

# **Genome-driven Search of Natural Products from Gram-negative Bacteria**

## **Genom-getriebene Suche nach Naturstoffen aus Gram-negativen Bakterien**

### **Dissertation**

der Mathematisch-Naturwissenschaftlichen Fakultät  
der Eberhard Karls Universität Tübingen  
zur Erlangung des Grades eines  
Doktors der Naturwissenschaften  
(Dr. rer. nat.)

vorgelegt von  
Andri Frediansyah  
aus Sleman/Indonesien

Tübingen  
2020

Gedruckt mit Genehmigung der Mathematisch-Naturwissenschaftlichen Fakultät der  
Eberhard Karls Universität Tübingen.

Tag der mündlichen Qualifikation:

25.09.2020

Stellvertretender Dekan:

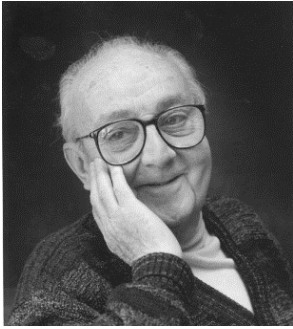
Prof. Dr. József Fortágh

1. Berichterstatter:

Prof. Dr. Harald Groß

2. Berichterstatter:

PD Dr. Bertolt Gust



*"All models are wrong, but some are useful".*

**George Box, 1976**



*"Kegagalan terjadi hanya bila kita menyerah".*

**B.J. Habibie**

## **Declaration**

I hereby declare that I alone wrote the doctoral work submitted here under the title 'Genome-driven Search of Natural Products from Gram-negative Bacteria, that I only used the sources and materials cited in work, and that all citations, whether the word for word or paraphrased are given as such. I declare that I adhered to the guidelines set forth by the University of Tübingen to guarantee proper academic scholarship (Senate Resolution 25.05.2000). I declare that these statements are true and that I am concealing nothing. I understand that any false statements can be punished with a jail term of up to three years or a financial penalty.

Andri Frediansyah

Tübingen, 01.08.2020

# Table of Contents

	Page
<b>Table of Contents</b>	i
<b>Publications, Posters, and Fellowship</b>	iv
<b>Contributions of Other Scientists to This Work</b>	v
<b>Abbreviations and Units</b>	vi
<b>Summary</b>	x
<b>Chapter 1. Introduction</b>	1
1.1. Bacterial natural products: dating back to the history to clinical matter	1
1.2. Bacterial natural product drug discovery today	9
1.2.1. OSMAC approach	10
1.2.2. Genome mining	12
1.2.3. Mass spectrometry-based metabolomics.	14
1.3. Gram-negative bacteria: from shape to function	15
1.3.1. Cell architecture	17
1.3.2. Emerging pathogens and their ubiquitous life	18
1.4. Underexplored of gram-negative proteobacteria: morphological characteristics, taxonomy, ecological niche, and their natural products	20
1.4.1. The genus <i>Massilia</i>	22
1.4.2. The genus <i>Telluria</i>	24
1.4.3. The genus <i>Janthinobacterium</i>	25
<b>Aims of the present study</b>	27
<b>Chapter 2. Materials and Methods</b>	28
2.1. Chemicals and media components	28
2.2. Columns	32
2.3. Kits	33
2.4. Media for bacterial cultivation	33
2.5. Antibiotics	35
2.6. Quorum sensing standards	36
2.7. Bacterial strains	39
2.8. Instrumentation	40
2.8.1. Mass spectroscopy	40
2.8.2. Reverse-phase VLC system	41
2.8.3. SEC system	41
2.8.4. HPLC system	42
2.8.5. NMR spectroscopy	43
2.8.6. UV spectroscopy	43
2.8.7. IR spectroscopy	44
2.8.8. Optical rotation	44
2.8.9. Bioinformatic analysis.	44

2.8.10. MS-Networking	45
2.9. Cultural Conditions	45
2.9.1. Cryo-culture preparation	45
2.9.2. Pre-culture preparation	45
2.9.3. Bacterial growth measurement	45
2.9.4. Large scale fermentation	45
2.10. Extraction, fractionation, and isolation of novel compounds	46
2.11. Cultivation, extraction, and profiling of AHL	47
2.12. Determination of absolute configuration of peptide	48
2.13. Siderophore detection-based CAS assay	49
2.14. Swimming motility assay	50
2.15. Biofilm assay	50
2.16. Sub-inhibitory assay by antibiotic	51
2.17. Fatty acid supplementation assay	51
2.18. Tyrosinase inhibition assay	51
2.19. Antibacterial assay	52
2.20. Cytotoxicity assay	52
2.21. Statistical analysis	53
<b>Chapter 3. Unveiling the specialized metabolites from the genus <i>Massilia</i> and the discovery of novel peptide</b>	54
3.1. Bioinformatic analysis of six type strains from the genus <i>Massilia</i>	54
3.2. Chemical investigation through OSMAC approach	56
3.3. Isolation and structure elucidation of novel tetrapeptide from <i>M. albidiflava</i>	57
3.4. Biological activities of novel tetrapeptide	68
3.5. Tyrosinase inhibitor – a mechanism and its bacterial production	70
<b>Chapter 4. Unveiling the specialized metabolites from the genus <i>Telluria</i> and the discovery of siderophore-like compounds</b>	72
4.1. Bioinformatic analysis of two type strains from the genus <i>Telluria</i>	72
4.2. Chemical investigation through OSMAC approach	73
4.3. The isolation and purification of serratiochelin C and its derivatives	74
4.4. Biosynthesis proposal of serratiochelin C from <i>T. chitinolytica</i>	82
4.5. Biological activity and CAS-assay of purified red-like compounds	85
<b>Chapter 5. Production and physiological function of acyl-homoserine lactones from the genera of <i>Massilia</i> and <i>Telluria</i></b>	86
5.1. Multiple genome comparison	86
5.2. Phylogenetic relationship and the assessment of genome similarity using ANI and <i>isDDH</i>	86
5.3. Acyl-homoserine lactones (AHLs) identity	90
5.4. Comparative AHLs production with an interval time of incubation.	92
5.5. AHL induce swimming motility.	94

5.6. AHL induce biofilm formation.	96
5.7. Effect of sub-inhibitory antibiotic concentration towards AHL production in <i>T. chitinolytica</i> and <i>M. lutea</i> .	98
5.8. The inhibition of FAb produced by <i>Burkholderia glumae</i> ICMP 3729 on swimming motility and biofilm formation.	100
5.9. AHLs within gram-negative bacteria – a novelty perspective	102
<b>Chapter 6. Chemical investigation of bacteria from the genus <i>Janthinobacterium</i></b>	108
6.1. Bioinformatic analysis of two strains from the genus <i>Janthinobacterium</i>	108
6.2. Chemical investigation employing the OSMAC approach	109
6.3. Isolation of purple-like compound and diamino acids	109
6.4. Biological activity of the purple-like compound and diamino acids	111
<b>Acknowledgments</b>	111
<b>Curriculum Vitae</b>	115
<b>References</b>	116
<b>Supplementary</b>	131

## Publications, Posters, and Fellowship

### Publications

Frediansyah, A., D., Straetener, J., Brötz-Oesterhelt, Gross, H., 2020. Massiliamide, a cyclic tetrapeptide with potent tyrosinase inhibitory properties from the Gram-negative bacterium *Massilia albidiflava* DSM 17472<sup>T</sup>. *Submitted*.

Chen, J., Frediansyah, A., Männle, D., Straetener, J., Brötz-Oesterhelt, H., Ziemert, N., Kaysser, L. and Gross, H., 2020. New nocobactin derivatives with antimuscarinic activity, terpenibactins A–C, revealed by genome mining of *Nocardia terpenica* IFM 0406. *ChemBioChem*, 21(15), pp. 2205-2213

Jiao, J., Du, J., Frediansyah, A., Jahanshah, G. and Gross, H., 2020. Structure elucidation and biosynthetic locus of trinickiabactin from the plant pathogenic bacterium *Trinickia caryophylli*. *The Journal of Antibiotics*, 73(1), pp.28-34.

Miess, H., Frediansyah, A., Göker, M. and Gross, H., 2020. Draft Genome Sequences of Six Type Strains of the Genus *Massilia*. *Microbiology Resource Announcements*, 9(18).

### Posters

Frediansyah, A. and Gross, H. A new tetrapeptide from underexplored gram-negative proteobacterium *Massilia albidiflava* and its tyrosinase inhibitor activity, presented at 16<sup>th</sup> Copenhagen Bioscience Conference: Natural Product-Discovery, Biosynthesis, and Application, by Novo Nordisk Foundation, 5<sup>th</sup>-9<sup>th</sup> May 2019, Copenhagen, Denmark; Abstract 048.

Frediansyah, A. and Gross, H. Genome-driven isolation of NRPS-based siderophore from *Telluria* sp., presented at International VAAM Workshop 2019, 15<sup>th</sup>-17<sup>th</sup> September 2019, Jena, Germany; Abstract P13.

### Fellowships

Ph.D. scholarship by Program for Research and Innovation in Science and Technology (RISET-Pro; World Bank loan no. 8245)

Selected conference fellowship by Novo Nordisk Foundation for attending Copenhagen Bioscience Conference: Natural Product-Discovery, Biosynthesis, and Application, 5<sup>th</sup>-9<sup>th</sup> May 2019 in Denmark.



## Contributions of Other Scientists to This Work

**Chapter 3:** This project was initially set up to find new chemistry of natural products from the genus *Massilia*. Antibacterial activities and cytotoxic against novel tetrapeptide produce by *M. albidiflava* have been conducted by Heike Brötz-Oesterhelt Lab (Department of Microbial Bioactive Compounds, Interfaculty Institute for Microbiology and Infection Medicine, University of Tübingen). The author also got help by several colleagues, including Dr. Arif Luqman (Microbial Genetics Department, University of Tuebingen) for technical assistance on recording tyrosinase inhibitory activity, Irina Helmle for technical support on recording NMR spectra, Hamada Saad for the professional assistant on analysis of amino acid configuration and Dr. Ghazaleh Jahanshah for technical assistance on recording polarimeter and FT/IR.

**Chapter 4:** This project was originally set up to find new chemistry of natural products from the genus *Telluria*. The author got help from Dr. Arif Luqman for technical assistance on recording bacterial activities against serratiochelin C.

**Chapter 5:** This project was originally set up in order to characterize QS molecules produced by members of the genus *Massilia* and *Telluria*. The author got help from several colleagues, including Dr. Arif Luqman and Dr. Nils Hauk, for technical assistance on the use of Tecan Infinite<sup>®</sup> 200 Pro microplate reader, Irina Helmle to help on operating and submitting the fatty acid metabolite of *B. glumae* ICMP 3729 to the NMR instrument.

**Chapter 6:** This project was initially set up in order to find new chemistry from the genus *Janthinobacterium*. The author got help by Dr. Arif Luqman technical assistance on the use of Tecan Infinite<sup>®</sup> 200 Pro microplate reader

**High-Resolution Mass Spectrometry (HRMS):** HRMS measurements and predicted molecular formula was obtained from Dr. Dorothee Wistuba (Institute of Organic Chemistry, University of Tübingen).

## Abbreviations and Units

°C	degrees Celsius
1D	one dimensional
2D	two dimensional
A	adenylation domain
AHL	Acyl-homoserine lactone
APCI	Atmospheric pressure chemical ionization
AT	acetyltransferase
ATP	Adenosine triphosphate
BGC	Biosynthetic Gene Cluster
C	condensation domain
Cy	cyclisation domain
d	(NMR) doublet
Da	Dalton
DAD	Diode Array Detector
DCL	deuterium chloride
DCM	dichloromethane
dd	(NMR) doublet of doublets
ddd	(NMR) doublet of doublet of doublets
DEPT	Distortionless Enhancement by Polarization Transfer
DiOC <sub>2</sub> (3)	3,3'-Diethyloxycarbocyanine iodides
DMSO	dimethyl sulphoxide

DMSO- <i>d</i> <sub>6</sub>	deuterated dimethyl sulphoxide
CCCP	carbonyl cyanide <i>m</i> -chlorophenyl hydrazone
EUCAST	European Committee on Antimicrobial Susceptibility Testing
ESI	electrospray ionization
Fe (III)	ferric iron
g	gram
GapDH	Glyceraldehyde-3-phosphate dehydrogenase
GNPS	Global Natural Product Social Molecular Networking
HCl	hydrochloric acid
HEPES	4-(2-hydroxyethyl)-1-piperazineethanesulfonic acid
HMBC	Heteronuclear Multiple Bond Correlation
HR	(MS) high resolution
HSQC	Heteronuclear Single Quantum Coherence
Hz	Hertz
IR	Infrared
L	liter
LC	Liquid Chromatography
LR	(MS) low resolution
m	(NMR) multiplet
<i>m/z</i>	mass to charge ratio
MeOH- <i>d</i> <sub>3</sub>	deuterated methanol with water
MeOH- <i>d</i> <sub>4</sub>	deuterated methanol

MeOH	methanol
mg	milligram
MHz	Megahertz
MIC	Minimum Inhibitory Concentration
min	minutes
mL	milliliter
MS	Mass Spectroscopy
MS/MS	Tandem Mass Spectrometry
MTT	3-(4,5-dimethyl-2-thiazolyl)-2,5-diphenyl-2H-tetrazolium bromide
nm	nanometer
NMR	Nuclear Magnetic Resonance
NOESY	Nuclear Overhauser Effect Spectroscopy
NRPS	Non-Ribosomal Peptide Synthetase
PBS	phosphate buffer saline
PCP	Peptidyl Carrier Protein
pH	potential of hydrogen
PKS	Polyketide Synthase
ppm	parts per million
QC	Quorum Quenching
QS	Quorum Sensing
qd	(NMR) quadruplet of doublets
RP	Reversed-Phase

s	(NMR) singlet
SEC	size-exclusion chromatography
SEM	Standard Error Mean
Ser	serine
T	thiolation
t	(NMR) triplet
TE	thioesterase
TOCSY	Total Correlation Spectroscopy
TOF	Time of Flight
TSB	Tryptic Soy Broth
UV	ultraviolet (spectroscopy)
VIS	visible (spectroscopy)
VLC	Vacuum Liquid Chromatography
$\alpha$	optical rotation (°)
$\delta$	NMR chemical shift (ppm)
$\Delta$	difference
$\epsilon$	(UV spectroscopy) molar attenuation coefficient
$\lambda$	wavelength
$\mu$	micro ( $10^{-6}$ )

## Summary

This thesis work constitutes an investigation of natural product production by three under-explored gram-negative genera, including *Massilia*, *Telluria*, and *Janthinobacterium*. The workflow started with bioinformatics analysis of the biosynthetic capacity to produce secondary metabolites, which were followed up by wet-lab experiments. For this purpose, the medium and cultivation conditions were optimized to trigger the production of the predicted compounds. Upon upscaling, pure compounds were isolated, and their biological effect was evaluated in biological assays.

### Chapter 3.

*Massilia albidiflava*, among eight strains, revealed the production of a novel cyclic tetrapeptide in the minimal culture broth. We successfully isolated and characterized its planar structure elucidated by spectroscopic analysis using extensive 1D- and 2D NMR experiments. The absolute configuration of the amino acid residues was determined by acid hydrolysis, followed by Marfey's derivatization coupled with LC-MS analysis. The final structure was determined to possess the amino acid sequence L-Pro-D-Tyr-L-Pro-D-Val and was designated massilamide. Massilamide potently inhibited the protein tyrosinase *in vitro* with an  $IC_{50}$  of  $1.15 \pm 1.04$ . However, it showed no antibacterial activity and cytotoxicity.

### Chapter 4.

*Telluria chitinolytica*, among two strains, revealed the production of the known compound serratiochelin C and its derivatives. Its biosynthesis has been proposed through this thesis on the base of the genome analysis. The serratiochelin C possesses antibacterial activity towards pathogenic bacteria.

### Chapter 5.

We present a comparative genomic analysis of bacteria from the genera *Massilia* and *Telluria* on the basis of Quorum Sensing production, specifically acyl-homoserine lactones/AHLs. We also investigated their physiological functions. The Multiple Reaction Monitoring-assisted analysis, in combination with molecular networking, showed that all

members from these genera produced C8-AHL, C4-AHL, and OH-C6-AHL. The swimming motility and biofilm formation were found to be dependent on the quorum-sensing system. The application of antibiotics in sub-inhibitory concentration did not disrupt their AHL production. However, the fatty acid metabolite (FAb) produced by *Burkholderia glumae* ICMP 3729 was found to reduce their AHL production significantly. This study was suggesting a cooperative interaction in their natural niche.

## **Chapter 6.**

*Janthinobacterium agaricidamnosum*, among two strains, revealed the production of the known compounds violacein, deoxy-violacein, and various types of a diketopiperazines. Some of these compounds possess antibacterial activity.

## Chapter 1. Introduction

### 1.1. Bacterial natural products: dating back to the history to clinical matter

Natural products (also known as secondary metabolites or as the end-product of gene expression) epitomize a group with chemically diverse structural entities, usually low-molecular-weight molecules, with various complex bioactive properties. They are not essential but provide an advantage for the organism. They can be produced by various organisms such as terrestrial plants, microbes, marine organisms, terrestrial vertebrates and invertebrates, and animals. Whichever as mixtures or pure form, these molecules act as the productive factory of therapeutic agents in different ailments.

Microbes are mainly known as remarkable sources of antibiotics. This knowledge began in 1928 when Alexander Fleming, a Scottish physician, discovered penicillin - a first-time non-ribosomal peptide antibiotic derived from mold, the filamentous fungus *Penicillium notatum* (Fleming, 1944).

In the same time interval - 1927, Selman Abraham Waksman, an Ukrainian scientist at the Rutgers Bacteriology Department, together with his colleague, Rene Dubois, -in collaboration with Oswald Avery from the Rockefeller Institute Hospital, found that their soil-bacillus-bacterium could attack the capsular polysaccharide of *Streptococcus pneumoniae* (Dubos, 1939). This encounter stirred Waksman to investigate more of their pre-existing antimicrobial bacteria in soil samples.

Thirteen years later, the growth inhibition zone technique- as proof of the natural product excreted from the bacterial colony with anti-pathogenic bacterial activity- has been discovered by Waksman and his colleague (Waksman and Woodruff, 1940). A year later, they published a pure form of the first-world-antibiotic from the gram-positive bacterium *Actinomyces antibioticus*, called actinomycin (Waksman and Woodruff, 1941). Its discovery was also noticeable as shifting meaningfully from plant to microbes as sources of natural products. Since then, Waksman was denoted as the true father of antibiotics (Kresge *et al.*, 2004).



Following actinomycin discovery, the era between the 1950s and 1960s is historically denoted as the 'Golden Era of Antibiotics', where various scientists have revealed an abundance of antibiotics. Most of them became long-lasting antimicrobial drugs including streptomycin which is produced by *Streptomyces griseus* (Waksman *et al.*, 1946), chloramphenicol from *S. venezuelae* (Bartz, 1948), streptocin from *S. griseus* (Waksman *et al.*, 1949), tetracycline from *S. aureofaciens* (Doerschuk *et al.*, 1959) and vancomycin from *S. orientalis* (Brigham and Pittenger, 1956).

As mentioned above, most of the natural products with antimicrobial function have been identified from *Actinobacteria*. *Bacillus* - a representative of the endospore-forming gram-positive bacilli, was also recognized as a decent source of antibiotics (Stein, 2005). In contrast, gram-negatives proved only occasionally to be also a trustworthy source of natural products, especially *Myxobacteria* (Reichenbach *et al.*, 1988; Schäberle *et al.*, 2014), the genus *Pseudomonas* (Gross and Loper, 2009), the genus *Burkholderia* (Kunakom and Eustáquio, 2019), and the phylum *Cyanobacteria* (Singh *et al.*, 2011).

There is an infinite number of gram-positive bacterial natural products that have been passed through clinical trials and which were approved as drugs (Raja and Prabakarana, 2011). Exemplary, some clinically used drugs of gram-positive but also of gram-negative origin (**Figure 1-1** and **1-2**) shall be highlighted in the following,

Tacrolimus (*syn.* FK506) -an immune-suppressive macrolide drug. It has been discovered for the first time from *Streptomyces tsukubaensis* (Tanaka *et al.*, 1987). Although it is not structurally like cyclosporin A, tacrolimus has been reported to have a similar effect as immunosuppressant *in vitro*, with the concentration 100 times lower to cyclosporin. Its immunosuppressive activity has also been studied *in vivo* using mice and mouse models (High and Washburn, 1997; Pereira *et al.*, 2006; Zhang *et al.*, 2009). Tacrolimus mediates its activity by the inhibition of calcineurin (*syn.* phosphatase 2B) through the production of the immunophilin-complex binding. Furthermore, it also disrupts calcium-dependent events, e.g., apoptosis, cell degranulation, nitrite oxide synthase, and transcription of the 2-interleukin genes (Thomson *et al.*, 1995). Tacrolimus has been used to minimize organ rejection and to induce immunosuppression via calcineurin blocking and interruption of the T-cell activation pathway (Migita and Eguchi, 2003). Its type of drug has been

conceded clinical trials passed phase IV, i.e., for renal transplantation (registered number NCT00935298), liver, and kidney transplantation (NCT01889758), the complication of transplant (NCT02014103) and nephrotic syndrome in children (NCT03347357). Up to recently, there are 602 completed clinical trials and 109 under the recruiting process for other tacrolimus trials. Today, among others, tacrolimus is available and sold in the market under the brand name Prograf® and Advagraf®. It is mainly used to help prevent organ rejection in people with transplantation of heart, liver, or kidney.

Polymyxins is a mixture of cationic polypeptide antibiotics composed of at least five chemically different compounds (polymyxins A to E) and have been discovered in 1947 (Stansley *et al.*, 1947). In their pure form, polymyxin B and polymyxin E have been isolated from gram-positive bacteria *Bacillus* spp. (Evans *et al.*, 1999). Polymyxin E is non-ribosomally synthesized from *B. polymyxa* subspecies *colistinus* (Komura and Kurahashi, 1979). Both have the same mode of action, which directly targets the membrane of the bacterial cell. Their cationic side interacts with anionic lipopolysaccharide molecules of the outer layers' gram-negative bacteria, supporting the displacement of calcium and magnesium that contribute to the stabilization of the lipopolysaccharide layer, thus effecting derangement of the membrane cell. This process elevates the permeability of membrane cells, cell leakage, and apoptosis (Gupta *et al.*, 2009). Colistin (polymyxin E) entered phase III for bacterial pneumonia-related *Acinetobacter baumannii* infection with the registered number of NCT01577862 and successfully entered phase IV for gram-negative bacterial infections (NCT01732250). The combination of colistin with imipenem could enter phase IV (NCT02683603). Polymyxin B hemoperfusion could enter phase III clinical trials for patients with severe sepsis from gram-negative infection (NCT00490477) and with modification with immobilized fiber column could entered phase IV for the same treatment (NCT00629382). In the market, polymyxins are sold as Colistin® (contains polymyxin E) and Polyspectran® (contains polymyxin B and additional bacitracin and neomycin).

Bacitracin- is a polypeptide topical antibiotic produce by *Bacillus licheniformis* ATCC 10716 and has been discovered for the first time in 1946 (Callow and Hart, 1946). Its production is connected with the sporulation time during the exponential phase of poorly

used nitrogen and carbon sources (Hanlon and Hodges, 1981). The neotype of ATCC 14580 also has been reported to produce the same compound (Haavik, 1975). Bacitracin has been reported with bactericidal activity towards gram-positive cells at low concentrations (Werner and Russell, 1999). It also exhibits antibacterial activity against streptococcal infections *in vivo* using mice (Johnson *et al.*, 1945) and *Clostridium difficile* which cause pathogen-related related colitis and diarrhea (Chang *et al.*, 1980; Young *et al.*, 1985). The mode of action of bacitracin has been demonstrated using the gram-positive pathogen *Staphylococcus aureus*. The bacteriostatic effect on *S. aureus* involves growth inhibition, lysis induction of the membrane, suppression of enzyme synthesis, and the reduction of triphenyl-tetrazolium chloride (Smith and Weinberg, 1962). However, the primary mode of action is the binding of bacitracin to C<sub>55</sub>-isoprenyl pyrophosphate, thereby preventing the dephosphorylation reaction, which is a prerequisite that the flippase can transfer the C<sub>55</sub>-P arm back through the cell membrane, so that the next peptidoglycan building unit can be transported across the membrane (Storm, 1974). In clinical trials, bacitracin in combination with topical tranexamic 5% passed phase IV to treat patients with arteriovenous fistula (NCT02106962). For patients with contact dermatitis and paranasal sinus disease, it only could enter up to phase II (NCT00132600 and NCT01222832, respectively). In the market, bacitracin is sold under the brand of Nebacetin®.

Streptozocin or streptozotocin- is a glucosamine-containing nitrosourea anticancer agent produced for the first time by *Streptomyces achromogene* var. *streptozoticus* (Bergy *et al.*, 1962). It has been reported to inhibit the synthesis of pyridine nucleotide in a mouse model (Schein and Loftus, 1968). The early anticancer activity of streptozocin has been shown against a panel of six human cell lines (Carter *et al.*, 1971). Later in 1972, within the frame of a phase II clinical trial, the compound showed half reduction magnitude tumor to three patients and less than fifty percent reduction to additional four people (Stolinsky *et al.*, 1972). The mode of action of this molecule is the inhibition of DNA synthesis which in turn affects the cell cycle of bacteria and mammalians cells (Broder and Carter, 1973). It has a wide variety of anticancer activity, including carcinoid, islet, and liver tumors (Gyves *et al.*, 1983). The first study of streptozocin biosynthesis was conducted in 1979 using a classical feeding experiment and suggesting the incorporation of D-glucosamine

(Singaram *et al.*, 1979). Streptozocin has passed clinical trials related to adrenal cortical carcinoma (NCT00094497) and has been sold under the brand name Zanosar®.

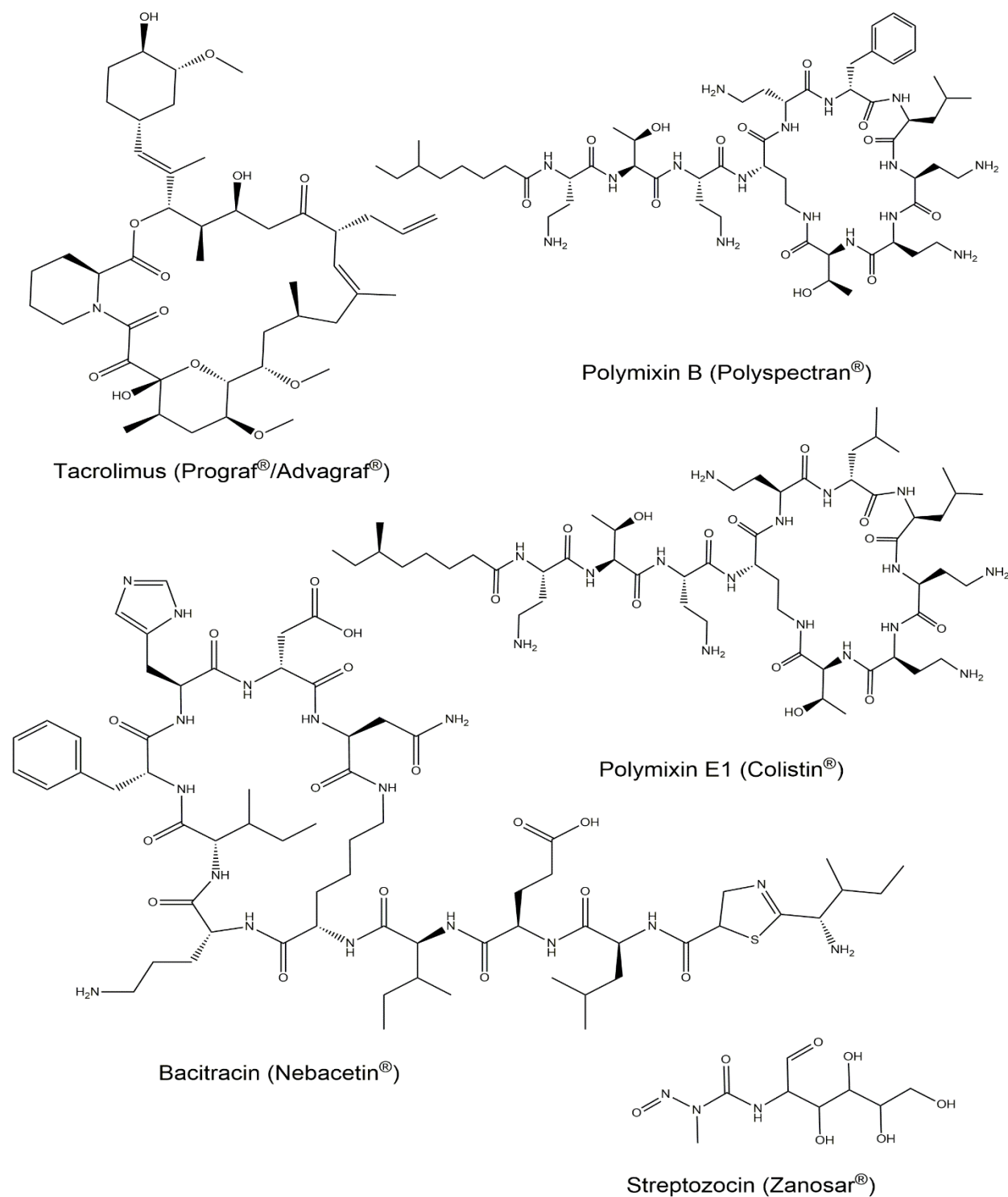


**Figure 1-1.** Clinically approved drugs produced by gram-positive bacteria.

Compared with gram-positives, there are less clinically approved drugs from gram-negative bacteria even though numerous compounds have been so far discovered. To the best of our knowledge, only three drugs from gram-negative bacteria (cyanobacteria excluded) have been passed through clinical trials and sold on the market.

Epothilone is a 16-membered macrolide anticancer drug that has been discovered at the beginning of the 1990s from mycobacterium *Sorangium cellulosum*. At the first time of isolation, epothilone A and B have shown, beside antifungal properties, remarkable cytotoxic activity *in vitro* to human cell lines (Gerth *et al.*, 1996; Höfle *et al.*, 1996). These molecules had paclitaxel-like activity as its activity is mediated by stabilizing microtubulin and polymerization, leading to programmed cell death -termed as apoptosis (Wessjohann, 1997). These attractive preclinical outcomes led to further in-depth studies as an anti-cancer drug. Currently, several types of epothilones underwent clinical trials. Among 88 completed trials, epothilone D (KOS-862 from Kosan Biosciences) could enter Phase II for colorectal cancer treatment (NCT00077259) and natural epothilone B (EPO906 or patupilon from Novartis) has been efficaciously progressed into Phase III for ovarian cancer treatment (NCT00262990). The drug has been launched to the market under the name Ixempra®.

Another drug from gram-negative bacteria is called mupirocin and represents a topical antibacterial drug (Sutherland *et al.*, 1985). It belongs to polyketide-antibiotics encompassing a pyran ring, and a saturated fatty acid- called as 9-hydroxynonanoic acid. At the first time of its discovery, it was termed pseudomonic acid A, a mono-carboxylic acid, and was isolated from *Pseudomonas fluorescens* (Fuller *et al.*, 1971). It has bactericidal activity against clinical skin isolates of *Staphylococcus aureus* and went from *in vitro* into clinical studies (Casewell and Hill, 1985; 1986; Frank *et al.*, 1989). Ward and Campoli-Richards (1986) explained that more than 90% of these colonies inhabited at a concentration below 0.12 mg/L, followed by methicillin-resistant strains, *S. pyogenes*, and *S. pneumonia* at a concentration under 1 mg/L, and the most insensitive species was *S. faecalis*. However, mupirocin showed less sensitivity to gram-positive strains and was ineffective towards gram-negative pathogens. However, it furthermore possesses antifungal activity against a variety of fungi *in vitro* and *in vivo* (Nicholas *et al.*, 1999). The

mode of action study showed that mupirocin inhibits RNA synthesis and bacterial protein synthesis activity through selective binding to the isoleucyl-tRNA synthetase (IleS), thereby interfering with protein biosynthesis (Casewell and Hill, 1987). Since then, this drug belongs to antibiotics with direct action onto tRNA by inhibiting its aminoacylation. The biosynthesis of mupirocin also has been classically studied since 1977, using feeding experiments through radio-isotopically labeled substrates (Feline *et al.*, 1977).

Further studies were conducted with other strains, such as *P. fluorescens* NCIMB 10586, using biochemical tests and sequencing (El-Sayed *et al.*, 2003). In the US, mupirocin successfully entered phase IV clinical studies as an efficacious drug against Staphylococcal infection (NCT02284555) and chronic rhinosinusitis (NCT02218307). This antibiotic also passed phase III clinical trial to treat impetigo, a highly contagious skin infection in children and infants (NCT04287777). The drug was then marketed under the name Bactroban®.

Ecteinascidin (*syn.* ET-743) is an anticancer drug and was discovered for the first time in the marine tunicate *Ecteinascidia turbinata* from the Caribbean (Rinehart *et al.*, 1990). Recently, with the increasing technology, an endosymbiont of the tunicate called *Candidatus Endoecteinascidia frumentensis*, a gamma proteobacterium, was identified as the true producer of ET-743 (Moss *et al.*, 2003; Tianero *et al.*, 2015). *In vitro* studies projected that ecteinascidin has anticancer activity against human cancer cell lines, including prostate, ovarian, non-small cell lung, melanoma, and breast cancer (Ghielmini *et al.*, 1998; Izbiccka *et al.*, 1998). The same activity towards these cancer types could be reproduced in mouse models through *in vivo* studies (Valoti *et al.*, 1998; Hendriks *et al.*, 1999). The preclinical *in vivo* studied showed that the cytotoxicity of the ecteinascidin drug could be achieved in  $\mu\text{g}/\text{m}^2$  doses and resilient nanomolar plasma concentration (Rosing *et al.*, 1998). Consequently, ecteinascidin was nominated for clinical development by the US National Cancer Institute in 1993 (Aune *et al.*, 2002) because of its excellent activities. The mechanism of action ecteinascidin is the alkylation of guanine N2 in the DNA minor groove through an electrophilic iminium ion that occurs after the conversion of the carbinolamine (Aune *et al.*, 2002). In cellular pharmacology, the drug slows down cell progression in the S phase and arrests cells in G2 followed by an increase of p53 as an

alert of DNA damage, ultimately leading to apoptosis (Takebayashi *et al.*, 2001). In clinical trials, esteinascidin has passed III phase clinical trials for anti-leiomyosarcoma, liposarcoma, synovial sarcoma (NCT03773510), and ovarian cancer (NCT00113607). The drug has been sold under the name Yondelis®.

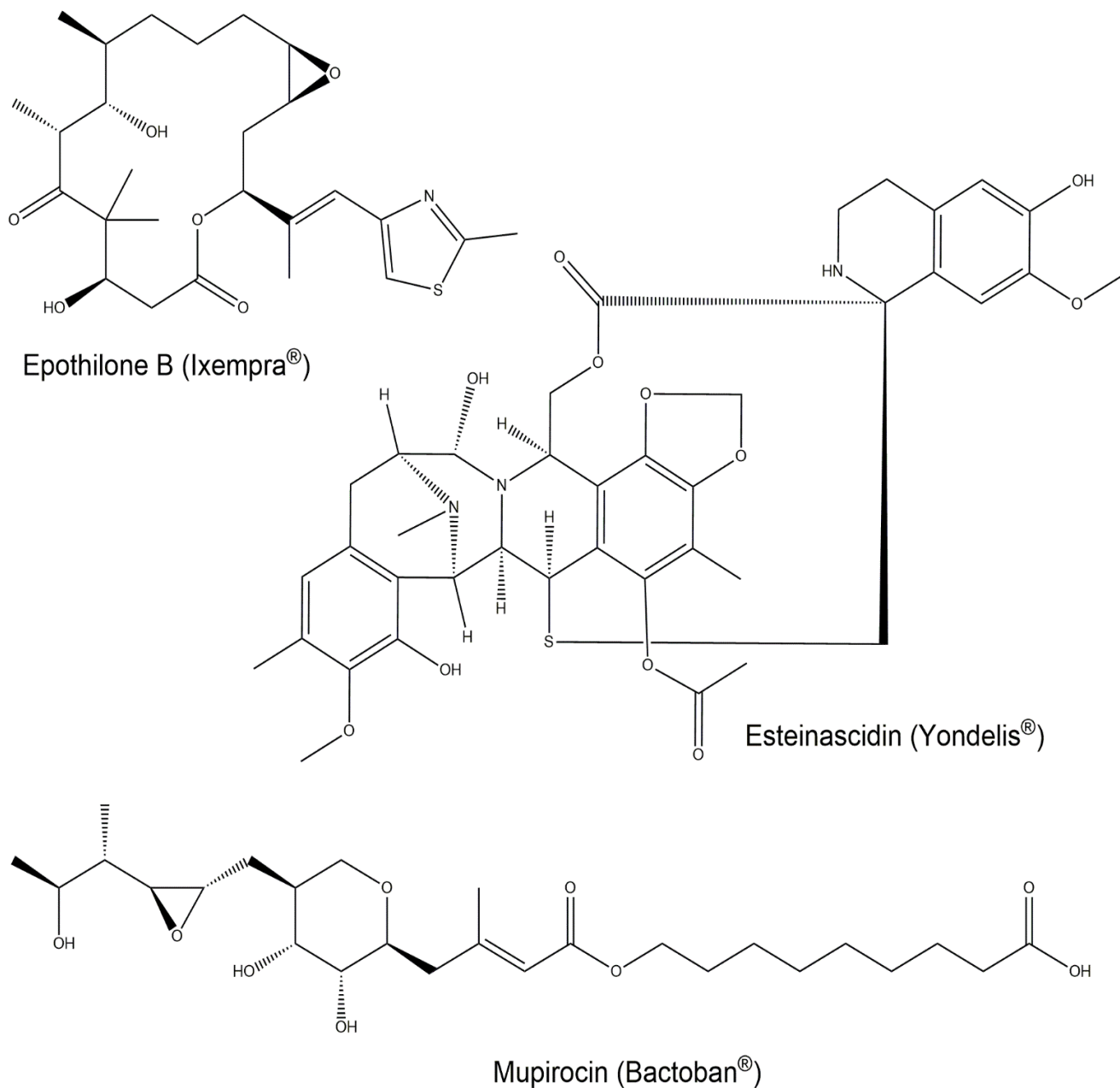


**Figure 1-2.** Clinically approved drugs produced by gram-negative bacteria.

## 1.2. Bacterial natural product drug discovery today

The natural product (NP) itself has a full function in terms of variation of biological activity and proves to be more than just “secondary metabolites.” Natural products always inspired the development of pharmaceutical-lead drugs. More than 80% (Sneader, 1997) of approved drugs stem from either unmodified NPs, altered NPs by semi-synthesis, or from NP-synthesis by total synthesis (Newman and Cragg, 2016). In 2008, natural products from bacteria had been reported to contribute about 11.11% and have been placed as third after plant and semi-synthetically that lead to preclinical and clinical stages (Harvey, 2008). Bacterial natural products play an essential role as anti-infective, anti-cancer, immunomodulatory agents, and other miscellaneous (Demain, 2014; Newman and Cragg, 2016).

Bacteria are persistently recognized as an inexhaustible reservoir of new drug leads. Their chemical assembly is often unrivaled to any synthetically reference library of small molecules and bears to prompt avant-garde findings chemistry and biological functions. Bacterial secondary metabolites also demonstrated its value, particularly in the history of antibiotic discovery and development. Their encounter has been reflected by their sustained use and the diminution in morbidity and mortality from bacterial contagions over the past five decades. However, recently, the elevation of the number of multidrug-resistant bacteria (MDR) has led to the prophecy that we are returning to a pre-antibiotic era (Ash, 1996). Thus, new chemical structures with biological functions against MDR bacteria or other pharmacological functions are required.

However, bacterial natural product screening efforts have not coped well in the current timelines and did not afford a noteworthy new pharmaceutical-lead compound. While bacterial diversity remains mostly unexplored, the re-discovery of known compounds through traditional strategies outweighed pharmaceutically lead bioactive discoveries regardless of significant advances. This fact has to lead to a weighty undesirable for all kinds of natural product programs in bulky pharmaceutical companies (Pye *et al.*, 2017). Without the right target and plan, its exploration remains costly, time-consuming, and ineffective for pharmaceutical industries (Demain, 2014). Thus, in the past 2-3 decades, most of them switched their drug discovery program to synthetic combinatorial libraries



instead of natural products. Nevertheless, bacteria persist as an influential source for the unearthing of pharmaceutically lead compounds. Various strategies and technologies can be used in order to diminish the rediscovery rate of known natural products, including OSMAC, genome mining, and MS/MS molecular networking approaches.

### 1.2.1. OSMAC approach

Presently, many compounds are still discovered by employing classical methods, for example, the direct-isolation method, i.e., isolation from bacterial fermentation broth and determination of the structure solely as a pure compound. Bioactivity-guided fractionation principle is typically integrated to facilitate the search. However, recently, this method is not considered relevant anymore, due to the high rate of re-discovery of known molecules. As secondary metabolites are end-products of gene clusters, the identification, prediction, and activation of gene clusters are needed to facilitate the production of bioactive compounds in bacteria. Because most of these gene clusters are silent or cryptic under the standard fermentation conditions, mimicking the bacterial native environment, could result in the activation of their diverse-cryptically metabolic pathways. One relatively simple and versatile strategy represents the OSMAC (one strain-many compound)-approach, which principally varies cultivation conditions (Bode *et al.*, 2002). Its cultivation-dependent approach can be categorized as abiotic and biotic. An abiotic approach can be influenced either by chemical or physical elicitors. Chemical elicitors can exert a strong influence on the awakening of the cryptic gene cluster (Seyedsayamdost, 2014). A further example represents the addition of the antibiotic trimethoprim at a sub-inhibitory level to the culture broth of *Burkholderia thailandensis*, which led to the increase of the production of acybolin (Okada *et al.*, 2016).

Furthermore, the addition of a quorum-sensing molecule induced the production of secondary metabolites such as fragin, an antifungal compound, produced by *B. cenocepacia* (Jenul *et al.*, 2018); and jessenipeptin and mupirocin from *Pseudomonas* sp., associated with an amoeba (Arp *et al.*, 2018). The addition of metal ions, in combination with a quorum-sensing molecule, was able to regulate the production of the amphiphilic enterobactin along with numerous related siderophores in *Vibrio harveyi* (McRose *et al.*, 2018a). Alteration in the chemical composition of growth media can also

profoundly change the secondary metabolite profile. Changing the medium composition as a report by Jiao *et al.* (2020) showed that *Trinickia caryophylli*, one of the gram-negative bacteria, belonging to *Burkholderia sensu lato*, was only produced in SRM<sub>HG</sub> media instead of MM9 media. The SRM<sub>HG</sub> contains only L-histidine as nitrogen sources, however MM9 content mix nitrogen sources from casamino acid. The use of a suitable saline concentration also affects the production of rhamnolipids by *P. aeruginosa* (Prieto *et al.*, 2008).

Various scientists have also demonstrated a physical method that influences the production of new secondary metabolites. Awad *et al.* (2005) reported that UV mutagenesis could influence the production of a new antibiotic in *Aspergillus ochraceous*. Another example is the use of a shake flask instead of a roller bottler that could induce the production of antibiotics in a marine bacterium *Bacillus* sp. (Yan *et al.*, 2002). Bode *et al.* (2002) also explained that the alteration of new secondary metabolites can be even influenced by hydrostatic pressure.

The biotic approach is using the entire organism also to activate the biosynthetic gene cluster and stimulate either a new chemical structure or various tremendous amounts of known natural products, i.e., by co-cultivation or by mix cultivations. Reports showed that the production of the known natural product lateropyrone increased up to 78-fold in co-cultivation when compared with mono-cultivation (Ola *et al.*, 2013) and increased up to 100-fold the production of emericellamides compared with the natural fermentation (Oh *et al.*, 2007). Co-cultivation of *Pseudomonas aeruginosa* with the fungus *Fusarium tricinctum* could influence the production of various antifungal phenazine and quorum-sensing signals (Moussa *et al.*, 2020). A similar co-interaction between gram-negative bacteria and fungi could also be seen in the production of pestalone that involved the gram-negative bacterium *Thalassospira* sp. with marine fungus *Pestalotia* (Cueto *et al.*, 2001). Rhodostreptomycins A and B had been produced by co-cultivation of *Rhodococcus fascians* and *Streptomyces pandanus* as a result of the horizontal gene cluster (Kurosawa *et al.*, 2008). The production of istamycins A and B also resulted in co-cultivation between *Streptomyces tenjimariensis* and unidentified marine bacteria (Slattery *et al.*, 2001). However, fungi are the most applicable microorganisms concerning

the production of new secondary metabolites through co-cultivation, such as the production of marinamide (Zhu and Lin, 2006), enniatin (Wang *et al.*, 2013), acremostatin (Degenkolb *et al.*, 2002), libertellenones (Oh *et al.*, 2005), and aspergicin (Zhu *et al.*, 2011).

### 1.2.2. Genome mining

In 2002 and 2003, two bacterial genomes belonging to bacteria that were widely known as natural product producers, namely *Streptomyces coelicolor* (Bentley *et al.*, 2002) and *S. avermitilis* (Ikeda *et al.*, 2003) respectively, opened the fact that these genomes still carries a hidden potential to produce further secondary metabolites. Fundamentally, genomes are necessary data from creatures that could be excavated. The term is derived from the term 'data mining' that includes the systematic assortment, analysis, and interpretation of embankments of data to determine new significant traits, associations, patterns or tendencies (archetypally but not unavoidably used to envisage forthcoming events). Following its term, classical genome mining was born by recognizing the enzymes or deeper into genes (GATC, triplet codon, and two directions readable) that cipher the putative enzymes that contribute to the respective biosynthesis of secondary metabolites.

Thus, since then, the process of activating cryptic genes was aided by genome mining. It is a process of extracting information from genome sequences information to explore the secondary metabolite biosynthetic gene clusters (BGCs) and to predict the production of the secondary metabolite of interest *in silico*. Despite that microbial natural products shows a high diversity concerning the chemical structure, the enzymes that contribute to the biosynthetic machinery to build these molecules are frequently high conserved. It is also reflected in the amino acid sequence of many of the core biosynthetic enzymes. The conserved pieces of the BGCs machinery are regulated at the transcription level. Generally, the code for biosynthetic enzymes, comprise polyketide synthases (PKS), non-ribosomally synthesized peptide synthetases (NRPS), ribosomally- and post-translationally modified peptides (RiPPs), transporters, decorating enzymes, i.e., oxidases, cyclases, and halogenates.

There are several types of sequencing platforms to facilitate high-throughput genome mining of natural products, including Illumina (short read length sequences), PacBio (long read length sequences), and Oxford nanopore (long read length sequences). The best sequence quality of genomic data can be provided by the combination of short-read sequence technology (e.g., Illumina) that provides error correction of the long read -with long-read sequence technologies (e.g., PacBio or Nanopore) which provide scaffolding power. In order to mine the BGCs, several tools can be used as a facilitator, as shown in **Table 1-1**. These software technologies had been developed by bioinformaticians to detect and decipher all types of BGCs. In some instances, the programs are functionated to provide a prediction of the chemical scaffold of the metabolites, especially for NRPS, types 1 PKS, and RiPPs. However, the information is limited to other molecule classes, including glycosylated natural compounds.

**Table 1-1.** Available genome mining tools.

Genome mining tools	Function	URL
antiSMASH 5.0	To mine general BGCs	<a href="https://antismash.secondarymetabolites.org">https://antismash.secondarymetabolites.org</a>
PRISM 3	To mine general BGCs	<a href="http://grid.adapsyn.com/prism">http://grid.adapsyn.com/prism</a>
BAGEL 4	To mine RiPP BGSs	<a href="http://bagel4.molgenrug.nl/">http://bagel4.molgenrug.nl/</a>
RODEO	To mine RiPP BGCs	<a href="http://ripp.rodeo/">http://ripp.rodeo/</a>
RiPPMiner	To mine RiPP BGCs	<a href="http://www.nii.ac.in/~priyesh/lantipepDB/new_predictions/index.php">http://www.nii.ac.in/~priyesh/lantipepDB/new_predictions/index.php</a>
SBSPKS	To mine PKS BGCs	<a href="http://202.54.249.142/~pkssdb/sbspks/master.html">http://202.54.249.142/~pkssdb/sbspks/master.html</a>
PKMiner	To mine PKS BGCs	<a href="http://pks.kaist.ac.kr/pkminer/">http://pks.kaist.ac.kr/pkminer/</a>
CASSIS/SMIPS	To mine PKS and NRPS	<a href="https://sbi.hki-jena.de/cassis/">https://sbi.hki-jena.de/cassis/</a>
NaPDoS	To mine domain of BGCs	<a href="http://napdos.ucsd.edu/">http://napdos.ucsd.edu/</a>
antiSMASH database	Database of microbial BGCs	<a href="https://antismash-db.secondarymetabolites.org/">https://antismash-db.secondarymetabolites.org/</a>
Natural Products Atlas	Database of natural products	<a href="https://www.npatlas.org/">https://www.npatlas.org/</a>
StreptomeDB 2.0	Database of natural products from Streptomyces	<a href="http://132.230.56.4/streptomedb2/">http://132.230.56.4/streptomedb2/</a>

---

AntiBase	Database of natural products from Microbes	software
SciFinder	Database of chemical structure	<a href="https://sso.cas.org">https://sso.cas.org</a>
SIRIUS 4.4	To predict chemical structure against a compound database	<a href="https://bio.informatik.uni-jena.de/software/sirius/">https://bio.informatik.uni-jena.de/software/sirius/</a>
SeMPI	To predict chemical structure against a compound database	<a href="http://132.230.56.4/SeMPI/">http://132.230.56.4/SeMPI/</a>
BactiBase	To predict chemical structure against bacteriocin database	<a href="http://bactibase.hammamilab.org/">http://bactibase.hammamilab.org/</a>

---

There are several compounds from gram-negative bacteria that have been discovered through genome mining, such as compound class PKS-NRPS hybrid, i.e., jagaricin and rhizoxin; trans-AT-polyketides, i.e., rhizopodin and elansolide D; NRPS, i.e., gacamide, massiliachelin, trinickiabactin, poeamide, orfamide, endopyrroles, and gramibactins.

### 1.2.3. Mass spectrometry-based metabolomics

MS-based metabolomics could also be used to prioritize, to dereplicate, and to assess new chemistry-based secondary metabolites in bacterial cultures. This technique involves analytical tools (i.e., mass spectrometry) in combination with computational and statistical treats, referred to as 'omics' tools. Thus, metabolomics enables quick identification and quantification of small metabolites produced by creatures at a definite time point, analyzable by the preferred technique. Undeniably, the latter cultures can be unswervingly evaluated without the need for isolation and purification, and large data sets can be handled on one occasion. So, this technique could minimize the isolation of known compounds produced by bacteria.

MS spectrometry is a compassionate tool, and the sample of interest could be used in small volume or even in complex mixtures. It also can be coupled with various detectors (i.e., UV, DAD) and chromatography techniques. Moreover, MS/MS fragmentation (i.e., MS<sup>1</sup> and MS<sup>2</sup>) provides additional essential information for structural elucidation and

comparison with natural product databases such as the mass search tools called MASST (Wang *et al.*, 2020). Tandem MS (MS/MS) molecular networking has evolved and fruitfully employed over the last half decades to conduct dereplication of known bacterial secondary metabolites production through an open-access database for organizing and sharing raw, processed or recognized MS/MS spectral information, called as Global Natural Products Social Molecular (GNPS) networking (Wang *et al.*, 2016). MASST is also a part of this system. This technique is clustering and organizing MS/MS data using spectral similarity. So, it can split unknown from known natural compounds based on their structural similarity through MS/MS fragmentation. In order to ease the organizing of more extensive raw MS data set in a specific time point, MetaboScape® could be used as a pre-processed data set.

There are many examples of bioactive compounds that have been discovered using this technique, such as nocobactin-like siderophores derivatives from *Nocardia terpenica* (Chen *et al.*, 2020), acybolin from *Burkholderia thailandensis* (Okada *et al.*, 2016) and cyanotoxins from a cyanobacterial bloom in Green Lake, Seattle (Teta *et al.*, 2015).

### 1.3. Gram-negative bacteria: from shape to function

Nowadays, Gram staining cannot be continuously used to evaluate familial relations of bacteria. Nonetheless, staining consistently gives reliable information about the composition of the cell membrane. Gram-negatives are distributed in the various phyla of bacteria. There are four significant phyla of gram-negative bacteria, including *Proteobacteria*, *Cyanobacteria*, *Bacteroidetes*, and *Candidatus Tectomicrobia*, as shown in **Figure 1-3**. The known pathogens of humans, animals, and most plants are *Proteobacteria*. *Cyanobacteria* is the phylum that is found abundantly in the aquatic ecosystem from fresh to saline water (Singh *et al.*, 2011).

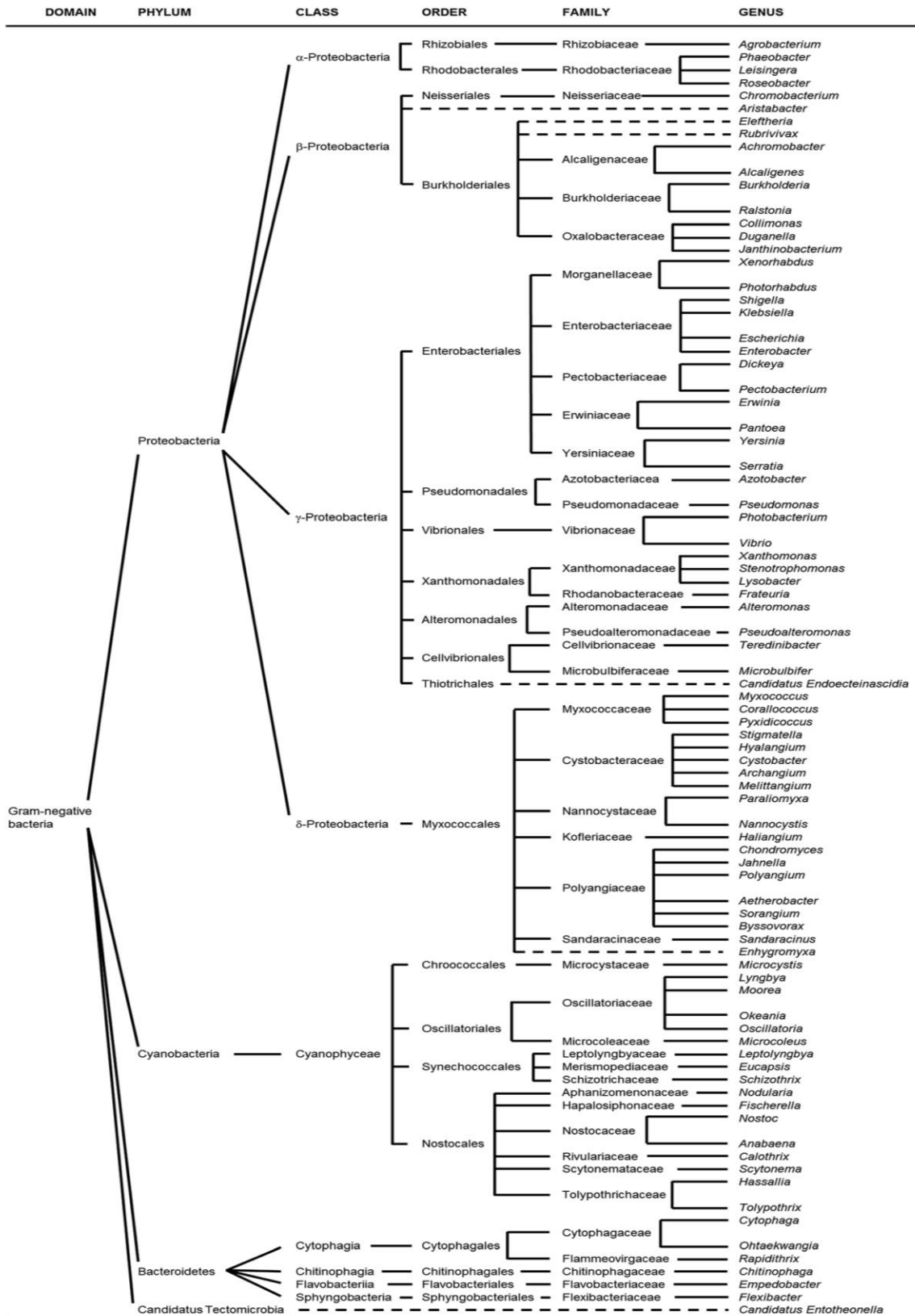


Figure 1-3. Taxonomical overview of gram-negative bacteria (Masschelein et al., 2017).

### 1.3.1. Cell architecture

The architecture of gram-negative bacteria has differed from gram-positive bacteria. At large, the main construction of the bacterial cell wall is peptidoglycan, also termed murein, which is a macromolecular polymer consisting of sugars and peptides. The sugar part is assembled by other residues of N-acetylglucosamine (NAG) and N-acetylmuramic acid (MurNAc). They are allied by a  $\beta$ -(1,4)- glycosidic bond. In gram-negative bacteria, using *Escherichia coli* as an example, a peptide chain straddling from three to five amino acids containing L-alanine, D-alanine, D-glutamic acid, and meso-diaminopimelic acid. In gram-positive bacteria such as *Staphylococcus aureus*, a peptide chain consists of L-alanine, L-lysine, D-alanine, and D-glutamine. Its chain was connected to 5-glycine. Overall, these edifices are attached to MurNAc, which in turn allows cross-linking to take place, hence providing the intertwined-like structure of the layer, also the strength required to counteract the osmotic pressure of the cytoplasm. Concerning cross-linking, it is made conceivable through the action of the DD-transpeptidase enzyme. It is imperative to note that the mentioned above amino acid arrangement and molecular edifice vary among bacterial species. In *Mycobacteria*, cell walls have an additional mycolic acid, which offers a waxy outer layer (**Figure 1-4**).

Even though the gram-negative bacterial cell wall is also unruffled of peptidoglycan, it contrasts in the means that the peptidoglycan is a single thin layer compared to the thick layers in gram-positive cells. Its thin layer does not retain the initial crystal violet dye but picks up the pink color from the safranin counterstain during Gram-staining. However, the cell wall architecture of gram-negative bacteria possesses a more complex structure than that of gram-positive creatures. It is sandwiched between the plasma membrane and the thin peptidoglycan sheet like a gel matrix called periplasmic space. Unlike gram-positive bacteria, gram-negative bacteria have an outer membrane layer that is external to the peptidoglycan cell wall. Another unique characteristic is that gram-negative bacteria contain lipopolysaccharide (LPS) molecules on the outer membrane. It is important to note that LPS has pyrogenic qualities (endotoxins) that can cause inflammation and a septic shock, and abnormal release of prostaglandins via the hypothalamus.



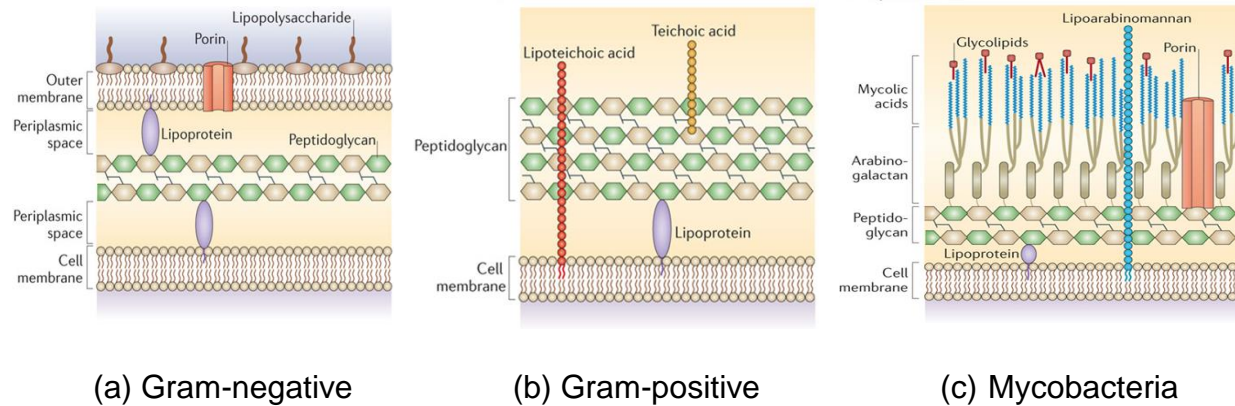


**Figure 1-4.** Overview of the cell wall structure of gram-positive and gram-negative bacteria, and *Mycobacteria* (Brown *et al.*, 2015).

### 1.3.2. Emerging pathogens and their ubiquitous life

Gram-negative bacteria are known to contain human pathogens that contribute to global infections (Breijyeh *et al.*, 2020). They cause several clinical outcomes, including bacteremia, ventilator-associate pneumonia, urinary tract infection, and intra-abdominal infections. These groups were often more prevalent than in gram-positive bacteria and developed antibiotic resistance due to their unique resistant mechanisms and limited treatment options (Thomson and Bonomo, 2005). Gram-negative pathogens usually produce beta-lactamase that hydrolyzes beta-lactam in order to develop a resistance mechanism of beta-lactam drugs on the market, including penicillin, cephalosporin, oxacillin, and metallo-beta-lactamases.

The resistant pathogens are a serious public health problem facing people's world. In the US, more than 35,000 people have been reported dead due to these infections, and about 2.8 million people living with antibiotic resistance infection each year (CDC, 2019). The majority of the deaths is related to gram-negative infections, including carbapenem-resistant *Acinetobacter*, carbapenem-resistant *Enterobacteriaceae*, drug-resistant *Neisseria gonorrhoeae*, extended-spectrum beta-lactamase-producing *Enterobacteriaceae*, multidrug-resistant *Pseudomonas aeruginosa*, drug-resistant nontyphoidal *Salmonella*, drug-resistant *Shigella*, and drug-resistant *Salmonella* serotype *Typhi*.

Utmost critical emergent associated with antibiotic resistance are the ESKAPE pathogens that belongs to six bacteria; three thereof are gram-negative pathogens, including *A. baumannii*, *P. aeruginosa*, and *Enterobacteriaceae*. They can escape the outcome of antimicrobial drugs and cause widespreadding hospital-acquired infections (Boucher *et al.*, 2009). In addition, *Klebsiella pneumoniae*, *K. oxytoca*, and *Escherichia coli* also contribute to human infections (Hadziyannis *et al.*, 2000).

Some rod shape gram-negative bacteria also represent a pathogen and a parasite to animals. They cause diseases in animals, such as *Brucella* spp. that causes brucellosis or undulant fever in cattle, pigs, sheep, and goats (Gul and Khan, 2007); *Chlamydia* causes chlamydiosis in livestock (Wheelhouse and Longbottom, 2012); bloodborne *Bartonella* causes bacteremia in dear, cat, rodent and cattle (Breitschwerdt and Kordick, 2000); and *Burkholderia pseudomallei* causes melioidosis, a fatal disease of animals (also human), by the type III secretion system (Ribot and Ulrich, 2006).

The pathogenicity of several gram-negative bacteria was also found in plants causing diseases, such as the members of the genus *Xanthomonas* cause blight, leaf streak, and spot to various plants (Yang and Bogdanove, 2013). Other gram-negative species, such as *Xylella fastidiosa* and *Ralstonia solanacearum*, also belong to soil-borne plant pathogens (Salanoubat *et al.*, 2002). *X. fastidiosa* subspecies *pauca* has been reported as an emerging olive quick decline syndrome disease agent which economically affected olive farms across Europe, especially in Greece, Italy, and Spain since 2013 (Guo, 2020).

In another story, gram-negative bacteria also have a ubiquitous environment except as pathogenic creatures to an organism. As these genomes vary in size 0.4 to >6 Mb with the GC content ranging from 25 to 80%, gram-negative cells could adapt to a broad type of environmental fitness (Masschelein *et al.*, 2017). Thus, they are belonging to the massive cluster with taxonomically diverse and distributed in an extensive environmental niche within the earth, including terrestrial, freshwater, and marine habitat (Campbell *et al.*, 2006; Dangi *et al.*, 2020). They play an essential role in biological evolution and maintaining the balance of the biosphere. The versatility of the bacteria is reflected in the wide variety of the ecological functions and phenotypic of these individual species. Gram-negative bacteria can be found in different temperature zones in nature. Some of them

belong to psychrophiles, bacteria that live at low temperatures (below 5°C) such as *Janthinobacterium* spp. (Tan *et al.*, 2020), *Iodobacter* sp. (Atalah *et al.*, 2020), *Flavobacterium sandaracinum*, *F. caseinilyticum*, and *F. hiemivividum* (Chaudhary *et al.*, 2020); thermophiles, a group of bacteria living at more than 45°C, such as *Thermaurantimonas aggregans* (Iino *et al.*, 2020), *Vulcaniibacterium gelatinicum* (Niu *et al.*, 2020), *Elioraea thermophila* (Habib *et al.*, 2020), and *Tepidiforma bonchosmolovskayae* (Kochetkova *et al.*, 2020). The rest of the bacteria that live under reasonable conditions from 5 to 45°C belong to mesophiles.

In nature, gram-negative bacteria are living together with other colonies or other organisms. They can live together in commensalism (Rhee *et al.*, 2000), mutualism (Koropatnick *et al.*, 2004), or even parasitism (Raidal *et al.*, 1998). In order to adapt to the environment, gram-negative bacteria produce a series of specialized metabolites with various biological functions to support their life. This metabolite could be a simple form to a massive one with a complicated architecture. They also maintain the rhizosphere by producing some degrading enzymes, for example, keratinase (Bach *et al.*, 2011), atrazine de-gradating molecules (Rousseaux *et al.*, 2001), and cellulose (Ueki *et al.*, 2007). In the marine ecosystem, they adapt to stress environment by generating membrane lipid with specific compositions such as in *Vibrio marinus*, which contains large amounts of long-chain polyunsaturated fatty acids (DeLong and Yayanos, 1986) and long-chain saturated ranging from C14:0, C16:0, and C18:0 lipid species in *Prochlorococcus* (Biller *et al.*, 2014).

#### **1.4. Underexplored of gram-negative proteobacteria: morphological characteristics, taxonomy, ecological niche, and their natural products.**

As mentioned above, the genome of gram-negative bacteria varies from 0.4 to > 6 Mb, with 25 to 80% of GC content (Masschelein *et al.*, 2017). It is smaller than Actinobacteria (Ventura *et al.*, 2007). Proteobacteria constitute a significant phylum of gram-negative cells, including the fore-mentioned pathogenic cells, i.e., *E. coli*, *Salmonella*, *Shigella*, *Pseudomonas*, *Klebsiella*, *Acinetobacter*, *Burkholderia*, and other *Enterobacteria*. They have been studied well in terms of pathogenicity to humans, animals, and even plants. Based on genome analyses from prokaryotic cells, as shown in **Figure 1-5**, it could be

deduced that gram-negative Proteobacteria also contain numerous gene cluster families. This evidence could provide a qualitative standpoint on bacterial secondary metabolite biosynthesis machinery. Their cluster families are also comparable to gram-positive *Actinobacteria*, a well-known historical group for antibiotic producers. Therefore, it means that they have a hidden potential to generate new chemistry. However, the majority of their secondary metabolites remain un-touched, un-isolated, and un-characterized except for *Pseudomonas* (Gross and Loper, 2009), *Burkholderia* (Kunakom and Eustáquio, 2019) and *Myxobacteria* (Schäberle *et al.*, 2014). Therefore, along with their shreds of evidence, we consider them as underexplored bacteria. There are many underexplored bacteria, among them, e.g., the genera *Massilia*, *Telluria*, and *Janthinobacterium*.

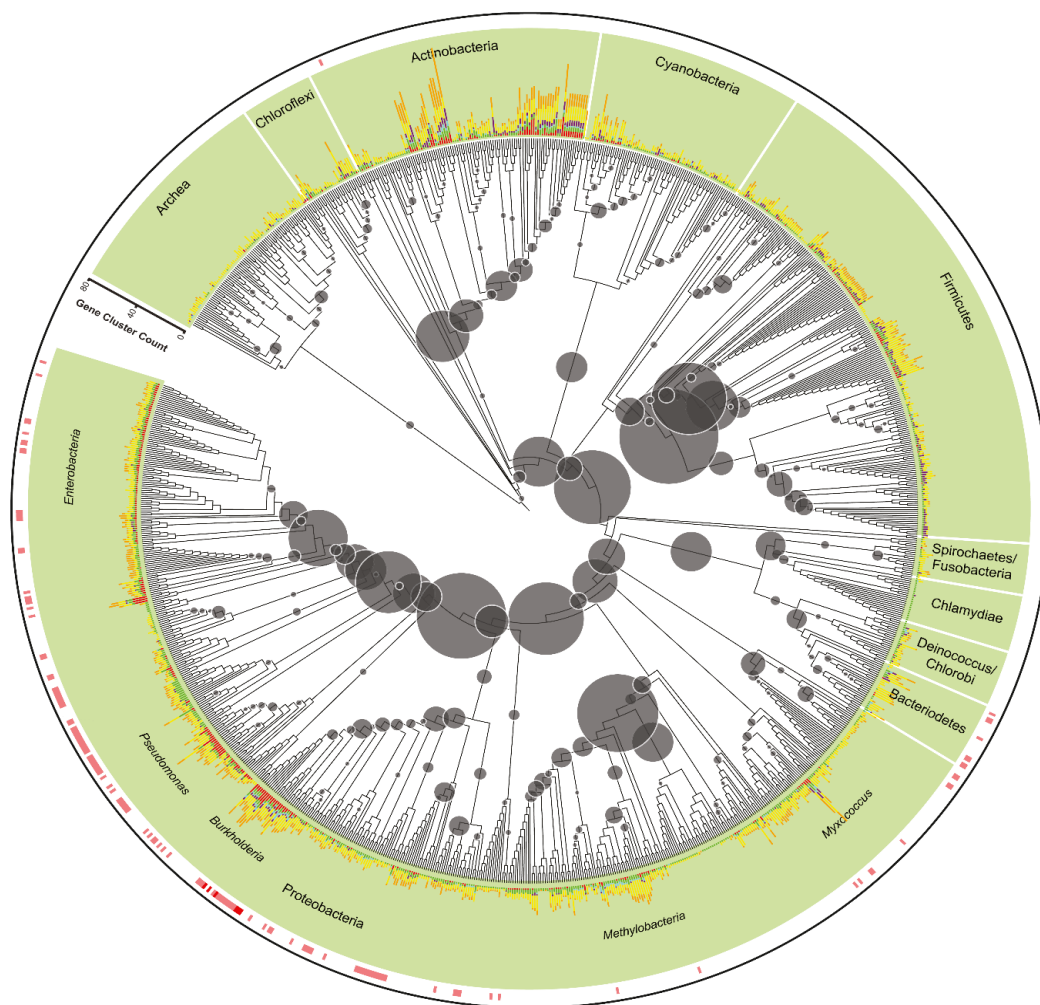


**Figure 1-5.** Distribution of BGCs (Cimermanic *et al.*, 2014).

### 1.4.1. The genus *Massilia*

The name of *Massilia* (*Mas.sil' i.a*) derives from the Latin name of Marseille, France. *Massilia* is one of a non-fermentative aerobic gram-negative class of  $\beta$ -Proteobacteria. Bacteria of this genus are non-spore-forming, rod-shaped and flagellated with a slow-growing characteristic (La Scola *et al.*, 1998; Kampfner *et al.*, 2000; Lindquist *et al.*, 2003). The genus *Massilia* was revealed for the first time in 1998 as *Massilia timonae* (CIP 105350) and has been isolated from an immune-compromised patient with a cerebellar lesion (La Scola *et al.*, 1998). Two years after its discovery, the 16S rRNA sequence has been used as a reference and led to the identification of the second isolate of *M. timonae*, this time from a wound infection of a 36-year-old man with orthopedic surgical treatment in New South Wales, Australia (Sintchenko *et al.*, 2000). Other types of *M. timonae* like bacteria were found in the US (strain 85A2206). One was isolated from the femur of a 29-year-old male with a benign bone tumor. Three more strains including 96A14209 were isolated from the cerebrospinal fluid of 49-year-old female with cerebral pseudo-tumor, 97A4424 isolated from the blood of 41-year-old with renal disease, diabetic nephropathy and hypertension (Sintchenko *et al.*, 2000), and 99A9205 isolated from the blood of a 39-year-old female with massive swelling on the thigh (Lindquist *et al.*, 2003). The genus of *Massilia* seems pervasive in environmental samples. In the following years, the report of cultivable *Massilia* from other environmental samples has become more frequent, including soil, rock, air, freshwater, ice core, eye, and blood, as presented in **Table 1-2**. Uncultured *Massilia* spp. were also found in the dust (Pakarinen *et al.*, 2008), air (Fahlgren *et al.*, 2011), aerosol (Blatny *et al.*, 2011), soil (Ferrari *et al.*, 2005; Nagy *et al.*, 2005), and leaves (Zhou *et al.*, 2010).

In a pathogenic context, *M. timonae* is known to cause infections to humans, triggering lymphadenopathy, corneal abscesses, and wound infection (Sintchenko *et al.*, 2000; Van Craenenbroeck *et al.*, 2011). The genus *Massilia* is considered underexplored in terms of natural product discovery. So far, merely the discovery of dimethyl disulfide, violacein, N-acetyl-homoserine lactone, and a siderophore called massiliachelin has been reported (D'Angelo-Picard *et al.*, 2005; Agematu *et al.*, 2011; Feng *et al.*, 2016; Diettrich *et al.*, 2019).

**Table 1-2.** Members of the genus *Massilia*.

<b>Species</b>	<b>Origin</b>	<b>Country</b>
<i>M. albidiflava</i> DSM 17472 <sup>T</sup>	Soil	China
<i>M. dura</i> DSM 17513 <sup>T</sup>	Soil	China
<i>M. lutea</i> DSM 17473 <sup>T</sup>	Soil	China
<i>M. plicata</i> DSM 17505 <sup>T</sup>	Soil	China
<i>M. flava</i> DSM 26639 <sup>T</sup>	Soil	China
<i>M. umbonata</i> DSM 26121 <sup>T</sup>	Soil	Spain
<i>M. niastensis</i> DSM 21313 <sup>T</sup>	Air	South Korea
<i>M. niabensis</i> DSM 21312 <sup>T</sup>	Air	South Korea
<i>M. solisilvae</i> JCM 31607 <sup>T</sup>	Soil	South Korea
<i>M. terrae</i> JCM 31606 <sup>T</sup>	Soil	South Korea
<i>M. agilis</i> JCM 31605 <sup>T</sup>	Soil	South Korea
<i>M. lurida</i> KCTC 23880 <sup>T</sup>	Soil	China
<i>M. arvi</i> KCTC 42609 <sup>T</sup>	Soil	South Korea
<i>M. tieshanensis</i> KACC 14940 <sup>T</sup>	Soil	China
<i>M. armeniaca</i> DSM 104676 <sup>T</sup>	Soil	China
<i>M. neuiana</i> BCRC 81061 <sup>T</sup>	Soil	China
<i>M. violacea</i> LMG 28941 <sup>T</sup>	Soil	Mexico
<i>M. pinisoli</i> JCM 31316 <sup>T</sup>	Soil	South Korea
<i>M. aurea</i> DSM 18055 <sup>T</sup>	Freshwater	Spain
<i>M. namucuoensis</i> DSM 25159 <sup>T</sup>	Soil	China
<i>M. yuzhufengensis</i> KACC 16569 <sup>T</sup>	Ice core	China
<i>M. aerilata</i> DSM 19289 <sup>T</sup>	Air	South Korea
<i>M. glaciei</i> JCM 30271 <sup>T</sup>	Ice core	China
<i>M. agri</i> JCM 31661 <sup>T</sup>	Soil	Nepal
<i>M. psychrophile</i> JCM 30813 <sup>T</sup>	Ice core	China
<i>M. buxea</i> DSM 103547 <sup>T</sup>	Rock	China

<i>M. norwichensis</i> LMG 28164 <sup>T</sup>	Air	United Kingdom
<i>M. oculi</i> CCUG 43427A <sup>T</sup>	Eye	Sweden
<i>M. atriviolacea</i> LMG 30840 <sup>T</sup>	Soil	China
<i>M. eurypsychrophila</i> JCM 30074 <sup>T</sup>	Ice core	China
<i>M. violaceinigra</i> DSM 19531 <sup>T</sup>	Ice core	China
<i>M. putida</i> DSM 27523 <sup>T</sup>	Soil	China
<i>M. jejuensis</i> DSM 21311 <sup>T</sup>	Air	South Korea
<i>M. phosphatilytica</i> LMG 29956 <sup>T</sup>	Soil	China
<i>M. umbonata</i> DSM 26121 <sup>T</sup>	Soil	Spain
<i>M. brevitalea</i> DSM 18925 <sup>T</sup>	Soil	Germany
<i>M. consociata</i> CCM 7792 <sup>T</sup>	Blood	Sweden
<i>M. timonae</i> DSM 16850 <sup>T</sup>	Blood	France
<i>M. chloroacetimidivorans</i> KACC 18674 <sup>T</sup>	Soil	South Korea
<i>M. varians</i> DSM 21873 <sup>T</sup>	Eye	Norway
<i>M. haematophila</i> DSM 21946 <sup>T</sup>	Blood	Sweden
<i>M. suwonensis</i> DSM 21311 <sup>T</sup>	Air	South Korea
<i>M. alkalitolerans</i> DSM 1746 <sup>T</sup>	Soil	China
<i>M. kyonggiensis</i> KACC 17471 <sup>T</sup>	Soil	South Korea
<i>M. guangdongensis</i> KACC 21312 <sup>T</sup>	Stream water	China
<i>M. humi</i> KCTC 42737 <sup>T</sup>	Soil	South Korea
<i>M. arenosa</i> LMG 31737 <sup>T</sup>	Soil	USA
<i>M. arenae</i> JCM 32744 <sup>T</sup>	Soil	China

---

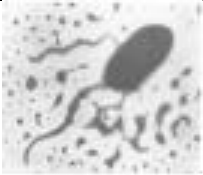

\* based on International Journal of Systematic and Evolutionary Microbiology and Antonie van Leeuwenhoek Journal.

#### 1.4.2. The genus *Telluria*

The name of *Telluria* (*Tel.lu.ri.a*) originated from the Roman goodness of the earth Tellus, also the ground or earth. *Telluria* spp. are aerobic gram-negative and belong to the class of  $\beta$ -Proteobacteria. They are filamentous rod-shaped cells, up to 30  $\mu$ m in size, mixed flagellar, motile, show a complex polysaccharide-dependent growth, are intolerant

towards the presence of NaCl more than 1.5%, and show optimal growth at 30-35°C (Sly and Fegan, 2005; 2015). Up to recent, only two species belonging to this genus have been yet discovered, which are *Telluria mixta* and *T. chitinolytica*, as presented in **Table 1-3**. *Telluria* is commonly found in the rhizosphere soils (Bowman *et al.*, 1988; Bowman *et al.*, 1993; Ndour *et al.*, 2008). It has been reported as a biocontrol agent control the root-knot nematode *Meloidogyne javanica* (Chet *et al.*, 2004) and as a removal agent of 5-hydroxy-2-methyl furfural (HMF)-polluted soil (Bandounas *et al.*, 2009).

**Table 1-3.** Members of the genus *Telluria*.

Species	Electron micrograph	Origin	Country
<i>Telluria mixta</i> ACM 1762 <sup>T</sup>		Soil	Australia
<i>T. chitinolytica</i> ACM 3522 <sup>T</sup>		Soil	Israel

\* based on International Journal of Systematic and Evolutionary Microbiology.

#### 1.4.3. The genus *Janthinobacterium*

The name of *Janthinobacterium* (*Jan.thin.o.bac.te' ri.um*) as a small violet-colored rod was constructed from *janthinus* violet-colored and *bakterion* a small rod. A *Janthinobacterium* is an aerobic gram-negative bacterium belonging to the class of  $\beta$ -Proteobacteria. It is motile, shows an optimum growth at 25°C with pH 7-8, but no growth below pH 5, and is oxidase- and catalase-positive (Gillis and Logan, 2015). Nevertheless, in many cases, members of the genus of *Janthinobacterium* are misidentified as *Chromobacterium*, *Duganella*, *Alteromonas*, *Massilia*, and *Pseudoalteromonas*, which also yield violet pigments (Gauthier, 1982; Yang *et al.*, 2007; Kämpfer *et al.*, 2012; Aruldass *et al.*, 2015; Embarcadero-Jiménez *et al.*, 2016). However, the phenotypic features differentiating the genera *Janthinobacterium* and *Chromobacterium* have been reported by De Ley *et al.* (1978).



Up to recent, only six species belong to *Janthinobacterium* have been discovered, as presented in **Table 1-4**. *Janthinobacteria* is ubiquitous in environmental samples. Members have also been found in tropical peatland soils (Hashidoko *et al.*, 2008), glacier (Kim *et al.*, 2012), and the coastal sea (Shi *et al.*, 2008). *J. lividum*, a butter rod shape bacterium, has also been found in soil (Shivaji *et al.*, 1991; Schloss *et al.*, 2010) and in human blood (Patjanasontorn *et al.*, 1992). Recently, numerous *Janthinobacterium* species had been isolated from a cold area such as Antarctica and Alaska (Schloss *et al.*, 2010; Mojib *et al.*, 2011; Huang *et al.*, 2012; Martinez-Rosales *et al.*, 2015; Chiriac *et al.*, 2018).

In a pathogenic context, *J. lividum* is one of the foremost infections to humans, causing septicemia (Patjanasontorn *et al.*, 1992). It has been reported to cause fish *Oncorhynchus mykiss* infection in the United Kingdom (Austin *et al.*, 1992), and *J. agaricidamnosum* acts as a soft rot pathogen to *Agaricus bisporus* (Lincoln *et al.*, 1999). A member of *Janthinobacterium* also has been reported involved in the spoilage of pasteurized milk (Eneroth *et al.*, 2000) and carcass rabbit (Giaccone *et al.*, 2008).

In the pharmaceutical field, *J. lividum* could yield janthinocins A-C, cyclic decapeptide lactones, which are forceful against gram-positive bacteria, including *Staphylococcus aureus* infection in mice (Johnson *et al.*, 1990; O'Sullivan *et al.*, 1990). Its bacterium has also been reported as a violacein producer that is effective against *Escherichia coli*, *Chromobacterium violaceum*, *Pseudomonas fragi*, *P. pastorianus*, and *Bacillus subtilis* var. natto (Naito *et al.*, 1986). The purple violacein itself also possesses activity against phytopathogenic fungi such as the *Rosellinia necatrix* (Shirata *et al.*, 1997). Moreover, violacein exhibits antitumor activity (Masuelli *et al.*, 2016). Another colored compound called prodigiosin – a red form is produced by the psychotropic strain *J. lividum* (Schloss *et al.*, 2010)

The genus *Janthinobacterium* also have been reported to produce antifungal compounds, such as janthinopolynemycins A and B under co-culture conditions (Anjum *et al.*, 2018). Another antifungal compound called jagaricin -a lipopeptide molecule which also has been isolated from *J. agaricidamnosum* (Graupner *et al.*, 2012). The mode of action of its

compound has also been studied using two molds *Candida albicans* and *C. glabrata* and showed that it relies on a membrane disruption mechanism (Fischer *et al.*, 2019).

In nature, *Janthinobacterium* spp. also lives in a mutualism symbiosis to the host. *J. lividum* produces an antifungal against *Batrachochytrium dendrobatidis* in the skin of salamander *Plethodon cinereus* (Brucker *et al.*, 2008; Ackleh *et al.*, 2016) and green frog *Lithobates clamitans* (Rebollar *et al.*, 2016). One of the *Janthinobacterium* species produces alkaline  $\beta$ -propeller phytase with its insect symbiont *Batocera horsfieldi* (Zhang *et al.*, 2011).

**Table 1-4.** Members of the genus *Janthinobacterium*.

Species	Origin	Country
<i>Janthinobacterium lividum</i> DSM 1522 <sup>T</sup>	Butter	-
<i>J. agaricidamnosum</i> DSM 9628 <sup>T</sup>	<i>Agaricus bisporus</i>	United Kingdom
<i>J. violaceinigrum</i> KACC 21319 <sup>T</sup>	Stream water	China
<i>J. aquaticum</i> KACC 21468 <sup>T</sup>	Stream water	China
<i>J. rivuli</i> KACC 21469 <sup>T</sup>	Stream water	China
<i>J. svalbardensis</i> DSM 25734 <sup>T</sup>	Glacier ice	Arctic

\* based on International Journal of Systematic and Evolutionary Microbiology.

## Aims of the present study

As previously discussed, the value of investigating the natural products from underexplored gram-negative bacteria for application in various human-beneficial aspects is tremendous. This thesis shall be, therefore, mainly concerned with the isolation and structural characterization of new chemistry of natural products from gram-negatives, integrating the OSMAC approach coupled with MS analysis and genome mining approaches from underexplored gram-negatives of the genera *Massilia*, *Telluria*, and *Janthinobacterium*.

## Chapter 2. Materials and Methods

### 2.1. Chemicals and media components

To conduct studies, we used various chemicals and media components as follows:

All L-type of amino acid: alanine, arginine, asparagine, cysteine, glutamine glycine, histidine, isoleucine, leucine, lysine, methionine, phenylalanine proline, serine, threonine, tryptophan, tyrosine, valine (Aldrich Chemistry, Steinheim, Germany)

Acetylcholine chloride (Sigma-Aldrich Chemie GmbH, Steinheim, Germany)

Acetonitrile (Honeywell, Riedel-de Haen<sup>TM</sup>. Seelze, Germany)

Acetonitrile LCMS (Chemsolute<sup>®</sup>, Th. Geyer GmbH & Co. KG, Renningen, Germany)

Acetone (Aldrich Chemistry, Steinheim, Germany)

Acetone-*d*<sub>6</sub> for NMR spectroscopy (Aldrich Chemistry, Steinheim, Germany)

Agar (Sigma-Aldrich Chemie GmbH, Steinheim, Germany)

Arbutin (Sigma-Aldrich Chemie GmbH, Steinheim, Germany)

Amberlite<sup>®</sup> XAD16N (Sigma-Aldrich Chemie GmbH, Steinheim, Germany)

Amberlite<sup>®</sup> XAD4 (Supelco-Sigma-Aldrich Chemie GmbH, Steinheim, Germany)

Amberlite<sup>®</sup> XAD<sup>®</sup>2 (Supelco-Sigma-Aldrich Chemie GmbH, Steinheim, Germany)

Ammonium acetate (AppliChem, Darmstadt, Germany)

Ammonium chloride (AppliChem, Darmstadt, Germany)

Ammonium iron (II) sulfate hexahydrate (Sigma-Aldrich Chemie GmbH, Steinheim, Germany)

Ammonium molybdate tetrahydrate (Sigma-Aldrich Chemie GmbH, Steinheim, Germany)

Butan-1-ol, ≥ 99.5% (Fischer Chemical, Loughborough, UK)

Bromobenzoic acid (-3) (Sigma-Aldrich Chemie GmbH, Steinheim, Germany)

Bacto™ Peptone (BD, Maryland, USA)

Bacto™ Proteose Peptone (BD, Maryland, USA)

Bacto™ Yeast Extract (BD, Maryland, USA)

Bacto™ Tryptic Soy Broth (BD, Maryland, USA)

Bacto™ Triptone (BD, Maryland, USA)

Boric acid (Merck KGaA, Damstadt, Germany)

Casamino acids (MP, Ohio, USA)

Calcium carbonate (Roth, Karlsruhe, Germany)

Calcium chloride (Roth, Karlsruhe, Germany)

Cobalt (II) Nitrate Hexahydrate (Fluka™, Germany)

Cobalt (II) Chloride Hexahydrate (Fluka™, Germany)

Chromazurol S (Merck KGaA, Damstadt, Germany)

Chloroform (WWR Chemicals, France)

Chloroform-*d* for NMR spectroscopy (Aldrich Chemistry, Steinheim, Germany)

Chlorobenzoic acid (-3) (Sigma-Aldrich Chemie GmbH, Steinheim, Germany)

Copper sulfate pentahydrate (AppliChem, Damstadt, Germany)

Cotton Seed Flour (Pharmamedia®)

Davis minimal broth without dextrose (Sigma-Aldrich Chemie GmbH, Steinheim, Germany)

Deuterium chloride solution (Aldrich Chemistry, Stenheim, Germany)

Diaion® HP-20 (Supelco-Sigma-Aldrich Chemie GmbH, Steinheim, Germany)

Dichlormethane (Chemsolute<sup>®</sup>, Th. Geyer GmbH & Co. KG, Renningen, Germany)

Dimethyl sulfoxide (Merck KGaA, Darmstadt, Germany)

N, N-Dimethylformamide-*d*<sub>7</sub> for NMR spectroscopy (Aldrich Chemistry, Steinheim, Germany)

Dimethylsulfoxide-*d*<sub>6</sub> for NMR spectroscopy (Aldrich Chemistry, Steinheim, Germany)

Dimethylsulfoxide for analysis (Merck KGaA, Darmstadt, Germany)

Difco<sup>™</sup> Soluble starch (BD, Maryland, USA)

D-proline (Sigma-Aldrich Chemie GmbH, Steinheim, Germany)

D-valine (Sigma-Aldrich Chemie GmbH, Steinheim, Germany)

D-tyrosine (Sigma-Aldrich Chemie GmbH, Steinheim, Germany)

Ethylendiaminetetra acetic acid (Sigma-Aldrich Chemie GmbH, Steinheim, Germany)

Ethylacetate

Formic acid (Sigma-Aldrich Chemie GmbH, Steinheim, Germany)

Fructose (Sigma-Aldrich Chemie GmbH, Steinheim, Germany)

HEPES (Roth, Karlsruhe, Germany)

Hydrochloric acid (Sigma-Aldrich Chemie GmbH, Steinheim, Germany)

n-Hexane (Chemsolute<sup>®</sup>, Th. Geyer GmbH & Co. KG, Renningen, Germany)

n-Hexane (Honeywell, Riedel-de Haen<sup>™</sup>, Seelze, Germany)

Glycerol (Chemsolute<sup>®</sup>, Th. Geyer GmbH & Co. KG, Renningen, Germany)

D-Glucose (Sigma-Aldrich Chemie GmbH, Steinheim, Germany)

(s)-(+)-Ibuprofen (Sigma-Aldrich Chemie GmbH, Steinheim, Germany)

Iron (II) sulfate heptahydrate (Sigma-Aldrich Chemie GmbH, Steinheim, Germany)

Iron (III) chloride hexahydrate (Sigma-Aldrich Chemie GmbH, Steinheim, Germany)

Kojic acid (Sigma-Aldrich Chemie GmbH, Steinheim, Germany)

Manganese (II) chloride tetrahydrate (Roth, Karlsruhe, Germany)

Magnesium sulfate heptahydrate (Sigma-Aldrich Chemie GmbH, Steinheim, Germany)

Magnesium chloride hexahydrate (Sigma-Aldrich Chemie GmbH, Steinheim, Germany)

Manitol (-L) (Sigma-Aldrich Chemie GmbH, Steinheim, Germany)

Meat extract (Sigma-Aldrich Chemie GmbH, Steinheim, Germany)

Methanol for HPLC, gradient grade,  $\geq 99.5\%$  (Sigma-Aldrich Chemie GmbH, Steinheim, Germany)

Marfey's reagent FDAA (Thermo scientific, Illinois, USA)

Methanol for LC-MS (Chemsolute<sup>®</sup>, Th. Geyer GmbH & Co. KG, Renningen, Germany)

Methanol- $d_3$  for NMR spectroscopy (Merck KGaA, Darmstadt, Germany)

Methanol- $d_4$  for NMR spectroscopy (Aldrich Chemistry, Steinheim, Germany)

Nutrient broth CM0001 (Oxoid Ltd., Hants, UK)

N-Z-case<sup>®</sup> (Fluka, Sigma-Aldrich Chemie GmbH, Steinheim, Germany)

Polygoprep<sup>®</sup> 60-50 C<sub>18</sub> (Macherey-Nagel GmbH & Co. KG, Düren, Germany)

Probenecid (Sigma-Aldrich Chemie GmbH, Steinheim, Germany)

2-Propanol, 99.9% (Sigma-Aldrich Chemie GmbH, Steinheim, Germany)

n-Propanol for LC-MS (Chemsolute<sup>®</sup>, Th. Geyer GmbH & Co. KG, Renningen, Germany)

Potassium phosphate monobasic (Sigma-Aldrich Chemie GmbH, Steinheim, Germany)

Potassium phosphate dibasic (Sigma-Aldrich Chemie GmbH, Steinheim, Germany)

Potassium sulfat (Roth, Karlsruhe, Germany)

Pyridine-*d*<sub>5</sub> for NMR spectroscopy (Aldrich Chemistry, Steinheim, Germany)

Sephadex™ LH-20 (GE Healthcare Bio-Sciences AB, Uppsala, Sweden)

Silica gel 60 H (Merck KGaA, Darmstadt, Germany)

Silica gel high purity grade (Sigma-Aldrich Chemie GmbH, Steinheim, Germany)

Sodium molybdate dihydrate (Roth, Karlsruhe, Germany)

Sodium bicarbonate (Sigma-Aldrich Chemie GmbH, Steinheim, Germany)

Sodium chloride (Sigma-Aldrich Chemie GmbH, Steinheim, Germany)

Sodium pyruvate (Sigma-Aldrich Chemie GmbH, Steinheim, Germany)

Soybean flour type I (Sigma-Aldrich Chemie GmbH, Steinheim, Germany)

Starch (Roth, Karlsruhe, Germany)

Sucrose (Merck KGaA, Darmstadt, Germany)

Trifluoroacetic acid (Honeywell, Fluka, Seelze, Germany)

Zinc Sulfate Heptahydrate (AppliChem, Darmstadt, Germany)

## 2.2. Columns

To isolate and purify the compounds produced by all bacteria used in this study, we used several columns, including:

Luna® Omega 5 μm PS C18 100 Å, 250 x 4.6 mm (Phenomenex®)

Luna® Omega 3 μm Polar C18 100 Å, 250 x 4.6 mm (Phenomenex®)

Luna® 5 μm C18(2) 100 Å, 250 x 10 mm (Phenomenex®)

Luna® 5 μm C18(2) 100 Å, 250 x 4.6 mm (Phenomenex®)

Luna® 3 μm C18(2) 100 Å, 250 x 4.6 mm (Phenomenex®)

Luna<sup>®</sup> 5u C5 100 Å, 250 x 4.6 mm (Phenomenex<sup>®</sup>)

Aeris<sup>™</sup> 3.6 µm PEPTIDE XB-C18 100 Å, 250 x 4.6 mm (Phenomenex<sup>®</sup>)

Kinetex<sup>®</sup> 5 µm EVO C18 100 Å, 250 x 4.6 mm (Phenomenex<sup>®</sup>)

Kinetex<sup>®</sup> 5 µm XB-C18 100 Å, 250 x 4.6 mm (Phenomenex<sup>®</sup>)

Kinetex<sup>®</sup> 5 µm PFP 100 Å, 250 x 4.6 mm (Phenomenex<sup>®</sup>)

Kinetex<sup>®</sup> 5 µm F5 Å, 250 x 4.6 mm (Phenomenex<sup>®</sup>)

### 2.3. Kits

To perform the tyrosinase inhibitor activity of the novel peptide, we used:

Tyrosinase Inhibitor Screening Kit-MAK257 (Sigma-Aldrich Chemie GmbH, Steinheim, Germany).

### 2.4. Media for bacterial cultivation

Bacterial culture media were used either with or without 1.5-2% agar before sterilization (w/v) as follows in **Table 2-1**. The medium was sterilized using autoclave for 15 min at 121°C or 2 bars (Systec, VX-150, Systex GmbH, Linden, Germany). If required, antibiotics and other heat-unstable substances were added after autoclaving using the sterilized filter, as showed in section **2.5. Antibiotic**. All media were prepared with distilled water (ddH<sub>2</sub>O) from the output of PURELAB flex (ELGA LabWater VWS Ltd., UK). The media were then stored at room temperature or 4°C.

**Table 2-1.** Media for pre- and main cultivation.

Cultivation Media	Constituent per L
Luria-Bertani (LB):	10 g tryptone, 5 g yeast extract, 10 g NaCl, final pH 7.5±2 at 25°C
Mueller-Hinton (MH)	21 g ready use Mueller-Hinton <sup>®</sup> , final pH 7.4±2 at 25°C
Nutrient broth (NB):	5 g peptone, 2 g yeast extract, and 5 g NaCl or 13 g ready use NB CM0001, final pH 7.4±2 at 25°C



King's B medium (KB):	20 g proteose peptone, 1.5 g K <sub>2</sub> HPO <sub>4</sub> , 1.5 g MgSO <sub>4</sub> , 15 g glycerol, 7.5±2 at 25°C
Massilia meat (MM):	2% soluble starch, 1% glucose, 0.2% meat extract, 0.2% yeast extract, 0.5% N-Z-case <sup>®</sup> , 0.2% CaCO <sub>3</sub> , final pH 7.4±2 at 25°C
Reasoner's 2 A (R2A):	0.5 g yeast extract, 0.5 g protease peptone, 0.5 g casamino acids, 0.5 g dextrose, 0.5 g soluble starch, 0.3 g sodium pyruvate, 0.3 g KH <sub>2</sub> PO <sub>4</sub> , 50 mg MgSO <sub>4</sub> ·7H <sub>2</sub> O, final pH 7.2±2 at 25°C
Davis minimal broth with glycerol (DMBGly):	10.6 g Davis minimal broth without dextrose, 1.83 mL 100% glycerol, pH adjustment is not necessary
Modified DMB I:	5.3 g Davis minimal broth without dextrose, 0.56 g HEPES buffer, 5.1 g sucrose, 1 mg methionine, 1 ml A5+co trace metal mix, final pH 6.6±2 at 25°C
Tryptic soy broth (TSB):	17 g tryptone, 3 g soybean flour, 2.5 g dextrose, 5 g NaCl, 2.5 g KH <sub>2</sub> PO <sub>4</sub> , final pH 7.3±2 at 25°C
Shipworm basal medium (SBM) without sea salt: (Han <i>et al.</i> , 2013)	15.3 mg KH <sub>2</sub> PO <sub>4</sub> , 10 mg Na <sub>2</sub> CO <sub>3</sub> , 2.5 mg Na <sub>2</sub> MoO <sub>4</sub> ·2H <sub>2</sub> O, 0.5 mg EDTA, 3 mg C <sub>6</sub> H <sub>8</sub> FeNO <sub>7</sub> , 5.2 g HEPES buffer, 1mL A5-co trace metal mix, pH adjustment is not necessary
Modified SBM:	15.3 mg KH <sub>2</sub> PO <sub>4</sub> , 10 mg Na <sub>2</sub> CO <sub>3</sub> , 2.5 mg Na <sub>2</sub> MoO <sub>4</sub> ·2H <sub>2</sub> O, 0.5 mg EDTA, 5.2 g HEPES buffer, 1mL A5+co trace metal mix, 0.267 g NH <sub>4</sub> Cl, 5 g sucrose, without sea salt, 5 mg L-methionine, final pH 7.2±2 at 25°C
MM9:	900 ml Solution C, 20 ml Solution A, 20 ml Solution B, 16.7 ml 100mM L-leucine, 5 ml 60mM L-histidine, 10 ml 100 mM L-lysine, 10 ml 40 mM L-tryptophane, 10

	ml 40 mM L-methionine, 20 ml 50% (w/v) glucose, 1 mL A5-co trace metal mix, pH adjustment is not necessary
SRM <sub>HG</sub> : (Jiao <i>et al.</i> , 2020)	4 g L-histidine, 1.6 mg FeCl <sub>3</sub> , 0.89 g KH <sub>2</sub> PO <sub>4</sub> , 0.8 g K <sub>2</sub> HPO <sub>4</sub> , 0.20 g, MgSO <sub>4</sub> ·7H <sub>2</sub> O, 10 g glucose, 1 g fructose, pH adjustment is not necessary
Modified SRM <sub>HG</sub> :	4 g L-histidine, 1.6 mg FeCl <sub>3</sub> , 0.89 g KH <sub>2</sub> PO <sub>4</sub> , 0.8 g K <sub>2</sub> HPO <sub>4</sub> , 0.20 g, MgSO <sub>4</sub> ·7 H <sub>2</sub> O, 10 g glucose, 1 g fructose, 3 mg ibuprofen, 5 g casamino acid, final pH 7.2±2 at 25°C
A5+Co trace metal mix:	2.86 g H <sub>3</sub> BO <sub>3</sub> , 1.81 g MnCl <sub>2</sub> ·4H <sub>2</sub> O, 0.222 g ZnSO <sub>4</sub> ·7H <sub>2</sub> O, 0.390 mg Na <sub>2</sub> MoO <sub>4</sub> ·2H <sub>2</sub> O, 79 mg CuSO <sub>4</sub> ·5H <sub>2</sub> O, 49 mg Co (NO <sub>3</sub> ) <sub>2</sub> ·6H <sub>2</sub> O, pH adjustment is not necessary
Solution A:	100 g KH <sub>2</sub> PO <sub>4</sub> , 350 g K <sub>2</sub> HPO <sub>4</sub> , pH adjustment is not necessary
Solution B:	50 g (NH <sub>4</sub> ) <sub>2</sub> SO <sub>4</sub> , 5 g MgSO <sub>4</sub> , pH adjustment is not necessary
Solution C:	2 g of each amino acid (L-arginine, L-alanine, L-asparagine, L-aspartate, L-cysteine, L-glutamine, L-glutamate, L-glycine, L-isoleucine, L-proline, L-serine, L-threonine, L-tyrosine, L-valine, and L-phenylalanine) or 30 g casamino acid, final pH 7.2±2 at 25°C

---

## 2.5. Antibiotics

Antibiotics, as mentioned below, were dissolved in an appropriate solvent (i.e., DMSO, ddH<sub>2</sub>O, and ethanol) and kept at -20°C. The aqueous solutions were bypassing through

sterilized a 22 µm filter. For antibiotic selection, the required antibiotics were added to the cooled media at room temperature at an appropriate concentration.

Tetracycline (Roth, Karlsruhe, Germany)

Kanamycin (Roth, Karlsruhe, Germany)

Trimethoprim (Sigma-Aldrich Chemie GmbH, Steinheim, Germany)

Neomycin (Sigma-Aldrich Chemie GmbH, Steinheim, Germany)

Gentamicin (Sigma-Aldrich Chemie GmbH, Steinheim, Germany)

Vancomycin (Roth, Karlsruhe, Germany)

## 2.6. Quorum sensing standards

Quorum sensing standards, as shown in **Table 2-2** and **Figure 2-1** have been used as fragmentation standards and to calculate the quantity of AHL production in *Massilia* and *Telluria*, as shown in **Chapter 5**.

**Table 2-2.** AHL standards

AHL	MW	Synonym	Manufacturer
C4-AHL	171	N-Butanoyl-L-homoserine lactone	Sigma-Aldrich Chemie GmbH, Steinheim, Germany
3-OH-C6-AHL	215	N-(3-Hydroxyhexanoyl)-L-homoserine lactone	University of Nottingham, UK
3-oxo-C6-AHL	213	N-(3-Oxohexanoyl)-L-homoserine lactone	University of Nottingham, UK
C6-AHL	199	N-Hexanoyl-L-homoserine lactone	Sigma-Aldrich Chemie GmbH, Steinheim, Germany
3-OH-C8-AHL	243	N-(3-Hydroxyoctanoyl)-L-homoserine lactone	Cayman Chemical, Michigan, USA

3-oxo-C8-AHL	241	N-(3-Oxooctanoyl)-L-homoserine lactone	Sigma-Aldrich Chemie GmbH, Steinheim, Germany
C8-AHL	227	N-Octanoyl-L-homoserine lactone	Cayman Chemical, Michigan, USA
C9-AHL	241	N-Nonanoyl-L-homoserine lactone	Santa Cruz Biotechnology, USA
3-OH-C10-AHL	271	N-3-hydroxydecanoyl-L-homoserine lactone	Cayman Chemical, Michigan, USA
3-oxo-C12-AHL	297	N-(3-Oxododecanoyl)-L-homoserine lactone	Sigma-Aldrich Chemie GmbH, Steinheim, Germany

---

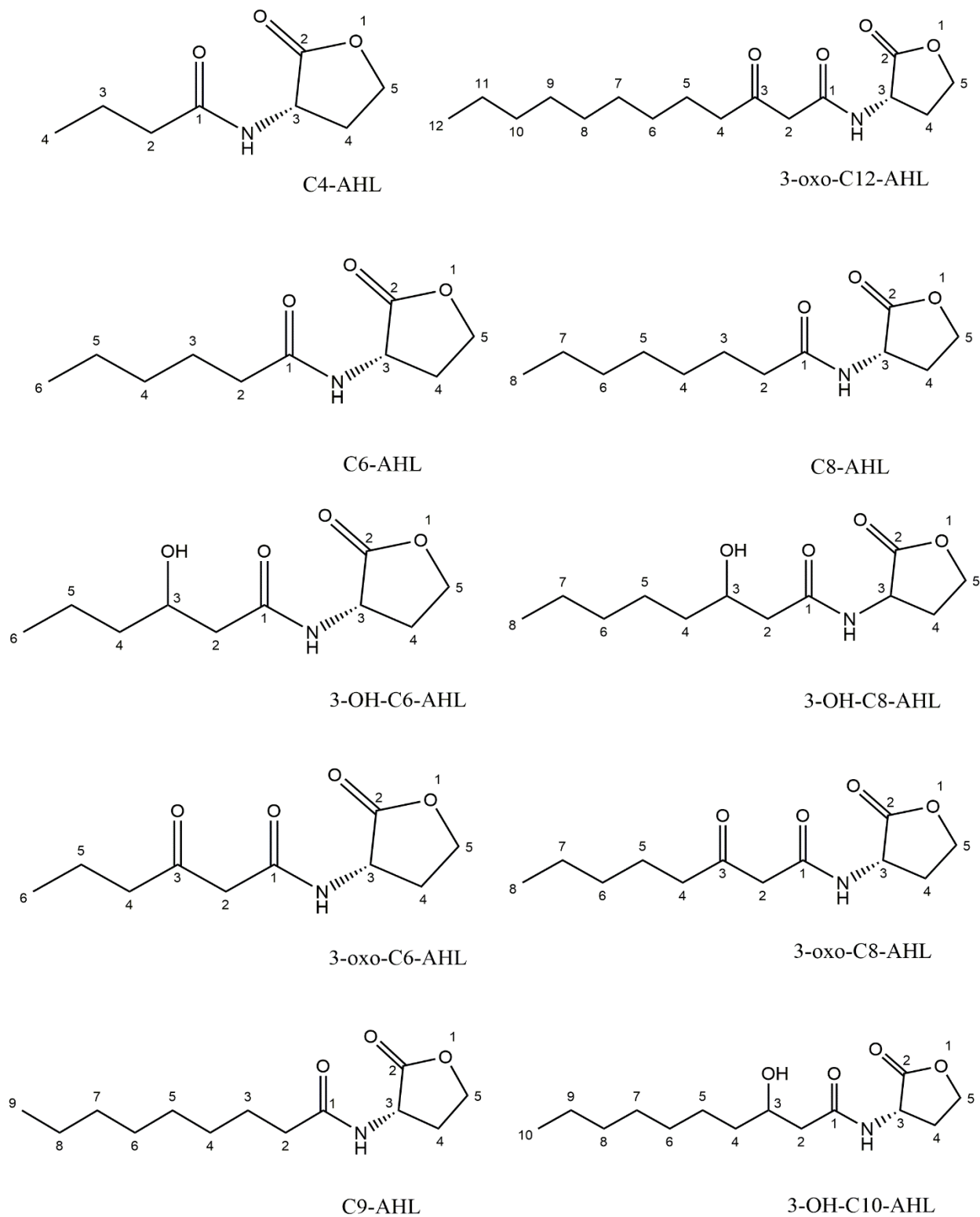


**Figure 2-1.** The structure of AHL standards.

## 2.7. Bacterial strains

To conduct studies, we used various genus from gram-negative bacteria as followed:

**Table 2-3.** Bacterial materials

Genus	Purpose study	Chapter
<b><i>Massilia</i></b>		
<i>Massilia albidiflava</i> DSM 17472 <sup>T</sup>	Discovery new natural products & QS study	3 & 5
<i>M. dura</i> DSM 17513 <sup>T</sup>	Discovery new natural products & QS study	3 & 5
<i>M. flava</i> DSM 26639 <sup>T</sup>	Discovery new natural products & QS study	3 & 5
<i>M. lutea</i> DSM 17473 <sup>T</sup>	Discovery new natural products & QS study	3 & 5
<i>M. plicata</i> DSM 17505 <sup>T</sup>	Discovery new natural products & QS study	3 & 5
<i>M. umbonata</i> DSM 26121 <sup>T</sup>	Discovery new natural products & QS study	3 & 5
<i>M. timonae</i> LMG 21530	Discovery new natural products & QS study	3 & 5
<i>M. haloabium</i> / <i>Empedobacter</i> ATCC 31962	Discovery new natural products & QS study	3 & 5
<b><i>Telluria</i></b>		
<i>Telluria chitinolytica</i> ACM 3522 <sup>T</sup>	Discovery new natural products & QS study	4 & 5
<i>T. mixta</i> DSM 29330 <sup>T</sup>	Discovery new natural products & QS study	4 & 5
<b><i>Janthinobacterium</i></b>		
<i>Janthinobacterium lividum</i> DSM 1522	Discovery new natural products	6
<i>J. agaricidamnosum</i> DSM 9628	Discovery new natural products	6
<b><i>Burkholderia</i></b>		
<i>Burkholderia glumae</i> ICMP 3729	Discovery new natural products	5

***Pseudomonas***

*P. aeruginosa* TUEPA7472      Swarming motility study      5

***Other bacteria that do not include in this thesis***

*E. coli* with BL21 pMev Duet vector empty      Research collaboration with Dr. Olaf Tyc, - Netherlands Institute of Ecology (NIOO-KNAW), Netherland

*E. coli* with BL21 pMev Duet SqhC gene

*E. coli* with BL21 pMev Duet YtpB gene

*E. coli* with BL21 pMev Duet with SqhC + HepS\_HepTYtpB gene

*Paenibacillus* sp. AD64

---

**2.8. Instrumentation****2.8.1. Mass spectroscopy**

HR-ESI-TOF-MS was carried out using Bruker Daltonik maXis 4G, which acquired at the Department of Organic Chemistry, University of Tübingen, Germany. The data (including MS<sup>1</sup> and MS<sup>2</sup>) were then analyzed using Bruker Compass DataAnalysis 4.4 SR1(x64).

Low-resolution MS was analyses using the 1100 Series HPLC system (Agilent Technologies, Waldbronn, Germany). The Agilent HPLC components (G1322A degasser, G1312A binary pump, G1329A autosampler, G1315A diode array detector) were connected to ABSCIEX 3200 Q TRAP LC/MS/MS mass spectrometer (AB Sciex, Germany GmbH, Darmstadt, Germany). The data (including MS<sup>1</sup> and MS<sup>2</sup>) were then analyzed using Analyst<sup>®</sup> 1.6.3.

### 2.8.2. Reverse-phase VLC system

VLC system has been set up using sintered glass filters contained Polygoprep<sup>®</sup> 60-50 C<sub>18</sub>, vacuum connection, adapter, round-bottom flask, and dry vacuum pump system (Welch<sup>®</sup>, Thomas Industries Inc., Illinois, USA) as shown in **Figure 2-2**. This system was used to fractionate crude extract on a solid phase to minimize the matrix by applying a stepwise gradient with elevating eluting power. The crude extract was dissolved in the first-time eluent mixture MeOH: dH<sub>2</sub>O 10/90 (v/v) and allowed to soak the column bed up to 100 % MeOH and followed by final dichloromethane elution. All fractions were then evaporated in *vacuo* using a rotary evaporator (Heidolph, Schwabach, Germany).

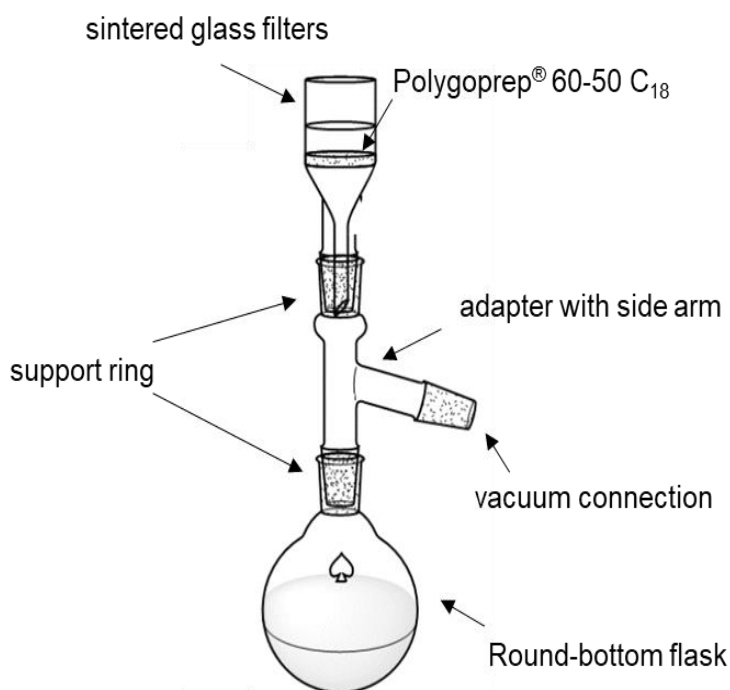


**Figure 2-2:** Equipment set-up for the VLC system.

### 2.8.3. SEC system

SEC or gel filtration system has been set up using the Sephadex<sup>®</sup> LH-20 column (length 50 cm, diameter 3 cm) under atmospheric pressure, as shown in **Figure 2-3**. SEC sort out the molecules by differences in size as they pass through a bead packed in a column. The crude extract was dissolved in the first-time eluent mixture MeOH: dH<sub>2</sub>O 0/100 (v/v) or higher contain water to 100 % MeOH. Molecules more massive than the pores are not capable of drawn-out into the beads, so they elute first.



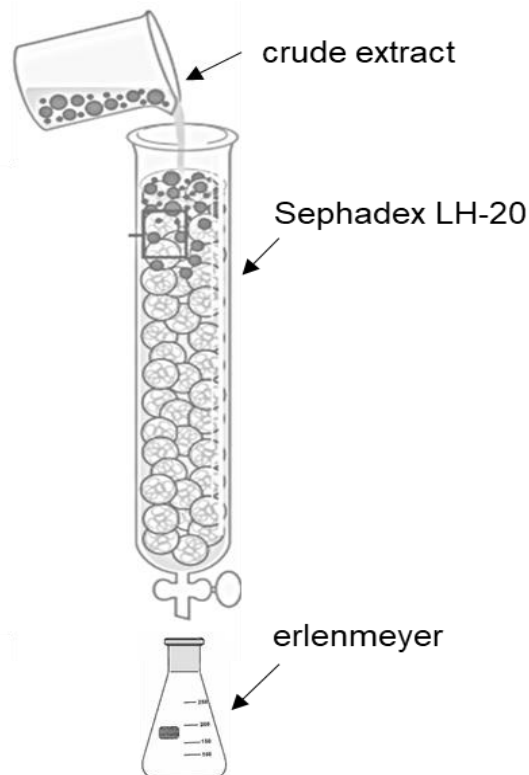


**Figure 2-3.** Equipment set-up for SEC system.

#### 2.8.4. HPLC system

Three HPLC systems as shown below were used to fractionate, isolate, and purify the compound of interest

HPLC system 1	Merck-Hitachi L-7420 LaChrom UV-Vis Detector (Merck-Hitachi), L-6200A Intelligent Pump (Merck-Hitachi), Interface Box (Knauer), Millenium 3.2 software
HPLC system 2	Waters 1525 Photodiode Array Detector, Water 996 Pump, degasser (Kromega), Millenium 3.2 software, Windows XP system
HPLC system 3	Waters 2996 Photodiode Array Detector, Water 1525 Pump and Degasser, Millenium 3.2 software, Windows XP system

### 2.8.5. NMR spectroscopy

1D- and 2D NMR spectra were measured on a Bruker Avance III HD 400 (BRUKER DALTONIK GmbH, Bremen, Germany) using 5 mm and 1 mm SMART probe head. The spectra were recorded at 293 K using NMR solvent quality, as shown in **Table 2-4**. The spectra were then collected and referenced to the residual solvent signal as follows. Spectra of pure compounds were processed using TopSpin 3.5 pl2 and MestReNova v14.0. The planar structural assignment was based on spectra from one or more of following NMR experiment:  $^1\text{H}$ - $^1\text{H}$ ,  $^1\text{H}$ - $^{13}\text{C}$ , DEPT-135, DEPT-90,  $^1\text{H}$ - $^1\text{H}$  COSY,  $^1\text{H}$ - $^1\text{H}$  NOESY,  $^1\text{H}$ - $^{13}\text{C}$  edited HSQC,  $^1\text{H}$ - $^{13}\text{C}$  HMBC, un-calibrated  $^1\text{H}$ - $^{15}\text{N}$  HSQC, un-calibrated  $^1\text{H}$ - $^{15}\text{N}$  HMBC, and broadband selective HMBC.

**Table 2-5.** NMR solvent references.

NMR solvent	Residual hydrogenated solvent signal references (ppm)	
	$\delta\text{H}$	$\delta\text{C}$
DMSO- <i>d</i> 6	2.5	39.51
DMF- <i>d</i> 7	2.75/2.92/8.03	29.76/34.89/163.15
MeOH- <i>d</i> 4	3.31	49.0
MeOH- <i>d</i> 3	3.31	49.0
pyridine- <i>d</i> 5	7.22/7.58/9.74	123.87/135.91/150.35
chloroform- <i>d</i>	7.24	77.23

### 2.8.6. UV spectroscopy

UV spectra were recorded on a Perkin-Elmer Lambda 25 UV/VIS spectrometer in 1.0 cm quartz cell. Compounds were diluted in methanol or DMSO. Dilutions were measured with UV-scan mode from 600 to 200 nm. The molar absorption coefficient  $\epsilon$  was calculated according to the Lambert-Beer-Law

$$\epsilon = \frac{A}{c \times d} \dots\dots\dots (\text{L}\cdot\text{mol}^{-1}\cdot\text{cm}^{-1})$$

Where A = absorption at peak maximum (non-dimensional), c = concentration ion mol/L, and D = layer thickness of solution in cm.

### 2.8.7. IR spectroscopy

Infrared spectra were analyzed by employing a Jasco FT/IR 4200 spectrometer, interfaced with a MIRacle ATR device (ZnSe crystal). The resulting data were reported and analyzed using Spectra Manager software packages V2.0 software.

### 2.8.8. Optical rotation

Optical rotation values were measured using a Jasco P-2000 polarimeter series in a 3.5 mm x 10 mm cylindrical quartz cell. The specific optical rotation  $[\alpha]_D^T$  was calculated according to:

$$[\alpha]_D^T = \frac{\alpha}{c \times l} \times 10^4$$

Where T = temperature in degree Celsius,  $\alpha$  = rotation angle in degree, D = sodium D line ( $\lambda=589$  nm), c= concentration in g/100 mL, l = cell length in mm. The rotation angles  $\alpha$  were determined as a mean value based on at least ten individual measurements.

### 2.8.9. Bioinformatic analysis

To facilitate genome mining of whole-genome sequence as part of finding new chemistry that possibly produces by bacteria. We applied several tools, as previously mentioned in **Table 1-1**, including antiSMASH v5.0 and manual annotation using a rapid prokaryotic genome annotation system (Prokka). Proportion identities and coverages between homologous genes were gained through the NCBI GenBank Blastp search algorithm. The resistant gene has been analyzed using Antibiotic-Resistant Target Seeker (ARTS).

Multiple alignments of genomic loci to facilitate phylogenetic tree analysis was performed using Mauve and MEGA version 10.1.8 (x64). We also used Easyfig 2.2.2 based python to create a linear comparison figure of multiple genomic loci. In the circular presentation, we employed BRIG 0.95 software coupled with Java 1.6. A local reference genome has been done using local BLASTn from the NCBI Blast+ 2.8.1.

### **2.8.10. MS-Networking**

We employed the public resource GNPS and Cytoscape v3.8.0 for 64 bit, to establish molecular networking from HR-ESI-MS data. The raw chromatogram data were converted to mzXML via ProteoWizard. Alternatively, we used Metabo<sup>®</sup>Scape 3.0 service release 1. The data were then compressed with FileZilla and uploaded to GNPS and Cytoscape for further analysis.

## **2.9. Cultural Conditions**

### **2.9.1. Cryo-culture preparation**

Each bacterial culture in this thesis was prepared in cryo by mixing 500 µl of a bacterial pellet containing growth media (LB) with 500 µl sterile glycerol with a concentration of 50% (v/v). The cryo culture was then kept at -86°C in Thermo Scientific<sup>™</sup> Forma<sup>™</sup> 900 Series (Ohio, USA).

### **2.9.2. Pre-culture preparation**

A defrosted cryo stock of bacterial strain was used for pre-culture cultivation by inoculating them into the LB agar plate and incubated at 30°C for 48 h and followed by inoculation into 6 ml of rich media (i.e., LB) in 15 mL sterile tube (Sarstedt). The pre-culture was then incubated for 24 h in a VWR orbital shaker model 3500 at 30°C, 250 rpm. The seed culture was then prepared by dilution to an OD<sub>600</sub> nm of 0.06 into a new 15 mL sterile tube.

### **2.9.3. Bacterial growth measurement**

A bacterial curve was measured based on OD<sub>600</sub> using Eppendorf BioPhotometer<sup>®</sup> D30, pH from broth culture was measured using Mettler Toledo FE20-ATC Kit FiveEasy<sup>™</sup> Benchtop pH Meter.

### **2.9.4. Large scale fermentation**

The pre-culture was then used for conduction of a more extensive fermentation in order to acquire enough sought compound.

For the discovery of massiliamide, seed culture ( $OD_{600}$  nm of 0.06) of *Massilia albidiflava* were prepared into fifteen of 15 mL sterile tube containing 6 mL LB and re-incubated for 24 h, at 30°C, 250 rpm. Each 6 mL 24-h seed culture was then inoculated to fifteen 5 L Erlenmeyer containing 2 L of Modified DMB I, equaling a sum of 30 L. Culture was then incubated for 48 h at 30°C, 140 rpm in a Multitron Pro orbital incubator shaker (INFORS HT, Bottmingen, Switzerland).

For the discovery of serratiochelin C, seed culture ( $OD_{600}$  nm of 0.06) of *Telluria chitinolytica* were prepared into fifteen of 15 mL sterile conical tube containing 6 mL LB and re-incubated for 48 h, at 30°C, 250 rpm. Each 2 mL 48-h seed culture was then inoculated to twenty 5 L Erlenmeyer containing 2 L of SBM without sea salt, equaling a sum of 40 L. Culture was then incubated for 48 h at 30°C, 160 rpm in a Multitron Pro orbital incubator shaker (INFORS HT, Bottmingen, Switzerland).

## 2.10. Extraction, fractionation, and isolation of novel compounds

For the discovery of massiliamide, a total of 30 L fermentation broth from *M. albidiflava* was centrifuged using Thermo Scientific Heraeus Multifuge 4 KR in each 1 L centrifugal tube to separate the supernatant and cell pellet. The condition was set up for 30 min at 10°C, 4400 rpm. The remained supernatant was then extracted using resin called Diaion<sup>®</sup> HP 20. In detail, about 30 g/L was employed in the Erlenmeyer containing supernatant, followed by shaking in in a Multitron Pro orbital incubator shaker (INFORS HT, Bottmingen, Switzerland) for four days, 5°C, 120 rpm. The resin was then filtered from the supernatant and washed twice with deionized water, and directly fractionated using VLC system to give five fractions (A-E). Fraction (MeOH: H<sub>2</sub>O) A, B, C, D, and E is 10:90, 25:75, 50:50, 75:25, 100 MeOH, respectively. The fraction C (76.34 mg) containing massiliamide were then subjected to RP-HPLC using a linear gradient from 10:90 to ACN: H<sub>2</sub>O containing 0.1% TFA over 19 min, followed by isocratic stage at 100 ACN for an additional 6 min using Luna<sup>®</sup> Omega 3  $\mu$ m Polar C18 100 Å, 250 x 4.6 mm (Phenomenex<sup>®</sup>), 0.8 mL/min flow rate, UV monitoring 254 and 280 nm. The purification of massiliamide has been done using a linear gradient from 10:80 to 100 ACN: H<sub>2</sub>O containing 0.1% TFA for 8 min, followed by isocratic stage at 100 ACN for additional 8 min using Luna<sup>®</sup> 5u C5 100 Å, 250 x 4.6 mm (Phenomenex<sup>®</sup>), with 0.5

mL/min flow rate, UV monitoring 254 and 280 nm.

For the discovery of serratiochelin C, a total of 40 L fermentation broth from *T. chitinolytica* was centrifuged in each 1 L centrifugal tube to separate the supernatant and cell pellet. The condition was set up for 30 min at 10°C, 4400 rpm. The remained supernatant was then extracted using Diaion® HP 20 using Erlenmeyer for four days 5°C, 120 rpm, then filtered, washed twice with deionized water, and directly fractionated using VLC system to give five fractions (A-E). Fraction (MeOH: H<sub>2</sub>O) A, B, C, D, and E is 10:90, 25:75, 50:50, 75:25, 100 MeOH, respectively. The fraction D (45.34 mg) containing serratiochelin C were then subjected to RP-HPLC using a linear gradient from 10:90 to 50:50 ACN: H<sub>2</sub>O containing 0.1% TFA over 7 min, followed by isocratic stage at 100 ACN for an additional 6 min using Aeris™ 3.6 μm PEPTIDE XB-C18 100 Å, 250 x 4.6 mm (Phenomenex®), 0.8 mL/min flow rate, UV monitoring 211, 255 and 280 nm. The purification of serratiochelin C has been done using the same method as mentioned before using different column, which was Luna® 3 μm C18(2) 100 Å, 250 x 4.6 mm (Phenomenex®), with 0.5 mL/min flow rate, UV monitoring 211, 255 and 280 nm.

### 2.11. Cultivation, extraction, and profiling of AHL

The strains were grown as a pre-culture for 24 hours in 10 ml LB at 30°C and 140 rpm. For primary cultures, each media was supplemented with 100 mM phosphate buffer (pH 6.5) to prevent degradation of AHL due to alkaline pH. Subsequently, 25 ml medium in 50 ml falcon flasks were inoculated with 100 μl pre-culture with an initial OD<sub>600</sub> of 0.06 and incubated at 30°C and 140 rpm. After 24 hours, 50 ml of the culture supernatants were doubly extracted (1:1) with ethyl acetate, then acidified with 0.1% acetic acid. The solvent phase was evaporated with a rotary evaporator with 150 rpm and 40°C until dry *in vacuo*. The extract of the supernatant was then resolved in 300 μl LC-MS grade-acetonitrile and vortex vigorously to dissolve the extracted AHLs. The mixture was subsequently centrifuged, and the presence of insoluble residues was discarded. The final mix was then inserted into LC-MS vials for mass spectrometry analysis.

The extracted AHLs of bacterial strain were qualitatively and quantitatively analyzed using the MRM method as previously reported from our lab with modification (Bauer *et al.*, 2016). In general, AHLs were identified via comparison of the retention time and the fragmentation pattern with commercially available reference standards and co-injection (1:1) of the standards and the crude extract. MRM analysis was performed with Low-resolution MS. MRM with LC-MS system was carried out on Luna<sup>®</sup> 5  $\mu$ m C18(2) 100 Å, 250 x 4.6 mm (Phenomenex<sup>®</sup>). For measurement, the gradient profile started at 70% water acidified with TFA (B), 50% acetonitrile (A) in 7 min with flow 0.6 mL/min reaching 100% A for an additional 8 min, then re-equilibrated with 70% B for the next 15 min. The flow was set continuously up 0.6 mL/min for the whole MRM time. Injection volume 20  $\mu$ L. MRM measurement was conducted in positive ionization mode using a source temperature of 450°C and ion spray voltage floating of 5500 V. Nitrogen gas was used as curtain gas pressure of 10 psi (Cur), nebulizer gas (GS1) with 20 psi and heated gas (GS2) with 20 psi. Other MS parameters were set as follows de-clustering potential (DP), entrance potential (EP), and collision energy (CE) at 46, 12, and 13 V, respectively. All MRM data were collected, analyzed, and visualized with Analyst<sup>®</sup> TF 1.7 software. To obtain MS/MS product ion spectra of AHL, MS parameters were optimized separately for each standard.

## 2.12. Determination of absolute configuration of peptide

One milligram of the compound was hydrolyzed with 2 mL 6M deuterium chloride solution. The reaction vessel was heated and maintained to 110°C and shaken at the same temperature for 24 h, as referred to the method of Kusumoto *et al.* (1981). The solvent was then evaporated *in vacuo*, and the remaining hydrolysis residue was re-dissolved in water (100  $\mu$ L). 200  $\mu$ L of 1% Marfey's reagent in acetone (1-fluoro-2-4-dinitrophenyl-5-L-alanine amide) and 40  $\mu$ L 1.0 M sodium bicarbonate solution was added. The reaction mixture was then heated with shaking for 1 h at 40 °C. Afterward, the solution was cooled at room temperature, and the reaction was stopped by the addition of 20  $\mu$ L of 2N HCL and centrifuged for 10 min, 3000 rpm. The analysis was performed on LC-MS/MS with the condition of CUR 25, TEM 40, GS1 and GS2 30, IS 4500, DP 50, EP 10 and the system was on position equipped with Luna<sup>®</sup> 5  $\mu$ m C18(2) 100 Å, 250 x 4.6 mm (Phenomenex<sup>®</sup>),

special UV monitoring at 340 nm. The gradient profile started at 10% (v/v) ACN in H<sub>2</sub>O containing 0.1% TFA in 5 min with flow 200  $\mu$ L/min reaching to 100% (v/v) ACN for additional 25 min, then subsequently re-equilibrate with 100% (v/v) ACN for the following 10 min, and re-condition to the same stage (10% (v/v) ACN) for additional 5 min. L- and D- amino acids standard for assignment, the absolute configuration was dissolved in 100  $\mu$ l H<sub>2</sub>O and treated in the same manner using FDAA. Each of Marfey's products was confirmed using retention time (L-pro, D-pro, L-val, D-val, L-tyr, and D-tyr was 29.58, 30.15, 32.42, 33.72, 34.65, and 35.48 minutes, respectively) and extracted ion of positive LC-MS [M+H]<sup>+</sup> m/z 368.1, 370.1, and 434.1 for L/D pro, L/D val, and L/D tyr, respectively.

### 2.13. Siderophore detection-based CAS assay

CAS assay agar plate was prepared according to Louden *et al.* (2011)., as shown in **Table 2-6**.

**Table 2.6.** CAS agar composition and detail instruction.

<b>A. Blue dye</b>	Solution 1, with 9 ml of Solution 2, subsequently added Solution 3—autoclave and store in a bottle containing free-trace elements.
Solution 1	0.06 g CAS was prepared in 50 ml of ddH <sub>2</sub> O.
Solution 2	0.0027 g FeCl <sub>3</sub> .6H <sub>2</sub> O was added to 10 ml of 10 mM HCl.
Solution 2:	0.073 g HDTMA was added to in 40 ml of ddH <sub>2</sub> O
<b>B. Mixture solution</b>	
MM9 salt stock	15 g KH <sub>2</sub> PO <sub>4</sub> , 25 g NaCl, and 50 g NH <sub>4</sub> Cl were dissolved in 500 ml ddH <sub>2</sub> O.
20% glucose stock	20 g glucose was dissolved in 100 ml ddH <sub>2</sub> O.
NaOH stock	25 g NaOH was dissolved in 150 ml ddH <sub>2</sub> O, pH adjusted to 12
Casamino acid	3 g Casamino acid was dissolved in 27 ml ddH <sub>2</sub> O, followed by extraction with 8-hydroxyquinoline in chloroform to discard trace iron, subsequently filter sterilized.
<b>C. CAS agar</b>	100 mL MM9 salt stock was added to 750 ml ddH <sub>2</sub> O; the pH was then adjusted to 6 and added 32.24 g PIPES, checked regularly the pH that should not more than 6.8, followed by addition of 15 g agar



and autoclave. After the solution, less than 50°C, 30 mL Casamino acid stock, and 10 ml sterilized 20% glucose was then added to the MM9-PIPES mixture. 100 ml Blue Dye was then added slowly through a glass wall. The final mixture was then aseptically poured into the plate.

---

#### **2.14. Swimming motility assay**

A bacterial surface movement called swimming motility was performed in all wild type in the genus of *Massilia* and *Telluria*. To prepare pre-cultured, about 2 ml of LB were inoculated with a single pure colony of each strain and incubated for 24 h at 30°C, 140 rpm. Each bacterium grown from pre-cultivation was then diluted with sterile ddH<sub>2</sub>O to achieve OD<sub>600</sub> of 0.06. Each ready-to-cultivate bacterium (5µl) was treated with the different type of exogenous AHL, namely 3-OH-C6-AHL, C4-AHL and C8-AHL with a final concentration 10µM, then subsequently inoculate agar plate, dried for another 10 to 15 min, and followed by incubation for 18 h at 30°C in the static condition. Each AHL used in this study was previously prepared in 10 mM with DMSO as a vehicle. The swimming motility of each bacterium was measured manually using a diameter caliper for the visualization of swimming motility, Bio-RAD Molecular Imager<sup>®</sup> Gel Doc<sup>™</sup> XR+ imaging system coupled with Image Lab<sup>™</sup> Software Version 5.1 with an imaged color of SYBR Green.

#### **2.15. Biofilm assay**

Overnight pre-culture of each strain was prepared in LB media and incubated for 30°C with agitation at 140 rpm. Each culture was then serially diluted with sterile water to achieve OD<sub>600</sub> of 0.06. About 100 µl of culture mixed with exogenous AHL was inoculated in limited media that contains only salt and carbon sources (DMBgly) and then incubated at 30°C for 24 h with a static condition in 96 well-plate. The final concentration of AHL in DMBgly containing bacteria was 10µM. The culture was then incubated overnight. Staining and quantifying the biofilm was conducted based on the protocol that has been performed by O'Toole (2011). In brief, 125 µl of crystal violet in water (0.1%) was mixed with a biofilm that adhered to the microplate well. The mixture was incubated then for 15

min and rinsed with water four times. After the microplate has been upside down and dried for a few hours, a qualitative assay can be achieved using a manual photograph. For the quantitative analysis, 125  $\mu\text{l}$  of 30% acetic acid was transferred to a microplate to solubilize the crystal violet, followed by the incubation for 15 min. About 125  $\mu\text{l}$  solubilized mixture was then transferred to new flat-bottomed micro-titer dish and measured at 550 nm using Tecan Infinite<sup>®</sup> 200 Pro microplate reader. For the blank used only 30% acetic acid.

### **2.16. Sub-inhibitory assay by antibiotic**

The initial  $\text{OD}_{600}$  of strains for the experiment was 0.06. Each culture was then treated with antibiotics, i.e., tetracycline, kanamycin, trimethoprim, neomycin, and gentamycin in DMSO with the final concentration of 30  $\mu\text{M}$  in 20 ml of 50 ml falcon tube. The agitation performed at 140 rpm, at 30°C for 24 h. Each antibiotic was prepared using DMSO with a final concentration of 10 mM as a stock. The AHL production of 3-OH-C6-AHL, C4-AHL, and C8-AHL monitored by MRM together with curve growth (as previously described) after exposed by antibiotic in sub-inhibitory concentration was monitored based on the previous method (2.16).

### **2.17. Fatty acid supplementation assay**

The initial  $\text{OD}_{600}$  of *T. chitinolytica* and *M. lutea* for this experiment was 0.06. Each culture was then treated with exogenous fatty acid (FAB) produce by *B. glumae* ICMP 3729 with the final concentration of 20  $\mu\text{M}$  in 20 ml of 50 ml falcon tube. FAB was prepared in DMSO in the final concentration of 10 mM as a stock. The 3-OH-C6-AHL, C4-AHL, and C8-AHL monitored by MRM, as previously described (2.12), for motility assay, was performed as previously described using FAB at the final concentration of 20 and 40  $\mu\text{M}$ .

### **2.18. Tyrosinase inhibition assay**

The tyrosinase activity was examined using tyrosinase inhibitor screening kit MAK257 and its protocol. In brief, 20  $\mu\text{L}$  peptide with various concentrations was added into 50  $\mu\text{L}$  tyrosinase enzyme solutions that contained 48  $\mu\text{L}$  MAK257A buffer and 2  $\mu\text{L}$  of tyrosinase. The mixture was then subsequently incubated for 10 min at 25°C, followed by addition of 30  $\mu\text{L}$  substrate solution contains 23  $\mu\text{L}$  MAK257A buffer, 2  $\mu\text{L}$  tyrosinase

substrate, and 5  $\mu$ L tyrosinase enhancer. The final reaction mix was then thawed and immediately monitored at 510 nm using Tecan Infinite<sup>®</sup> 200 Pro microplate reader using kinetic mode for 30-60 min. Kojic acid and arbutin was used as a positive control. The concentration ranges of tetrapeptide used for the assay was 0.05–5  $\mu$ M. Each measurement was made in three independent replications. The result was determined as % relative inhibition as follows: % Relative = [Slope (EC)–Slope(S)]/Slope (EC) x 100. The EC means as enzyme activity control and S means as a test sample. The IC<sub>50</sub> value, the concentration with 50 % inhibition of tyrosinase activity, was determined by interpolation of dose-response curves from the log(inhibitor) vs. normalized relative inhibition using GraphPad Prism 7.0.

### **2.19. Antibacterial assay**

The antibacterial activity analysis of pure compounds against bacterial pathogen was performed in 96-well plate using the broth dilution method according to EUCAST guideline (European Committee for Antimicrobial Susceptibility Testing of the European Society of Clinical and Infectious, 2003). In brief, 100  $\mu$ l of Mueller-Hinton Broth and 5  $\mu$ l of each bacterial pathogen (OD<sub>600</sub>= 0.2) were cultures in each well. The total of 200  $\mu$ l from the solution of 256  $\mu$ g/mL of pure compounds was dissolved in MeOH 10% was applied in the first vertical line of the 96-well plate. Serial dilutions were constructed to obtain ten different concentrations in each well: 128, 64, 32, 16, 8, 4, 2, 1, 0.5 and 0.25  $\mu$ g/mL. MeOH 10% was used as a negative control. The 96-well plates were then incubated for 24 h at 37°C; growth inhibition was measured using Tecan Plate Reader Infinite M200 at 600 nm. The MIC was determined in independent triplicate for each bacterial pathogen. The OD<sub>600</sub> data that represented bacterial growth were adjusted by the Gompertz equation to calculate the MIC (Lepe *et al.*, 2014).

### **2.20. Cytotoxicity assay**

Cytotoxicity test against the Hela cell line was performed using the 3-(4,5-dimethyl-2-thiazolyl)-2,5-diphenyl-2H-tetrazolium bromide (MTT). In brief, MTT was added to the cell after the incubation period to the final concentration of 1 mg/mL. The cells were then incubated for 60 min, followed by centrifugation for 5 min at 2315 rpm. The medium was then aspirated, and DMSO (100  $\mu$ L) was added to every well to produce formazan color

from the cells. After 25 min of the incubation, the absorbance at 650 nm and 570 nm, which were represented as reference wavelength and test wavelength, respectively, were measured using multiple readers.

### **2.21. Statistical analysis**

The quantitative data has been conducted using at least three independent replicates. The analysis output has been projected as mean value  $\pm$  SEM, and statistical analysis was generated by unpaired Student's t-test using GraphPad Prism 7. Probability ( $p$ -value) less than 0.05, the difference was considered as statistically significant

## Chapter 3. Unveiling the specialized metabolites from the genus *Massilia* and the discovery of novel peptide

### 3.1. Bioinformatic analysis of six type strains from the genus *Massilia*

Our previous studies revealed the whole genome sequence of six type strains of the genus *Massilia*, i.e., *Massilia albidiflava*, *M. dura*, *M. flava*, *M. lutea*, *M. plicata*, and *M. umbonata*. The size of the genomes varied from 5.9 to 7.5 Mb. This size-range is comparable with one of the bacteria of the genus *Burkholderia*, which is typically ranging between 2.4 to 11.5 Mb (Peeters *et al.*, 2017) and of the genus *Pseudomonas* (*sensu stricto*), mostly ranging between 6 to 7 Mb (Jensen *et al.*, 2004). Since the latter two genera are known to contain prolific secondary metabolite gram-negative Proteobacteria, we hypothesized that bacteria of the genus *Massilia* might also represent talented producers of new chemistry. In order to prove this hypothesis, at first, genome mining employing antiSMASH v5.0 was applied (**Figure 3-1**). Using default settings, the web-based tool predicted 6 to 11 BGCs per strains, unveiling already the biosynthetic potential of these species. All strains are bioinformatically denoted as terpene producers, which became apparent by the presence of a carotenoid BGC with 100% similarity against the database. Moreover, all members of the genus *Massilia* in this study also have the potential to produce NRPS-based compounds, homoserine lactones, siderophores, aryl-polyenes, type 1 polyketides, and bacteriocins.

**A**

Region	Type	From	To	Most similar known cluster	Similarity
Region 1	transAT-PKS-like <a href="#">↗</a> , transAT-PKS <a href="#">↗</a> , T3PKS <a href="#">↗</a> , PKS-like <a href="#">↗</a>	27,379	139,854	thailanstatin A <a href="#">↗</a>	NRP + Polyketide 30%
Region 2	NRPS <a href="#">↗</a> , T1PKS <a href="#">↗</a>	144,301	236,689	tubulylin A / tubulylin B / tubulylin C / tubulylin D / tubulylin E / tubulylin F / tubulylin G / tubulylin H / tubulylin I <a href="#">↗</a>	NRP + Polyketide 11%
Region 3	acyl_amino_acids <a href="#">↗</a>	337,134	397,876		
Region 4	terpene <a href="#">↗</a>	420,585	440,639	CDA1b / CDA2a / CDA2b / CDA3a / CDA3b / CDA4a / CDA4b <a href="#">↗</a>	NRP:Ca+-dependent lipopeptide 5%
Region 5	siderophore <a href="#">↗</a>	849,304	869,682	cupriachelin <a href="#">↗</a>	NRP:NRP siderophore 11%
Region 6	betalactone <a href="#">↗</a>	1,787,529	1,818,807		
Region 7	arylpolyene <a href="#">↗</a>	1,988,183	2,031,771	APE Vf <a href="#">↗</a>	Other 45%
Region 8	hserlactone <a href="#">↗</a>	3,971,501	3,990,376		
Region 9	hserlactone <a href="#">↗</a> , thiopeptide <a href="#">↗</a> , LAP <a href="#">↗</a>	4,130,352	4,164,118		
Region 10	terpene <a href="#">↗</a>	4,460,247	4,483,847	carotenoid <a href="#">↗</a>	Terpene 100%
Region 11	bacteriocin <a href="#">↗</a>	5,372,836	5,384,443		
Region 12	NRPS-like <a href="#">↗</a>	6,322,148	6,364,929		
Region 13	NRPS-like <a href="#">↗</a>	6,389,842	6,433,753	rhizomide A / rhizomide B / rhizomide C <a href="#">↗</a>	NRP 100%

**B**

Region	Type	From	To	Most similar known cluster	Similarity
Region 1	arylpolyene <a href="#">↗</a>	1,300,750	1,344,407	APE Vf <a href="#">↗</a>	Other 40%
Region 2	terpene <a href="#">↗</a>	3,021,427	3,040,737		
Region 3	acyl_amino_acids <a href="#">↗</a>	3,064,554	3,123,924		
Region 4	NRPS-like <a href="#">↗</a>	3,880,846	3,922,798	rhizomide A / rhizomide B / rhizomide C <a href="#">↗</a>	NRP 100%
Region 5	bacteriocin <a href="#">↗</a>	5,205,364	5,216,653		
Region 6	hserlactone <a href="#">↗</a>	5,599,146	5,619,727		
Region 7	NRPS <a href="#">↗</a> , bacteriocin <a href="#">↗</a>	6,066,204	6,108,401		
Region 8	terpene <a href="#">↗</a>	6,178,332	6,202,001	carotenoid <a href="#">↗</a>	Terpene 100%
Region 9	NRPS <a href="#">↗</a> , T1PKS <a href="#">↗</a>	6,354,866	6,422,944	tallysomylin A <a href="#">↗</a>	NRP:Glycopeptide + Polyketide:Modular type I + Saccharide:Hybrid/tailoring 5%
Region 10	acyl_amino_acids <a href="#">↗</a>	6,685,036	6,789,912	N-tetradecanoyl tyrosine <a href="#">↗</a>	Other 9%

**C**

Region	Type	From	To	Most similar known cluster	Similarity
Region 1	bacteriocin <a href="#">↗</a>	1,506,138	1,517,793		
Region 2	terpene <a href="#">↗</a>	2,350,190	2,372,734	carotenoid <a href="#">↗</a>	Terpene 100%
Region 3	NRPS <a href="#">↗</a> , T1PKS <a href="#">↗</a>	2,517,800	2,585,757	tallysomylin A <a href="#">↗</a>	NRP:Glycopeptide + Polyketide:Modular type I + Saccharide:Hybrid/tailoring 5%
Region 4	acyl_amino_acids <a href="#">↗</a>	2,833,440	2,894,003	O-antigen <a href="#">↗</a>	Saccharide 14%
Region 5	arylpolyene <a href="#">↗</a>	4,750,040	4,793,661	APE Vf <a href="#">↗</a>	Other 40%
Region 6	terpene <a href="#">↗</a>	6,444,066	6,465,756		

**D**

Region	Type	From	To	Most similar known cluster	Similarity
Region 2.1	terpene <a href="#">↗</a>	592,005	614,620	carotenoid <a href="#">↗</a>	Terpene 100%
Region 2.2	bacteriocin <a href="#">↗</a>	1,550,403	1,562,070		
Region 2.3	NRPS <a href="#">↗</a> , T1PKS <a href="#">↗</a>	2,542,586	2,610,672		
Region 2.4	acyl_amino_acids <a href="#">↗</a>	2,857,759	2,917,333	O-antigen <a href="#">↗</a>	Saccharide 14%
Region 2.5	arylpolyene <a href="#">↗</a>	4,786,040	4,829,688	APE Vf <a href="#">↗</a>	Other 45%
Region 2.6	thiopeptide <a href="#">↗</a> , LAP <a href="#">↗</a>	5,938,303	5,985,198		
Region 2.7	terpene <a href="#">↗</a>	6,393,804	6,415,493		
Region 2.8	acyl_amino_acids <a href="#">↗</a>	6,436,697	6,497,395		

Region	Type	From	To	Most similar known cluster	Similarity	
Region 1	NRPS-like	544,893	588,747	GE81112	NRP	7%
Region 2	acyl_amino_acids	1,074,814	1,133,710			
Region 3	terpene	1,572,118	1,591,963			
Region 4	arylpolyene	3,146,868	3,190,516	APE Vf	Other	45%
Region 5	linaridin	4,862,376	4,882,882			
Region 6	acyl_amino_acids	5,121,203	5,221,866	lipopolysaccharide	Saccharide:Lipopolysaccharide	8%
Region 7	terpene	5,614,891	5,638,605	carotenoid	Terpene	100%
Region 8	hserlactone	6,183,974	6,204,555			
Region 9	bacteriocin	6,532,317	6,544,002			

Region	Type	From	To	Most similar known cluster	Similarity	
Region 1	NRPS	193,033	250,549	turnerbactin	NRP	69%
Region 2	acyl_amino_acids	650,989	711,632			
Region 3	terpene	765,256	784,937			
Region 4	hserlactone	874,717	895,280	obafuorin	NRP	14%
Region 5	thiopeptide	1,049,428	1,084,749	lankacidin C	NRP + Polyketide	13%
Region 6	thiopeptide	3,187,902	3,220,154			
Region 7	acyl_amino_acids	3,436,732	3,497,295	O-antigen	Saccharide	14%
Region 8	terpene	4,059,867	4,080,817	carotenoid	Terpene	100%
Region 9	NRPS, arylpolyene	4,744,322	4,802,434	APE Vf	Other	10%
Region 10	bacteriocin	5,156,029	5,167,648			

**Figure 3-1.** Number of BGCs from bacteria of the genus *Massilia* through the antiSMASH v5.0 analysis. (a) *M. flava*, (b) *M. albidiflava*, (c) *M. lutea*, (d) *M. dura*, (e) *M. umbonata*, (f) *M. plicata*.

### 3.2. Chemical investigation through OSMAC approach

The six type strains mentioned above from the genus *Massilia* and two additional strains *M. timonae* and *M. haloabium* were used for metabolic profiling on a 5L-scale fermentation in various types of media as we believed that the OSMAC approach through media variation could activate cryptic BGCs. All cultivation approaches were conducted with shaking. Fermentation without shaking caused marginal growth and was not further followed up and examined. After 48 hours of fermentation, the broth was extracted with butanol and the resultant crude extract fractionated by VLC. The obtained fractions were then screened using low-resolution LC-MS. The screening dereplicated various known metabolites such as rhizomide A, rhizomide B,  $\beta$ -carotenoid, and epoxy-carotenoid. However, the analysis of the low-resolution LC-MS profile of *M. albidiflava* fraction showed also an unidentified peak, which could not be dereplicated, and we hypothesized the production of putative novel chemical entities. Subsequently, we collected the corresponding peak, and conducted initial  $^1\text{H}$  NMR analysis, and found that the compound has a peptide backbone. Thus, we further scaled-up the fermentation.

**Table 3-1.** Low-resolution LC-MS screening results based on the positive mode of the investigated strains.

No	Bacterial strains	Medium						
		SBM without salt	Modified DMB I	MM9	SRM <sub>HG</sub>	Modified SRM <sub>HG</sub>	LB	R2A
1	<i>Massilia lutea</i>	537.12 (β-carotenoid), 364.9, 670.3	-	-	537.12 (β-carotenoid)	537.12 (β-carotenoid)	537.12 (β-carotenoid)	-
2	<i>M. dura</i>	-	-	-	-	-	-	-
3	<i>M. albidiflava</i>	537.12 (β-carotenoid)	537.12 (β-carotenoid), Un-identified peak	748.1 (Rhizomide B)	-	537.12 (β-carotenoid)	-	537.12 (β-carotenoid)
4	<i>M. umbonata</i>	537.12 (β-carotenoid), 364.9, 670.3	-	-	-	-	-	537.12 (β-carotenoid)
5	<i>M. flava</i>	36.9	537.12 (β-carotenoid)	732.19 (Rhizomide A), 537.12 (β-carotenoid)	-	732.19 (Rhizomide A), 553.30 (epoxy-carotene suspected)	-	537.12 (β-carotenoid)
6	<i>M. plicata</i>	-	-	-	-	-	-	-
7	<i>M. timonae</i>	-	-	-	-	-	-	-
8	<i>M. haloabium</i>	-	-	-	-	-	-	-

### 3.3. Isolation and structure elucidation of a novel tetrapeptide from *M. albidiflava*

In order to obtain a sufficient amount of material for structural elucidation, fifteen of 5 L Erlenmeyer containing each 2 L modified DMB medium were prepared and inoculated, the supernatant was extracted with Diaion<sup>®</sup> HP 20 resin and subsequently partitioned into water and MeOH. The 50% of MeOH layer (termed as fraction C) was fractionated repeatedly using Luna<sup>®</sup> Omega 3 μm Polar C18 100 Å, LC column 250 x 4.6 mm to provide a semi-pure compound (**Figure 3-1**) and the next purification step was done using Phenomenex<sup>®</sup> Luna 5u C5, 4.6 x 250 mm to afford the pure compound. The final purification of the peptide yielded 5.1 mg of a yellow bright opaque solid.



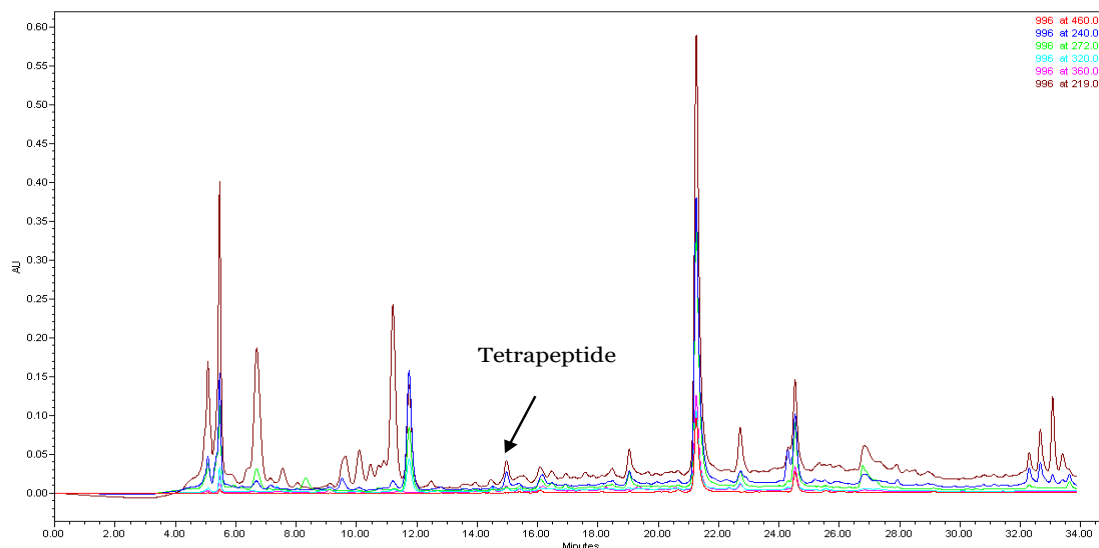


**Figure 3-2.** HPLC chromatogram of fraction C containing a novel tetrapeptide produced by *M. albidiflava* ( $t_R = 15$  min).

Spectroscopic analyses then elucidated its planar structure. All  $^1\text{H}$ - and  $^{13}\text{C}$ -NMR resonances were assigned using DEPT-135, COSY, HSQC, HSQC-TOCSY, NOESY, HMBC, and broadband selective HMBC (shift region of 27-36 and 165-171) spectra. In addition,  $^1\text{H}$ - $^{15}\text{N}$  NMR was assigned using non-calibrated HSQC and HMBC.

Overall, the  $^1\text{H}$ -NMR signals (**Figure 3-3**) were ranging from 0.84 to 7.98 ppm and showed aromatic protons at  $\delta_H$  6.63 to 7.04 ppm. The use of DMSO-*d*<sub>6</sub> solvent for  $^1\text{H}$ -NMR experimentation exhibited two amidic protons ( $\delta_H$  7.98 and 7.88) and one hydroxyl group ( $\delta_H$  9.2 ppm). Additionally, the  $^1\text{H}$  and  $^{13}\text{C}$ -NMR spectra suggested the manifestation of four  $\alpha$ -protons ( $\delta_H$  3.91, 4.05, 4.12, and 4.24 ppm), which were attached to four carbonyl carbons ( $\delta_C$  168.9, 165.2, 170.3, and 165.1 ppm, respectively). Hence, the  $^1\text{H}$  and  $^{13}\text{C}$  NMR spectra suggested that the compound (**1**) is peptidic (**Figure 3-3 and 3-4**).

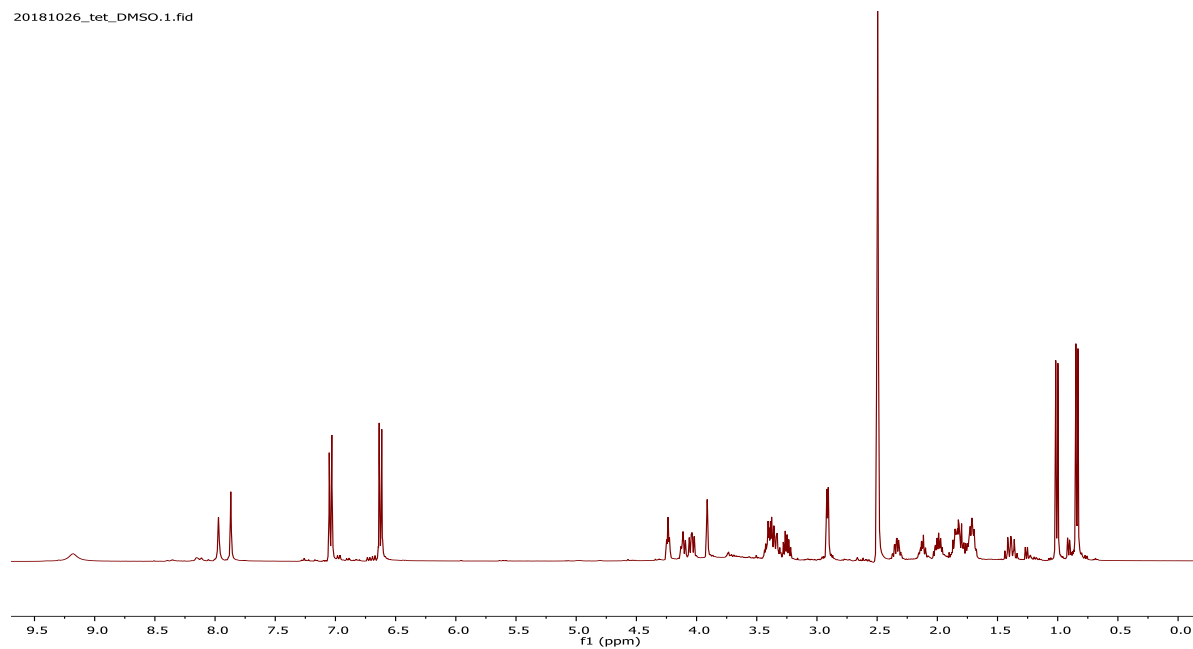


**Figure 3-3.**  $^1\text{H}$ -NMR spectrum of the novel tetrapeptide (**1**) in  $\text{DMSO-}d_6$ , 400 MHz.

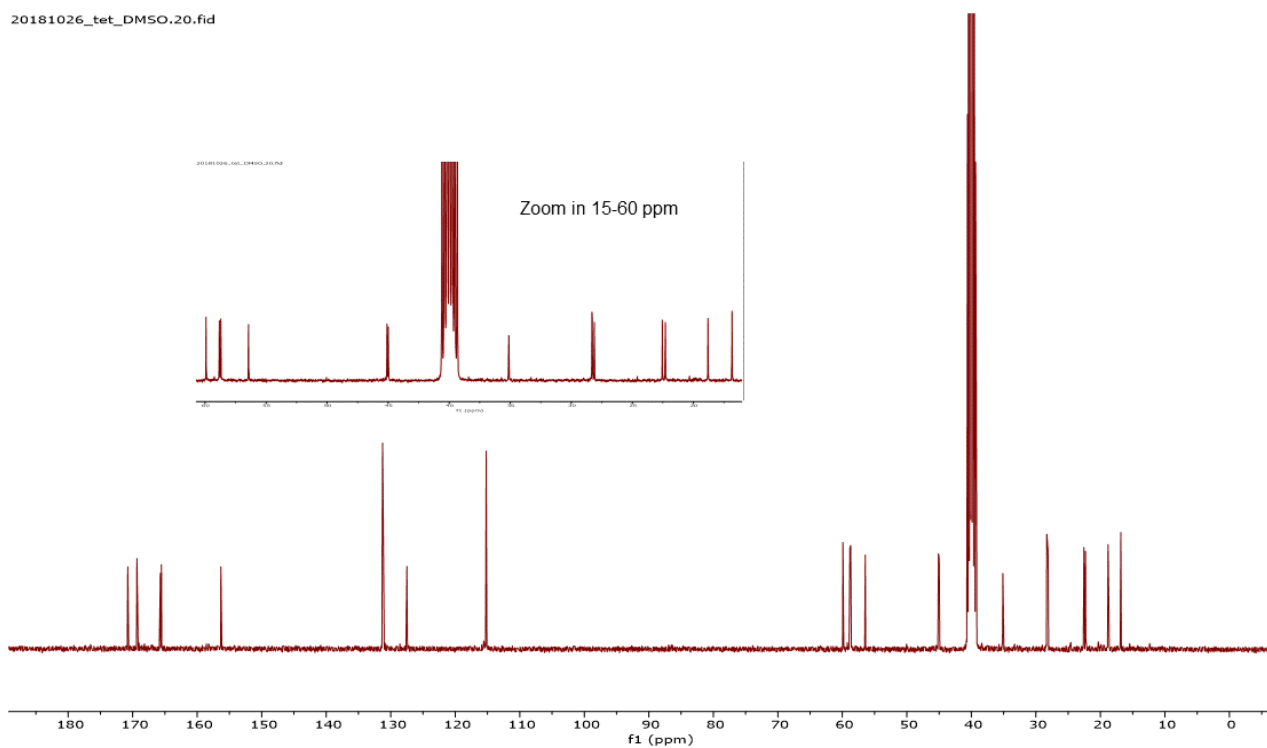


**Figure 3-4.**  $^{13}\text{C}$ -NMR spectrum of the novel tetrapeptide (**1**) in  $\text{DMSO-}d_6$ , 100 MHz.

Based on DEPT-135 and  $^{13}\text{C}$  NMR spectra (**Figures 3-4** and **3-5**), twenty-four carbons resonances have been assigned and consisted of two methyl, seven methylene, nine methine, and seven quaternary carbons.

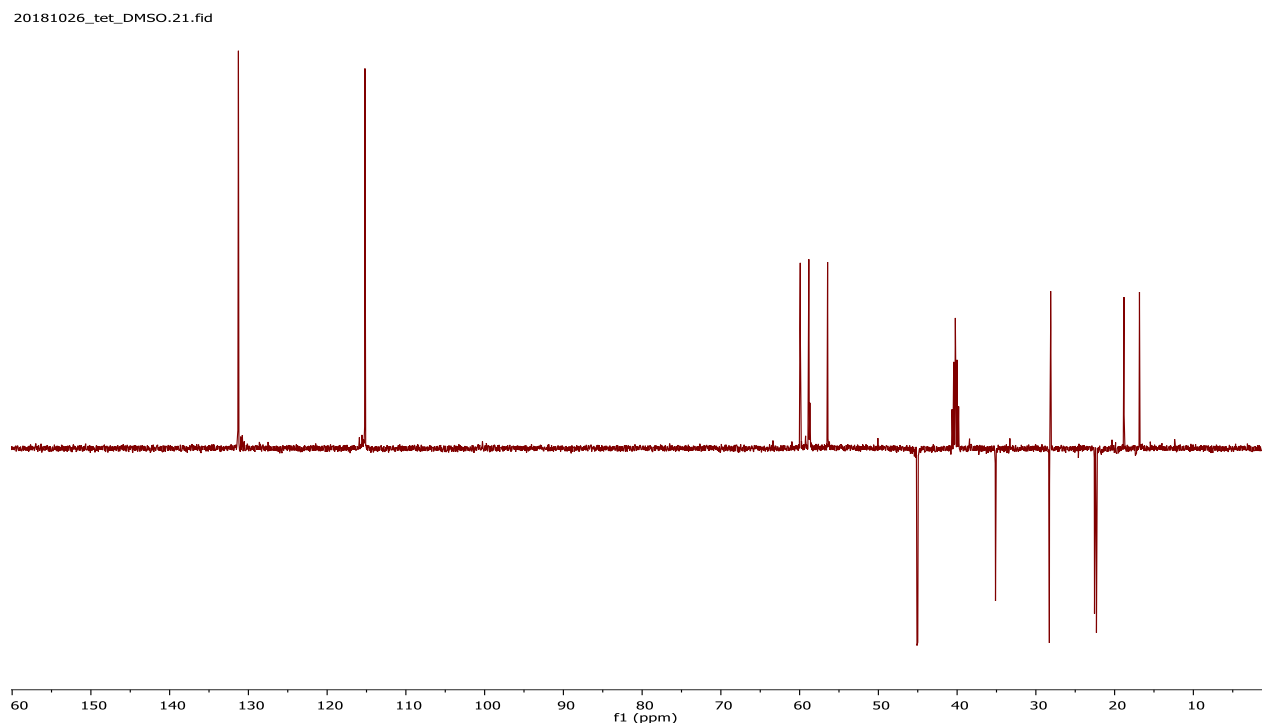


**Figure 3-5.** DEPT-135 spectrum of the novel tetrapeptide (**1**) in DMSO- $d_6$ , 100 MHz.

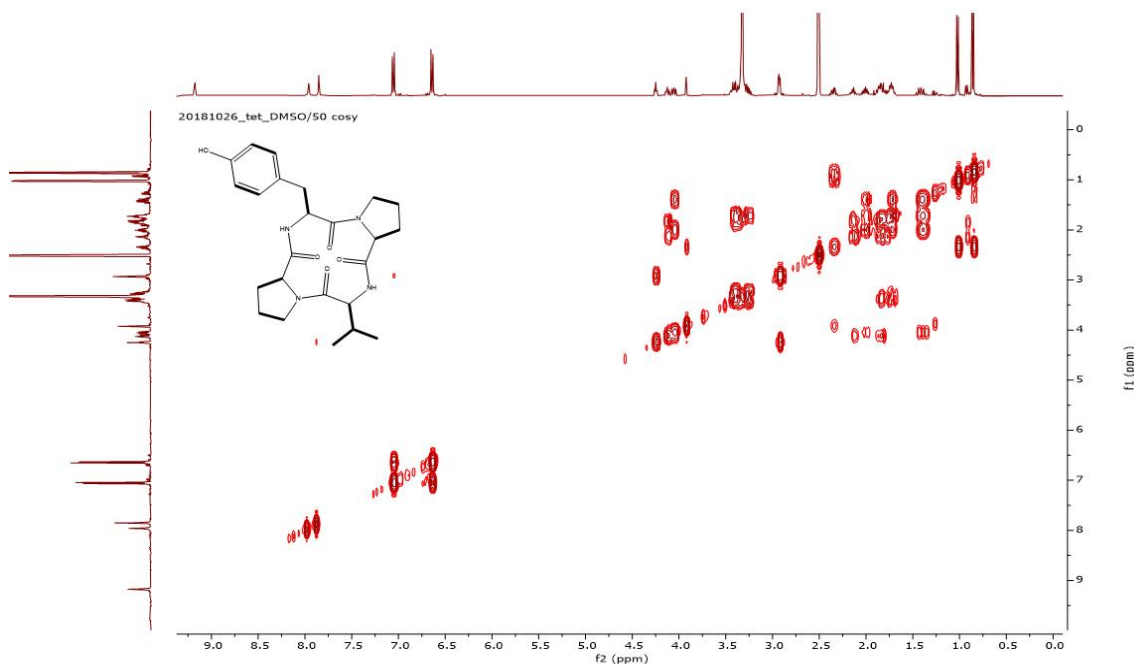


**Figure 3-6.**  $^1\text{H}$ - $^1\text{H}$  COSY spectrum of novel tetrapeptide (**1**) in DMSO- $d_6$ , 400 MHz.

As shown in **Figure 3-6**, two signals are ascending from neighboring protons in the five members' ring of proline in the  $^1\text{H}$ - $^1\text{H}$  COSY test. These signals have two repetitions, which means that the compound consists of two proline units. Moreover, two methyl

groups are coupled to the same  $\beta$ -proton, forming a valine residue. The doublet signals, at  $\delta_H$  6.63 and 7.04, represented each two magnetically equivalent aromatic protons, which was characteristic for a para-substituted aromatic unit. Together with the additional adjacent protons of 2.92 and 4.24 ppm undoubtedly showed the presence of tyrosine residue. Taken together, the  $^1\text{H}$ - $^1\text{H}$  COSY experiment could predict the three sequence amino acids, including proline, valine, and tyrosine.

To confirm these amino acid sequences, we performed an edited  $^1\text{H}$ - $^{13}\text{C}$  HSQC NMR experiment (**Figure 3-7**). It shows the correlation line of primary protons chemical shift (as displayed in the F2 axis) to the  $^{13}\text{C}$  chemical shift of their directly attached carbon through  $^1J_{\text{CH}}$  coupling (as projected in the F1 axis). There are eighteen protons that compartment to carbons an even (i.e., methylene) and odd number, i.e., (methyl and methane) of hydrogen. The combination with a TOCSY experiment, called  $^1\text{H}$ - $^{13}\text{C}$  HSQC-TOCSY, also has been performed to confirm the sequence of each amino acid since this experiment gives a long-ranged correlation between a  $^{13}\text{C}$ -attached  $^1\text{H}$  to all other coupled  $^1\text{H}$  including primarily  $^1\text{H}$ , but cannot pass hetero atoms. These connections confirm the presence of three amino acids, including double proline (2 x Pro), valine (Val), and tyrosine (Tyr), as shown in **Figure 3-8**.

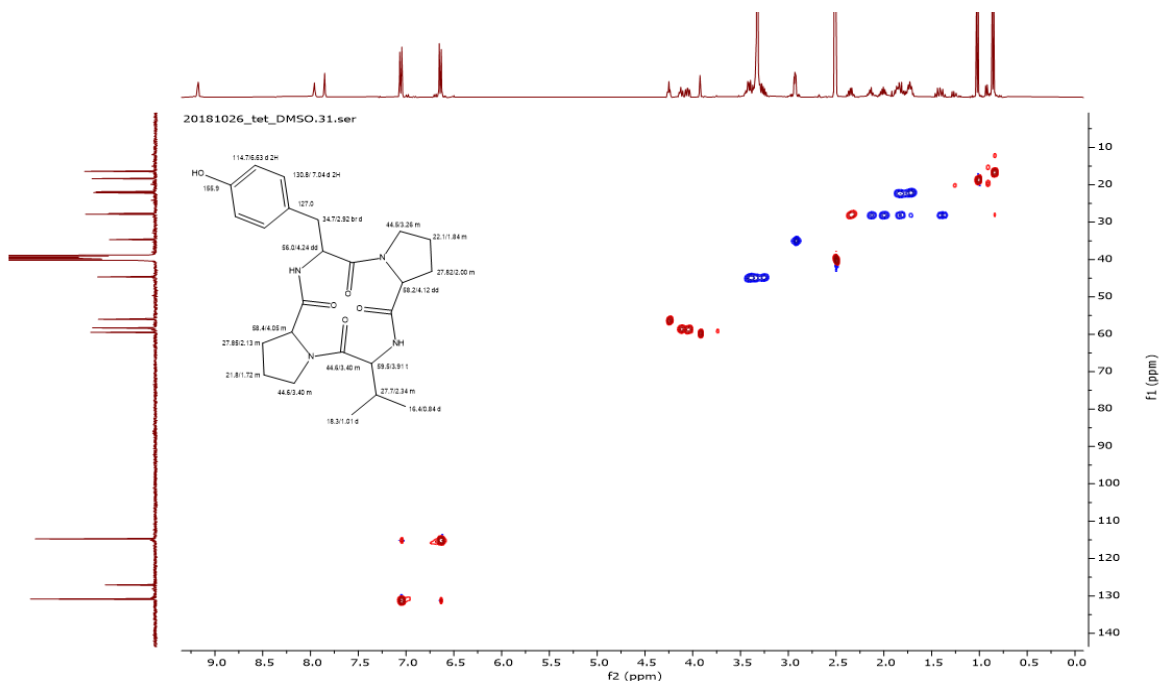


**Figure 3-7.**  $^1\text{H}$ - $^{13}\text{C}$  HSQC spectrum of the novel tetrapeptide (**1**) in  $\text{DMSO-}d_6$ , 400 MHz.

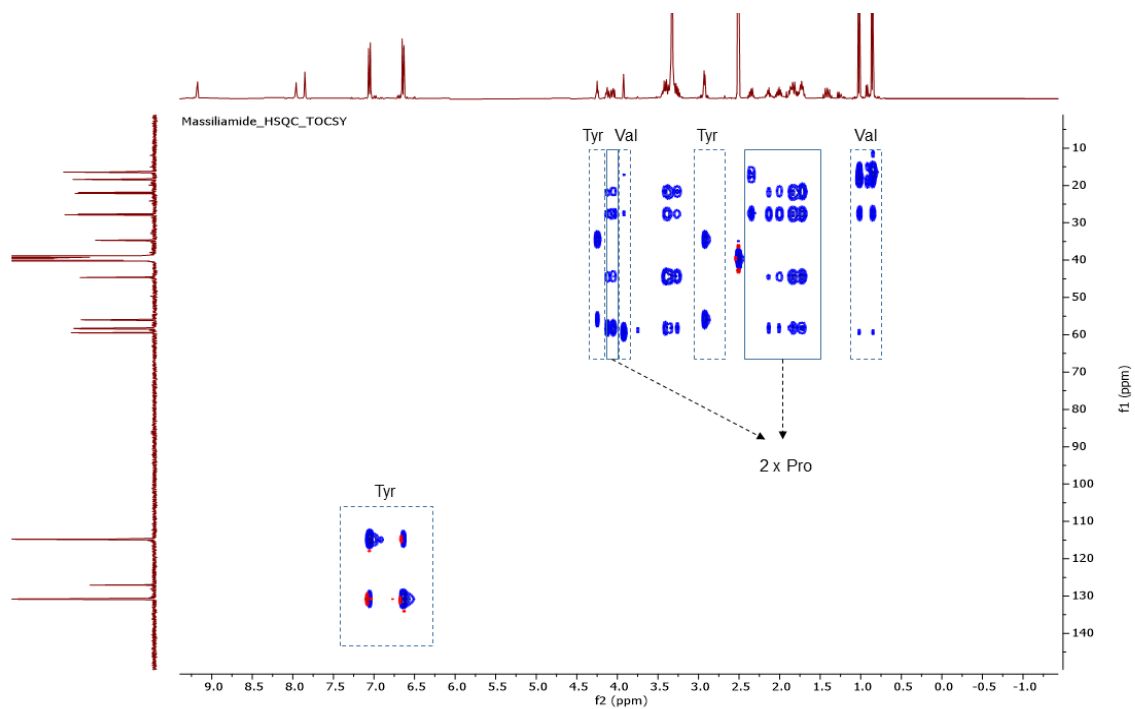


**Figure 3-8.**  $^1\text{H}$ - $^{13}\text{C}$  HSQC-TOCSY spectrum of the novel tetrapeptide (1) in  $\text{DMSO-}d_6$ , 400 MHz.

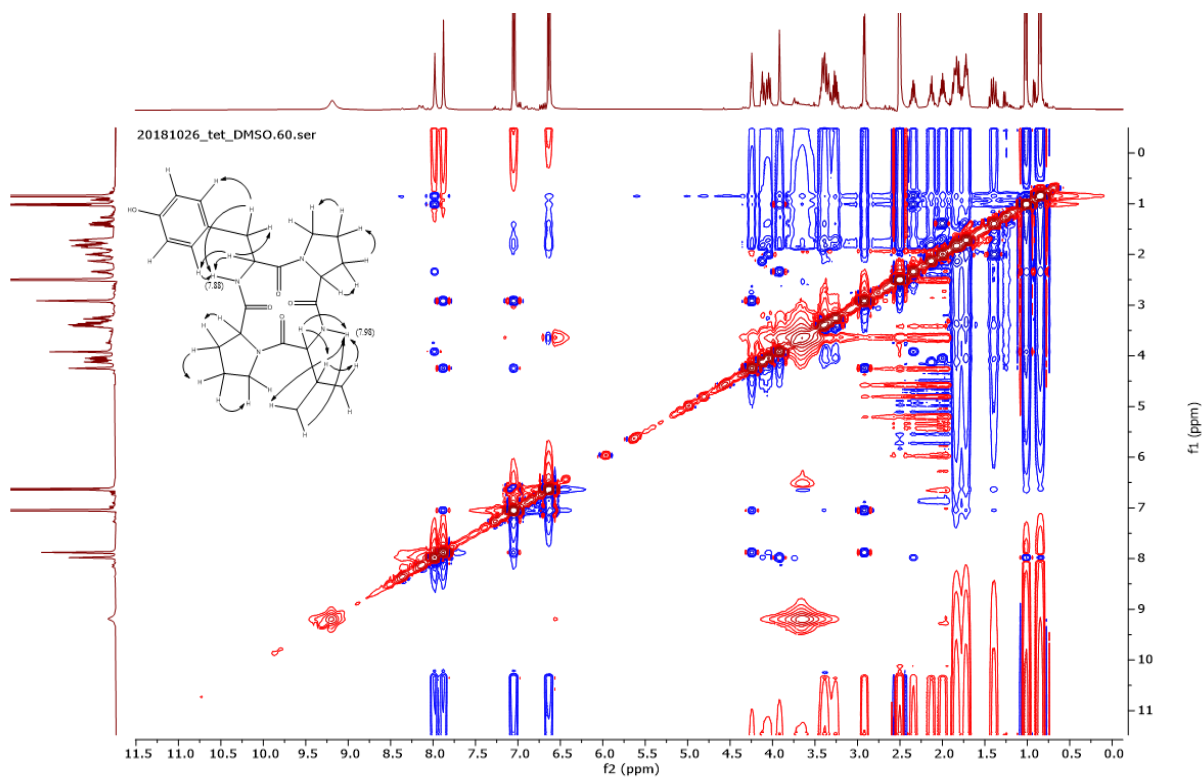


**Figure 3-9.**  $^1\text{H}$ - $^1\text{H}$  NOESY spectrum of the novel tetrapeptide (1) in  $\text{DMSO-}d_6$ , 400 MHz.

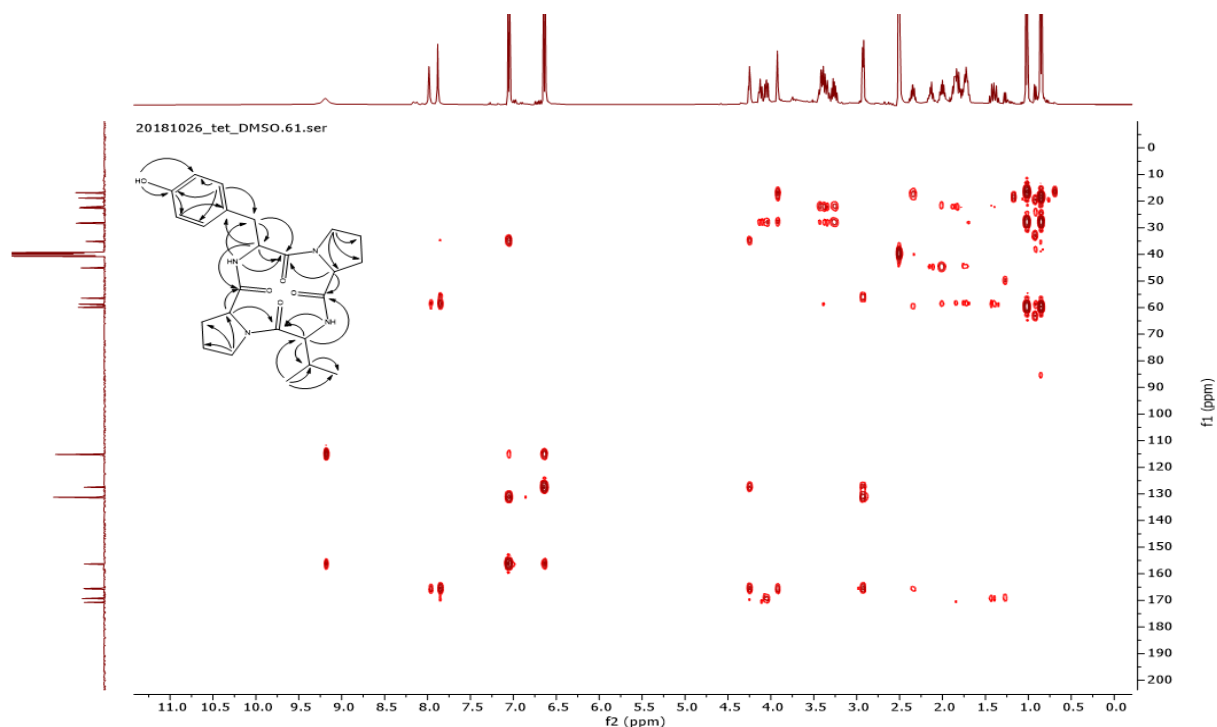


**Figure 3-10.**  $^1\text{H}$ - $^{13}\text{C}$  HMBC spectrum of the novel tetrapeptide (**1**) in  $\text{DMSO-}d_6$ , 400 MHz.

The connection between two amino acids could be performed through the interpretation of  $^1\text{H}$ - $^1\text{H}$  NOESY experiments, which reveals through space interactions up to 5 Å (**Figure 3-9**). As mentioned above, all amino acid signals could quickly be confirmed by this experiment through correlation of  $^1\text{H}$  through space and connected proline, valine, and tyrosine. In addition, two NH groups, which were located at 7.88 and 7.98 ppm, build connectivity through space to tyrosine and valine, respectively.

The linkage of these NHs to the amino, as mentioned above, acids were also confirmed by cross-linked protons to the  $^{13}\text{C}$  chemical shift using a  $^1\text{H}$ - $^{13}\text{C}$  HMBC experiment (**Figure 3-10**). Also, new connections of four quaternary carbonyl carbons could be observed in each amino acid (i.e.,  $\delta_{\text{H}}$  to  $\delta_{\text{C}}$ , 4.05 to 168.9, 3.91 to 165.2, 4.12 to 170.3, and 4.24 to 165.1 ppm). However, the connectivity between amide- to the corresponding carbonyl group was missing due to weak signals given in the  $^1\text{H}$ - $^{13}\text{C}$  HMBC spectrum. To overcome these obstacles, we performed  $^1\text{H}$ - $^{13}\text{C}$  band-selective HMBC experiments in the range of 164 to 171 ppm, as shown in **Figure 3-11**. From this experiment, we could see the connection between NH of 7.88 ppm to CO of 168.9 and 165.1; also, NH of 7.98 ppm to 170.3 and 165.2 ppm.

Moreover, to provide clear evidence of the presence of two proline sequences, since they show quite a similar proton and carbon chemical shift, we performed  $^1\text{H}$ - $^{13}\text{C}$  band selective HMBC in the range of 28 to 36 ppm, as shown in **Figure 3-12**. The result showed that distinctive signals between adjacent protons in the range of 0.84 to 4.24 ppm could be correlated to their adjacent carbons ( $\delta_{\text{C}}$  27.7, 27.82, 27.85 ppm).

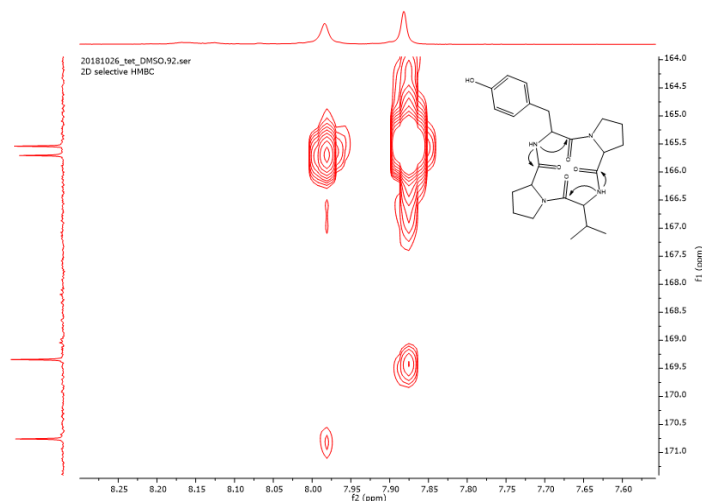


**Figure 3-11.**  $^1\text{H}$ - $^{13}\text{C}$  band-selective HMBC spectrum of the novel tetrapeptide (**1**) in  $\text{DMSO-}d_6$ , 400 MHz, in the range of 164 to 171 ppm.

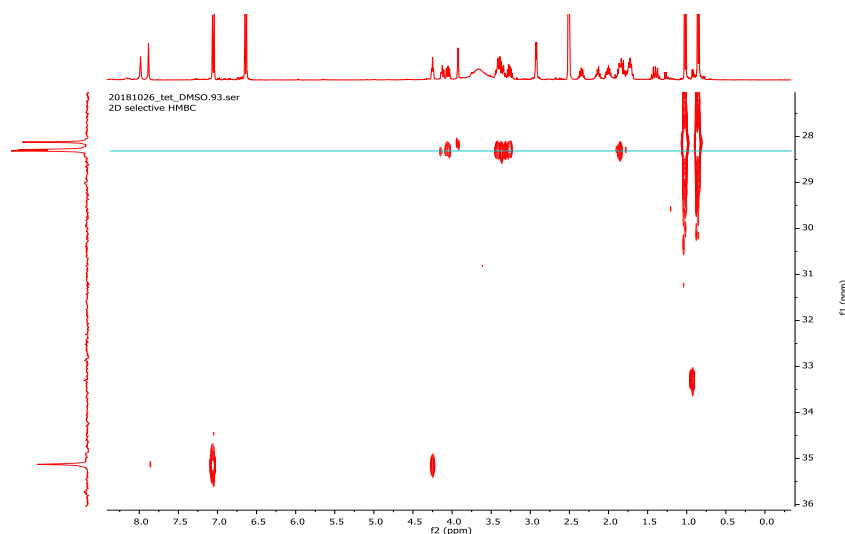


**Figure 3-12.**  $^1\text{H}$ - $^{13}\text{C}$  band-selective HMBC spectrum of the novel tetrapeptide (**1**) in  $\text{DMSO-}d_6$ , 400 MHz, in the range of 28 to 36 ppm.

Furthermore, the NMR experiment of an un-calibrated  $^1\text{H}$ - $^{15}\text{N}$  HSQC experiment gave strong evidence for the presence of an NH group, as we proposed before. The spectrum

showed the presence of two amide bonds ( $\delta_N > 100$  ppm; 111.8 and 117.0), as shown in **Figure 3-13**. The connection of these NHs through the nearest carbons could be seen using  $^1\text{H}$ - $^{15}\text{N}$  HMBC (**Figure 3-14**). The nitrogen at 111.8 and 117 ppm were connected to 2.00 and 2.92 ppm, respectively.

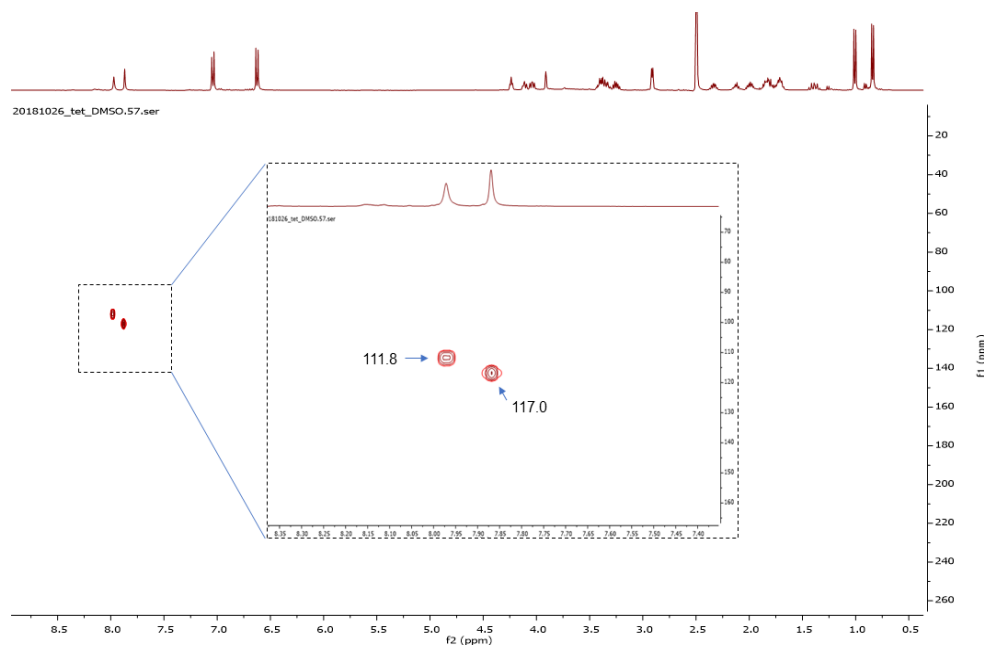


**Figure 3-13.**  $^1\text{H}$ - $^{15}\text{N}$  HSQC NMR spectrum of the novel tetrapeptide (**1**) in DMSO- $d_6$ , 400 MHz, –represents two amide bonds.

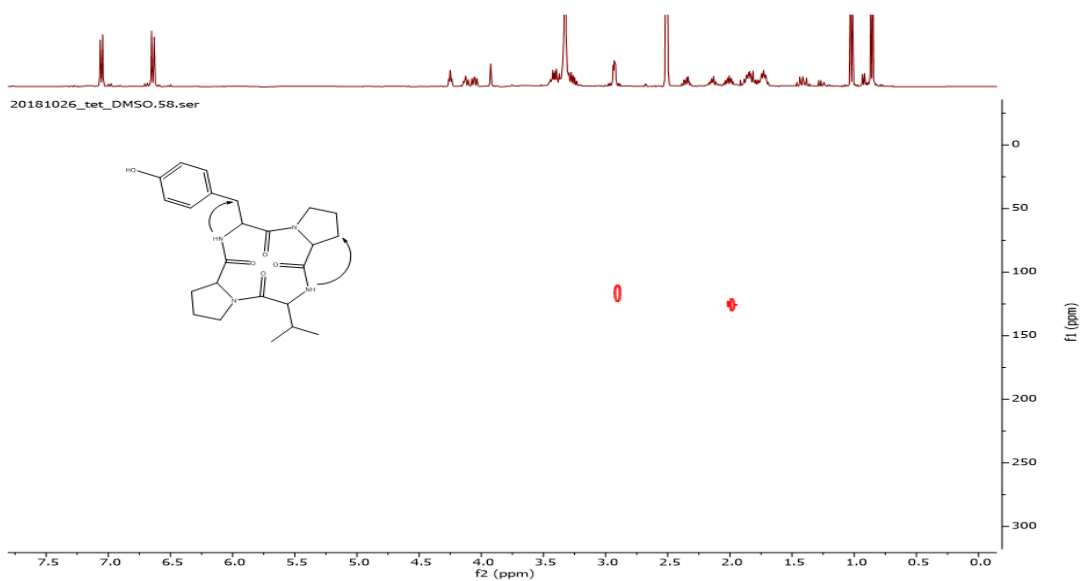


**Figure 3-14.**  $^1\text{H}$ - $^{15}\text{N}$  HMBC NMR spectrum of the novel tetrapeptide (**1**) in DMSO- $d_6$ , 400 MHz.



Taken into account the identified amino acids and the number of double bond equivalents with the value of 11 degrees unsaturation deduced from the predicted chemical formula of  $C_{24}H_{32}N_4O_5$  (HR-ESI-MS with  $m/z$  of 457.2443  $[M + H]^+$ , calc. for 457.2451  $\Delta$  -1.7 ppm) showed that **1** had to be cyclic. In summary, compound (**1**) was a cyclic structure consisting of four amino acids, including one tyrosine (Tyr), two proline (Pro-1 and Pro-2), and one valine (Val) residue. The detailed assignment of all carbon and proton signals is listed in **Table 3-2**. For **1** the trivial name massiliamide is proposed.

**Table 3-2.** NMR spectroscopic data for the novel tetrapeptide (**1**) in  $DMSO-d_6$ .

Unit	position	$\delta_{C,N}$ , mult.	$\delta_H$ , mult. (J, Hz)	
Pro1	N	126.0 <sup>a</sup>		
	$\alpha$	58.4, CH	4.05, dd (7.0, 7.0)	
	$\beta$		27.8, CH <sub>2</sub>	1.39, m
				2.00, m
	$\gamma$	21.8, CH <sub>2</sub>	1.72, m	
	$\delta$		44.5, CH <sub>2</sub>	3.26, m
				3.41, m
CO	168.9, qC			
Val	NH	111.8	7.98, brs	
	$\alpha$	59.5, CH	3.92, brs	
	$\beta$	27.7, CH	2.34, m	
	$\gamma$	16.4, CH <sub>3</sub>	0.84, d (6.9)	
	$\gamma'$	18.3, CH <sub>3</sub>	1.01, d (7.2)	
	CO	165.2, qC		
Pro2	N	125.6 <sup>a</sup>		
	$\alpha$	58.2, CH	4.12, m	
	$\beta$		27.9, CH <sub>2</sub>	1.84, m
				2.14, m
	$\gamma$	22.1, CH <sub>2</sub>	1.84, m	
	$\delta$	44.6, CH <sub>2</sub>	3.36, m	
		3.42, m		
CO	170.3, qC			
Tyr	NH	117.0	7.88, brs	
	a	56.0, CH	4.24, t (4.8)	
	b	34.7, CH <sub>2</sub>	2.92, dd (4.8, 1.0)	
	g	127.0, qC		
	<i>ortho</i>	130.8, CH	7.04, d (8.4)	
	<i>meta</i>	114.7, CH	6.63, d (8.4)	
	<i>para</i>	155.9, qC		
	OH		9.18, brs	
	CO	165.1, qC		

Note:  $^1H$  (400 MHz),  $^{13}C$  (100 MHz) and  $^{15}N$  (41 MHz)

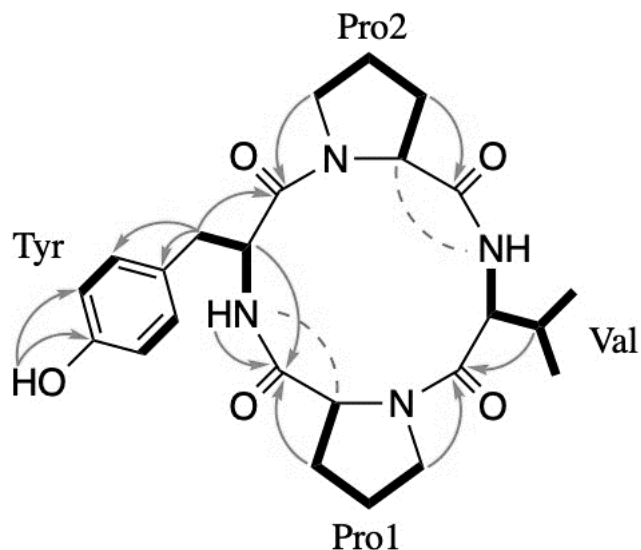


**Figure 3-15.** The proposed structure of massiliamide (**1**) – a novel cyclic tetra-peptide, from *M. albidiflava*.  $^1\text{H}$ - $^1\text{H}$ -COSY /  $^1\text{H}$ - $^{13}\text{C}$ -HSQC-TOCSY (bold lines),  $^1\text{H}$ - $^{13}\text{C}$ -HMBC (arrows) and  $^1\text{H}$ - $^1\text{H}$ -NOESY (dashed lines)

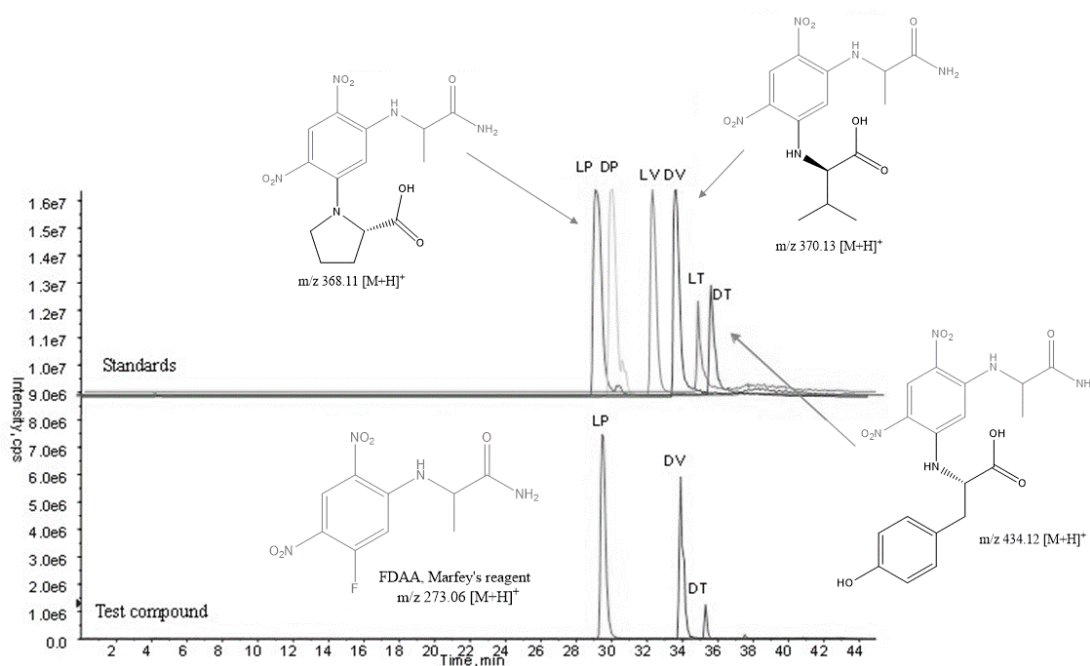


**Figure 3-16.** The absolute configuration of the novel tetrapeptide (**1**) using Marfey's method and LC-MS detection.

To get insight into the absolute configuration of each amino acid present in the compound, we subsequently performed Marfey's analysis, followed by mass spectroscopy analysis. Acid hydrolysis of the peptide followed by LC-MS analysis

of the hydrolysate after the derivatization with Marfey's reagent and comparison of the retention times, together with the mass of each amino acid standard fused to 1-fluoro-2,4-dinitrophenyl-5-L-alanine amide, revealed the D- and L- configuration of all residues. This experiment proved that the proline residues were L-configured while the Tyr and Val units were D-configured (**Figure 3-16**). Based on literature empirical rules,  $^{13}\text{C}$  NMR chemical shift differences between proline  $\beta$  and  $\gamma$  carbon resonances are characteristic of *trans* ( $\Delta\beta\gamma \sim 2\text{--}6$  ppm) vs. *cis* ( $\Delta\beta\gamma \sim 8\text{--}12$  ppm) rotamers, respectively. Thus, the  $^{13}\text{C}$  NMR data indicated that both proline peptide bonds were *trans* configured, as shown by the small chemical shift differences of Pro1  $\Delta\beta\gamma = 6.0$  and Pro2  $\Delta\beta\gamma = 5.8$ , respectively (**Table 3-2**).

Physical analysis of the novel tetrapeptide (**1**) showed amorphous and yellow bright opaque powder. As an optical rotation, a value of  $[\alpha]_{\text{D}_{25}}^{20} -20$  (c 0.040, MeOH) was determined. Absorption peaks in the FT-IR (ATR) spectrum of the novel tetrapeptide (**1**) was observed at 3300, 2950, 1660, 1560, 1410, and 1360  $\text{cm}^{-1}$ , which implied the presence of OH groups, amide bonds, and an aromatic system (as shown in **Supplementary Figure 3-1**).

### 3.4. Biological activities of novel tetrapeptide

The compound was *in vitro* tested for inhibitory activity towards tyrosinase and showed inhibition at a concentration of  $1.15 \pm 1.04$   $\mu\text{M}$ . The result showed a higher potency compared to two available standard tyrosinase inhibitors, which are commonly used as positive controls, i.e., arbutin and kojic acid. Compound **1** also showed higher inhibitory activity compared with a similar tetrapeptide produced by *L. helveticus* (Kawagishi *et al.*, 1993). In cytotoxicity assays, the isolated compound did not display activity against HeLa cells, indicating the potential absence of a cytotoxic effect ( $\text{IC}_{50} > 64$   $\mu\text{g/ml}$ ). In antibacterial assays, the compound showed no activity towards ESKAPE pathogens, such as *Enterococcus faecium*, *Staphylococcus aureus*, *Klebsiella pneumoniae*, *Acinetobacter baumannii*, *Pseudomonas aeruginosa*, and *Enterobacter* cells that commonly cause nosocomial infections (**Table 3-3**).

In conclusion, a new natural product has been isolated from the non-static fermentation of *M. albidiflava* with minimal media containing methionine. It is closely related to a cyclo-tetrapeptide, which was previously discovered in the broth of *Lactobacillus helveticus* and possessed a different absolute configuration. Compound **1** is more active as a tyrosinase inhibitor than the known tetrapeptide produced by *L. helveticus*, arbutin, and kojic acid. Interestingly, the compound has no cytotoxic and no antibacterial activity. This finding is also in agreement with the tetrapeptide hirsutide, a cyclo-L-NMePhe-L-Phe-L-NMePhe-L-Val, produced by *Hirsutella* sp. (Lang *et al.*, 2005). The cyclic tetrapeptide in this research represents, beside massiliachelin, the second secondary metabolite described from the gram-negative bacteria of the genus *Massilia*. The MS-guided approach from various broth extracts of *M. albidiflava* was successful and helped to identify this novel compound.

**Table 3-3.** Biological activity of novel tetrapeptide (**1**) isolated from *M. albidiflava*.

Biological activity	Tetrapeptide ( <b>1</b> ) IC <sub>50</sub> (μM)	Arbutin IC <sub>50</sub> (μM)	Kojic acid IC <sub>50</sub> (μM)
Tyrosinase inhibitor	1.15 ± 1.04	4.22 ± 1.02	37.09 ± 1.01
	<b>MIC (μg/ml)</b>		
Antibacterial			
<i>E. faecium</i> BM 4147-1	> 64		
<i>S. aureus</i> ATCC 2921	> 64		
<i>K. pneumonia</i> ATCC 12657	> 64		
<i>A. baumannii</i> 09987	> 64		
<i>P. aeruginosa</i> ATCC 27853	> 64		
<i>E. aerogenes</i> ATCC 13048	> 64		
<i>E. coli</i> ATCC 25922	> 64		
<i>B. subtilis</i> 168	> 64		
	<b>IC<sub>50</sub> (μg/ml)</b>		
Cytotoxicity			
HeLa cell line	> 64		

### 3.5. Tyrosinase inhibition – a mechanism and its bacterial production

Melanin is the primary brown pigment on human skin. It is produced in melanosomes by melanocytes through a complex process called melanogenesis. The presence of melanin plays an essential role in the skin homeostasis, including protection from ultraviolet radiation and scavenging toxic chemicals or drugs. However, the accumulation of abnormal melanin could induce a hyperpigmented spot that influences esthetic problems. The synthesis of melanin involves several enzymes as mediators, essential in melanocytes. One of them is tyrosinase (EC 1.14.18.1) that utilizes tyrosine as a substrate. It is a copper-containing enzyme that catalyzes the hydroxylation of L-tyrosine to 3,4-dihydroxy-l-phenylalanine (L-dopa), followed by oxidation, resulting in L-dopaquinone. Its quinone is highly reactive and influences the polymerization of melanin, which contributes in turn to the color of human skin.

The regulation of pigment production towards tyrosine by its inhibition is one of the crucial strategies in preventing hyperpigmentation due to the oxidation. Various tyrosinase inhibitors produced by plants (e.g., arbutin), found in food and synthetically developed, such as kojic acid, hydroquinone, azelaic acid, corticosteroid and resinoid. However, these agents have limitations such as a) their high cytotoxicity that could induce skin irritation, b) their insufficient skin penetration, and c) their storage instability.

Many tyrosinase inhibitors have also been discovered from the bacterial broth, such as pure cyclo-tetrapeptide from *L. helveticus* (Kawagishi *et al.*, 1993), the product of agaro-oligosaccharide from the application of beta agarose produced by *Pseudoalteromonas* sp. AG4 (Oh *et al.*, 2010), purified exo-polysaccharide from *L. sakei* Probio 65 (Bajpai *et al.*, 2016), purified lipoteichoic acid isolated from *L. plantarum* (Kim *et al.*, 2008), purified daidzein and equol from fermented soymilk with *L. plantarum* TWK10 (Chang and Tsai, 2016).

On the crude level, the use of *L. plantarum* KCCM 11613P in the fermentation of the *Inula britannica* petal flower also has tyrosinase inhibitor activity (Park *et al.*, 2017). The same activity was also found in fermented milk using *L. plantarum* M23 (Lim and Kim, 2012) and in the spent culture supernatant from *L. rhamnosus* (Tsai *et al.*, 2013).

This natural product potently inhibited tyrosinase *in vitro*, while no sign as either antibacterial or cytotoxicity. Thus, it means that massiliamide appears to be safe to be applied on the skin. The prospect will be to synthesize a similar structure to gain more amount since the pure product was only about 5.1 mg out of 30 L broth containing *M. albidiflava*. The synthetic derivatives could be used for an in-depth *in vivo* study of tyrosinase inhibitors.

## Chapter 4. Unveiling the specialized metabolites from the genus *Telluria* and the discovery of siderophore-like compounds

### 4.1. Bioinformatic analysis of two type strains from the genus *Telluria*

Two type strains of the genus *Telluria*, i.e., *Telluria chitinolytica* and *T. mixta*, possess a genome size of 7.4 and 6.4 Mb, respectively (as shown in **Table 4-1**). The size is typical for the genus *Massilia* and which is similar to bacteria from the genera *Pseudomonas* and *Burkholderia*. Thus, we hypothesized that these members of  $\beta$ -proteobacteria also represent talented producers of bioactive secondary metabolites. In order to support our hypothesis, we steered a genome analysis using the default setting of AntiSMASH v5.0, as shown in **Figure 4-1**.

**Table 4-1.** Genome properties of two type strain from the genus *Telluria*

Strain	Genome size (bp)	G+C content (mol%)
<i>T. chitinolytica</i> ACM 3522 <sup>T</sup>	6,387,078	66.27
<i>T. mixta</i> DSM 29330 <sup>T</sup>	7,444,617	65.92

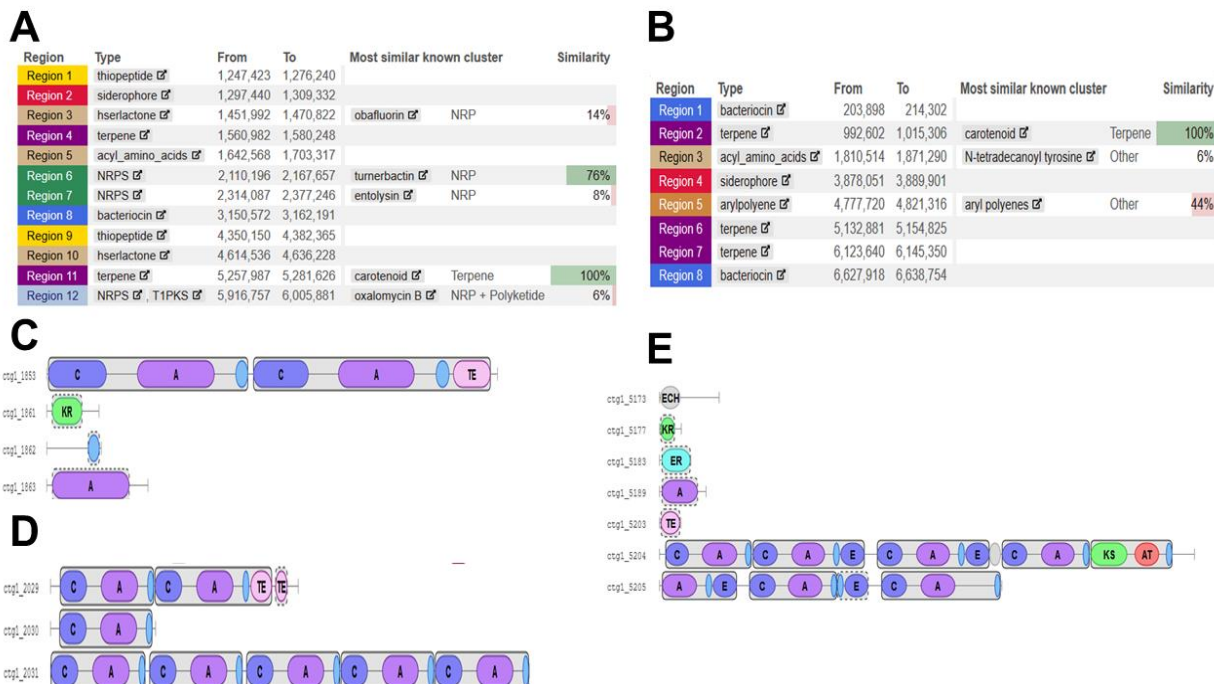


**Figure 4-1.** Number BGCs of the genus *Telluria* through the default setting analysis from AntiSMASH v5.0 (a) *T. chitinolytica*; (b) *T. mixta*; (c) (d) and (e) NRPS regions 6 and 7 and NRPS-hybrid region 12, respectively, from *T. chitinolytica*.

The genomic analysis predicted 12 and 8 BGCs for *T. chitinolytica* and *T. mixta*, respectively. Both strains are bioinformatically designated as carotenoid (terpene) producers whose BGC's showed 100% similarity against the database as a result of previously described *Massilia*. *T. chitinolytica* was predicted to produce two types of NRPS and 1 type NRPS hybrid-like compound. However, these types of natural product clusters could not be predicted in *T. mixta* (**Figure 4-1**). Both strains also were predicted to be siderophore producers.

#### 4.2. Chemical investigation employing the OSMAC approach

A subset of two type strains from the genus *Telluria* was used for metabolic profiling through 2.5 L- scale fermentation in various types of the media. After 72 hours of fermentation, we extracted all the broth containing strain with resin and subjected the extract to low-resolution LC-MS. The screening dereplicated various known dipeptides and DHB-ornithine-serine (DOS). However, the analysis of the low-resolution LC-MS profile of *T. chitinolytica* grown in minimal broth contained various novel masses, as shown in **Table 4-2** and **4-3**. Without shaking, only dipeptides were detected. Thus, we further initiated an up-scaled fermentation of the two strains in optimized media with shaking.

**Table 4-2.** Low-resolution LC-MS screening results based on the positive mode of the investigated strains cultivated in 2.5 L media with shaking.

No	Bacterial strains	Medium						
		SBM	Modified SBM	Modified DMB I	DMBGly	MM9	LB	R2A
1	<i>T. chitinolytica</i>	DOS, peptide, 1409, 1433, 1425, 1245, 1167, 430, 444, 452, 701.	dipeptide, DOS, ulbactin A, 656, 670, 637.	dipeptide	dipeptide	-	dipeptide	dipeptide
2	<i>T. mixta</i>	DOS, phthalate, phenylactic acid	dipeptide	dipeptide	-	-	dipeptide	-

\*number in m/z

**Table 4-3.** Low-resolution LC-MS screening results based on the positive mode of the investigated strains cultivated in 2.5 L media without shaking.

No	Bacterial strains	Medium						
		SBM	Modified SBM	Modified DMB I	DMBGly	MM9	LB	R2A
1	<i>T. chitinolytica</i>	dipeptide	dipeptide	-	-	-	dipeptide	dipeptide
2	<i>T. mixta</i>	-	-	dipeptide	-	dipeptide	-	-



### 4.3. The isolation and purification of serratiochelin C and its derivatives

A total amount of twenty sterilized 5 L Erlenmeyer flasks, each containing 2.5 L SBM medium, equaling a sum of 50 L, was used for the compound's production. The supernatant was then extracted with Diaion® HP 20 resin. The crude was then subjected to HR-ESI-MS and analyzed using GNPS based molecular networking, as shown in **Figure 4-2**. The remaining crude was then partitioned into water and MeOH using the VLC system. Fractions from A to E were acquired, each differing in its MeOH/water content (A: 10/90, B 25/75, C 50/50, D 75/25, E 100/0), as the fractionation procedure began with 10:90 MeOH/water mixture.

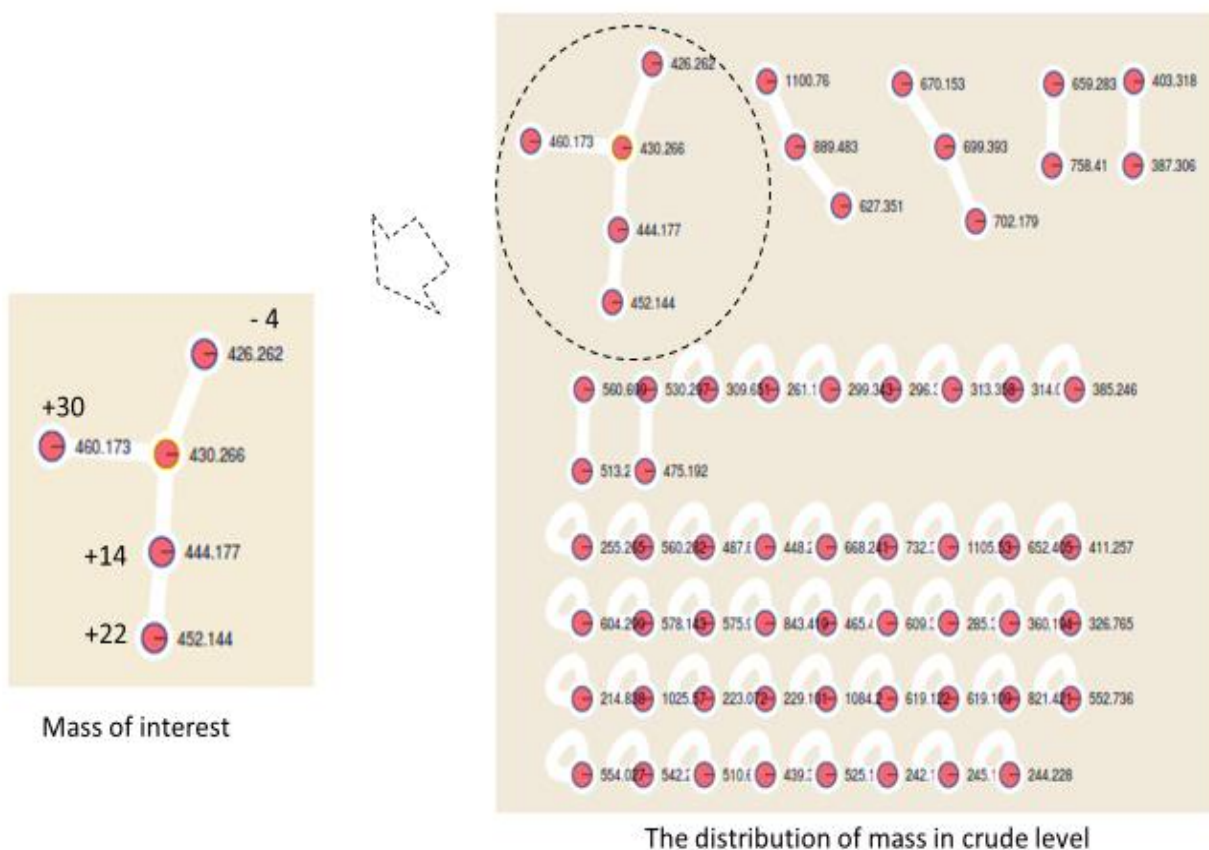


**Figure 4-2.** Mass distribution on crude extract level of SBM broth-containing *T. chitinolytica* analyzed by GNPS.

Faction D, which contained the compound of interest, was then subjected to RP-HPLC, equipped with a Luna Omega Polar C18 5  $\mu\text{m}$  100  $\text{\AA}$  250 x 4.6 mm column followed by Aeris C18 3.6  $\mu\text{m}$  100  $\text{\AA}$  250 x 4.6 mm column to afford pure compound (**Figure 4-3**).

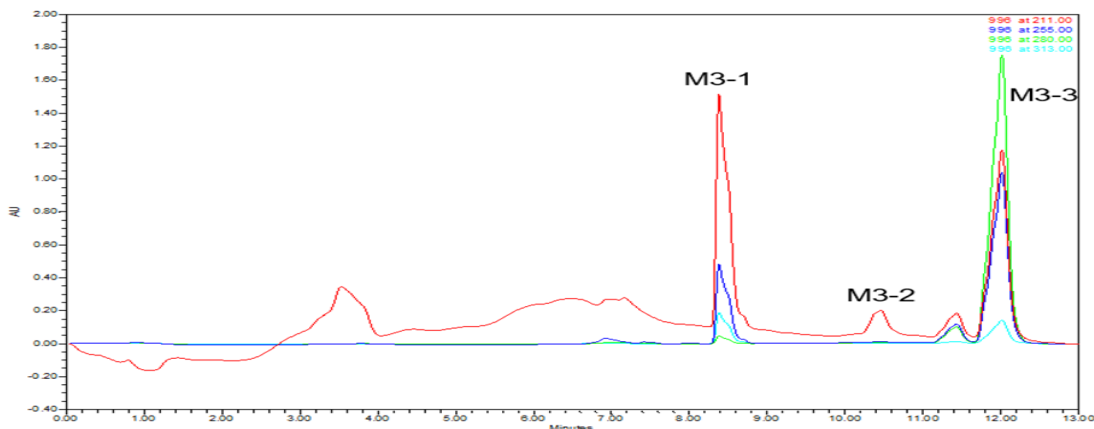


**Figure 4-3.** HPLC chromatogram of fraction D containing serratiochelin C produced by *T. chitinolytica* ( $t_R = 9.7$  min).

The mass of these compounds is  $m/z$  ( $[M+H]^+$ ) 430.1603, 444.1766, and 452.1430 for M3-1 (serratiochelin C), M3-2, and M3-3, respectively as shown in **Figure 4-4**.

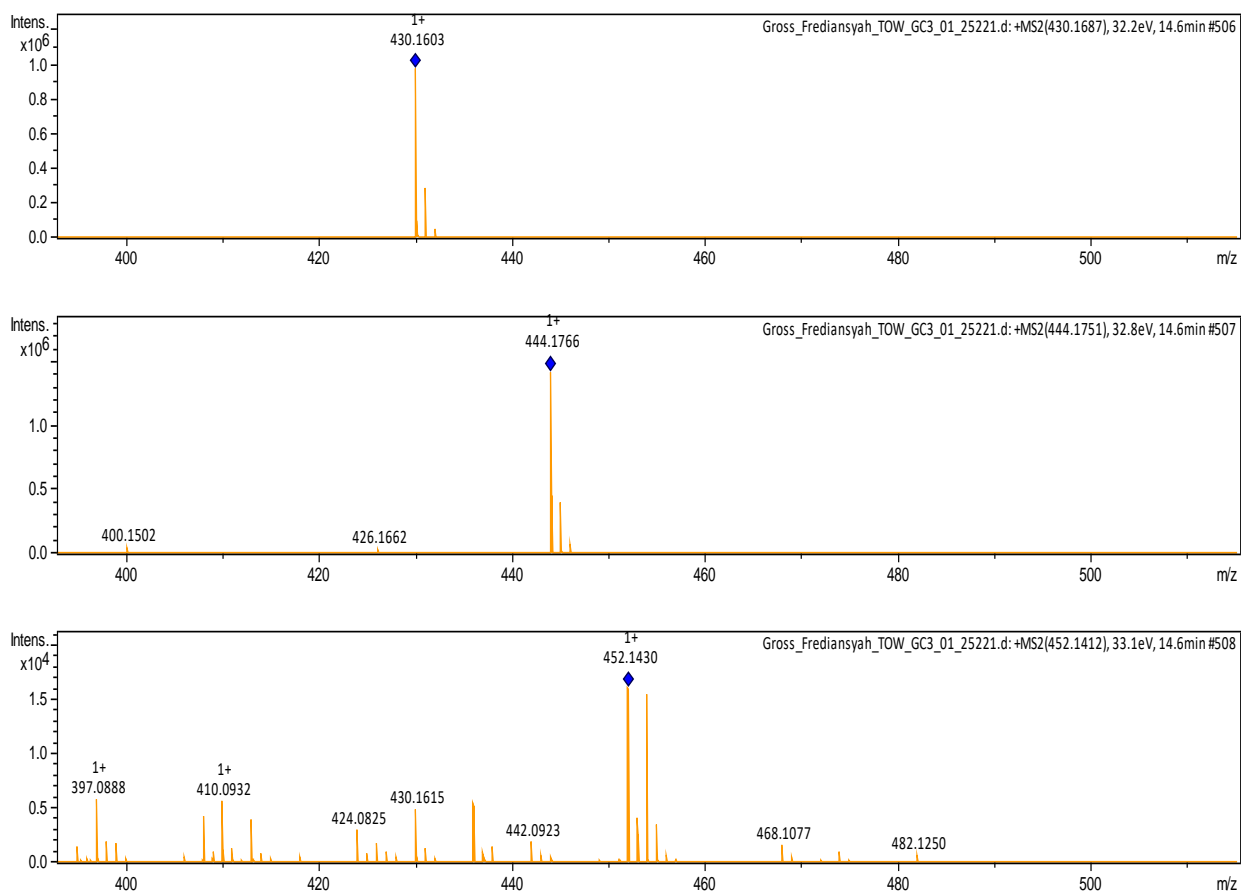


**Figure 4-4.** MS<sup>2</sup> spectra of M3-1, M3-2, and M3-3 from above to below, respectively.

As we believed that these three compounds represent siderophores, we then conducted a CAS assay as a preliminary confirmation. These peaks produced a positive result compared to broth extract as a negative control (**Figure 4-5**).

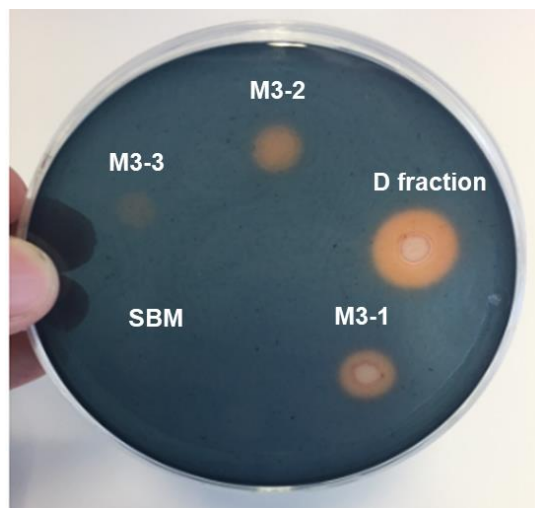


**Figure 4-5.** CAS assay of M3-1, M3-2, M3-3, fraction D, and SBM broth extract.

However, out of 40 L extract, only the amount of M3-1 was sufficient for structure elucidation through NMR. Fractions M3-2 and M3-3 were only obtained in quantities below 1.5 mg. Final purification of the compound M3-1 yielded 5.2 mg of serratiochelin C as a purple opaque solid.

All  $^1\text{H}$ - and  $^{13}\text{C}$ -NMR shifts were assigned using DEPT-135, COSY, NOESY, HSQC, and HMBC. In addition,  $^1\text{H}$ - $^{15}\text{N}$  NMR was assigned using a non-calibrated HSQC NMR experiment.

Overall, the  $^1\text{H}$ -NMR resonances (as shown in **Figure 4-6**) ranged from 1.38 to 12.70 ppm and exhibited aromatic protons at  $\delta_{\text{H}}$  6.68 to 7.40. The use of  $\text{DMSO-}d_6$  solvent for  $^1\text{H}$ -NMR experimentation bare the presence of three amidic protons ( $\delta_{\text{H}}$  8.40, 8.68, and 8.76) and four hydroxyl groups ( $\delta_{\text{H}}$  9.17, 9.51, 10.19, and 12.70).

The  $^{13}\text{C}$ -NMR signals (as shown in **Figure 4-7**) 21 signals were detected from 16.32 to 169.80 ppm. The spectra also suggested the manifestation of three carbonyls, which were  $\delta_{\text{C}}$  165.64, 168.08, and 169.80 ppm. The presence of resonances from 113.01 up to 149.60 ppm suggested that the compound contains two six-membered rings.

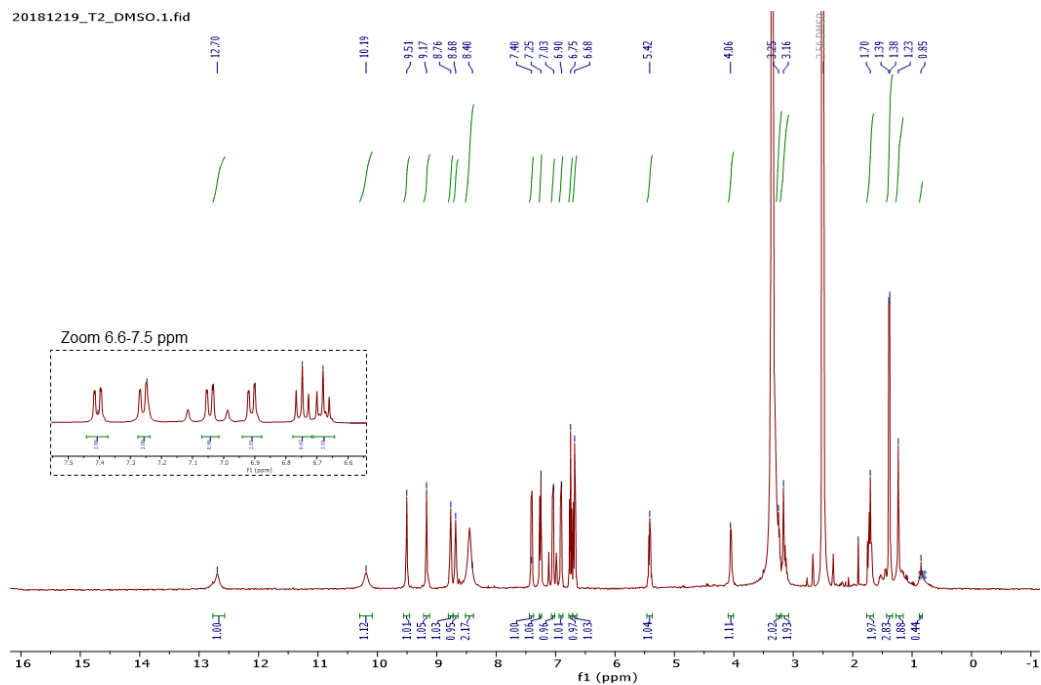


**Figure 4-6.**  $^1\text{H}$ -NMR spectrum of serratiochelin C in  $\text{DMSO-}d_6$ , 400 MHz.

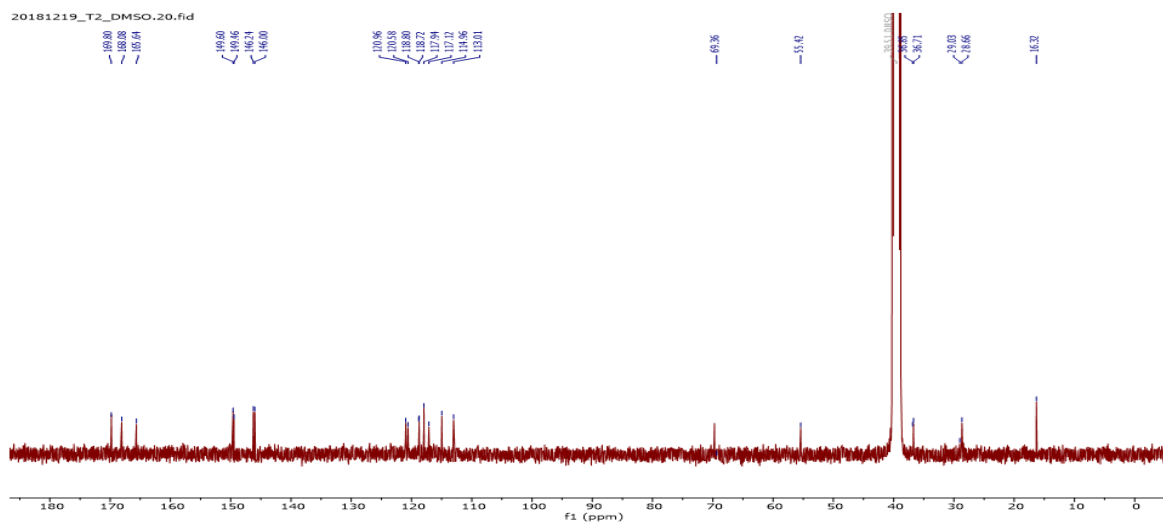


**Figure 4-7.**  $^{13}\text{C}$ -NMR spectrum of serratiochelin C in  $\text{DMSO-}d_6$ , 100 MHz.

Based on a DEPT-135 NMR experiment (**Figure 4-8**), only three carbon resonances have been assigned as methines, besides one methyl and seven methylene groups. The remaining carbons were found to be quaternary carbon. Except for quaternary carbons,

the correlation of primary protons chemical shift to the  $^{13}\text{C}$  chemical shift of their directly attached carbon was assigned by the  $^1J_{\text{CH}}$  coupling observed in an edited HSQC NMR spectrum (**Figure 4-9**).

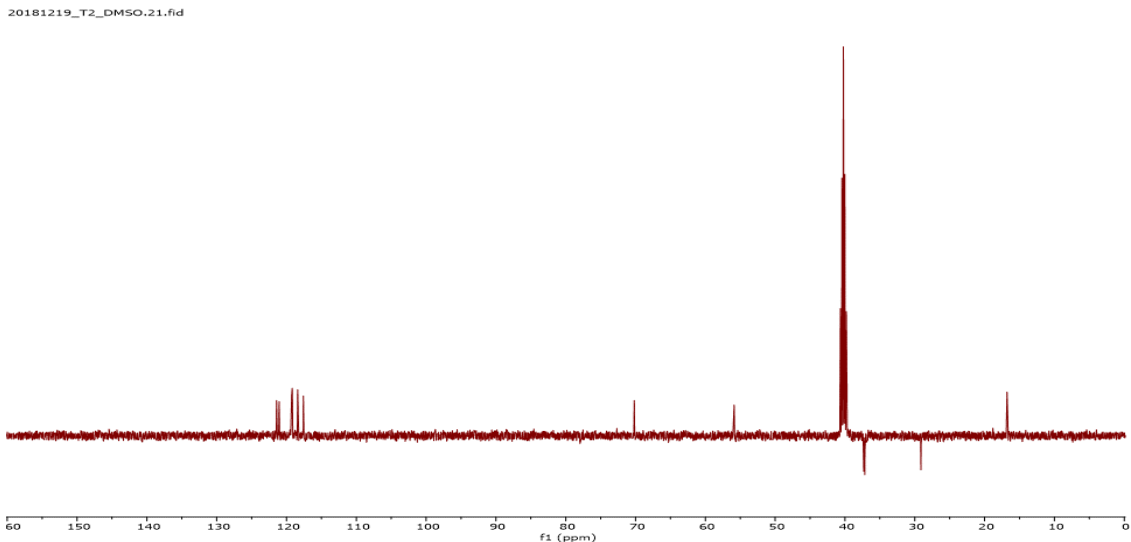


**Figure 4-8.** DEPT-135 spectrum of serratiochelin C in  $\text{DMSO-}d_6$ , 400 MHz.

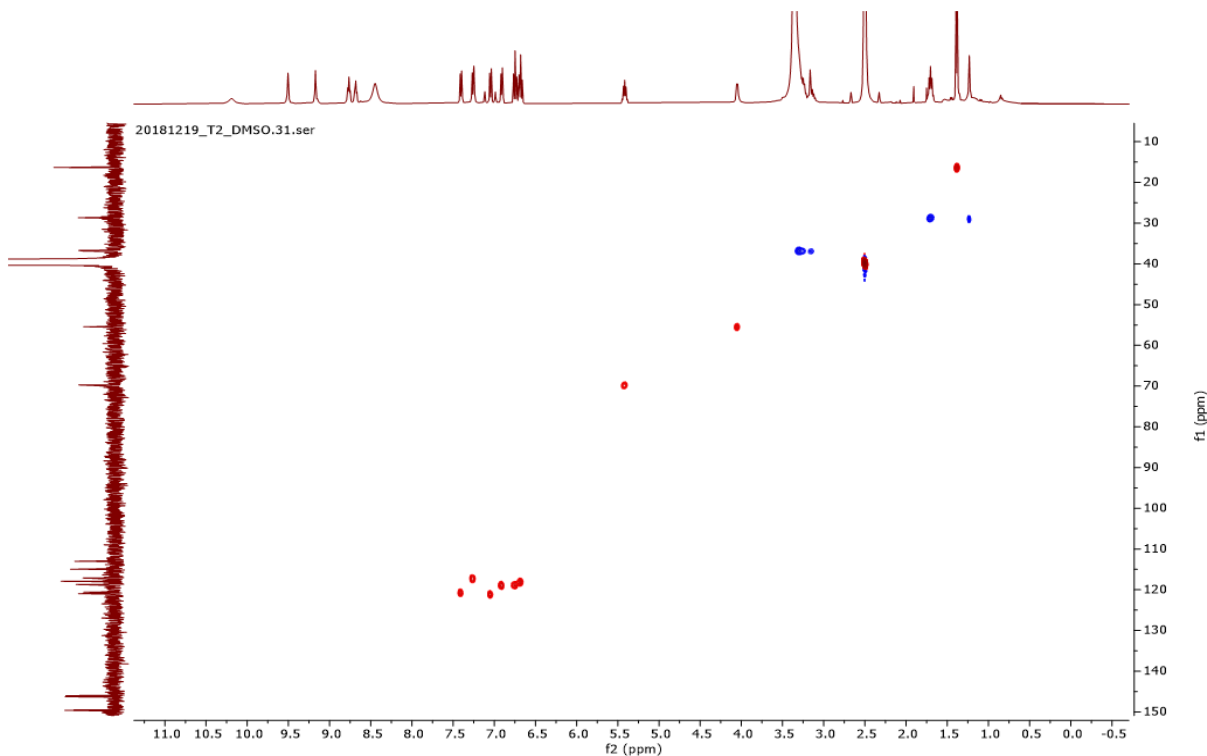


**Figure 4-9.**  $^1\text{H-}^{13}\text{C}$  HSQC of serratiochelin C in  $\text{DMSO-}d_6$ , 400 MHz.

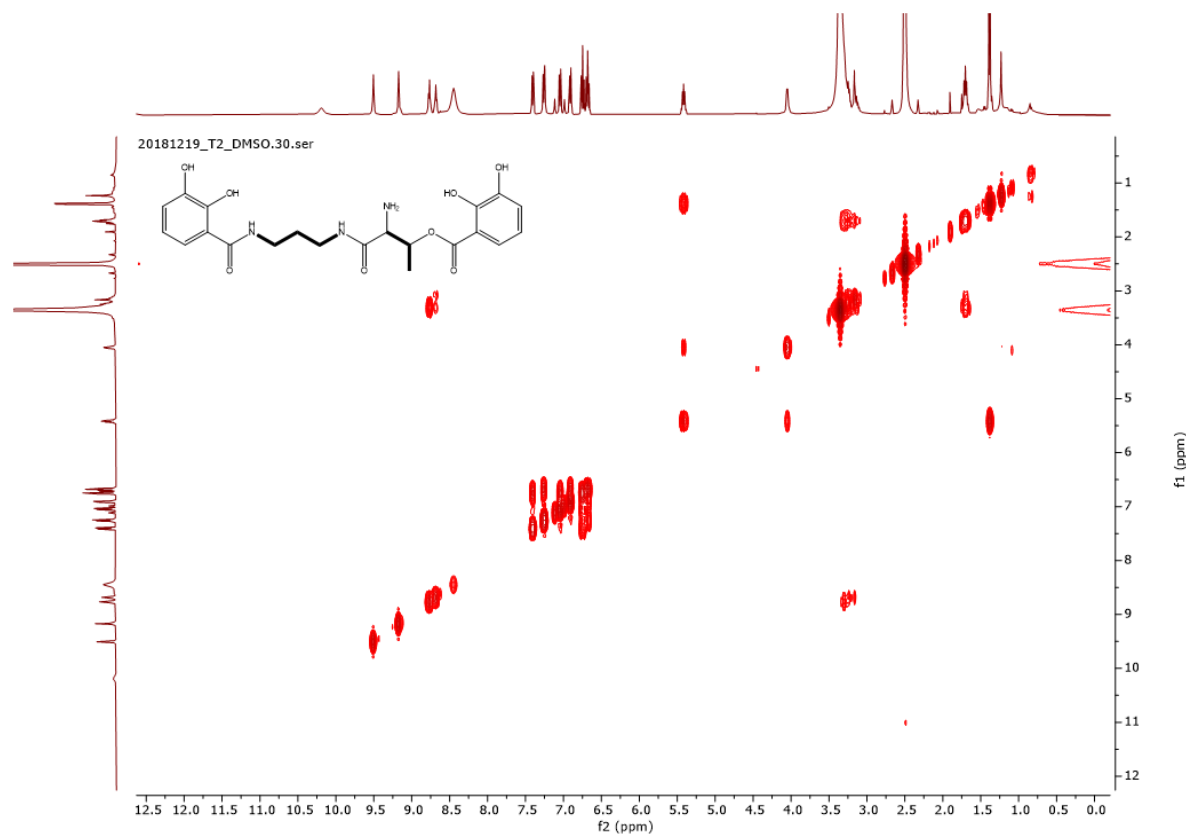


Figure 4-10.  $^1\text{H}$ - $^1\text{H}$  COSY of serratiochelin C in  $\text{DMSO-}d_6$ , 400 MHz.

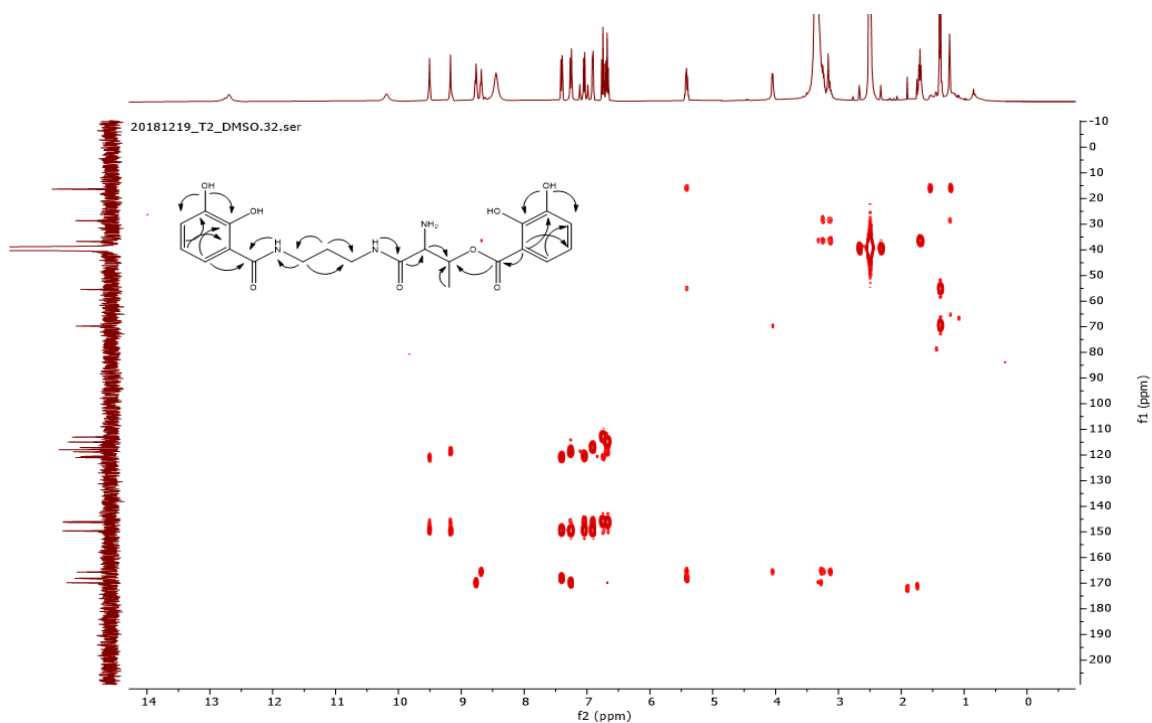
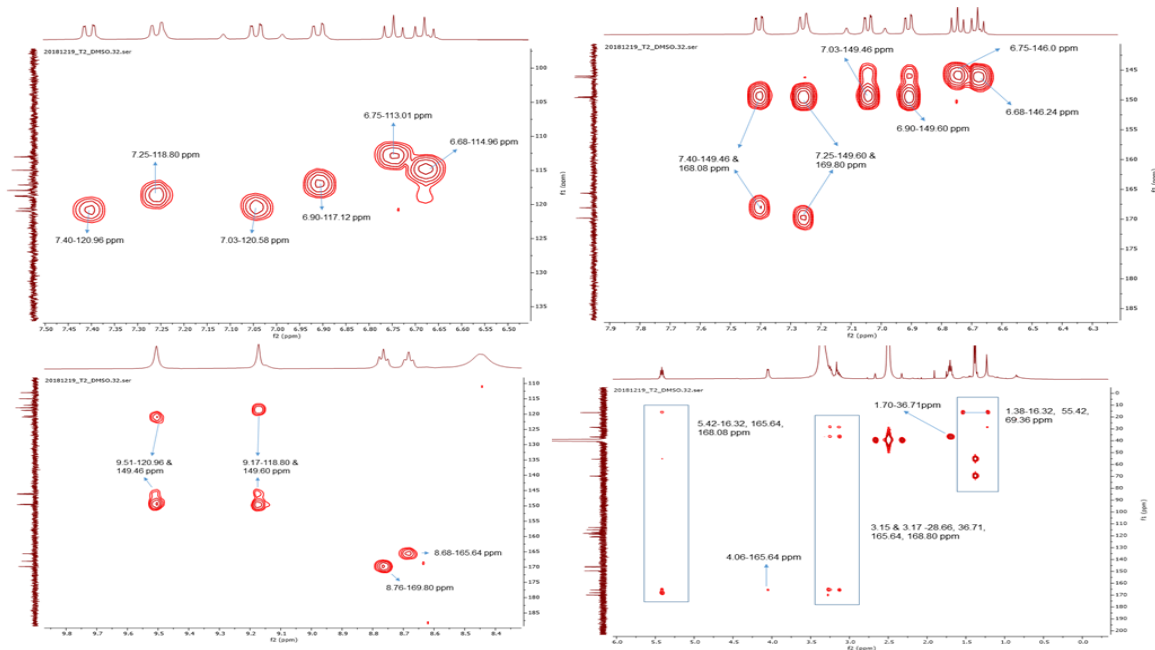
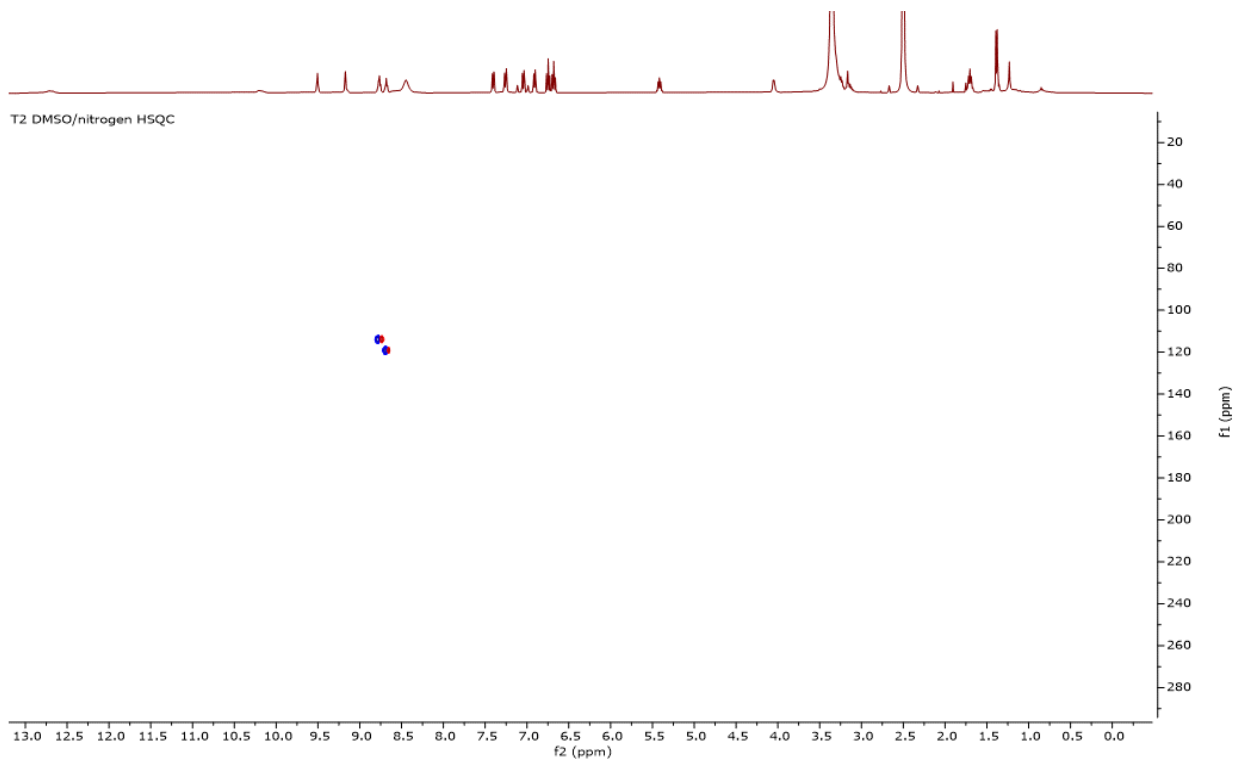


Figure 4-11.  $^1\text{H}$ - $^{13}\text{C}$  HMBC NMR of serratiochelin C in  $\text{DMSO-}d_6$ , 400 MHz.



**Figure 4-12.**  $^1\text{H}$ - $^{13}\text{C}$  HMBC NMR (with different zoom area) of serratiochelin C (1) in  $\text{DMSO-}d_6$ , 400 MHz.



**Figure 4-13.**  $^1\text{H}$ - $^{15}\text{N}$  HSQC NMR spectrum of serratiochelin C in  $\text{DMSO-}d_6$ , 400 MHz.

Therefore, the isolated compound has no agreement with the predicted molecular formula  $C_{21}H_{24}N_3O_7$  (HR-ESI-MS with  $m/z$  of 430.1063  $[M + H]^+$ , calc. for 430.1063,  $\Delta$  1.2 ppm, rdb. 12). The confirmation has also been conducted using various de-clustering potential in low-resolution LC-MS but always showed the same mass as HR-ESI-MS (**Supplementary Figure 4-1**). Thus, we believed that the compound formed a hydrate motive during the NMR analysis and was only present as its form during LC-MS analysis. Thus, the compound was still rebuttal as serratiochelin C based on NMR analysis, as shown in **Figure 4-15**. The comparison of M3-1 with published NMR shifts of serratiochelin C and B is shown in **Table 4.4**. Schneider *et al.* 2020 experienced a similar situation with the mass of serratiochelin C that was produced by the co-culture of *Serratia* sp. and *Shewanella* sp. They explained that serratiochelin C is present in an apo form and possess the ability to lose relatively easy during ESI-MS, especially in positive mode, and acquired two hydrogens (-16 dalton). However, our findings showed that serratiochelin C loss of water in both ESI positive and negative.

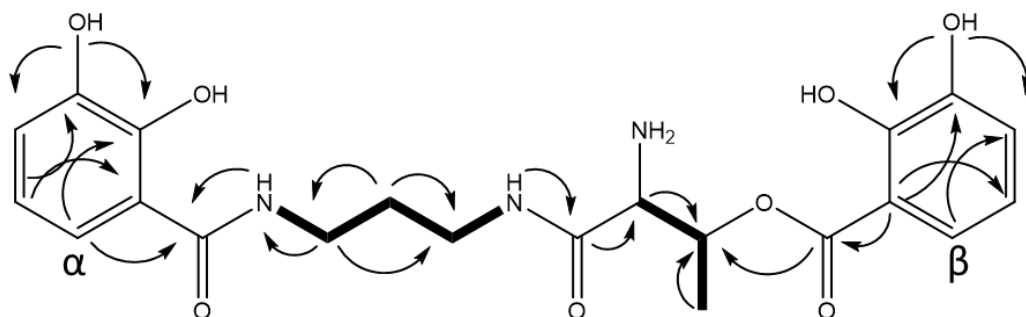


**Figure 4-15.** The proposed structure of serratiochelin C (1) – an NRPS-dependent siderophore from *T. chitinolytica*.

However, the number of ppm either proton and carbon and MS results are different from the published serratiochelin C from Seyedsayamdost *et al.* 2012 and Schneider *et al.* 2020, as shown in **Table 4-4**. It might represent a different stereochemistry or a different molecule organization.



**Table 4-4.** NMR spectroscopic data for serratiochelin C in DMSO-*d*<sub>6</sub> and MeOH-*d*<sub>4</sub>.

Unit	Serratiochelin C in MeOH- <i>d</i> <sub>4</sub> *		Serratiochelin in DMSO- <i>d</i> <sub>6</sub> *		M3-1 in DMSO- <i>d</i> <sub>6</sub> **		M3-1 in MeOH- <i>d</i> <sub>4</sub> **		Serratiochelin B in MeOH- <i>d</i> <sub>4</sub> *	
<b>DhB-α</b>	113.4	-	114.92	-	113.0	-	113.6	-	114.0	-
	150.9	-	149.81	-	149.6	-	151.5	-	153.9	-
	146.8	-	146.27	-	146.2	-	147.4	-	153.9	-
	122.0	7.03 dd	118.65	6.89, dd (7.8, 1.5)	118.7	6.90 dd	118.8	6.91dd	111.8	6.68 dd
	120.1	6.75 t	117.84	6.66, t (8.0)	118.8	6.75 t	120.4	6.75 t	118.1	6.57 t
	121.7	7.48 dd	117.04	7.25, dd (8.2, 1.5)	117.1	7.25 dd	122.4	7.45 dd	118.0	7.14 dd
	170.1	-	169.73	-	169.8	-	170.6	-	169.4	-
<b>DhB-δ</b>	116.3	-	116.77	-	115.0	-	116.6	-	114.0	-
	150.0	-	149.81	-	150.0	-	150.4	-	153.6	-
	147.0	-	146.12	-	146.0	-	147.5	-	153.6	-
	119.4	6.93 dd	118.19	6.92 dd (7.7, 1.5)	121.0	7.03 dd	119.8	6.75 dd	111.6	6.66 d
	119.4	6.71 t	117.77	6.69 t (7.9)	118.0	6.68 t	121.9	6.68 t	117.9	6.55 t
	118.4	7.22 dd	118.92	7.37, dd (8.1, 1.6)	120.6	7.40 dd	122.4	7.19 dd	117.9	7.11 dd
	171.4	-	168.01	-	168.1	-	171.9	-	169.2	-
<b>Thr</b>	71.3	5.65 dq	66.38	4.10 qd (6.1, 4.7)	69.4	5.42	70.7	5.63 t	68.1	4.31 m
	57.6	4.22 m	59.18	4.34, dd (8.0, 4.4)	55.4	4.09	58.3	4.12 d	60.6	4.44 d
	167.3	-	169.99	-	165.6	-	167.7	-	173.2	-
	16.8	1.53 d	20.30	1.09, d (6.4)	16.3	1.38/1.39	17.6	1.53 dd	20.1	1.25 d
<b>Diamine</b>	38.0	3.38 m, 3.37 m	36.58	3.29 q (6.7)	36.9	3.16 m	36.4	3.14 m	37.9	3.33 m
	29.7	1.79 dtd	28.96	1.67 p (7.0)	28.7	1.70 t	28.6	1.78 t	30.4	1.83 q
	37.4	3.43 m, 3.35 m	36.41	3.20-3.08 m	36.7	3.15 m	36.5	3.15 m	37.5	3.46 t

\*  $\delta_C$  and  $\delta_H$  (J in Hz) from publication (in MeOH-*d*<sub>4</sub> by Seyedsayamdost *et al.* 2012, in DMSO-*d*<sub>6</sub> by Schneider *et al.* 2020)

\*\*  $\delta_C$  and  $\delta_H$  (J in Hz) from the thesis produced by *T. chitinolytica*

#### 4.4. Biosynthesis proposal of serratiochelin C from *T. chitinolytica*.

The whole-genome sequenced of *T. chitinolytica* was screened for the BGC that is responsible for siderophore production. We analyzed using AntiSMASH v5.0, as shown in **Figure 4-16**. Interestingly, we found an NRPS-dependent siderophore BGC in cluster 6 within the genome of *T. chitinolytica*.

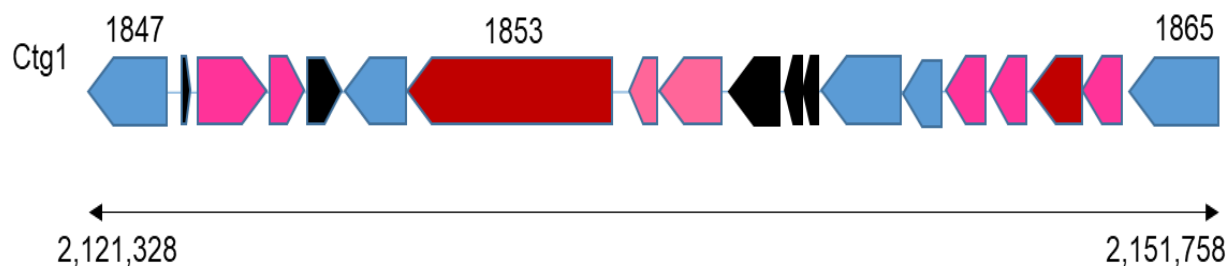


**Figure 4-16.** BGCs projection from nucleotide 2,121,328 to 2,151,758 from *T. chitinolytica*.

The details of the putative function have been assigned using NCBI Blast protein from these presented genes, as shown in **Table 4.5**

**Table 4-5.** BCG contains putative NRPS-dependent siderophore.

<b>Locus tag</b>	<b>Size (AA)</b>	<b>Putative function</b>	<b>Strains</b>	<b>% similarity</b>
Ctg1_1847	760	TonB-dependent siderophore receptor	<i>Massilia</i> sp. YMA4	100
Ctg1_1848	90	hypothetical protein	<i>Massilia armeniaca</i>	93
Ctg1_1849	750	NAD-dependent epimerase/dehydratase	<i>M. armeniaca</i>	100
Ctg1_1850	355	acyltransferase	<i>M. armeniaca</i>	90.2
Ctg1_1851	303	DUF72 domain-containing protein	<i>M. armeniaca</i>	94.3
Ctg1_1852	420	transporter	<i>M. armeniaca</i>	95.7
Ctg1_1853	2392	non-ribosomal peptide synthetase	<i>M. plicata</i>	99
Ctg1_1854	73	MbtH family NRPS accessory protein	<i>M. buxea</i>	99
Ctg1_1855	396	enterochelin esterase	<i>M. armeniaca</i>	89
Ctg1_1856	549	PepSY domain-containing protein	<i>M. armeniaca</i>	100
Ctg1_1857	97	hypothetical protein	<i>M. armeniaca</i>	94.8
Ctg1_1858	84	hypothetical protein	<i>Massilia</i> sp. YMA4	91.7
Ctg1_1859	1033	multidrug efflux RND transporter permease subunit	<i>Massilia</i> sp. YMA4	96
Ctg1_1860	385	efflux RND transporter periplasmic adaptor subunit	<i>Massilia</i> sp. YMA4	94
Ctg1_1861	277	2,3-dihydro-2,3-dihydroxybenzoate dehydrogenase	<i>Massilia</i> sp. YMA4	99
Ctg1_1862	289	isochorismatase	<i>M. armeniaca</i>	92

Ctg1_1863	537	(2,3-dihydroxybenzoyl)adenylate synthase	<i>M. armeniaca</i>	92.9
Ctg1_1864	380	isochorismate synthase	<i>M. armeniaca</i>	91
Ctg1_1865	655	TonB-dependent receptor	<i>M. armeniaca</i>	93.64

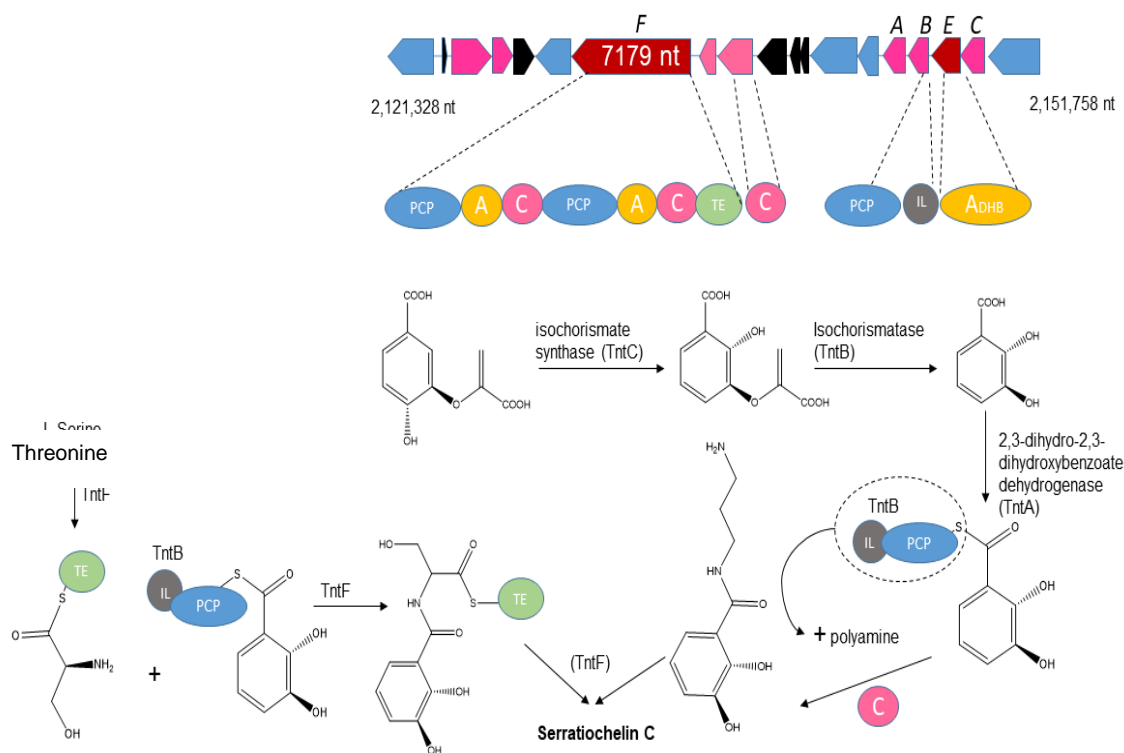


**Figure 4-17.** Proposed biosynthesis of serratiochelin C based on whole-genome analysis of *T. chitinolytica*.

As shown in **Figure 4-17**, chorismate is converted into 2,3-dihydro-2,3-dihydroxybenzoate (DHB) through enzymatic reactions catalyzed by TntC, TntB, TntA, and TntE. Followed by activation, using a 2,3-dihydroxy benzoyl adenylate synthase, then loaded onto a peptidyl carrier protein of TntB for incorporation into the nascent peptide chain. L-serine is also activated by the adenylation domain of TntF and loaded onto the thiolation domain. The condensation domain is responsible for incorporating intermediate molecules with a polyamine. Thus, via TntF of the NRPS system, these intermediates are incorporated into new molecules called serratiochelin C.

#### 4.5. Biological activity and CAS-assay of purified serratiochelin C.

**Table 4-7.** Biological activity of serratiochelin C isolated from *T. chitinolytica*.

Antibacterial activity	MIC ( $\mu\text{g/ml}$ ) *
<i>Pseudomonas aeruginosa</i> DSM 50071	60.68
<i>Paenibacillus</i> sp. AD64	53.07
<i>Staphylococcus aureus</i> USA300 LAC	18.86

\*see in **Supplementary Figure 4-1**

Serratiochelin C (M3-1) showed CAS activity. Thus, those rendered as siderophore members of compounds, as shown in **Figure 4-5** and **Figure 4-30**. Serratiochelin C is belonging to bis-catecholate siderophores and may be tetra- or hexadentate. Some siderophores also could be acted as an antibiotic. Colibactin has also known as an antibiotic against some bacteria (Faïs *et al.*, 2018). The previous study conducted by Jiao *et al.* 2020, showed that trinickiabactin has antibacterial activities toward gram-negative cells. In this study, as shown in **Table 4-7**, serratiochelin C has activities against gram-negative and gram-positive cells in the group of *Pseudomonas*, *Paenibacillus*, and *Staphylococcus*. However, the MIC values are more than 15  $\mu\text{g/ml}$ . This finding is relevant to a study conducted by Schneider *et al.* (2020). They found that serratiochelins either A and C produced from co-culture of *Serratia* sp. and *Shewanella* sp. showed antibacterial activities against *Coliform*, *Pseudomonas*, and *Staphylococcus* spp. However, the best activity was detected towards *S. aureus*. In addition, these two compounds also showed anticancer activities.

## Chapter 5. Production and physiological function of acyl-homoserine lactones from the genera of *Massilia* and *Telluria*

### 5.1. Multiple genome comparison

At the time of analysis, only six complete genome sequences were publicly available -at assembly-level from the NCBI database for the genera *Massilia* and *Telluria*, such as *Massilia* sp. NR 4-1, *Massilia* sp. WG5, *Massilia* sp. YMA4, *M. putida* 6NM-7T, *M. violaceinigra* B2, *M. oculi*, and *M. armeniaca*. In previous work, we conducted the genome sequencing of six type strains from the genus *Massilia* and two type strains from the genus *Telluria* to get a deep insight into the genomic organization and the content. The size of the genomes varied from 5.88 to 7.50 Mb, and the GC content was, on average 65.55 % (**See chapters 3 and 4**). The genomic comparison of these eight strains was performed using BRIG in circular visualization (**Figure 5-1**). The innermost ring shows the GC skew (purple and green) and the GC content (black). The third innermost ring shows the *Telluria mixta* genome followed by *T. chitinolytica*, *M. albidiflava*, *M. dura*, *M. flava*, *M. lutea*, *M. plicata*, and *M. umbonata*, respectively. They shared almost similar genes within each other that can be visualized in the pan-genome.

### 5.2. Phylogenetic relationship and the assessment of genome similarity using ANI and *isDDH*.

The relationship between each strain of *Massilia* and *Telluria* can be analyzed through the phylogenetic tree using the neighbor-joining with Tamura-Nei pairwise distance based on the 16S rRNA gene sequence and the sequence of a gene involved in the central metabolism. To get a more conserved selection, we used various functional genes that are present in our  $\beta$ -proteobacterial strains. We used nine-combined housekeeping gene *gyrA*, *gyrB*, *dnaK*, *radA*, *rpoD*, *metG*, *ileS*, *ftsZ*, and *lepA*. These genes also have been used in numerous taxonomical studies and represent conserved genes (Forsythe *et al.*, 2014; Cusick *et al.*, 2015; Jans *et al.*, 2016). We also conducted a phylogenetic tree using *rhtB* and *luxQ* that stand for homoserine lactone efflux RhtB and autoinducer two sensor kinase/phosphatase LuxQ, respectively. *T. chitinolytica* and *T. mixta* were clustered together based on 16S rRNA and *luxQ* gene (**Figure 5-2A and C**) but not in a

phylogenetic tree conducted using a concatenated sequence of nine housekeeping genes and the *rhtB* gene (**Figure 5-2B and D**). The taxonomical position of all bacteria used in our study was compared with other bacteria of the genera *Massilia* and *Telluria*, employing the neighbor-joining method (**Supplementary Figure 5-1**).

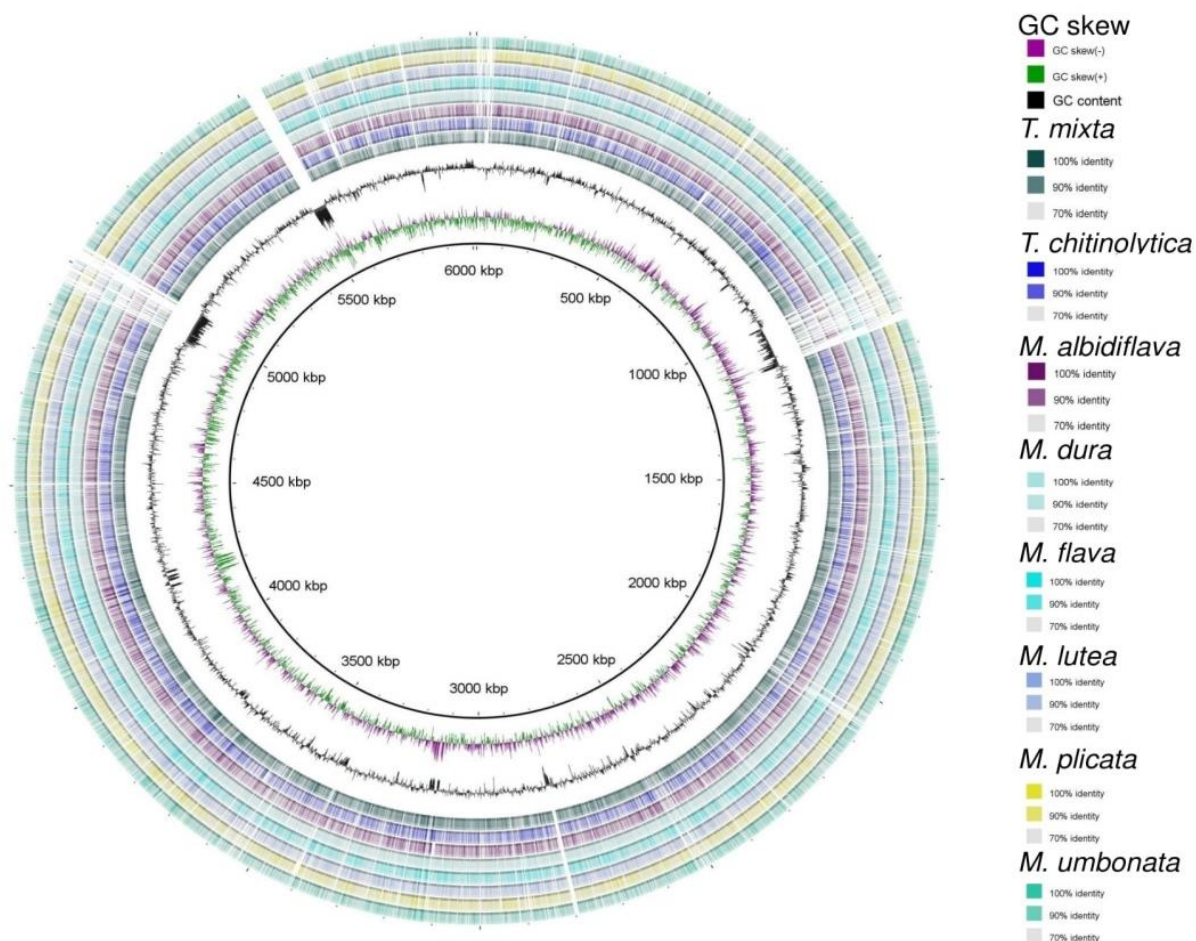


**Figure 5-1.** BRIG visualization from multiple genome comparisons of the genus *Massilia* and *Telluria*. A circular presentation of genome comparison of six type strains from *Massilia* and two strains from *Telluria* was generated using BRIG after performing a BLASTN.

The information provided from the phylogenetic analyses provided an insightful depiction of the evolutionary relationship among bacteria in our study, however, did not translate directly into the overall similarity of the genomes, which can be determined through DNA-DNA hybridization (DDH). Thus, we used two different *in silico* approaches, *isDDH*, and ANI (average nucleotide identity), to evaluate the genomic similarity among  $\beta$ -

proteobacteria in our study. We also assessed the congruence of both approaches. ANI values with a cut off more than 96% shows the same species, *isDDH* values with cutoff 70% displays similar species. The predicted point estimates of the *isDDH* values were obtained for all eight strains and were below 90%, which means these strains are different species. It was also proven by ANI value analysis, which gave values lower than 40% for all the bacteria in this study.

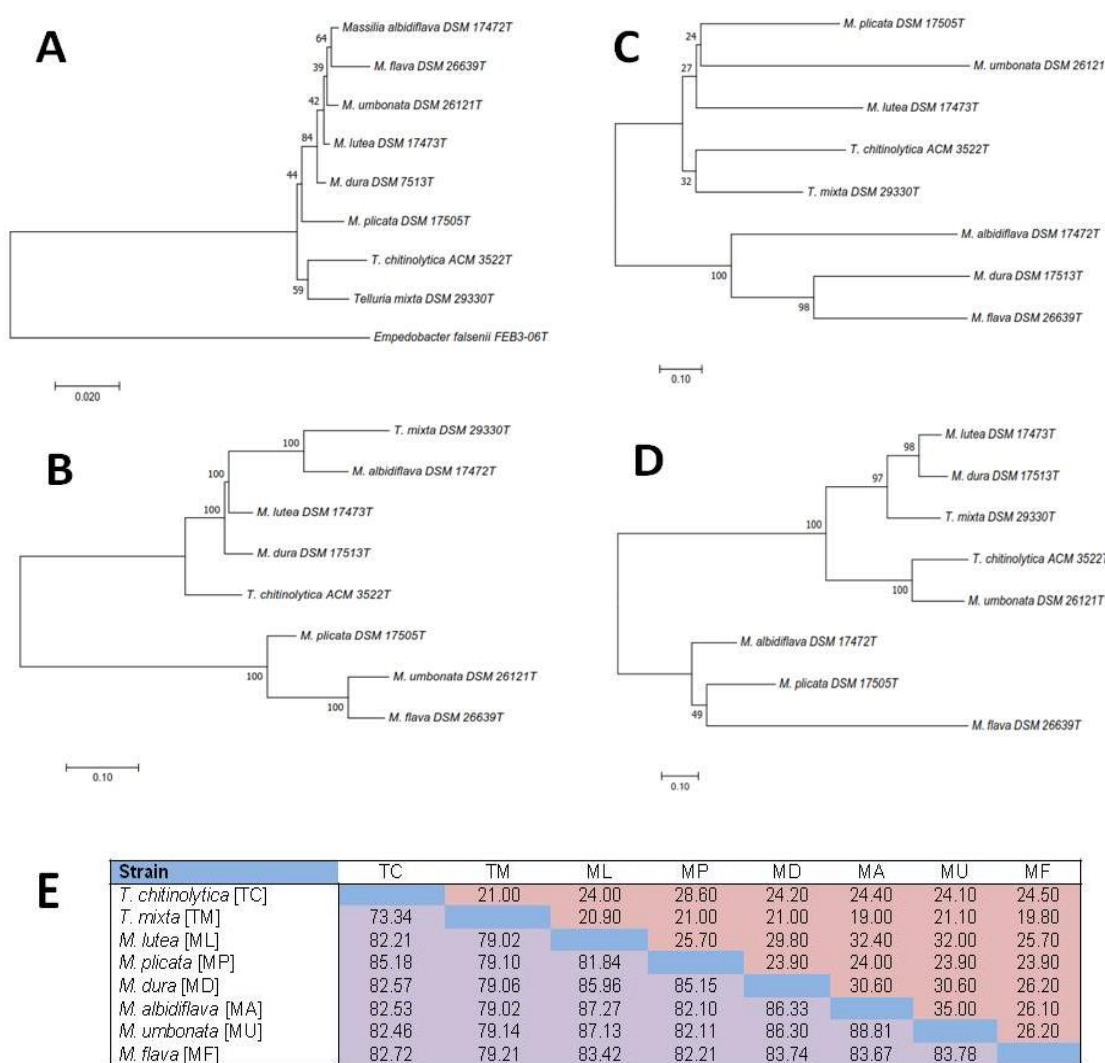


**Figure 5-2.** Phylogenetic tree and genome similarity based on ANI and *isDDH* within the genus *Massilia* and *Telluria*. A phylogenetic interference has been set up based on the neighbor-joining coupled with Tamura-Nei pairwise distance, and 1000 bootstrap replicates for *T. chitinolytica*, *T. mixta*, *M. lutea*, *M. albidiflava*, *M. flava*, *M. umbonata*, *M. dura*, *M. plicata*, *M. lutea*. The phylogenetic tree was constructed bases on (A) 16S rRNA using *Empedobacter falsenii* FEB3-06T as an outgroup (B) concatenated sequence of 9

housekeeping genes, including *gyrA*, *gyrB*, *dnaK*, *radA*, *rpoD*, *metG*, *ileS*, *ftsZ*, and *lepA* (C) *luxQ* gene (D) *rhtB* gene (E) ANI and *isDDH* values of *Massilia* and *Telluria*. The lower triangle represents ANI values, and the upper triangle displays the *isDDH* values.

Acyl homoserine lactone is an important autoinducer in gram-negative bacteria, including proteobacteria. Hence, to determine whether all strain in this study has a QS-related gene that presents within their genome, we conducted genome mining studies using antiSMASH v5.0, manual annotation, and gene synteny (Figure 5-3). Based on antiSMASH data, almost all the strains contained a homoserine lactone gene cluster within their genome, except *T. mixta*, *M. lutea*, and *M. dura*. However, all bacteria showed QS-contributed genes such as *rhtB*, *luxQ*, *motA*, and *motB* (Figure 5-3A). The RhtB-like protein plays an essential role in the QS system through the excretion of AHL from the bacterial trans-membrane to the environment (Zakataeva *et al.*, 1999; Zakataeva *et al.*, 2006). Once the concentration of AHL is high enough, it will bind to cognate transcription factors and thus affecting the transcription of genes within QS regulons (Asfahl and Schuster, 2018). Previous studies using radiolabeled AHL in *Rhodopseudomonas palustris*, *Bradyrhizobium*, *Vibrio fischeri*, and *Pseudomonas aeruginosa* cells show that autoinducers such as AHL are freely diffusible due to active efflux and a diffusion mechanism (Eberhard *et al.*, 1991; Ding *et al.*, 2018; Schaefer *et al.*, 2018). We also illustrated the *rhtB* gene using synteny Easyfig version 2.2 with *E. coli* and *Vibrio alginolyticus* for comparison (Figure 5-3B). The LuxQ-like protein plays a crucial role in kinase activity and phosphorylation that, in turn, has a contribution to signal communication using type 2 of autoinducers. The products of the genes *motA* and *motB* are vital for the bacterial flagellar motor rotation that contributes to motility on the surface area (Morimoto and Minamino, 2014; Terashima *et al.*, 2017). In *Escherichia coli*, the expression *motB* was induced by the presence of AHL (Weiss *et al.*, 2008). AHL contributes to the phenotypic switch in bacteria (Pietschke *et al.*, 2017). The gene *pvdQ* was also found almost in all strains except *T. mixta* and *M. lutea* (Figure 5-3A). *PvdQ* belongs to the Ntn-hydrolase superfamily, which hydrolyzes the peptide bond within the acyl chain and the homoserine lactone core to reduce the virulence (Bokhove *et al.*, 2010). Hence, this enzyme has the function to regulate the secretion of AHL. Furthermore, it is known that it plays an essential role in pyoverdine biosynthesis of *Pseudomonas aeruginosa* (Visca *et al.*, 2007). The genes *luxR* and *lasI* could only be



found in *M. flava*, *M. albidiflava*, and *M. umbonata* (**Figure 5-3A**). Generally, the AHL synthases and response regulators belong to the LuxI and LuxR protein family. Also, *lasI* is contributing directly to the synthesis of AHL in *P. aeruginosa* (Steindler *et al.*, 2009).

Thus, the comparative genome analysis of *Massilia* and *Telluria* spp. projected the first indications of possible QS production, the capability of coordinated activity like flagellar-driven motility, and biofilm formation. However, this represents only a bioinformatics prediction, which needs to be later experimentally confirmed.

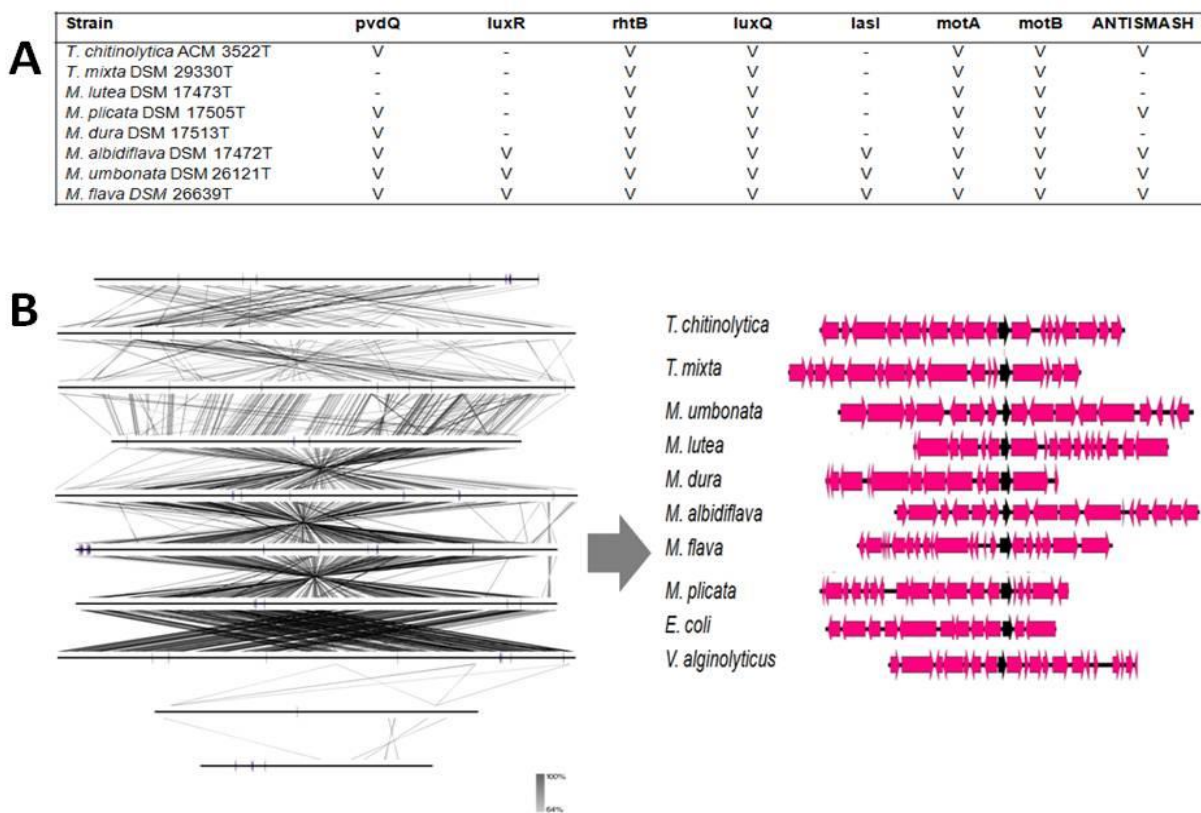


**Figure 5-3.** Genome mining of QS related genes in *Massilia* and *Telluria*. **(A)** Comparative gene and its cluster using antiSMASH v5.0 and manual annotation. **(B)** The synteny of *rhtB* within the genome using Easyfig 2.2. The black arrow indicated the *rhtB* gene and the pink arrow indicate neighbor genes.

### 5.3. Acyl-homoserine lactones (AHLs) identity

Many reports showed that an AHL is produced by all types of gram-negative bacteria (Ng and Bassler, 2009; Abisado *et al.*, 2018). However, the types of AHLs that are produced

by each bacterial species can be quite different. No report has been found about the type of AHLs produce either by *Massilia* and *Telluria*. As previously described, the QS-like genes are present in the whole genome of each *Massilia* and *Telluria* spp. The antiSMASH analysis also clearly showed that the homoserine lactone gene clusters were found in almost all the bacteria in our study (**Figure 5-3A**). Therefore, we studied the production of AHLs from bacteria of the genera *Massilia* and *Telluria* using Multiple Reaction Monitoring (MRM) in the LC-MS system. An overnight culture from liquid broth with an initial OD<sub>600</sub> of 0.06 from the incubation at 30°C and 140 rpm, was extracted twice with one volume of ethyl acetate. The organic parts were then mixed and evaporated entirely *in vacuo*. We experimented using both rich and limited liquid media, i.e., DMBgly and LB, respectively. The crude was then subjected to an LC-MS system coupled with MRM acquisition, which scanned for the presence of a highly characteristic amino-butyrolactone fragment in Q3 (fragment ion [M+H]<sup>+</sup> of  $m/z$  102±0.5, **Supplementary Figure 5-2**). Commercially available AHLs with acyl chain lengths ranging from C4 to C10 have been used to characterize the production of AHLs in both culture broths.

Interestingly, the C8-AHL and 3-OH-C6-AHL were found to be dominant in all strains (**Figure 5-4A and B**). Specifically, some strains produced other types of AHL, such as C4-AHL, C6-AHL, 3-oxo-C8-AHL, and 3-OH-C10-AHL. The production of C8-AHL in limited media is lower than those in rich media. With the best of our knowledge, this is the first report AHL production within the genus of *Massilia* and *Telluria*. The production of C8-AHL ([M+H]<sup>+</sup>  $m/z$  228.1598), C4-AHL ([M+H]<sup>+</sup>  $m/z$  172.0972), and 3-OH-C6-AHL ([M+H]<sup>+</sup>  $m/z$  216.1231) could also be observed in HR-MS analyses and were visualized in GNPS (**Supplementary Figure 5-3**).

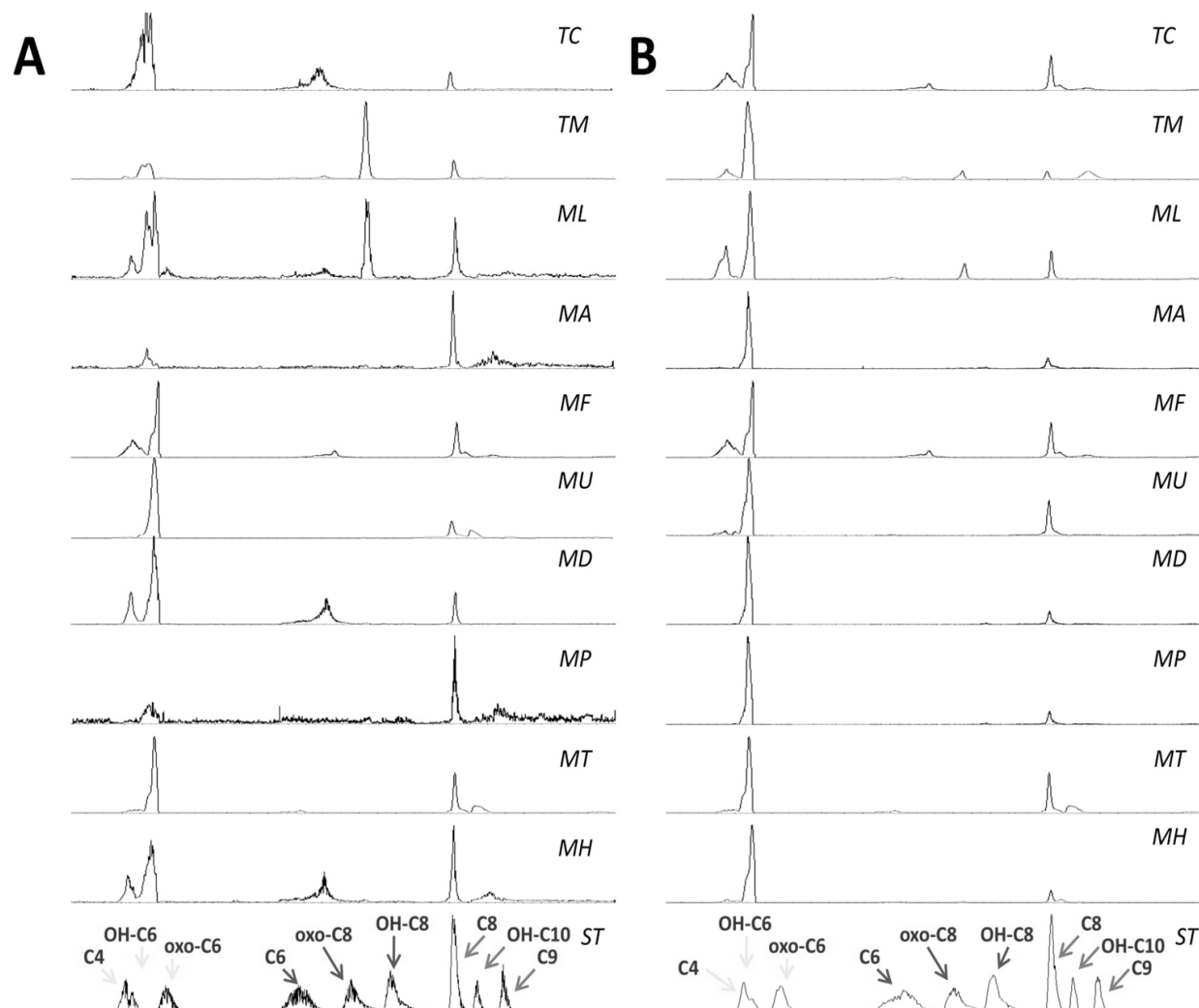


**Figure 5-4.** The AHLs production from the genus *Massilia* and *Telluria*. An MRM method has been developed in order to characterize the type of AHL production of each strain *T. chitinolytica* (TC), *T. mixta* (TM), *M. lutea* (ML), *M. albidiflava* (MA), *M. flava* (MF), *M. umbonata* (MU), *M. dura* (MD), *M. plicata* (MP), *M. lutea* (ML), and two other strains with have no genomic data *M. timonae* (MT) and *M. haloabium* (MH). **(A)** Comparative AHL production of each strain from rich media (LB broth) with nine types of standards as a comparison **(B)** Comparative AHL production from the crude of each strain from limited media (DMBgly broth) together with standards.

#### 5.4. Comparative AHLs production with an interval time of incubation.

To further characterize the output of C8-AHL, 3-OH-C6-AHL, and C4-AHL from each strain of our study, we extracted culture broth with different time intervals ranging from 2 to 40 h (**Figure 5-5A, B, and C**). We used the same condition and method using MRM, as described in the previous section. The calibration has been made with  $r \geq 0.99$  (**Supplementary Figure 5-4**) *T. chitinolytica* shows the highest production of these three

AHL, followed by *M. lutea* and *M. umbonata*. However, the output of 3-OH-C6-AHL in *M. lutea* remained lower when compared with *M. umbonata*. The production rate of 3-OH-C6-AHL and C-4 AHL in all test strains was increased in a time-dependent manner up to 24 h and only up to 18 h for C8-AHL. Generally, the AHL degradation was detected after 24 h, except for 3-OH-C6-AHL in *M. umbonata* (Figure 5-5A). The *pvdQ* gene found within the genome of most of the strains is responsible for the degradation of AHL to reduce virulence (Bokhove *et al.*, 2010). The bacterial growth (OD<sub>600</sub>) of all test strains also showed a time-dependent manner of up to 24 h, followed by the stationary phase (Figure 5-5D). The pH of the culture broth was ranging from 6.5 to 7.0, with monitoring time up to 70 h (Figure 5-5E).

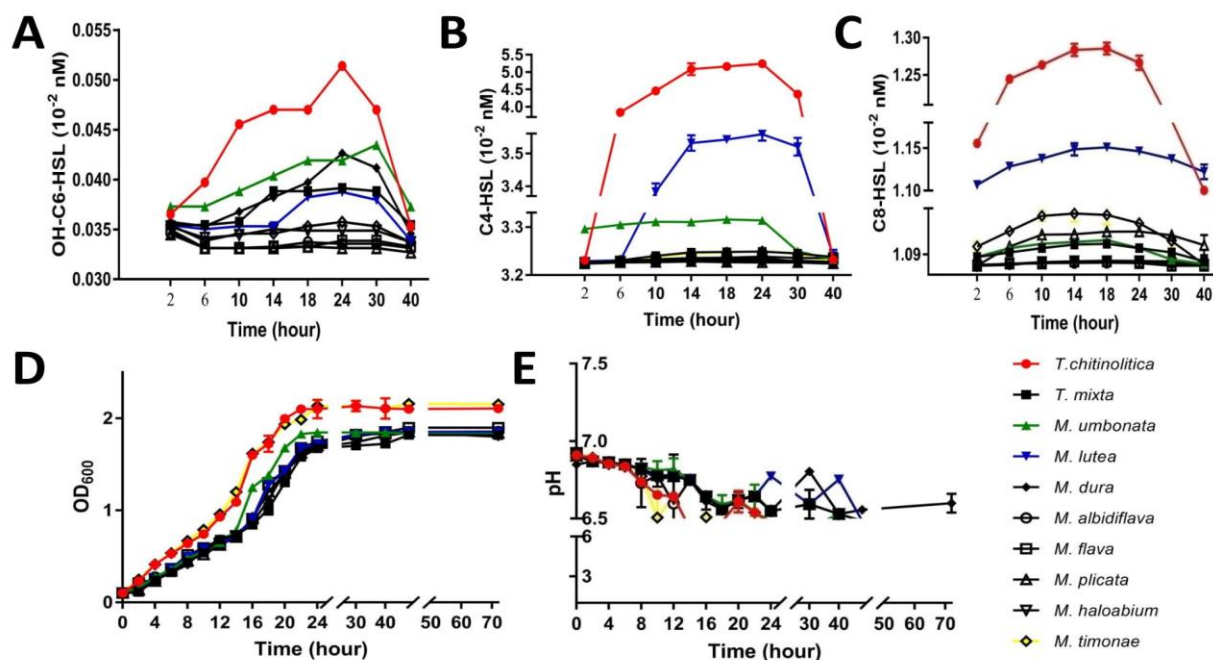


**Figure 5-5.** The AHLs production and curve growth from the genus *Massilia* and *Telluria*. A primary culture with OD<sub>600</sub> of 0.06 from LB liquid media with incubation of 30°C, 140 rpm was extracted within interval time 2 to 40 h using twice ethyl acetate and evaporated *in vacuo*. MRM method, as previously described, has been used for quantitative measurement of the AHL production-based intensity of serially diluted standard as a reference. The measure was subjected to ten strains, including *T. chitinolytica*, *T. mixta*, *M. lutea*, *M. albidiflava*, *M. flava*, *M. umbonata*, *M. dura*, *M. plicata*, *M. lutea*, *M. timonae*, and *M. haloabium*. (A) Comparative 3-OH-C6-AHL production of each strain (B) Comparative C4-AHL production of each strain (C) Comparative 3-OH-C6-AHL production of each strain (D) Curve growth of each strain for 70 h measurement (E) pH analysis of culture broth from each strain within 70 h. Three independent biological experiments were performed. Each value is given as Mean±SEM in each data point.

### 5.5. AHL induce swimming motility.

To test the hypothesis that AHL is contributed to the surface movement in *Massilia* and *Telluria*, we conducted an appropriate experiment using soft LB agar plates (0.4%). About 5µl of each bacterium grown from pre-cultivation in LB broth that contained OD<sub>600</sub> of 0.06 treated with exogenous AHL (in DMSO as a vehicle) with a final concentration of 10µM was centrally inoculated onto a quarter of agar plate and incubated for 18 h at 30°C. One crucial step in bacterial colonization and pathogenesis is surface movement, which can be achieved by swarming, sliding, or swarming motility. This motility is also needed to facilitate the bacteria to get a new source of nutrients and to speed up the biomass production.

Interestingly, *Massilia* and *Telluria* use swimming motility rather than other types of movement (**Figure 5-6B**). Swimming motility is explained as a coordinate, flagella-driven movement of individual bacteria across the surface of media. To compare with another type of motility, we used *Pseudomonas aeruginosa* strain TUEPA7472 as a control that uses swarming motility for the translocation (**Figure 5-6C**). Swarming motility is described as a collective movement of the bacterial group. We also found that exogenous provision of C8-AHL, 3-OH-C6-AHL, and C-4 AHL induced swimming motility in *Massilia* and *Telluria* within 18 h (**Figure 5-6A and B**). The swimming motility was ranging from 1 to 8-folds. The treatment with C8-AHL can speed up the performance of swim motility at least six-folds compared to the control for *T. mixta*, *M. umbonata*, and *M. albidiflava* (**Figure 5-6A**) while the untreated group performed limited cell swimming only 24 to 48 hours of incubation. The effect of these three exogenous AHL was statistically significant ( $p < 0.0001$ , unpaired Student's t-test) induced swimming motility in *T. chitinolytica*, *T. mixta*, *M. lutea*, *M. dura*, *M. albidiflava*, *M. umbonata*, *M. flava*, except C4-AHL whose effect was not statistically significant regarding the induction of motility of *T. mixta* and *M. dura*. Statistically significant induction of swimming motility compared to the control in *T. plicata* was achieved only by exogenous C8-AHL (**Figure 5-6A**). This evidence explained that AHLs play a vital role in the cell motility regulation in *Telluria* and *Massilia*. To the best of our knowledge, this is the first report suggesting the function of AHL in the provision of flagella driven migration called swimming motility in *Massilia* and *Telluria*. It

has also been previously reported that AHL-dependent quorum sensing control motility in *Burkholderia cenocepacia* (Schmid *et al.*, 2012), *Yersinia enterocolytica* (Ng *et al.*, 2018), *Serratia plymutica* (Liu *et al.*, 2011), and *Pseudomonas syringae* (Quiñones *et al.*, 2005).

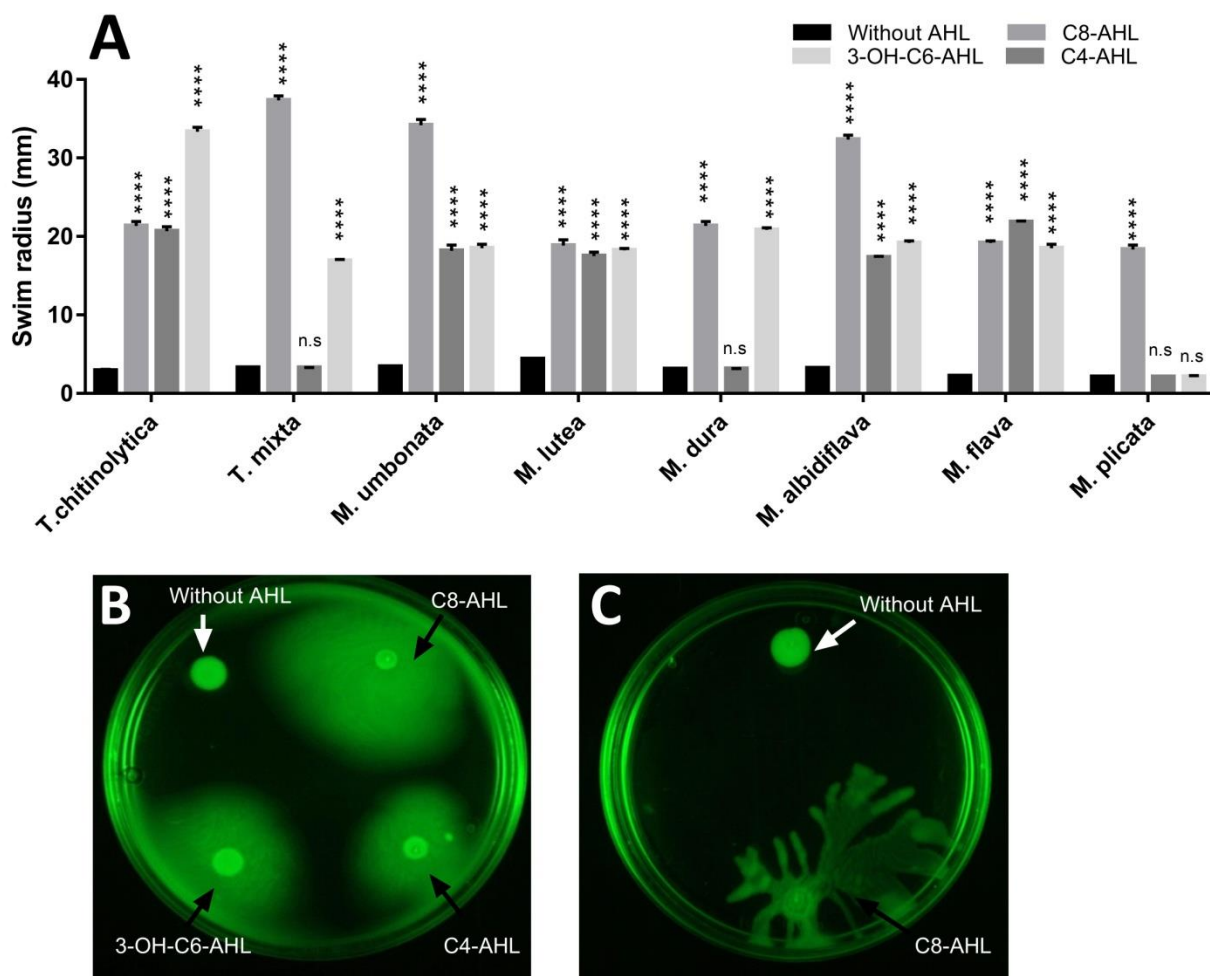


**Figure 5-6.** Swimming motility in *Massilia* and *Telluria*. Bacterial suspensions (5 $\mu$ l) with an OD<sub>600</sub> of 0.06 treated with exogenous AHL in DMSO with the final concentration of 10 $\mu$ M were inoculated centrally in each coordinate onto LB media agar (0.4%) plates. The negative control group was treated with DMSO without AHL. (A) Bacterial motility was monitored after 18-hour incubation at 30°C based on swim radius (mm). (B) A representative plate from *Massilia umbonata* without exogenous AHL treatment and treated with C8-AHL, C4-AHL, and 3-OH-C6-AHL. After 18 hours, the bacteria performed surface movement called swimming motility. (C) A representative plate of another type of bacterial surface movement called swarming motility was performed by *P. aeruginosa* strain TUEPA7472. Three independent biological experiments were performed. Values are given as Mean $\pm$ SEM. The student t-test of each time point was employed to determine the level of statistical differences between the control (without AHL) and the treated group.

While n.s. stand for not significantly different \*, \*\*, \*\*\* and \*\*\*\* represent statistically significant difference from control at  $p < 0.05$ ,  $p < 0.01$ ,  $p < 0.001$  and  $p < 0.0001$ , respectively.

## 5.6. AHLs induce biofilm formation.

To extend our hypothesis that AHLs are involved in the development of multi-cellular aggregates called biofilm in *Massilia* and *Telluria*, we performed an experiment that resulted in the formation of free-floating bacterial aggregates that can be seen by naked eyes from the side view or flat-bottom microplate. Overnight pre-cultures from liquid LB (100 $\mu$ l) with an OD<sub>600</sub> of 0.06 treated with exogenous AHL in DMSO with a final concentration of 10  $\mu$ M was inoculated in the limited broth that only contains salt and carbon sources (DMBgly) and is incubated for 24 h at 30°C under static conditions (without agitation). The cultivation using the shaker to give an agitation prevented the production of biofilm, and the bacteria remained in the planktonic state (data not shown). We found that *Massilia* and *Telluria* assemble a biofilm within 48 h, which are visible by naked eyes. These bacteria have free motiles, show a floating behavior, and form a multi-cellular aggregate to get the oxygen, which is located on the top wall of the micro-plate (**Figure 5-7B**), whereas no aggregates were visible in the negative control (**Figure 5-7B**, on the left side). To further corroborate the hypothesis that the exogenous provision of AHLs induces biofilm formation in *Massilia* and *Telluria*, quantitative analyses were initiated, using crystal violet dye for visualization of cell aggregates. Upon crystal violet, the biofilm aggregates tinted violet while the surrounding medium remained unstained. The multi-cellular aggregate was then diluted using acetic acid and measured by spectrophotometry at 550 nm. We found that exogenous provision of C8-AHL, 3-OH-C6-AHL, and C-4 AHL induced aggregate biofilm in *Massilia* and *Telluria* within 24 h (**Figure 5-5A**). The biofilm formation of each strain was formed, ranging from 1 to 3 folds after giving exogenous AHL when compared with the control (untreated AHL). Exogenous C8-AHL which has been fed into the bacterial culture was statistically significant ( $p < 0.0001$ , unpaired Student's t-test) and induced more biofilm aggregates in *T. chitinolytica*, *T. mixta*, *M. umbonata*, *M. lutea*, *M. dura*, *M. albidiflava*, except *M. flava* and *M. plicata* were not significant compared to each data point. The addition of C4-AHL into the culture was statistically significant ( $p < 0.0001$ , unpaired Student's t-test) and induced biofilm formation

of *T. chitinolytica*, *T. mixta*, *M. umbonata*, *M. dura*, *M. flava*, and *M. plicata*, except *M. lutea* and *M. albidiflava*. The exogenous induction by 3-OH-C6-HSL led to the same pattern to each bacterium in this study with an experiment that has been conducted using C4-AHL. However, its introduction to *T. chitinolytica* showed only  $p < 0.05$  (**Figure 5-7A**). All taken together explained that AHLs are playing an essential role in the multi-cellular biofilm aggregates in *Telluria* and *Massilia*. We believe that this is the first experiment that confirmed that AHLs are involved in the development of biofilm architecture in *Massilia* and *Telluria*.

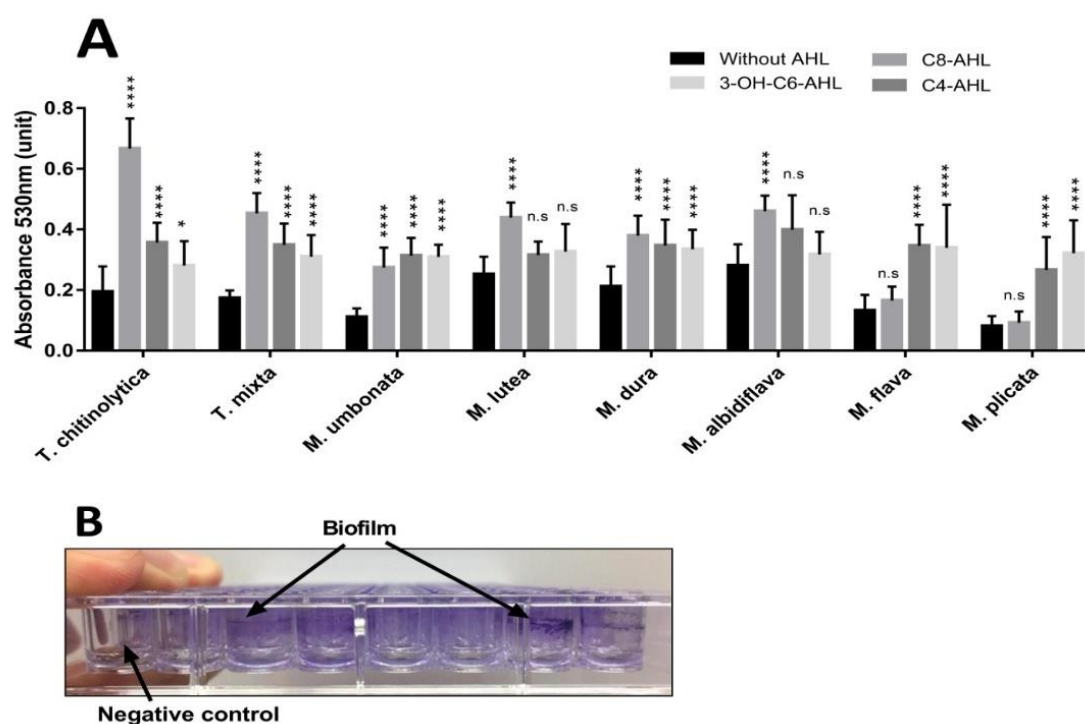


**Figure 5-7.** Biofilm production by *Massilia* and *Telluria* spp. Bacterial suspensions (5 $\mu$ l) with an OD<sub>600</sub> of 0.06 treated with exogenous AHL in DMSO with the final concentration of 10 $\mu$ M were inoculated onto DMBGly liquid media. The control group was treated with DMSO without AHL. (A) Biofilm production was spectrophotometrically monitored (OD<sub>530</sub> nm) after 24-hour incubation at 30°C (B) A representative microplate from *T. chitinolytica* (right arrow) and *M. flava* (left arrow) treated with exogenous C8-AHL. After 24 hours, the bacteria performed biofilm formation. Data represent as Mean $\pm$ SEM from four independent experiments with three technical replicates each. Statistical analysis of the difference between the untreated group (without exogenous AHL) and the treated group was performed using Student's t-test for each data point. No significant difference: n.s and \*, \*\*, \*\*\* and \*\*\*\* represent statistically significant difference from control at  $p < 0.05$ ,  $p < 0.01$ ,  $p < 0.001$  and  $p < 0.0001$ , respectively.



### 5.7. Effect of sub-inhibitory antibiotic concentration towards AHL production in *T. chitinolytica* and *M. lutea*.

In our study, we also tested whether the presence of antibiotics at sub-inhibitory concentration disrupts the signal mechanism of two bacteria from the genus *Telluria* and *Massilia*, i.e., *T. chitinolytica* and *M. lutea*. We performed an appropriate study using five types of antibiotics, such as tetracycline, trimethoprim, kanamycin, neomycin, and gentamycin. About 5 µl of each bacterium grown overnight with an initial OD<sub>600</sub> of 0.06 was subsequently inoculated to 25 ml of liquid LB in a 50 ml falcon tube with a final concentration of 30 µM from each antibiotic. Each antibiotic has been previously prepared as a 10 mM stock in DMSO. The culture was then incubated for at 30°C for 18h at 140 rpm. We found that the provision of each antibiotic with a concentration of 30 µM was not statistically significant and reduced the production of C8-AHL in *T. chitinolytica* and *M. lutea*. Solely, kanamycin and gentamycin reduced the output of C8-AHL in *M. lutea*. The provision of antibiotics did also not have a significant effect on the reduction of C4-AHL except kanamycin and trimethoprim to *T. chitinolytica* ( $p < 0.05$ , Student's t-test), and neomycin and gentamycin to *M. lutea* ( $p < 0.01$ , Student's t-test). However, the addition of each antibiotic had a significant effect on the reduction of 3-OH-C6-AHL production for both bacteria in our study. The p-value varied from  $p < 0.05$  to  $p < 0.0001$  based on an unpaired Student's t-test. (**Figure 5-8A and B**). To see the growth pattern of both strains, we performed a growth curve based on OD<sub>600</sub> within the time interval from 0 to 30 h. The growth pattern of *T. chitinolytica* and *M. lutea* was not far different after the induction with each antibiotic compared to the untreated group as a control (**Figure 5-8C and D**). In order to get insight into the whole genome data that has been sequenced in our previous work, we performed an *in-silico* antibiotic-resistant analysis using ARTS (<https://arts.ziemertlab.com/>). Based on this analysis, we found that generally, all the strains that we used in our study showed antibiotic-resistant in the range of 80-90% to tetracycline, trimethoprim, neomycin, and gentamycin. Most of the strains also showed antibiotic-resistance in the range of 50-80% except for *T. chitinolytica* and *M. umbonata*, which showed higher ranges (**Figure 5-8E**). Thus, these observations suggested that the provision of each antibiotic at a sub-inhibitory concentration (30 µM) did not result in a bactericidal effect and not in a reduction of the QS signal. Several previous studies

showed that the presence of antibiotics at the sub-inhibitory level correlates with the activation of some QS signals (Shen *et al.*, 2008; Cummins *et al.*, 2009; Liu *et al.*, 2013). The use of trimethoprim at a sub-inhibitory concentration in *Burkholderia thailandensis* activated the QS regulon and the production of acybolin (Okada *et al.*, 2016). However, the exogenous antibiotic application at a sub-inhibitory concentration to the culture also disrupts the production of AHL (Garske *et al.*, 2004; Skindersoe *et al.*, 2008; Babić *et al.*, 2010).

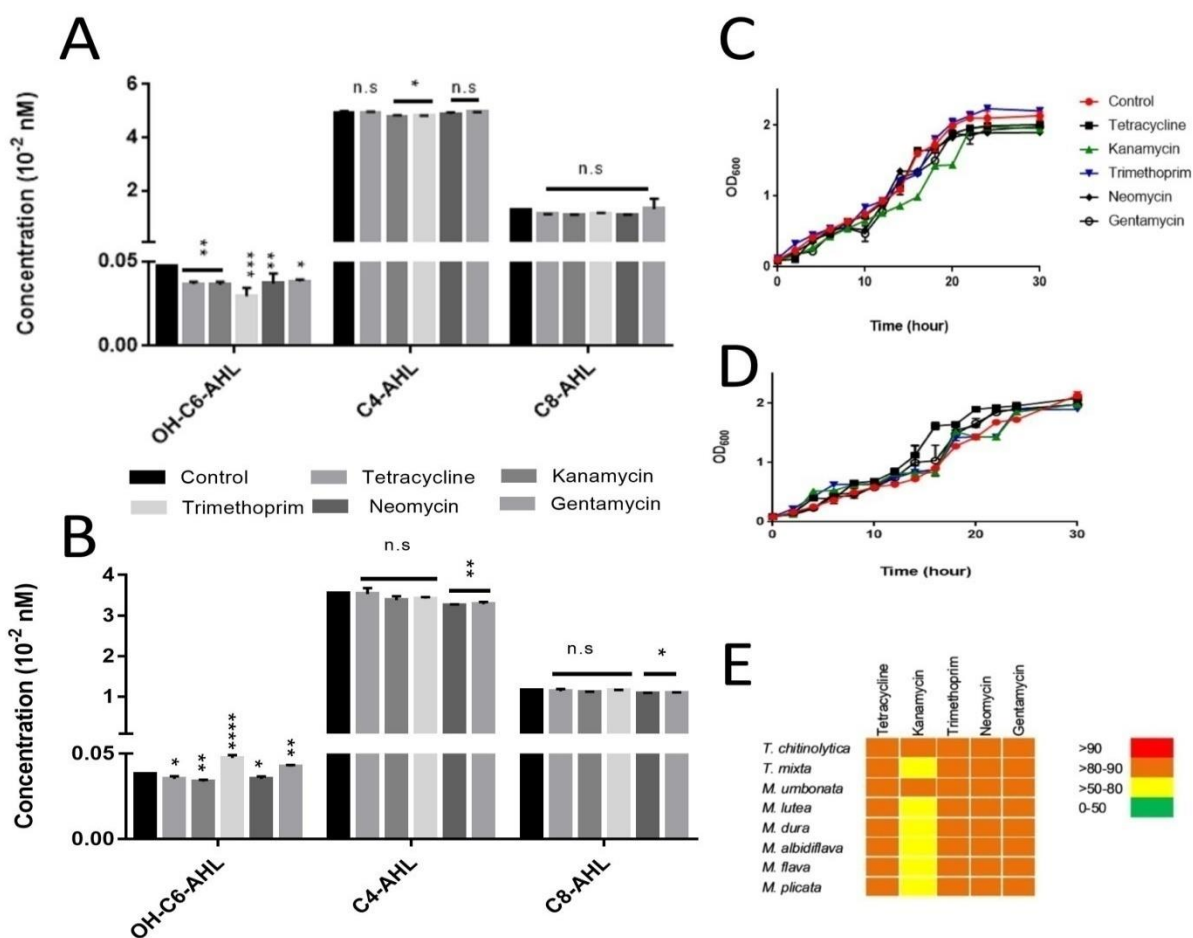


**Figure 5-8.** Sub-inhibitory effect of antibiotics to the growth curves and AHL production of *T. chitinolytica* and *M. lutea*. The initial OD<sub>600</sub> of the bacterial culture for the experiment was 0.06 and then treated with an antibiotic in DMSO with the final concentration of 30 μM. The sub-inhibitory treatment, including tetracycline, kanamycin, trimethoprim, neomycin, and gentamycin, the control group treated with only DMSO as a vehicle. (A) AHL production by *T. chitinolytica* after 18-hour incubation at 30°C, 140 rpm treated with various antibiotics. (B) AHL production by *M. lutea* after grown 18h at 30°C and 140 rpm

treated with various antibiotics. (C) The growth curve was performed by *T. chitinolytica* after treated with various antibiotics with the same condition for in AHL production experiment. (D) Same experiment with C for *M. lutea* (E) Antibiotic-resistant based on *in silico* analysis of the whole bacterial genome of each strain from *Massilia* and *Telluria* using Antibiotic-Resistant Target Seeker (ARTS). Data represent as Mean $\pm$ SEM from three independent experiments. Statistical analysis of the difference between the untreated group (without antibiotics) and a treated group was performed using the unpaired Student's t-test for each data point. No significant difference: n.s and \*, \*\*, \*\*\* and \*\*\*\* represent statistically significant difference from control at  $p < 0.05$ ,  $p < 0.01$ ,  $p < 0.001$  and  $p < 0.0001$ , respectively.

### 5.8. The inhibition of FAb produced by *Burkholderia glumae* ICMP 3729 on swimming motility and biofilm formation.

FAb is a fatty acid metabolite produced by *B. glumae* ICMP 3729. Previous reports also showed that *Burkholderia* produced 2-dodecenoic acid referred to as BDSF, a *Burkholderia* diffusible signal factor that synthesized by the enoyl-CoA-hydratase RpfF (Boon *et al.*, 2008). The structure elucidation using 1D and 2D NMR (**Supplementary Figure 5-5**) showed that this bioactive has no similarity against a database such as SciFinder. The structure of the compound is a fatty acid with  $[M+H]^+$   $m/z$  281.2487, based on HRMS (**Supplementary Figure 5-6**). While the previous experiment visualized that the AHLs of *T. chitinolytica* and *M. lutea*, contribute to the swimming motility (**Figure 5-6**), fatty acids have been reported to interfere with the QS system. Hence, to address whether FAb produced by *B. glumae* ICMP 3729 also disrupts the production of AHL and biofilm in *T. chitinolytica* and *M. lutea*, we performed experiments as previously described using 40  $\mu$ M of FAb. We found that the supplementation of FAb in both bacterial cultures could statistically significantly reduce the production of C4-AHL and C8-AHL ( $p < 0.0001$ , unpaired Student's t-test). The reduction of 3-OH-C6-AHL was also significant at  $p < 0.05$  for *T. chitinolytica* but did not apply to *M. lutea* (n.s,  $p > 0.05$ ) (**Figure 5-9B and C**). At the concentration of 20 and 40  $\mu$ M, FAb showed suppression to the motility of both strains at 18 h incubation; for the positive control, C8-AHL (**Fig 5-9D and E**). To the best of our knowledge, this is the first evidence suggesting that fatty acid produced by *B. glumae* ICMP 3729 reduces the production of AHL and inhibit flagella driven migration through swim motility in *T. chitinolytica* and *M. lutea*.

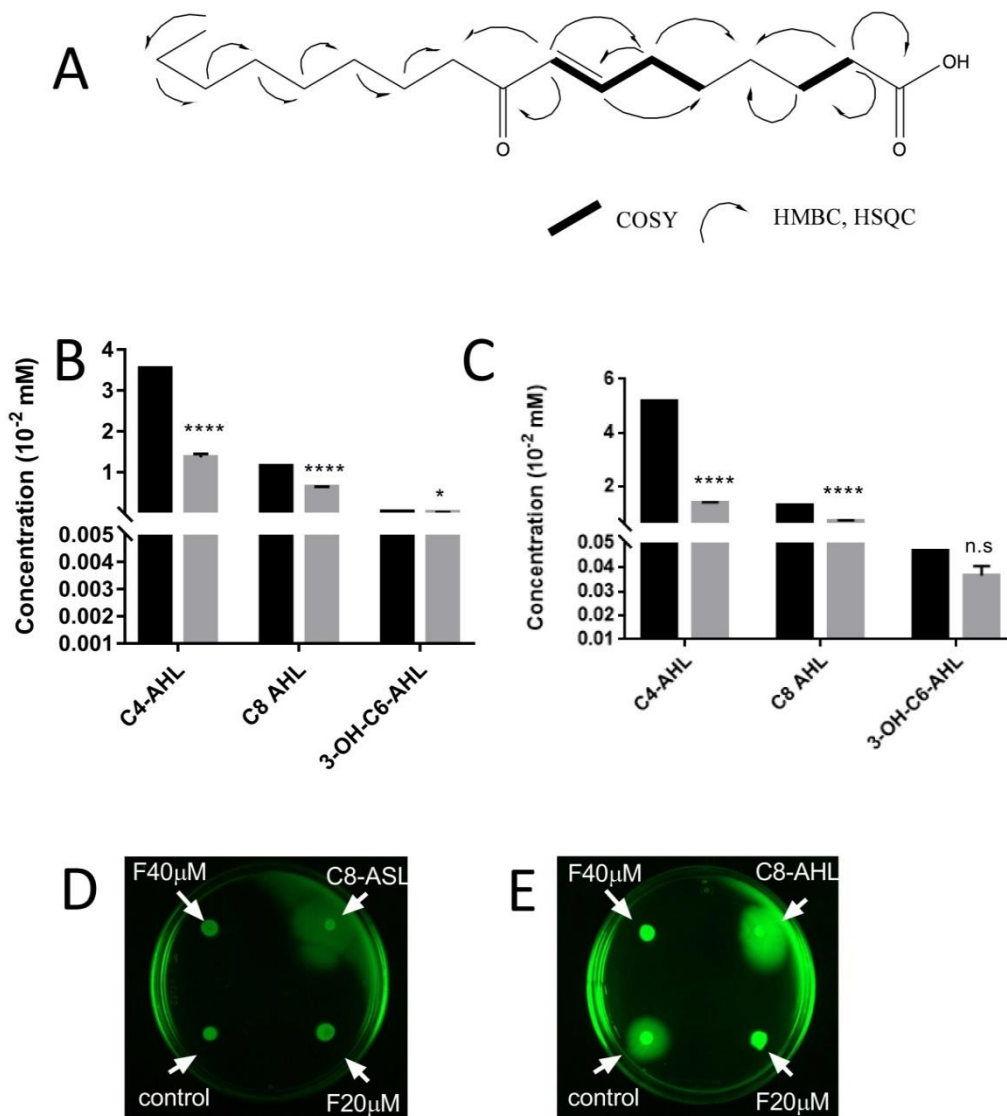


**Figure 5-9.** The effect of exogenous fatty acid (FAb) produced by *Burkholderia glumae* ICMP 3729 to the swimming motility and AHL production by *T. chitinolytica* and *M. lutea*. The initial OD<sub>600</sub> of the bacterial culture for the experiment was 0.06 and treated with FAb in DMSO with the final concentration of 20  $\mu$ M. (A) The structure elucidation of new fatty acid produced by *B. glumae* ICMP 3729 is based on 1D and 2D NMR. (B) AHL production by *M. lutea* after grown 18h at 30°C and 140 rpm treated with FAb 20  $\mu$ M. (C) The same experiment as B but conducted with *T. chitinolytica*. (D). Swimming motility in *M. lutea* after exposed by FAb 20  $\mu$ M and 40  $\mu$ M. (E). The same experiment has been conducted similarly as D using another AHL producer strain, *T. chitinolytica*. Statistical analysis of the difference between the untreated group (without FAb instead of DMSO) and treated group was performed using Student's t-test for each data point. No significant difference:

n.s and \*, \*\*, \*\*\* and \*\*\*\* represent statistically significant difference from control at  $p < 0.05$ ,  $p < 0.01$ ,  $p < 0.001$  and  $p < 0.0001$ , respectively.

### 5.9. AHLs within gram-negative bacteria – a novelty perspective

Bacteria, including gram-negative, live together as a community in nature. They do not exist as solitaire organisms. They are communicating with each other through cell-to-cell interaction by secreting diffusible low-molecular-weight signaling molecules (Novick and Geisinger, 2008). This communication system is called quorum sensing (QS). The bacteria mediate cooperative cell-cell interaction to facilitate them to alter gene expression and to coordinate their population. QS also use as mediation to produce a natural product such as antibiotics, antifungal, antiviral, cytotoxic, or even siderophores. The production of QS relies on a cell-density dependent manner. The QS molecules are produced in a small amount at low density, then diffuse into the environment. At high density, the QS molecules concentration has been reached, and the accumulated complex signal then influences the special biological activities.

The QS system was first discovered in gram-negatives, but later, an equivalent system was also found in gram-positives. However, in gram-positive bacteria, the QS molecules are often modified peptides, while in gram-negative bacteria, acyl-homoserine lactones (AHLs) are the decisive QS molecules. AHLs are produced by LuxI-type synthases that tightly bind to LuxR-type receptors in the cytoplasm to exert a regulatory outcome (Thoendel *et al.*, 2011).

QS communication can also be observed at the interspecies level. In human microflora, the morphology of *C. albicans* is affected by the excretion of the QS signal 3-oxo-C12-AHL from *P. aeruginosa* (Lindsay and Hogan, 2014). Other studies showed that the virulence factor of *B. cepacia* is influenced by the QS excretion of *P. aeruginosa* (McKenney *et al.*, 1995). The secretion of 3-oxo-C12-AHL inhibits the biofilm production of *Staphylococcus epidermidis* (Singh *et al.*, 2007), while the growth of *Salmonella* was influenced by the excretion of AHLs from *Pectobacterium carotovorum* (Noel *et al.*, 2010).

A recent study showed that AHLs induced the production of a cyclic lipopeptide called jessenipeptin and the polyketide mupirocin in a *Pseudomonas* bacterium associated with amoeba (Arp *et al.*, 2018). An experiment by Morel's group displayed that QS, together

with Fe regulates the biosynthesis of the siderophore amphi-enterobactin in *Vibrio harveyi* (McRose *et al.*, 2018b). A further study presented that the QS molecule cyclo (Phe-Pro) of *V. vulnificus* inhibits the RIG-I-mediated antiviral innate immunity (Lee *et al.*, 2018). Fragin, an antifungal compound produced by *Burkholderia cenocepacia*, is also controlled by QS (Jenul *et al.*, 2018). The QS system has also been involved in virulence and pathogenesis. The virulence factor malleilactone, which is cytotoxic to mammalian cells, is produced by *B. pseudomallei* under the regulation of QS and antibiotics (Klaus *et al.*, 2018). Numerous types of AHLs have also been discovered from other gram-negative bacteria, as presented in **Table 5-1**

**Table 5-1.** AHLs produced by various gram-negative bacteria

Strain	QS product	Regulated function
<i>Acinetobacter</i> sp.	3-oxo-C12-AHL and 3-hydroxy-C12- AHL	virulence factor
<i>Serratia proteamaculans</i>	3-oxo-C6- AHL	biofilm
<i>S. liquefaciens</i>	C4-AHL	virulence factor
	C6-AHL	
<i>Burkholderia</i> sp.	3-oxo-C6-AHL	virulence factor
	C8-AHL	
	3-hydroxy-C8-AHL	
	C9-AHL	
<i>B. pyrrocinia</i>	C8-AHL	antifungal
<i>B. vietnamiensis</i>	decanoyl-AHL	No information
<i>B. thailandensis</i>	3-oxo-C8-AHL	antibiotic
	3-oxo-C10-AHL	
<i>B. glumae</i>	C6-AHL	toxoflavin
	C8-AHL	production,
<i>Ralstonia solanacearum</i>	C8-AHL	pathogenicity
<i>Agrobacterium tumefaciens</i>	3-oxo-C8-AHL	conjugal transfer
<i>Pseudomonas aeruginosa</i>	C4-AHL	virulence factor
	3-oxo-C12-AHL	bacteriostatic
<i>P. chlororaphis</i>	C6-AHL	phenazine
<i>Erwinia carotovora</i>	3-oxo-C6-AHL	antibiotic
<i>Vibrio anguillarum</i>	3-hydroxy-C8-AHL, 3- hydroxy-C10-AHL, and 3-oxo-C12-AHL	influence serotype
<i>Vibrio scopthalmi</i>	3-hydroxy-C12-AHL	no information
<i>Vibrio tasmaniensis</i>	C10-AHL, hydroxy- C12-AHL, oxo-C12- AHL C14-AHL	no information
<i>Aeromonas hydrophila</i>	C4-AHL	protease and biofilm

<i>Pectobacterium</i> sp.	3-oxo-C6-AHL 3-oxo-C8-AHL	pathogenicity
<i>Chromobacterium violaceum</i>	C6-AHL	violacein production

As previously mentioned, the genera of *Massilia* and *Telluria* are ubiquitous in the environmental samples. They are mostly found in soils, air, and water. However, the functions of these genera in terms of contribution to the natural ecosystem and the production of secondary metabolites have not been thoroughly investigated. Quorum sensing is one of the ways to understand their physiological interaction and to elucidate more their functionality in the ecosystem.

In this study, the relationship of eight strains of the genera *Massilia* and *Telluria* was visualized using BRIG after performing a BLASTN. To accomplish this analysis, the whole genome of each strain was required. To get more insight, we also performed phylogenetic trees using 16sRNA, concatenated nine housekeeping genes as described above; particular-gene related QS that present in all the bacteria in these studies, i.e., *luxQ* and *rhtB*. We also investigated their similarity based on whole-genome sequence using *in silico* DDH and ANI. These data were suggesting that the eight bacteria in our study represent different species indeed. However, they are significantly related to each other. This condition also could be explained using big phylogenetic trees using other species in the genera *Massilia* and *Telluria*, respectively (**Supplementary Figure 5-1**).

In this study, we focused on whether *Massilia* and *Telluria* can produce diffusible autoinducers as a part of their QS system communication. This hypothesis relies on the general information that gram-negative bacteria can produce QS signals as a part of their interaction (Abisado *et al.*, 2018). Herein, we reported that we found several QS-related genes within their whole genome. Based on bioinformatics studies, we found that most of the bacteria in our studies have a homoserine lactone cluster in their genome. However, this analysis did not apply to *T. mixta*, *M. lutea*, and *M. dura*. Using manual annotation with BLAST and gene synteny, we found the QS-contributing genes, called *rhtB*, *luxQ*, *motA*, and *motB*, are present in all the bacteria. Most of them have also *pvdQ* within their genome except *T. mixta* and *M. lutea*. Also, *M. flava*, *M. albidiflava*, *M. umbonata*, and *M. dura* have *luxR* and *LasI*, which are known as a QS regulator in *P. aeruginosa* (Steindler *et al.*, 2009). The RhtB-like protein has a pivotal role in the QS system through the

excretion of AHL from bacterial trans-membrane into the environment (Zakataeva *et al.*, 2006). This evidence could explain more about the hypothesis of whether AHLs could be easily extracted in the supernatant of culture broth. Thus, we also performed *rhtB* synteny and compared it with *V. alginolyticus* and *E. coli*.

To prove the hypothesis of whether all strains produce the predicted AHLs under laboratory conditions, we performed an MRM study as previously described. Generally, they produce C8-AHL and 3-OH-C6-AHL; several strains also produce C4-AHL, C6-AHL, 3-oxo-C8-AHL, and 3-OH-C10-AHL. The production in minimal media was lower than in rich media. However, they showed a similar pattern, and C8-AHL was found to be dominant in all strains. In general, the AHL production is active up to 18 h and starts to enter the stationary phase and degradation after its time. AHL production in *Massilia* and *Telluria* relied on a growth curve-dependent manner but was independent of pH.

In order to understand the role of AHLs in their physiological context, we performed motility tests and biofilm studies. Interestingly, we found that *Massilia* and *Telluria* use swimming motility as their flagella-driven surface movement. This movement is different from *P. aeruginosa* that always used swarming motility. Herein, we also reported that exogenous provision of C8-AHL, 3-OH-C6-AHL, and C-4 AHL statistically induced swimming motility in *Massilia* and *Telluria* within 18 h, compared to the control. Without the addition of AHLs, the bacteria need at least 24-48 h to become motile.

Moreover, these exogenous AHL also significantly induced biofilm formation in *Massilia* and *Telluria* within 24 h, compared to the control. Biofilm assays conducted in limited media might promote aggregate formation due to the minimum availability of some essential nutrients that bacteria might need. Within these three AHLs, C8-AHL gives the highest role in the induction of both assays. Thus, AHLs play an essential role in the cell motility regulation and aggregate biofilm formation in *Telluria* and *Massilia*.

Many antibiotics are derived from secondary microbial metabolites. Generally, the existing antibiotics in the environment are naturally occurring to fight against competitors (Hoffman *et al.*, 2005). Consequently, the competitors develop a defense strategy to protect themselves by producing a resistant mechanism to antibiotics. On the other hand, the natural concentration of antibiotics present in the environment is significantly lower



than the minimum inhibitory level to kill the general microbial population. Whereas, we also conducted antibiotic exposure tests at sub-inhibitory concentration, using two representative soil bacterial strains that belong to *Massilia* and *Telluria* - *T. chitinolytica* and *M. lutea* and monitored their production of AHL using the MRM method. Thus, these data suggested that the provision of exogenous antibiotics at sub-inhibitory concentration were not bactericidal and did not reduce the QS signal in both bacteria. These results were corresponding with several previously reported that the level of antibiotic in the sub-inhibitory level activates the QS signal (Shen *et al.*, 2008; Liu *et al.*, 2013). Moreover, its supplementation can enable the QS system to produce secondary metabolites, i.e., acybolin (Okada *et al.*, 2016).

To gain more knowledge about the compound that can disrupt the AHL regulation and the motility of *T. chitinolytica* and *M. lutea*, we used a fatty acid metabolite (FAB) from *B. glumae* ICMP 3729, that might be found in the same niche. *Burkholderia*, *Massilia*, and *Telluria* were found to be dominant in the root community (Weisskopf *et al.*, 2011). As previously described, fatty acid production by *B. cenocepacia* can interfere with *Candida albicans* (Boon *et al.*, 2008). Here, we identified that the FAB significantly reduced the production of AHL, consistent with the previous report that fatty acids interrupt the QS signal in *P. aeruginosa* (Kwan *et al.*, 2011; Twomey *et al.*, 2012; Deng *et al.*, 2013). We also found that FAB inhibited the swimming motility of *T. chitinolytica* and *M. lutea*. The fatty acid also acted as a dispersion agent in microbial biofilms (Davies and Marques, 2009; Sepehr *et al.*, 2014).

This work highlights the various AHLs produced by *Massilia* and *Telluria*, with the majority of C8-AHL is found in the highest concentration in both minimal and rich media. This evidence is consistent with genome mining studies. To the broad understanding of the physiological function of AHL production, the use of exogenous AHLs at a higher level than those that are naturally produced by each strain may elucidate how AHLs contribute to these behaviors *in vitro*. At the physiological level, AHL regulates the flagellar-driven swimming motility and induce the multi-cellular aggregate known as biofilm within less than 24 h. For the particular assay, in *M. lutea* and *T. chitinolytica*, the sub-inhibition of antibiotics did not disrupt the production of AHL and their growth curve. However, the fatty

acid metabolite produced by *B. glumae* showed inhibition to their function in terms of AHL production and flagellar-driven motility. Such systematic studies will provide a basis for the creation of secondary metabolites based on AHL-driven regulation and give more ideas in developing FAb-inspired compounds as an anti-virulence compound towards strains that are human pathogenic, such as *M. timonae*.

## Chapter 6. Chemical investigation of bacteria from the genus *Janthinobacterium*

### 6.1. Bioinformatic analysis of two strains from the genus *Janthinobacterium*

The publicly available genome sequencing data of *Janthinobacterium agaricidamnosum* DSM 9628 and *J. lividum* DSM 1552 were extracted from the NCBI and analyzed with AntiSMASH v5.0 with the default setting, as shown in **Figure 7.1**.

Cluster	Type	From	To	Most similar known cluster	MIBiG BGC-ID
The following clusters are from record NZ_HG322949.1:					
Cluster 1	Nrps	172517	246041	Jagaricin_biosynthetic_gene_cluster (100% of genes show similarity)	BGC0001127_c1
Cluster 2	Bacteriocin	264050	274907	-	-
Cluster 3	Indole	1188768	1211818	Violacein_biosynthetic_gene_cluster (100% of genes show similarity)	BGC0000831_c1
Cluster 4	T1pks-Nrps	1500808	1558071	-	-
Cluster 5	Nrps	1878131	1945825	Serobactins_biosynthetic_gene_cluster (30% of genes show similarity)	BGC0000424_c1
Cluster 6	Terpene	2601041	2622782	-	-
Cluster 7	Acyl_amino_acids	2874876	2935622	O-antigen_biosynthetic_gene_cluster (14% of genes show similarity)	BGC0000781_c1
Cluster 8	Nrps	3319919	3407242	Myxochelin_biosynthetic_gene_cluster (41% of genes show similarity)	BGC0001345_c1
Cluster 9	Bacteriocin	4462389	4474032	-	-
Cluster 10	Nrps	5611727	5667113	Syringomycin_biosynthetic_gene_cluster (17% of genes show similarity)	BGC0000437_c1
Cluster 11	Thiopeptide	5696297	5731458	-	-
Cluster 12	Bacteriocin	5741483	5752334	-	-
Cluster	Type	From	To	Most similar known cluster	MIBiG BGC-ID
The following clusters are from record c00003_gi1078..:					
Cluster 1	Bacteriocin	12988	23917	-	-
The following clusters are from record c00008_gi1078..:					
Cluster 2	Nrps	1	4167	Cupriachelin_biosynthetic_gene_cluster (17% of genes show similarity)	BGC0000330_c1
The following clusters are from record c00010_gi1078..:					
Cluster 3	Nrps	1	6465	Poaeamide_B_biosynthetic_gene_cluster (100% of genes show similarity)	BGC0001347_c2
The following clusters are from record c00026_gi1078..:					
Cluster 4	T1pks	31020	62781	Enacyloxin_biosynthetic_gene_cluster (29% of genes show similarity)	BGC0001094_c1
The following clusters are from record c00037_gi1078..:					
Cluster 5	Acyl_amino_acids	20152	80898	O-antigen_biosynthetic_gene_cluster (14% of genes show similarity)	BGC0000781_c1
The following clusters are from record c00038_gi1078..:					
Cluster 6	Nrps	1	10869	Cupriachelin_biosynthetic_gene_cluster (35% of genes show similarity)	BGC0000330_c1

**Figure 6-1.** Number of BGCs through the antiSMASH v5.0 analysis. (top) *J. agaricidamnosum*, (bottom) *J. lividum*.

The genomic analysis predicted 12 and 6 BGCs for *J. agaricidamnosum* and *J. lividum*, respectively. Based on 100% similarity, *J. agaricidamnosum* was readily identified to be

a producer of jagaricin and violacein, while *J. lividum* was predicted to be to produce NRPS-based lipopeptide poeamide (**Figure 7-1**).

## 6.2. Chemical investigation employing the OSMAC approach

The two strains mentioned above were used for metabolic profiling on a 5L- scale. Eight different culture conditions were applied, always with shaking. After 48 hours of fermentation, the broth was extracted with ethyl acetate, and the resultant crude extract screened using low-resolution LC-MS. The screening dereplicated various known metabolites such as poeamide, violacein, and diketopiperazines.

**Table 6-1.** Low-resolution LC-MS screening results based on the positive mode of the investigated strains.

Bacteria	Medium							
	S	M	M1	M2	P	L	R	K
JA	-	violacein	violacein, dipeptide	violacein, dipeptide	-	-	-	-
JV	dipeptide	-	-	dipeptide	-	poeamide	poeamide	-

Note: JA: *Janthinobacterium agaricidamnorum*, JL: *J. lividum*, S: SBM, M: MM9, M1: Modified DMBgly, M2: DMBgly, P: pharma media, L: LB, R: R2AA, K: KB

## 6.3. Isolation of purple-like compound and diamino acids

In order to obtain enough material for structural elucidation, 15 x 5 L Erlenmeyer, each containing 2 L DMB medium was prepared, inoculated and cultivated. Subsequently, the supernatant was extracted with Diaion® HP 20 resin and partitioned into water and MeOH employing a VLC system. The 50% of MeOH layer (termed as fraction C) was fractionated repeatedly using Luna® Omega 3 µm Polar C18 100 Å, LC column 250 x 4.6 mm to provide semi-pure compounds as shown in **Figure 7-2**. A final purification step using a Phenomenex® Luna 5u C5, 4.6 X 250 mm column afforded the target compounds in a pure form.

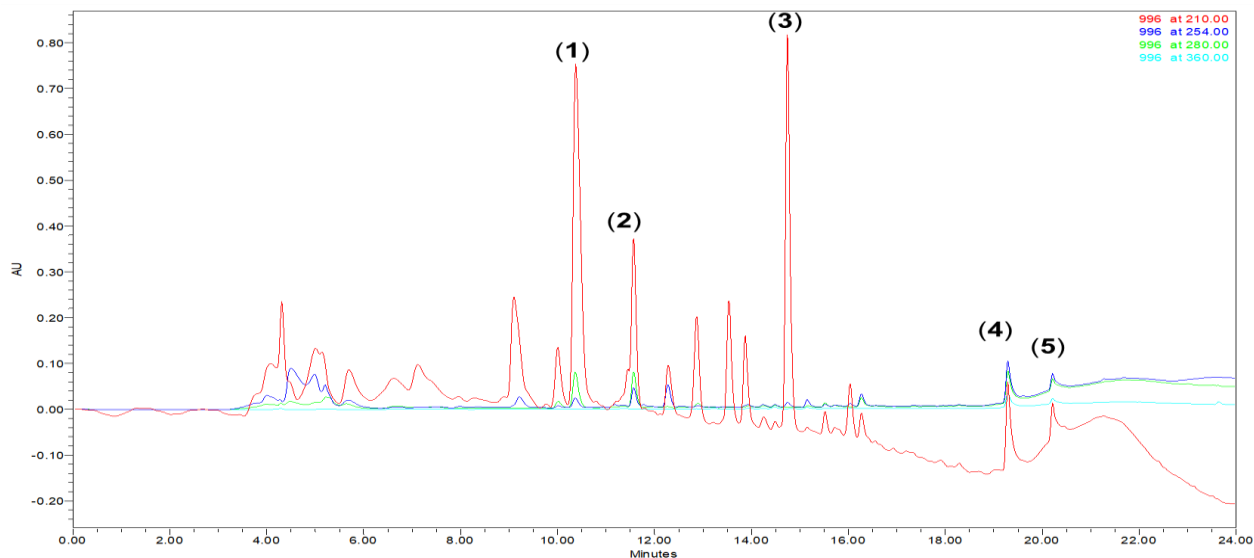


**Figure 6-2.** HPLC chromatogram of fraction C containing various secondary metabolites produced by *J. agaricidamnosum*.

Thus, we isolated and dereplicated several known compounds from the isolated peaks using HR-ESI-MS and 1-D NMR, as shown in **Figure 6.3**. We, therefore, could not find any new secondary metabolites from the strains.

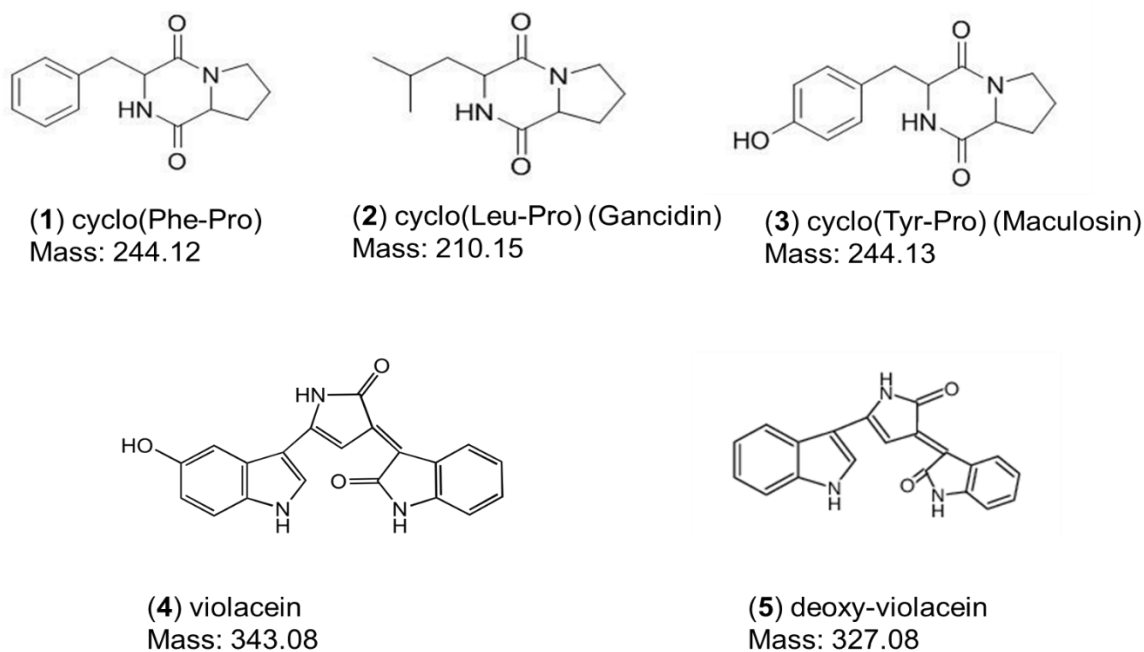


**Figure 6-3.** Dereplication of various known compounds from *J. agaricidamnosum* based on isolation, 1-D NMR, and mass spectrometry.

#### 6.4. Biological activity of the purple-like compound and diamino acids

**Table 6.2.** Biological activity of the purple-like compound and diamino acids produced by *J. agaricidamnorum*.

Antibacterial activity	MIC ( $\mu\text{g/ml}$ ) *				
	(1)	(2)	(3)	(4)	(5)
<i>Pseudomonas aeruginosa</i> DSM 50071	> 64	> 64	> 64	19.81	24.79
<i>Yersinia tuberculosis</i> YPIII	> 64	> 64	> 64	nd	nd
<i>Paenibacillus</i> sp. AD64	> 64	> 64	> 64	14.49	15.35
<i>Bacillus subtilis</i> ATCC 6051	> 64	> 64	> 64	nd	nd
<i>Mycobacterium phlei</i>	nd	nd	nd	> 64	> 64
<i>Staphylococcus aureus</i> USA300 LAC	nd	nd	nd	7.89	8.02

\***Supplementary Figure 7-1**, nd: did not conduct

All diketopiperazines produced by *J. agaricidamnorum* showed no antibacterial properties against the selected pathogens, as shown in **Table 7.2**. However, violacein, a natural pigment, derived from tryptophan, and its deoxy form showed antibacterial activities against *Pseudomonas*, *Paenibacillus*, and *Staphylococcus* in this study. A previous report by Aruldass *et al.* 2017 also showed that violacein produced by *Chromobacterium violaceum* has antibacterial activities towards *S. aureus* and MRSA. Its activities have also been previously reported by Cazoto *et al.* 2011.

There are many modes of action (MOA) of violacein suggested, but it appears that it is still not fully understood up to now. Some authors suggest that violacein is disrupting the membrane permeabilization, which causes leakage of ATP, while other studies showed that violacein also acts as a disruption agent to the structure and permeability of liposomes. However, it emerges the general idea that violacein is mainly mediating its antibacterial effect by damaging membranes.

## Acknowledgments

In these 3.5 years of my Ph.D. journey, I have evolved in many ways. As a biologist, I learned to be a chemist to solve many structures, discovering new chemistry from extracts of fermented bacterial broth. I strove for excellence in every aspect that I tackled. However, sometimes there were ups, and sometimes there were downs. My biological knowledge also helped to finalize every project. We were realized or not; every new entity needs a biological perspective to generate its function. Nevertheless, I feel a great deal of gratefulness to those who conveyed me along the way.

In the first instance, I would like to express my sincere gratitude to my supervisor, Prof. Dr. Harald Gross, who approved me to join and access his lab and continuously supported my Ph.D. study and related research. I found in him a supervisor with immense knowledge, cheerfulness, patience, and friendliness. He also creative in creating ideas, much motivation, and perpetual optimism. His consistent guidance also helped me in finalizing my thesis.

I am also thankful to my second supervisor, PD Dr. Bertolt Gust, for supporting me in conducting my Ph.D. studies in this institute. He is a flexible person and gave valuable comments on my project during a weekly group meeting of the department. I would also like to extend thanks to Prof. Dr. Friedrich Götz and Prof. Dr. Nadine Ziemert, for their willingness to accompany my supervisors as members of my oral defense committee.

I would also like to express my appreciation to Research and Innovation in Science and Technology (RISET-Pro) World Bank Loan No. 8245 for a three-year Ph.D. scholarship, giving me a chance to conduct my Ph.D. studies and research in one of the world's top 100 best universities based on Times Higher Education version in 2020. I would also thank to BMBF-Forschungsprojekte: TTU 09.705 for supporting my study.

I would also like to thank Wolfgang for his extensive help in some essential chemical-related research and delivering some pure compounds to collaborators. He is also friendly and has an easy-going character – also Patricia, who was responsible for providing me some chemicals before Wolfgang joined the lab. She is a warm and excellent organizer.

Thus, the lab was organized very well in her hand. She also managed some HiWi people that helped to provide us with some clean glassware. I would also like to thank Dr. Dorothee Wistuba of the MS measurements, which were valuable in all parts of my work.

Further, I would like to thank my fellow Ph.D. students in the Pharmaceutical Biology department over the years. Hamada, a person that is knowledgeable in chemistry, especially in NMR and mass spectrometry. I learned a lot from him, particularly about how to solve some structures and how to analyze the MS data. He was always the first person that I asked when I had difficulties related to elucidation and dereplication. He looks serious and disciplined, but he has a caring character and is helpful and friendly. The second person that I intended to go to solve my chemistry problems was Julia. However, she finished her studies one year after I arrived in this lab. Irina is also a chemist, and she helped me a lot regarding chemistry problems and the submission of my pure compounds to the NMR facility in the Gross group. She is accommodating and has a pleasant nature.

I would also thank Aziz. I feel home when talking with Aziz, as he also comes from Indonesia. On the other hand, his fatherly nature gives me a feeling of being at a family home. He also contributed to some research related to the 16s rRNA sequencing of my isolated strains from Indonesia. Junjing, my friendly mate, also makes me feel at home, as our food is not very different. Sometimes, we enjoyed eating together in a Chinese restaurant with other Gross lab members. I also extend thanks to Carolina and Lina: both are very friendly, they also gave me the feeling of being in my own country, as when I met them in the morning, they liked to say, "Hello! How are you?" together with a smile. A simple gesture, but it made me feel better when starting the day. They also sometimes helped me solve problems related to molecular biology. Another friendly guy is Niraj. He also has an easy-going manner, and so made my Ph.D. life feel a bit more liveable. I also would like to thank my seniors: a pleasant character, Ghazaleh, and a dynamic person, Anina. Their experience helped me to solve and build my strategy to research in this lab. I also thank Keshab, Thomas, and Tarik for their pleasant companionship in the lab, and some help. Keshab and Thomas are both good at organic chemistry. Thus, they also sometimes gave me some hints related to chemistry.



As other companions on this Ph.D. journey, I also thank my Master module M6 students (Christian, Mariana, Philip, Luke Tu, and Kristian). All their work was valuable in my Ph.D. research. I am also grateful for the considerable efforts of members of Pharmaceutical Biology Department on the sixth floor, including Junior Prof. Leo and Prof. Heide with their valuable comments in my work during group meetings, Corinna who helped me to finalize the documents related to Ph.D. studies, Alicia who organized the coffee machine for us, Tomke who organized the weekly group meetings; Marius with his cheerful and friendly manner; Emmanuel, Alexandra, Daniel, Felix, Nicole, Nils, Franziska, Tobias, Roger, Nhomsai, Cathrin, Gesa, Simon, and other members that were also part of my life as a Ph.D. student.

I also would like to thank my flatmates -Jenny and Andres, for their understanding during my studies and when writing my thesis. Also, thanks to Franky, who helped me during difficulties that raised when living in Germany. I'm grateful for Kengo, a Ph.D. student from Japan, who consistently accompanied me to exercise together at McFit. I also thank all Indonesian students in Tübingen who helped me during my stay and made me feel at home, including Karlina, Arif, Kunio, Bahrain, Ojik, Jejen, Mbak Dewi, and her family, and others.

I would also like to deliver my heartfelt and sincere thanks to my mother and father - who now rest in peace in a better place at heaven. Thanks for giving me approval and support to conduct studies abroad for my master's and my Ph.D. I also wish to place on records heartfelt and thanks to my beautiful wife -Winda, and my friendly sister -Linda, who also give me support, even at a distance, and their patience to pursue my Ph.D. in Germany. Their sacrifices have paid off. Finally, I thank my God for His unfailing love and blessing on every single life that touched mine during my journeys.

## Curriculum Vitae

### Personal Details

Andri Frediansyah, M.Sc.

Permanent residence: Celeban UH III/622 (A6), 55167 Yogyakarta, Indonesia

Temporary residence: Eberhardstrasse 22, 72108 Rottenburg Am Neckar, Germany

Place/Date of birth: Sleman/15<sup>th</sup> January 1989

Nationality: Indonesian

Telephone: +49 15223407444

Email: microbiologii@gmail.com or andri.frediansyah@lipi.go.id

### Education and Experiences

<i>Ph.D. in Pharmacy (Pharmaceutical Biology)</i> Supervisor: Prof. Dr. Harald Groß, Pharmaceutical Biology, Pharmaceutical Institute, Eberhard Karls Universität Tübingen, Germany Scholarship: RASET-Pro	May 2017 – September 2020
<i>Master of Science in Applied Biological Sciences</i> Supervisor: Prof. Dr. Panida Navasumrit Chulabhorn Graduate Institute, Bangkok, Thailand Scholarship: ASEAN Foundation	June 11, 2013 – May 22, 2015
<i>Research scientist</i> Research Division for Natural Product Technology, Indonesian Institute of Sciences (LIPI)	December 2010 – present
<i>Laboratory assistant (for six subjects)</i> Faculty of Biology Gadjah Mada University, Yogyakarta, Indonesia	July 2017- May 2010
<i>Bachelor of Science in Biology</i> Supervisor: Prof. Dr. Endang Sutariningsing S. Gadjah Mada University, Yogyakarta, Indonesia Scholarship: Tanoto Foundation	September 1, 2006 – July 19, 2010
Senior High School 6 Yogyakarta, Indonesia	July 2003 – June 2006
Junior High School 13 Yogyakarta, Indonesia	July 2001- June 2003
Elementary School Tahunan II Yogyakarta, Indonesia	July 1994- June 2000

## References

- Abisado, R.G., Benomar, S., Klaus, J.R., Dandekar, A.A., and Chandler, J.R. (2018). Bacterial quorum sensing and microbial community interactions. *MBio* 9.
- Ackleh, A.S., Carter, J., Chellamuthu, V.K., and Ma, B. (2016). A model for the interaction of frog population dynamics with *Batrachochytrium dendrobatidis*, *Janthinobacterium lividum* and temperature and its implication for chytridiomycosis management. *Ecological modelling* 320, 158-169.
- Agematu, H., Suzuki, K., and Tsuya, H. (2011). *Massilia* sp. BS-1, a novel violacein-producing bacterium isolated from soil. *Bioscience, biotechnology, and biochemistry* 75, 2008-2010.
- Anjum, K., Sadiq, I., Chen, L., Kaleem, S., Li, X.-C., Zhang, Z., and Lian, X.-Y. (2018). Novel antifungal janthinopolyenemycins A and B from a co-culture of marine-associated *Janthinobacterium* spp. ZZ145 and ZZ148. *Tetrahedron Letters* 59, 3490-3494.
- Arp, J., S., Mukherji, R., Mattern, D.J., García-Altres, M., Klapper, M., Brock, D.A., Brakhage, A.A., Strassmann, J.E., and Queller, D.C. (2018). Synergistic activity of cosecreted natural products from amoebae-associated bacteria. *Proceedings of the National Academy of Sciences* 115, 3758-3763.
- Aruldass, C.A., Venil, C.K., and Ahmad, W.A. (2015). Violet pigment production from liquid pineapple waste by *Chromobacterium violaceum* UTM5 and evaluation of its bioactivity. *Rsc Advances* 5, 51524-51536.
- Asfahl, K.L., and Schuster, M. (2018). Additive effects of quorum sensing anti-activators on *Pseudomonas aeruginosa* virulence traits and transcriptome. *Frontiers in Microbiology* 8, 2654.
- Ash, C. (1996). Antibiotic resistance: the new apocalypse? *Trends in microbiology* 4, 371-372.
- Atalah, J., Blamey, L., Muñoz-Ibacache, S., Gutierrez, F., Urzua, M., Encinas, M.V., Pérez, M., Sun, J., and Blamey, J.M. (2020). Isolation and characterization of violacein from an Antarctic *Iodobacter*: a non-pathogenic psychrotolerant microorganism. *Extremophiles* 24, 43-52.
- Aune, G.J., Furuta, T., and Pommier, Y. (2002). Ecteinascidin 743: a novel anticancer drug with a unique mechanism of action. *Anti-cancer drugs* 13, 545-555.
- Austin, B., Gonzalez, C.J., Stobie, M., Curry, J.I., and Mcloughlin, M.F. (1992). Recovery of *Janthinobacterium lividum* from diseased rainbow trout, *Oncorhynchus mykiss* (Walbaum), in Northern Ireland and Scotland. *Journal of Fish Diseases* 15, 357-359.
- Awad, G., Mathieu, F., Coppel, Y., and Lebrihi, A. (2005). Characterization and regulation of new secondary metabolites from *Aspergillus ochraceus* M18 obtained by UV mutagenesis. *Canadian journal of microbiology* 51, 59-67.
- Babić, F., Venturi, V., and Maravić-Vlahoviček, G. (2010). Tobramycin at subinhibitory concentration inhibits the RhII/R quorum sensing system in a *Pseudomonas aeruginosa* environmental isolate. *BMC infectious diseases* 10, 148.
- Bach, E., Daroit, D.J., Corrêa, A.P.F., and Brandelli, A. (2011). Production and properties of keratinolytic proteases from three novel Gram-negative feather-degrading bacteria isolated from Brazilian soils. *Biodegradation* 22, 1191.
- Bajpai, V.K., Rather, I.A., and Park, Y. (2016). Partially Purified Exo-Polysaccharide from *Lactobacillus Sakei* Probio 65 with Antioxidant,  $\alpha$ -Glucosidase and Tyrosinase Inhibitory Potential. *Journal of Food Biochemistry* 40, 264-274.
- Bandounas, L., De Winde, J.H., and Ruijssenaars, H.J. (2009). Isolation and characterization of *Cupriavidus basilensis* HMF14 for biological removal of inhibitors from lignocellulosic hydrolysate. *Microbial Biotechnology* 3, 336-343.
- Bartz, Q.R. (1948). Isolation and characterization of chloromycetin. *J. Biol. Chem* 172, 445-450.
- Bauer, J.S., Hauck, N., Christof, L., Mehnaz, S., Gust, B., and Gross, H. (2016). The systematic investigation of the quorum sensing system of the biocontrol strain *Pseudomonas*

- chlororaphis subsp. aurantiaca PB-St2 unveils aurl to be a biosynthetic origin for 3-oxo-homoserine lactones. *PLoS one* 11, e0167002.
- Bentley, S.D., Chater, K.F., Cerdeño-Tárraga, A.-M., Challis, G.L., Thomson, N., James, K.D., Harris, D.E., Quail, M.A., Kieser, H., and Harper, D. (2002). Complete genome sequence of the model actinomycete *Streptomyces coelicolor* A3 (2). *Nature* 417, 141-147.
- Bergy, M.E., De, B.C., Alma, D., Eble, T.E., Herr, R.R., and Le Roy, E.J. (1962). "Streptozotocin and its production". Google Patents).
- Biller, S.J., Schubotz, F., Roggensack, S.E., Thompson, A.W., Summons, R.E., and Chisholm, S.W. (2014). Bacterial vesicles in marine ecosystems. *science* 343, 183-186.
- Blatny, J.M., Ho, J., Skogan, G., Fykse, E.M., Aarskaug, T., and Waagen, V. (2011). Airborne *Legionella* bacteria from pulp waste treatment plant: aerosol particles characterized as aggregates and their potential hazard. *Aerobiologia* 27, 147-162.
- Bode, H.B., Bethe, B., Höfs, R., and Zeeck, A. (2002). Big effects from small changes: possible ways to explore nature's chemical diversity. *ChemBioChem* 3, 619-627.
- Bokhove, M., Jimenez, P.N., Quax, W.J., and Dijkstra, B.W. (2010). The quorum-quenching N-acyl homoserine lactone acylase PvdQ is an Ntn-hydrolase with an unusual substrate-binding pocket. *Proceedings of the National Academy of Sciences* 107, 686-691.
- Boon, C., Deng, Y., Wang, L.-H., He, Y., Xu, J.-L., Fan, Y., Pan, S.Q., and Zhang, L.-H. (2008). A novel DSF-like signal from *Burkholderia cenocepacia* interferes with *Candida albicans* morphological transition. *The ISME journal* 2, 27-36.
- Boucher, H.W., Talbot, G.H., Bradley, J.S., Edwards, J.E., Gilbert, D., Rice, L.B., Scheld, M., Spellberg, B., and Bartlett, J. (2009). Bad bugs, no drugs: no ESKAPE! An update from the Infectious Diseases Society of America. *Clinical infectious diseases* 48, 1-12.
- Bowman, J., Sly, L., and Hayward, A. (1988). *Pseudomonas mixta* sp. nov., a bacterium from soil with degradative activity on a variety of complex polysaccharides. *Systematic and Applied Microbiology* 11, 53-59.
- Bowman, J., Sly, L., Hayward, A., Spiegel, Y., and Stackebrandt, E. (1993). *Telluria mixta* (*Pseudomonas mixta* Bowman, Sly, and Hayward 1988) gen. nov., comb. nov., and *Telluria chitinolytica* sp. nov., soil-dwelling organisms which actively degrade polysaccharides. *International Journal of Systematic and Evolutionary Microbiology* 43, 120-124.
- Breijyeh, Z., Jubeh, B., and Karaman, R. (2020). Resistance of Gram-negative bacteria to current antibacterial agents and approaches to resolve it. *Molecules* 25, 1340.
- Breitschwerdt, E.B., and Kordick, D.L. (2000). Bartonella infection in animals: carriership, reservoir potential, pathogenicity, and zoonotic potential for human infection. *Clinical microbiology reviews* 13, 428-438.
- Brigham, R., and Pittenger, R. (1956). *Streptomyces orientalis*, n. sp., the source of vancomycin. *Antibiotics & chemotherapy (Northfield, Ill.)* 6, 642-647.
- Broder, L.E., and Carter, S.K. (1973). Pancreatic islet cell carcinoma: II. Results of therapy with streptozotocin in 52 patients. *Annals of Internal Medicine* 79, 108-118.
- Brown, L., Wolf, J.M., Prados-Rosales, R., and Casadevall, A. (2015). Through the wall: extracellular vesicles in Gram-positive bacteria, mycobacteria and fungi. *Nature Reviews Microbiology* 13, 620-630.
- Brucker, R.M., Harris, R.N., Schwantes, C.R., Gallaher, T.N., Flaherty, D.C., Lam, B.A., and Minbiole, K.P.C. (2008). Amphibian chemical defense: antifungal metabolites of the microsymbiont *Janthinobacterium lividum* on the salamander *Plethodon cinereus*. *Journal of chemical ecology* 34, 1422-1429.
- Callow, R., and Hart, P.A. (1946). Antibiotic material from *Bacillus licheniformis* (Weigmann, emend. Gibson) active against species of *Mycobacteria*. *Nature* 157, 334-335.
- Campbell, B.J., Engel, A.S., Porter, M.L., and Takai, K. (2006). The versatile epsilon-proteobacteria: key players in sulphidic habitats. *Nature Reviews Microbiology* 4, 458-468.

- Carter, S.K., Broder, L., and Williams, R.B. (1971). Streptozotocin and metastatic insulinoma. *Annals of internal medicine* 74, 445-446.
- Casewell, M., and Hill, R. (1985). In-vitro activity of mupirocin 'pseudomonic acid' against clinical isolates of *Staphylococcus aureus*. *Journal of Antimicrobial Chemotherapy* 15, 523-531.
- Casewell, M., and Hill, R. (1986). Elimination of nasal carriage of *Staphylococcus aureus* with mupirocin ('pseudomonic acid')—a controlled trial. *Journal of Antimicrobial Chemotherapy* 17, 365-372.
- Casewell, M., and Hill, R. (1987). Mupirocin ('pseudomonic acid')—a promising new topical antimicrobial agent. *Journal of Antimicrobial Chemotherapy* 19, 1-5.
- Cdc (2019). Antibiotic Resistance Threats in the United States,.
- Chang, C.-J., and Tsai, T.-Y. (2016). Antimelanogenic effects of the novel melanogenic inhibitors daidzein and equol, derived from soymilk fermented with *Lactobacillus plantarum* strain TWK10, in B16F0 mouse melanoma cells. *Journal of Functional Foods* 22, 211-223.
- Chang, T.-W., Gorbach, S.L., Bartlett, J.G., and Saginur, R. (1980). Bacitracin treatment of antibiotic-associated colitis and diarrhea caused by *Clostridium difficile* toxin. *Gastroenterology* 78, 1584-1586.
- Chaudhary, D.K., Dahal, R.H., Kim, D.-U., and Kim, J. (2020). *Flavobacterium sandaracinum* sp. nov., *Flavobacterium caseinilyticum* sp. nov., and *Flavobacterium hiemivividum* sp. nov., novel psychrophilic bacteria isolated from Arctic soil. *International Journal of Systematic and Evolutionary Microbiology* 70, 2269-2280.
- Chen, J., Frediansyah, A., Männle, D., Straetener, J., Brötz-Oesterhelt, H., Ziemert, N., Kaysser, L., and Gross, H. (2020). New Nocobactin Derivatives with Antimuscarinic Activity, Terpenibactins AΓÇôC, Revealed by Genome Mining of *Nocardia terpenica* IFM 0406. *ChemBioChem*.
- Chet, I., Spiegel, Y., and Sharon, E. (Year). "Mechanisms and Improved Biocontrol of the Root-Knot Nematodes by *Trichoderma* spp", in: *VI International Symposium on Chemical and non-Chemical Soil and Substrate Disinfestation-SD2004* 698), 225-228.
- Chiriac, C., Baricz, A., and Coman, C. (2018). Draft genome sequence of *Janthinobacterium* sp. strain ROICE36, a putative secondary metabolite-synthesizing bacterium isolated from Antarctic snow. *Genome Announc.* 6, e01553-01517.
- Cimermancic, P., Medema, M.H., Claesen, J., Kurita, K., Brown, L.C.W., Mavrommatis, K., Pati, A., Godfrey, P.A., Koehrsen, M., and Clardy, J. (2014). Insights into secondary metabolism from a global analysis of prokaryotic biosynthetic gene clusters. *Cell* 158, 412-421.
- Cueto, M., Jensen, P.R., Kauffman, C., Fenical, W., Lobkovsky, E., and Clardy, J. (2001). Pestalone, a new antibiotic produced by a marine fungus in response to bacterial challenge. *Journal of Natural Products* 64, 1444-1446.
- Cummins, J., Reen, F.J., Baysse, C., Mooij, M.J., and O'gara, F. (2009). Subinhibitory concentrations of the cationic antimicrobial peptide colistin induce the *Pseudomonas aeruginosa* quinolone signal in *Pseudomonas aeruginosa*. *Microbiology* 155, 2826-2837.
- Cusick, K.D., Fitzgerald, L.A., Cockrell, A.L., and Biffinger, J.C. (2015). Selection and evaluation of reference genes for reverse transcription-quantitative PCR expression studies in a thermophilic bacterium grown under different culture conditions. *PLoS One* 10, e0131015.
- D'angelo-Picard, C., Faure, D., Penot, I., and Dessaux, Y. (2005). Diversity of N-acyl homoserine lactone-producing and-degrading bacteria in soil and tobacco rhizosphere. *Environmental microbiology* 7, 1796-1808.
- Dangi, S., Gao, S., Duan, Y., and Wang, D. (2020). Soil microbial community structure affected by biochar and fertilizer sources. *Applied Soil Ecology* 150, 103452.
- Davies, D.G., and Marques, C.Í.N.H. (2009). A fatty acid messenger is responsible for inducing dispersion in microbial biofilms. *Journal of bacteriology* 191, 1393-1403.

- De Ley, J., Segers, P., and Gillis, M. (1978). Intra- and intergeneric similarities of *Chromobacterium* and *Janthinobacterium* ribosomal ribonucleic acid cistrons. *International Journal of Systematic and Evolutionary Microbiology* 28, 154-168.
- Degenkolb, T., Heinze, S., Schlegel, B., Strobel, G., and Gräfe, U. (2002). Formation of new lipoaminopeptides, acremostatins A, B, and C, by co-cultivation of *Acremonium* sp. Tbp-5 and *Mycogone rosea* DSM 12973. *Bioscience, biotechnology, and biochemistry* 66, 883-886.
- Delong, E.F., and Yayanos, A.A. (1986). Biochemical function and ecological significance of novel bacterial lipids in deep-sea prokaryotes. *Appl. Environ. Microbiol.* 51, 730-737.
- Demain, A.L. (2014). Importance of microbial natural products and the need to revitalize their discovery. *Journal of industrial microbiology & biotechnology* 41, 185-201.
- Deng, Y., Boon, C., Chen, S., Lim, A., and Zhang, L.-H. (2013). Cis-2-dodecenoic acid signal modulates virulence of *Pseudomonas aeruginosa* through interference with quorum sensing systems and T3SS. *BMC microbiology* 13, 1-11.
- Dietrich, J., Kage, H., and Nett, M. (2019). Genomics-inspired discovery of massiliachelin, an agrochelin epimer from *Massilia* sp. NR 4-1. *Beilstein journal of organic chemistry* 15, 1298-1303.
- Ding, F., Oinuma, K.-I., Smalley, N.E., Schaefer, A.L., Hamwy, O., Greenberg, E.P., and Dandekar, A.A. (2018). The *Pseudomonas aeruginosa* orphan quorum sensing signal receptor QscR regulates global quorum sensing gene expression by activating a single linked operon. *MBio* 9.
- Doerschuk, A.P., McCormick, J.R.D., Goodman, J.J., Szumski, S.A., Growich, J.A., Miller, P.A., Bitler, B.A., Jensen, E.R., Matrishin, M., and Petty, M.A. (1959). Biosynthesis of tetracyclines. I. The halide metabolism of *Streptomyces aureofaciens* mutants. The preparation and characterization of tetracycline, 7-chloro-36-tetracycline and 7-bromotetracycline. *Journal of the American Chemical Society* 81, 3069-3075.
- Dubos, R.J. (1939). Bactericidal effect of an extract of a soil bacillus on gram positive cocci. *Proceedings of the Society for Experimental Biology and Medicine* 40, 311-312.
- Eberhard, A., Longin, T., Widrig, C.A., and Stranick, S.J. (1991). Synthesis of the lux gene autoinducer in *Vibrio fischeri* is positively autoregulated. *Archives of microbiology* 155, 294-297.
- El-Sayed, A.K., Hothersall, J., Cooper, S.M., Stephens, E., Simpson, T.J., and Thomas, C.M. (2003). Characterization of the mupirocin biosynthesis gene cluster from *Pseudomonas fluorescens* NCIMB 10586. *Chemistry & biology* 10, 419-430.
- Embarcadero-Jiménez, S., Peix, Á., Igual, J.M., Rivera-Orduña, F.N., and Wang, E.T. (2016). *Massilia violacea* sp. nov., isolated from riverbank soil. *International journal of systematic and evolutionary microbiology* 66, 707-711.
- Eneroeth, Å., Ahrné, S., and Molin, G. (2000). Contamination routes of Gram-negative spoilage bacteria in the production of pasteurised milk, evaluated by randomly amplified polymorphic DNA (RAPD). *International Dairy Journal* 10, 325-331.
- European Committee for Antimicrobial Susceptibility Testing of the European Society of Clinical, M., and Infectious, D. (2003). Determination of minimum inhibitory concentrations (MICs) of antibacterial agents by broth dilution. *Clinical Microbiology and Infection* 9.
- Evans, M.E., Feola, D.J., and Rapp, R.P. (1999). Polymyxin B sulfate and colistin: old antibiotics for emerging multiresistant gram-negative bacteria. *Annals of Pharmacotherapy* 33, 960-967.
- Fahlgren, C., Bratbak, G., Sandaa, R.-A., Thyraug, R., and Zweifel, U.L. (2011). Diversity of airborne bacteria in samples collected using different devices for aerosol collection. *Aerobiologia* 27, 107-120.
- Fais, T., Delmas, J., Barnich, N., Bonnet, R., and Dalmasso, G. (2018). Colibactin: more than a new bacterial toxin. *Toxins* 10, 151.

- Feline, T.C., Jones, R.B., Mellows, G., and Phillips, L. (1977). Pseudomonic acid. Part 2. Biosynthesis of pseudomonic acid A. *Journal of the Chemical Society, Perkin Transactions 1*, 309-318.
- Feng, G.-D., Yang, S.-Z., Li, H.-P., and Zhu, H.-H. (2016). *Massilia putida* sp. nov., a dimethyl disulfide-producing bacterium isolated from wolfram mine tailing. *International journal of systematic and evolutionary microbiology* 66, 50-55.
- Ferrari, B.C., Binnerup, S.J., and Gillings, M. (2005). Microcolony cultivation on a soil substrate membrane system selects for previously uncultured soil bacteria. *Appl. Environ. Microbiol.* 71, 8714-8720.
- Fischer, D., Gessner, G., Fill, T.P., Barnett, R., Tron, K., Dornblut, K., Kloss, F., Stallforth, P., Hube, B., and Heinemann, S.H. (2019). Disruption of Membrane Integrity by the Bacterium-Derived Antifungal Jagaricin. *Antimicrobial Agents and Chemotherapy* 63, e00707-00719.
- Fleming, A. (1944). The discovery of penicillin. *British Medical Bulletin* 2, 4-5.
- Forsythe, S.J., Dickins, B., and Jolley, K.A. (2014). *Cronobacter*, the emergent bacterial pathogen *Enterobacter sakazakii* comes of age; MLST and whole genome sequence analysis. *BMC genomics* 15, 1121.
- Frank, U., Lenz, W., Damrath, E., Kappstein, I., and Daschner, F. (1989). Nasal carriage of *Staphylococcus aureus* treated with topical mupirocin (pseudomonic acid) in a children's hospital. *Journal of Hospital Infection* 13, 117-120.
- Fuller, A., Mellows, G., Woolford, M., Banks, G., Barrow, K., and Chain, E. (1971). Pseudomonic acid: an antibiotic produced by *Pseudomonas fluorescens*. *Nature* 234, 416-417.
- Garske, L.A., Beatson, S.A., Leech, A.J., Walsh, S.L., and Bell, S.C. (2004). Su-inhibitory concentrations of ceftazidime and tobramycin reduce the quorum sensing signals of *Pseudomonas aeruginosa*. *Pathology* 36, 571-575.
- Gauthier, M. (1982). Validation of the name *Alteromonas luteoviolacea*. *International Journal of Systematic and Evolutionary Microbiology* 32, 82-86.
- Gerth, K., Bedorf, N., Höfle, G., Irschik, H., and Reichenbach, H. (1996). Epothilons A and B: antifungal and cytotoxic compounds from *Sorangium cellulosum* (Myxobacteria). *The Journal of antibiotics* 49, 560-563.
- Ghielmini, M., Colli, E., Erba, E., Bergamaschi, D., Pampallona, S., Jimeno, J., Faircloth, G., and Sessa, C. (1998). In vitro schedule-dependency of myelotoxicity and cytotoxicity of Ecteinascidin 743 (ET-743). *Annals of oncology* 9, 989-993.
- Giaccone, V., Alberghini, L., Biscotto, A., and Milandri, C. (Year). "Unusual spoilage in rabbit carcasses caused by *Janthinobacterium lividum*": World Rabbit Science Association), 1349-1352.
- Gillis, M., and Logan, N.A. (2015). *Janthinobacterium*. *Bergey's Manual of Systematics of Archaea and Bacteria*, 1-12.
- Graupner, K., Scherlach, K., Bretschneider, T., Lackner, G., Roth, M., Gross, H., and Hertweck, C. (2012). Imaging mass spectrometry and genome mining reveal highly antifungal virulence factor of mushroom soft rot pathogen. *Angewandte Chemie International Edition* 51, 13173-13177.
- Gross, H., and Loper, J.E. (2009). Genomics of secondary metabolite production by *Pseudomonas* spp. *Natural product reports* 26, 1408-1446.
- Gul, S.T., and Khan, A. (2007). Epidemiology and epizootology of brucellosis: A review. *Pakistan veterinary journal* 27, 145.
- Guo, Y. (2020). The fate of European olives. *Nature Food* 1, 255-255.
- Gupta, S., Govil, D., Kakar, P.N., Prakash, O., Arora, D., Das, S., Govil, P., and Malhotra, A. (2009). Colistin and polymyxin B: a re-emergence. *Indian journal of critical care medicine: peer-reviewed, official publication of Indian Society of Critical Care Medicine* 13, 49.

- Gyves, J.W., Stetson, P., Ensminger, W.D., Meyer, M., Walker, S., Gilbertson, S., and Janis, M.A. (1983). Hepatic arterial streptozocin: a clinical pharmacologic study in patients with liver tumors. *Cancer drug delivery* 1, 63-68..
- Haavik, H.I. (1975). Bacitracin production by the neotype: *Bacillus licheniformis* ATCC 14580. *Acta Pathologica Microbiologica Scandinavica Section B Microbiology* 83, 534-540.
- Habib, N., Khan, I.U., Xiao, M., Hejazi, M.S., Tarhriz, V., Zhi, X.-Y., and Li, W.-J. (2020). *Elioraea thermophila* sp. nov., a thermophilic bacterium from hot spring of the class Alphaproteobacteria, emended description of the genus *Elioraea* and proposal of *Elioraeaceae* fam. nov. *International Journal of Systematic and Evolutionary Microbiology* 70, 1300-1306.
- Hadziyannis, E., Tuohy, M., Thomas, L., Procop, G.W., Washington, J.A., and Hall, G.S. (2000). Screening and confirmatory testing for extended spectrum beta-lactamases (ESBL) in *Escherichia coli*, *Klebsiella pneumoniae*, and *Klebsiella oxytoca* clinical isolates. *Diagnostic microbiology and infectious disease* 36, 113-117.
- Han, A.W., Sandy, M., Fishman, B., Trindade-Silva, A.E., Soares, C.a.G., Distel, D.L., Butler, A., and Haygood, M.G. (2013). Turnerbactin, a novel triscatecholate siderophore from the shipworm endosymbiont *Teredinibacter turnerae* T7901. *PLoS one* 8, e76151.
- Hanlon, G., and Hodges, N.A. (1981). Bacitracin and protease production in relation to sporulation during exponential growth of *Bacillus licheniformis* on poorly utilized carbon and nitrogen sources. *Journal of bacteriology* 147, 427-431.
- Harvey, A.L. (2008). Natural products in drug discovery. *Drug discovery today* 13, 894-901.
- Hashidoko, Y., Takakai, F., Toma, Y., Darung, U., Melling, L., Tahara, S., and Hatano, R. (2008). Emergence and behaviors of acid-tolerant *Janthinobacterium* sp. that evolves N<sub>2</sub>O from deforested tropical peatland. *Soil Biology and Biochemistry* 40, 116-125.
- Hendriks, H.R., Fiebig, H.H., Giavazzi, R., Langdon, S.P., Jimeno, J.M., and Faircloth, G.T. (1999). High antitumor activity of ET743 against human tumor xenografts from melanoma, non-small-cell lung and ovarian cancer. *Annals of Oncology* 10, 1233-1240.
- High, K.P., and Washburn, R.G. (1997). Invasive aspergillosis in mice immunosuppressed with cyclosporin A, tacrolimus (FK506), or sirolimus (rapamycin). *Journal of Infectious Diseases* 175, 222-225.
- Hoffman, L.R., D'argenio, D.A., Maccoss, M.J., Zhang, Z., Jones, R.A., and Miller, S.I. (2005). Aminoglycoside antibiotics induce bacterial biofilm formation. *Nature* 436, 1171-1175.
- Höfle, G., Bedorf, N., Steinmetz, H., Schomburg, D., Gerth, K., and Reichenbach, H. (1996). Epothilone A and B-Novel 16-Membered Macrolides with Cytotoxic Activity: Isolation, Crystal Structure, and Conformation in Solution. *Angewandte Chemie International Edition in English* 35, 1567-1569.
- Huang, J.P., Mojib, N., Goli, R.R., Watkins, S., Waites, K.B., Ravindra, R., Andersen, D.T., and Bej, A.K. (2012). Antimicrobial activity of PVP from an Antarctic bacterium, *Janthinobacterium* sp. Ant5-2, on multi-drug and methicillin resistant *Staphylococcus aureus*. *Natural products and bioprospecting* 2, 104-110.
- Iino, T., Kawai, S., Yuki, M., Dekio, I., Ohkuma, M., and Haruta, S. (2020). *Thermaurantimonas aggregans* gen. nov., sp. nov., a moderately thermophilic heterotrophic aggregating bacterium isolated from microbial mats at a terrestrial hot spring. *International Journal of Systematic and Evolutionary Microbiology* 70, 1117-1121.
- Ikeda, H., Ishikawa, J., Hanamoto, A., Shinose, M., Kikuchi, H., Shiba, T., Sakaki, Y., Hattori, M., and Ōmura, S. (2003). Complete genome sequence and comparative analysis of the industrial microorganism *Streptomyces avermitilis*. *Nature biotechnology* 21, 526.
- Izbicka, E., Lawrence, R., Raymond, E., Eckhardt, G., Faircloth, G., Jimeno, J., Clark, G., and Vonhoff, D.D. (1998). In vitro antitumor activity of the novel marine agent, ecteinascidin-743 (ET-743, NSC-648766) against human tumors explanted from patients. *Annals of Oncology* 9, 981-987.



- Jans, C., De Wouters, T., Bonfoh, B., Lacroix, C., Kaindi, D.W.M., Anderegg, J., BCK, D.S.E., Vitali, S., Schmid, T., and Isenring, J. (2016). Phylogenetic, epidemiological and functional analyses of the *Streptococcus bovis*/*Streptococcus equinus* complex through an overarching MLST scheme. *BMC microbiology* 16, 117.
- Jensen, L.J., Skovgaard, M., Sicheritz-Pontén, T., Hansen, N.T., Johansson, H., Jørgensen, M.K., Kiil, K., Hallin, P.F., and Ussery, D. (2004). "Comparative genomics of four *Pseudomonas* species," in *Pseudomonas*. Springer), 139-164.
- Jenul, C., Sieber, S., Daepfen, C., Mathew, A., Lardi, M., Pessi, G., Hoepfner, D., Neuburger, M., Linden, A., and Gademann, K. (2018). Biosynthesis of fragin is controlled by a novel quorum sensing signal. *Nature communications* 9, 1-13.
- Jiao, J., Du, J., Frediansyah, A., Jahanshah, G., and Gross, H. (2020). Structure elucidation and biosynthetic locus of trinickiabactin from the plant pathogenic bacterium *Trinickia caryophylli*. *The Journal of antibiotics* 73, 28-34.
- Johnson, B.A., Anker, H., and Meloney, F.L. (1945). Bacitracin: a new antibiotic produced by a member of the *B. subtilis* group. *Science* 102, 376-377.
- Johnson, J.H., Tymiak, A.A., and Bolgar, M.S. (1990). Janthinocins A, B and C, novel peptide lactone antibiotics produced by *Janthinobacterium lividum*. *The Journal of antibiotics* 43, 920-930.
- Kampfer, P., Lodders, N., Martin, K., and Falsen, E. (2000). A revision of *Massilia*. *La Scola et al*, 1528-1533.
- Kämpfer, P., Wellner, S., Lohse, K., Martin, K., and Lodders, N. (2012). *Duganella phyllosphaerae* sp. nov., isolated from the leaf surface of *Trifolium repens* and proposal to reclassify *Duganella violaceinigra* into a novel genus as *Pseudoduganella violaceinigra* gen. nov., comb. nov. *Systematic and applied microbiology* 35, 19-23.
- Kawagishi, H., Somoto, A., Kuranari, J., Kimura, A., and Chiba, S. (1993). A novel cyclotetrapeptide produced by *Lactobacillus helveticus* as a tyrosinase inhibitor. *Tetrahedron letters* 34, 3439-3440.
- Kim, H.G., Kim, N.-R., Gim, M.G., Lee, J.M., Lee, S.Y., Ko, M.Y., Kim, J.Y., Han, S.H., and Chung, D.K. (2008). Lipoteichoic acid isolated from *Lactobacillus plantarum* inhibits lipopolysaccharide-induced TNF- $\alpha$  production in THP-1 cells and endotoxin shock in mice. *The Journal of Immunology* 180, 2553-2561.
- Kim, S.J., Shin, S.C., Hong, S.G., Lee, Y.M., Lee, H., Lee, J., Choi, I.-G., and Park, H. (2012). "Genome sequence of *Janthinobacterium* sp. strain PAMC 25724, isolated from alpine glacier cryoconite". *Am Soc Microbiol*.
- Klaus, J.R., Deay, J., Neuenswander, B., Hursh, W., Gao, Z., Bouddhara, T., Williams, T.D., Douglas, J., Monize, K., and Martins, P. (2018). Malleilactone is a *Burkholderia pseudomallei* virulence factor regulated by antibiotics and quorum sensing. *Journal of bacteriology* 200.
- Kochetkova, T.V., Zayulina, K.S., Zhigarkov, V.S., Minaev, N.V., Chichkov, B.N., Novikov, A.A., Toshchakov, S.V., Elcheninov, A.G., and Kublanov, I.V. (2020). *Tepidiforma bonchosmolovskayae* gen. nov., sp. nov., a moderately thermophilic Chloroflexi bacterium from a Chukotka hot spring (Arctic, Russia), representing a novel class, *Tepidiformia*, which includes the previously uncultivated lineage OLB14. *International Journal of Systematic and Evolutionary Microbiology* 70, 1192-1202.
- Komura, S., and Kurahashi, K. (1979). Partial purification and properties of L-2, 4-diaminobutyric acid activating enzyme from a polymyxin E producing organism. *The Journal of Biochemistry* 86, 1013-1021.
- Koropatnick, T.A., Engle, J.T., Apicella, M.A., Stabb, E.V., Goldman, W.E., and Mcfall-Ngai, M.J. (2004). Microbial factor-mediated development in a host-bacterial mutualism. *Science* 306, 1186-1188.

- Kresge, N., Simoni, R.D., and Hill, R.L. (2004). Selman Waksman: the father of antibiotics. *Journal of Biological Chemistry* 279, e7-e7.
- Kunakom, S., and EustáQuio, A.S. (2019). Burkholderia as a source of natural products. *Journal of natural products* 82, 2018-2037.
- Kurosawa, K., Ghiviriga, I., Sambandan, T., Lessard, P.A., Barbara, J.E., Rha, C., and Sinskey, A.J. (2008). Rhodostreptomycins, antibiotics biosynthesized following horizontal gene transfer from Streptomyces padanus to Rhodococcus fascians. *Journal of the American Chemical Society* 130, 1126-1127.
- Kusumoto, S., Matsukura, M., and Shiba, T. (1981). A new method for the determination of optical purity of synthetic peptides. *Biopolymers: Original Research on Biomolecules* 20, 1869-1875.
- Kwan, J.C., Meickle, T., Ladwa, D., Teplitski, M., Paul, V., and Luesch, H. (2011). Lyngbyoic acid, a tagged atty acid from a marine cyanobacterium, disrupts quorum sensing in Pseudomonas aeruginosa. *Molecular BioSystems* 7, 1205-1216.
- La Scola, B., Birtles, R.J., Mallet, M.-N.L., and Raoult, D. (1998). Massilia timonae gen. nov., sp. nov., isolated from blood of an immunocompromised patient with cerebellar lesions. *Journal of clinical microbiology* 36, 2847-2852.
- Lang, G., Blunt, J.W., Cummings, N.J., Cole, A.L.J., and Munro, M.H.G. (2005). Hirsutide, a cyclic tetrapeptide from a spider-derived entomopathogenic fungus, Hirsutella sp. *Journal of natural products* 68, 1303-1305.
- Lee, W., Lee, S.-H., Kim, M., Moon, J.-S., Kim, G.-W., Jung, H.-G., Kim, I.H., Oh, J.E., Jung, H.E., and Lee, H.K. (2018). Vibrio vulnificus quorum-sensing molecule cyclo (Phe-Pro) inhibits RIG-I-mediated antiviral innate immunity. *Nature communications* 9, 1-13.
- Lepe, J.A., Domínguez-Herrera, J., Pachón, J., and Aznar, J. (2014). Determining accurate vancomycin MIC values for methicillin-resistant Staphylococcus aureus by the microdilution method. *Journal of Antimicrobial Chemotherapy* 69, 136-138.
- Lim, S.-D., and Kim, K.-S. (2012). Optimization of tyrosinase inhibitory activity in the fermented milk by Lactobacillus plantarum M23. *Food Science of Animal Resources* 32, 678-684.
- Lincoln, S.P., Fermor, T.R., and Tindall, B.J. (1999). Janthinobacterium agaricidamnosum sp. nov., a soft rot pathogen of Agaricus bisporus. *International Journal of Systematic and Evolutionary Microbiology* 49, 1577-1589.
- Lindquist, D., Murrill, D., Burran, W.P., Winans, G., Janda, J.M., and Probert, W. (2003). Characteristics of Massilia timonae and Massilia timonae-like isolates from human patients, with an emended description of the species. *Journal of clinical microbiology* 41, 192-196.
- Lindsay, A.K., and Hogan, D.A. (2014). Candida albicans: molecular interactions with Pseudomonas aeruginosa and Staphylococcus aureus. *Fungal Biology Reviews* 28, 85-96.
- Liu, X., Jia, J., Popat, R., Ortori, C.A., Li, J., Diggle, S.P., Gao, K., and Cámara, M. (2011). Characterisation of two quorum sensing systems in the endophytic Serratia plymuthica strain G3: Differential control of motility and biofilm formation according to life-style. *BMC microbiology* 11, 1471-2180.
- Liu, Z., Wang, W., Zhu, Y., Gong, Q., Yu, W., and Lu, X. (2013). Antibiotics at subinhibitory concentrations improve the quorum sensing behavior of Chromobacterium violaceum. *FEMS Microbiology letters* 341, 37-44.
- Louden, B.C., Haarmann, D., and Lynne, A.M. (2011). Use of blue agar CAS assay for siderophore detection. *Journal of microbiology & biology education: JMBE* 12, 51.
- Martinez-Rosales, C., Marizcurrena, J.J., Iriarte, A., Fullana, N., Musto, H., and Castro-Sowinski, S. (2015). Characterizing proteases in an Antarctic Janthinobacterium sp. isolate: Evidence of a protease horizontal gene transfer event. *Adnace in Polar Science* 26, 88-95.

- Masschelein, J., Jenner, M., and Challis, G.L. (2017). Antibiotics from Gram-negative bacteria: a comprehensive overview and selected biosynthetic highlights. *Natural product reports* 34, 712-783.
- Masuelli, L., Pantanella, F., La Regina, G., Benvenuto, M., Fantini, M., Mattera, R., Di Stefano, E., Mattei, M., Silvestri, R., and Schippa, S. (2016). Violacein, an indole-derived purple-colored natural pigment produced by *Janthinobacterium lividum*, inhibits the growth of head and neck carcinoma cell lines both in vitro and in vivo. *Tumor Biology* 37, 3705-3717.
- Mckenney, D., Brown, K.E., and Allison, D.G. (1995). Influence of *Pseudomonas aeruginosa* exoproducts on virulence factor production in *Burkholderia cepacia*: evidence of interspecies communication. *Journal of bacteriology* 177, 6989-6992.
- Mcrose, D.L., Baars, O., Seyedsayamdost, M.R., and Morel, F.O.M. (2018a). Quorum sensing and iron regulate a two-for-one siderophore gene cluster in *Vibrio harveyi*. *Proceedings of the National Academy of Sciences* 115, 7581-7586.
- Mcrose, D.L., Baars, O., Seyedsayamdost, M.R., and Morel, F.O.M.M. (2018b). Quorum sensing and iron regulate a two-for-one siderophore gene cluster in *Vibrio harveyi*. *Proceedings of the National Academy of Sciences* 115, 7581-7586.
- Migita, K., and Eguchi, K. (2003). FK506: anti-inflammatory properties. *Current Medicinal Chemistry-Anti-Inflammatory & Anti-Allergy Agents* 2, 260-264.
- Mojib, N., Andersen, D.T., and Bej, A.K. (2011). Structure and function of a cold shock domain fold protein, CspD, in *Janthinobacterium* sp. Ant5-2 from East Antarctica. *FEMS microbiology letters* 319, 106-114.
- Morimoto, Y.V., and Minamino, T. (2014). Structure and function of the bi-directional bacterial flagellar motor. *Biomolecules* 4, 217-234.
- Moss, C., Green, D.H., Perez, B., Velasco, A., Henriquez, R., and McKenzie, J.D. (2003). Intracellular bacteria associated with the ascidian *Ecteinascidia turbinata*: phylogenetic and in situ hybridisation analysis. *Marine biology* 143, 99-110.
- Moussa, M., Ebrahim, W., Kalscheuer, R., Liu, Z., and Proksch, P. (2020). Co-culture of the bacterium *Pseudomonas aeruginosa* with the fungus *Fusarium tricinctum* induces bacterial antifungal and quorum sensing signaling molecules. *Phytochemistry Letters* 36, 37-41.
- Nagy, M.L., Prez, A., and Garcia-Pichel, F. (2005). The prokaryotic diversity of biological soil crusts in the Sonoran Desert (Organ Pipe Cactus National Monument, AZ). *FEMS Microbiology Ecology* 54, 233-245.
- Naito, S., Shiga, I., and Yamaguchi, N. (1986). Studies on protection of microbiological deterioration of packaged food, 14: Antimicrobial activity of violet pigment produced by *Janthinobacterium lividum* isolated from Yudemen [boiled Japanese noodle]. *Journal of Japanese Society of Food Science and Technology (Japan)*.
- Ndour, N.Y.B., Achouak, W., Christen, R., Heulin, T., Brauman, A., and Chotte, J.-L. (2008). Characteristics of microbial habitats in a tropical soil subject to different fallow management. *applied soil ecology* 38, 51-61.
- Newman, D.J., and Cragg, G.M. (2016). Natural products as sources of new drugs from 1981 to 2014. *Journal of natural products* 79, 629-661.
- Ng, W.-L., and Bassler, B.L. (2009). Bacterial quorum-sensing network architectures. *Annual review of genetics* 43, 197-222.
- Ng, Y.-K., Grasso, M., Wright, V., Garcia, V., Williams, P., and Atkinson, S. (2018). The quorum sensing system of *Yersinia enterocolitica* 8081 regulates swimming motility, host cell attachment, and virulence plasmid maintenance. *Genes* 9, 307.
- Nicholas, R., Berry, V., Hunter, P.A., and Kelly, J.A. (1999). The antifungal activity of mupirocin. *Journal of Antimicrobial Chemotherapy* 43, 579-582.
- Niu, X.-K., Narsing Rao, M.P., Dong, Z.-Y., Kan, Y., Li, Q.-R., Huang, J., Zhao, L., Wang, M.-Z., Shen, Z.-P., and Kang, Y.-Q. (2020). *Vulcaniibacterium gelatinicum* sp. nov., a moderately

- thermophilic bacterium isolated from a hot spring. *International Journal of Systematic and Evolutionary Microbiology*, ijssem003934.
- Noel, J.T., Joy, J., Smith, J.N., Fatica, M., Schneider, K.R., Ahmer, B.M.M., and Teplitski, M. (2010). Salmonella SdiA recognizes N-acyl homoserine lactone signals from *Pectobacterium carotovorum* in vitro, but not in a bacterial soft rot. *Molecular plant-microbe interactions* 23, 273-282.
- Novick, R.P., and Geisinger, E. (2008). Quorum sensing in staphylococci. *Annual review of genetics* 42, 541-564.
- O'sullivan, J., Mccullough, J., Johnson, J.H., Bonner, D.P., Clark, J.C., Dean, L., and Trejo, W.H. (1990). Janthinocins A, B and C, novel peptide lactone antibiotics produced by *Janthinobacterium lividum*. *The Journal of antibiotics* 43, 913-919.
- O'toole, G.A. (2011). Microtiter dish biofilm formation assay. *JoVE (Journal of Visualized Experiments)*, e2437.
- Oh, C., Nikapitiya, C., Lee, Y., Whang, I., Kim, S.-J., Kang, D.-H., and Lee, J. (2010). Cloning, purification and biochemical characterization of beta agarase from the marine bacterium *Pseudoalteromonas* sp. AG4. *Journal of industrial microbiology & biotechnology* 37, 483-494.
- Oh, D.-C., Jensen, P.R., Kauffman, C.A., and Fenical, W. (2005). Libertellenones A-G: induction of cytotoxic diterpenoid biosynthesis by marine microbial competition. *Bioorganic & medicinal chemistry* 13, 5267-5273.
- Oh, D.-C., Kauffman, C.A., Jensen, P.R., and Fenical, W. (2007). Induced production of emericellamides A and B from the marine-derived fungus *Emericella* sp. in competing coculture. *Journal of natural products* 70, 515-520.
- Okada, B.K., Wu, Y., Mao, D., Bushin, L.B., and Seyedsayamdost, M.R. (2016). Mapping the trimethoprim-induced secondary metabolome of *Burkholderia thailandensis*. *ACS chemical biology* 11, 2124-2130.
- Ola, A.R., Thomy, D., Lai, D., Broetz-Oesterhelt, H., and Proksch, P. (2013). Inducing secondary metabolite production by the endophytic fungus *Fusarium tricinctum* through coculture with *Bacillus subtilis*. *Journal of natural products* 76, 2094-2099.
- Pakarinen, J., Hyvärinen, A., Salkinoja-Salonen, M., Laitinen, S., Nevalainen, A., Mäkelä, M.J., Haahtela, T., and Von Hertzen, L. (2008). Predominance of Gram-positive bacteria in house dust in the low-allergy risk Russian Karelia. *Environmental microbiology* 10, 3317-3325.
- Park, E.-H., Bae, W.-Y., Kim, J.-Y., Kim, K.-T., and Paik, H.-D. (2017). Antimelanogenic effects of *Inula britannica* flower petal extract fermented by *Lactobacillus plantarum* KCCM 11613P. *Journal of Zhejiang University-Science B* 18, 816-824.
- Patjanasontorn, B., Boonma, P., Wilailackana, C., and Sittikesorn, J. (1992). Hospital acquired *Janthinobacterium lividum* septicemia in Srinagarind Hospital. *Journal medical association of Thailand* 75, 6-6.
- Peeters, C., Cooper, V.S., Hatcher, P.J., Verheyde, B., Carlier, A.L., and Vandamme, P. (2017). Comparative genomics of *Burkholderia multivorans*, a ubiquitous pathogen with a highly conserved genomic structure. *PLoS one* 12, e0176191.
- Pereira, R., Medeiros, Y.S., and Fröde, T.S. (2006). Antiinflammatory effects of Tacrolimus in a mouse model of pleurisy. *Transplant Immunology* 16, 105-111.
- Pietschke, C., Treitz, C., S., Schultze, A., Künzel, S., Tholey, A., Bosch, T.C.G., and Fraune, S. (2017). Host modification of a bacterial quorum-sensing signal induces a phenotypic switch in bacterial symbionts. *Proceedings of the National Academy of Sciences* 114, E8488-E8497.
- Prieto, L., Michelon, M., Burkert, J., Kalil, S., and Burkert, C. (2008). The production of rhamnolipid by a *Pseudomonas aeruginosa* strain isolated from a southern coastal zone in Brazil. *Chemosphere* 71, 1781-1785.

- Pye, C.R., Bertin, M.J., Lokey, R.S., Gerwick, W.H., and Linington, R.G. (2017). Retrospective analysis of natural products provides insights for future discovery trends. *Proceedings of the National Academy of Sciences* 114, 5601-5606.
- Quiñones, B., Dulla, G., and Lindow, S.E. (2005). Quorum sensing regulates exopolysaccharide production, motility, and virulence in *Pseudomonas syringae*. *Molecular plant-microbe interactions* 18, 682-693.
- Raidal, S., Ohara, M., Hobbs, R., and Prince, R. (1998). Gram-negative bacterial infections and cardiovascular parasitism in green sea turtles (*Chelonia mydas*). *Australian Veterinary Journal* 76, 415-417.
- Raja, A., and Prabakarana, P. (2011). Actinomycetes and drug-an overview. *American Journal of Drug Discovery and Development* 1, 75-84.
- Rebollar, E.A., Simonetti, S.J., Shoemaker, W.R., and Harris, R.N. (2016). Direct and indirect horizontal transmission of the antifungal probiotic bacterium *Janthinobacterium lividum* on green frog (*Lithobates clamitans*) tadpoles. *Appl. Environ. Microbiol.* 82, 2457-2466.
- Reichenbach, H., Gerth, K., Irschik, H., Kunze, B., and Höfle, G. (1988). Myxobacteria: a source of new antibiotics. *Trends in Biotechnology* 6, 115-121.
- Rhee, S.-K., Lee, S.-G., Hong, S.-P., Choi, Y.-H., Park, J.-H., Kim, C.-J., and Sung, M.-H. (2000). A novel microbial interaction: obligate commensalism between a new gram-negative thermophile and a thermophilic *Bacillus* strain. *Extremophiles* 4, 131-136.
- Ribot, W.J., and Ulrich, R.L. (2006). The animal pathogen-like type III secretion system is required for the intracellular survival of *Burkholderia mallei* within J774. 2 macrophages. *Infection and immunity* 74, 4349-4353.
- Rinehart, K.L., Holt, T.G., Fregeau, N.L., Stroh, J.G., Keifer, P.A., Sun, F., Li, L.H., and Martin, D.G. (1990). Ecteinascidins 729, 743, 745, 759A, 759B, and 770: potent antitumor agents from the Caribbean tunicate *Ecteinascidia turbinata*. *The Journal of Organic Chemistry* 55, 4512-4515.
- Rosing, H., Hillebrand, M.J.X., Jimeno, J.M., Gomez, A., Floriano, P., Faircloth, G., Cameron, L., Henrar, R.E.C., Vermorken, J.B., and Bult, A. (1998). Analysis of Ecteinascidin 743, a new potent marine-derived anticancer drug, in human plasma by high-performance liquid chromatography in combination with solid-phase extraction. *Journal of Chromatography B: Biomedical Sciences and Applications* 710, 183-189.
- Rousseaux, S., Hartmann, A., and Soulas, G. (2001). Isolation and characterisation of new Gram-negative and Gram-positive atrazine degrading bacteria from different French soils. *FEMS Microbiology Ecology* 36, 211-222.
- Salanoubat, M., Genin, S., Artiguenave, F.O., Gouzy, J., Mangenot, S., Arlat, M., Billault, A., Brottier, P., Camus, J.C., and Cattolico, L. (2002). Genome sequence of the plant pathogen *Ralstonia solanacearum*. *Nature* 415, 497-502.
- Schäberle, T.F., Lohr, F., Schmitz, A., and König, G.M. (2014). Antibiotics from myxobacteria. *Natural product reports* 31, 953-972.
- Schaefer, A.L., Harwood, C.S., and Greenberg, E.P. (2018). "Hot stuff": The many uses of a radiolabel assay in detecting acyl-homoserine lactone quorum-sensing signals," in *Quorum Sensing*. Springer), 35-47.
- Schein, P.S., and Loftus, S. (1968). Streptozotocin: depression of mouse liver pyridine nucleotides. *Cancer research* 28, 1501-1506.
- Schloss, P.D., Allen, H.K., Klimowicz, A.K., Mlot, C., Gross, J.A., Savengsuksa, S., Mcellin, J., Clardy, J., Ruess, R.W., and Handelsman, J. (2010). Psychrotrophic strain of *Janthinobacterium lividum* from a cold Alaskan soil produces prodigiosin. *DNA and cell biology* 29, 533-541.
- Schmid, N., Pessi, G., Deng, Y., Aguilar, C., Carlier, A.L., Grunau, A., Omasits, U., Zhang, L.-H., Ahrens, C.H., and Eberl, L. (2012). The AHL-and BDSF-dependent quorum sensing

- systems control specific and overlapping sets of genes in *Burkholderia cenocepacia* H111. *PLoS One* 7, e49966.
- Schneider, Y., Jenssen, M., Isaksson, J., Hansen, K.Ø., Andersen, J.H., and Hansen, E.H. (2020). Bioactivity of Serratiochelin A, a Siderophore Isolated from a Co-Culture of *Serratia* sp. and *Shewanella* sp. *Microorganisms* 8, 1042.
- Sepehr, S., Rahmani-Badi, A., Babaie-Naiej, H., and Soudi, M.R. (2014). Unsaturated fatty acid, cis-2-decenoic acid, in combination with disinfectants or antibiotics removes pre-established biofilms formed by food-related bacteria. *PloS one* 9, e101677.
- Seyedsayamdost, M.R. (2014). High-throughput platform for the discovery of elicitors of silent bacterial gene clusters. *Proceedings of the National Academy of Sciences* 111, 7266-7271.
- Shen, L., Shi, Y., Zhang, D., Wei, J., Surette, M.G., and Duan, K. (2008). Modulation of secreted virulence factor genes by subinhibitory concentrations of antibiotics in *Pseudomonas aeruginosa*. *The Journal of Microbiology* 46, 441-447.
- Shi, Y.-L., Lu, X.-Z., and Yu, W.-G. (2008). A new beta-agarase from marine bacterium *Janthinobacterium* sp. SY12. *World Journal of Microbiology and Biotechnology* 24, 2659-2664.
- Shirata, A., Tsukamoto, T., Yasui, H., Kato, H., Hayasaka, S., and Kojima, A. (1997). Production of bluish-purple pigments by *Janthinobacterium lividum* isolated from the raw silk and dyeing with them. *The Journal of Sericultural Science of Japan* 66, 377-385.
- Shivaji, S., Ray, M., Kumar, G.S., Reddy, G., Saisree, L., and Wynn-Williams, D. (1991). Identification of *Janthinobacterium lividum* from the soils of the islands of Scotia Ridge and from Antarctic peninsula. *Polar biology* 11, 267-271.
- Singaram, S., Lawrence, R.S., and Hornemann, U. (1979). Studies on the biosynthesis of the antibiotic streptozotocin (streptozocin) by *Streptomyces achromogenes* var. *streptozoticus*. *The Journal of antibiotics* 32, 379-385.
- Singh, R.K., Tiwari, S.P., Rai, A.K., and Mohapatra, T.M. (2011). Cyanobacteria: an emerging source for drug discovery. *The Journal of antibiotics* 64, 401-412.
- Singh, V.K., Utaida, S., Jackson, L.S., Jayaswal, R.K., Wilkinson, B.J., and Chamberlain, N.R. (2007). Role for *dnaK* locus in tolerance of multiple stresses in *Staphylococcus aureus*. *Microbiology* 153, 3162-3173.
- Sintchenko, V., Jelfs, P., Sharma, A., Hicks, L., Gilbert, G., and Waller, C. (2000). *Massilia timonae*: an unusual bacterium causing wound infection following surgery. *Clinical Microbiology Newsletter* 22, 149-151.
- Skindersoe, M.E., Alhede, M., Phipps, R., Yang, L., Jensen, P.O., Rasmussen, T.B., Bjarnsholt, T., Tolker-Nielsen, T., Høiby, N., and Givskov, M. (2008). Effects of antibiotics on quorum sensing in *Pseudomonas aeruginosa*. *Antimicrobial agents and chemotherapy* 52, 3648-3663.
- Slattery, M., Rajbhandari, I., and Wesson, K. (2001). Competition-mediated antibiotic induction in the marine bacterium *Streptomyces tenjimariensis*. *Microbial Ecology* 41, 90-96.
- Sly, L.I., and Fegan, M. (2005). Genus VI. *Telluria* Bowman, Sly, Hayward, Spiegel and Stackebrandt 1993b, 123VP.
- Sly, L.I., and Fegan, M. (2015). *Telluria*. *Bergey's Manual of Systematics of Archaea and Bacteria*, 1-8.
- Smith, J., and Weinberg, E. (1962). Mechanisms of antibacterial action of bacitracin. *Microbiology* 28, 559-569.
- Sneider, W. (1997). Drug prototypes and their exploitation. *European Journal of Medicinal Chemistry* 1, 91.
- Stansley, P., Shepherd, R., and White, H. (1947). Polymixin: A New Antibiotic Agent. *Bull. Johns Hopkins Hosp.* 81, 43.

- Stein, T. (2005). Bacillus subtilis antibiotics: structures, syntheses and specific functions. *Molecular microbiology* 56, 845-857.
- Steindler, L., Bertani, I., De Sordi, L., Schwager, S., Eberl, L., and Venturi, V. (2009). LasI/R and RhII/R quorum sensing in a strain of Pseudomonas aeruginosa beneficial to plants. *Applied and environmental microbiology* 75, 5131-5140.
- Stolinsky, D.C., Sadoff, L., Braunwald, J., and Bateman, J.R. (1972). Streptozotocin in the treatment of cancer: Phase II study. *Cancer* 30, 61-67.
- Storm, D.R. (1974). Mechanism of bacitracin action: a specific lipid-peptide interaction. *Annals of the New York Academy of Sciences* 235, 387-398.
- Sutherland, R., Boon, R., Griffin, K., Masters, P., Slocombe, B., and White, A. (1985). Antibacterial activity of mupirocin (pseudomonic acid), a new antibiotic for topical use. *Antimicrobial agents and chemotherapy* 27, 495-498.
- Takebayashi, Y., Goldwasser, F.O., Urasaki, Y., Kohlhagen, G., and Pommier, Y. (2001). Ecteinascidin 743 induces protein-linked DNA breaks in human colon carcinoma HCT116 cells and is cytotoxic independently of topoisomerase I expression. *Clinical cancer research* 7, 185-191.
- Tan, I.K.P., Foong, C.P., Tan, H.T., Lim, H., Zain, N.-a.A., Tan, Y.C., Hoh, C.C., and Sudesh, K. (2020). Polyhydroxyalkanoate (PHA) synthase genes and PHA-associated gene clusters in Pseudomonas spp. and Janthinobacterium spp. isolated from Antarctica. *Journal of biotechnology*.
- Tanaka, H., Kuroda, A., Marusawa, H.E.U., Hashimoto, M., Hatanaka, H., Kino, T., Goto, T., and Okuhara, M. (Year). "Physicochemical properties of FK-506, a novel immunosuppressant isolated from Streptomyces tsukubaensis", in: *Transplantation proceedings*, 11-16.
- Terashima, H., Kawamoto, A., Morimoto, Y.V., Imada, K., and Minamino, T. (2017). Structural differences in the bacterial flagellar motor among bacterial species. *Biophysics and Physicobiology* 14, 191-198.
- Teta, R., Della Sala, G., Glukhov, E., Gerwick, L., Gerwick, W.H., Mangoni, A., and Costantino, V. (2015). Combined LCF-MS/MS and molecular networking approach reveals new cyanotoxins from the 2014 cyanobacterial bloom in Green Lake, Seattle. *Environmental science & technology* 49, 14301-14310.
- Thoendel, M., Kavanaugh, J.S., Flack, C.E., and Horswill, A.R. (2011). Peptide signaling in the staphylococci. *Chemical reviews* 111, 117-151.
- Thomson, A., Bonham, C., and Zeevi, A. (1995). Mode of action of tacrolimus (FK506): molecular and cellular mechanisms. *Therapeutic drug monitoring* 17, 584-591.
- Thomson, J.M., and Bonomo, R.A. (2005). The threat of antibiotic resistance in Gram-negative pathogenic bacteria: beta-lactams in peril! *Current opinion in microbiology* 8, 518-524.
- Tianero, M.D.B., Kwan, J.C., Wyche, T.P., Presson, A.P., Koch, M., Barrows, L.R., Bugni, T.S., and Schmidt, E.W. (2015). Species specificity of symbiosis and secondary metabolism in ascidians. *The ISME journal* 9, 615-628.
- Tsai, C.-C., Chan, C.-F., Huang, W.-Y., Lin, J.-S., Chan, P., Liu, H.-Y., and Lin, Y.-S. (2013). Applications of Lactobacillus rhamnosus spent culture supernatant in cosmetic antioxidation, whitening and moisture retention applications. *Molecules* 18, 14161-14171.
- Twomey, K.B., O'connell, O.J., Mccarthy, Y., Dow, J.M., O'toole, G.A., Plant, B.J., and Ryan, R.P. (2012). Bacterial cis-2-unsaturated fatty acids found in the cystic fibrosis airway modulate virulence and persistence of Pseudomonas aeruginosa. *The ISME journal* 6, 939-950.
- Ueki, A., Akasaka, H., Satoh, A., Suzuki, D., and Ueki, K. (2007). Prevotella paludivivens sp. nov., a novel strictly anaerobic, Gram-negative, hemicellulose-decomposing bacterium isolated from plant residue and rice roots in irrigated rice-field soil. *International journal of systematic and evolutionary microbiology* 57, 1803-1809.
- Valoti, G., Nicoletti, M.I., Pellegrino, A., Jimeno, J., Hendriks, H., D'incalci, M., Faircloth, G., and Giavazzi, R. (1998). Ecteinascidin-743, a new marine natural product with potent

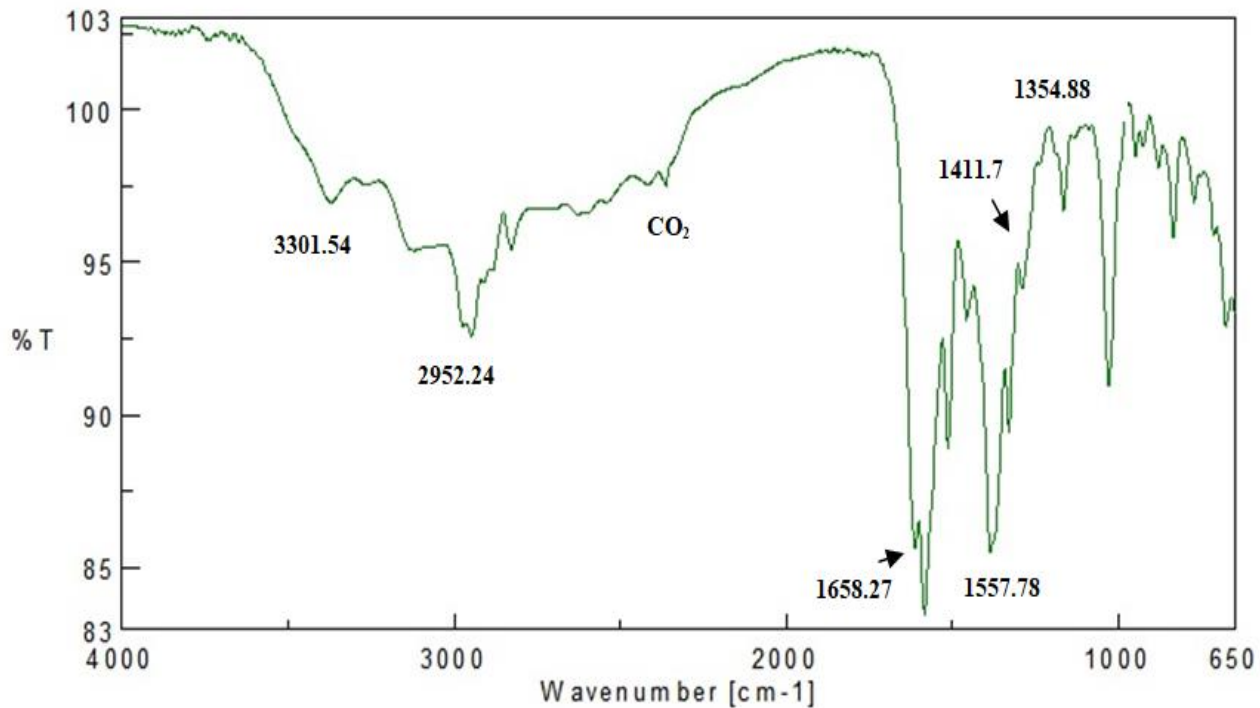
- antitumor activity on human ovarian carcinoma xenografts. *Clinical Cancer Research* 4, 1977-1983.
- Van Craenenbroeck, A.H., Camps, K., Zachée, P., and Wu, K.L. (2011). Massilia timonae infection presenting as generalized lymphadenopathy in a man returning to Belgium from Nigeria. *Journal of clinical microbiology* 49, 2763-2765.
- Ventura, M., Canchaya, C., Tauch, A., Chandra, G., Fitzgerald, G.F., Chater, K.F., and Van Sinderen, D. (2007). Genomics of Actinobacteria: tracing the evolutionary history of an ancient phylum. *Microbiol. Mol. Biol. Rev.* 71, 495-548.
- Visca, P., Imperi, F., and Lamont, I.L. (2007). Pyoverdine siderophores: from biogenesis to biosignificance. *Trends in microbiology* 15, 22-30.
- Waksman, S.A., Harris, D.A., Kupferberg, A., Singher, H., and Styles, H. (1949). Streptocin, Antibiotic Isolated from Mycelium of Streptomyces griseus, Active Against Trichomonas vaginalis, and Certain Bacteria. *Proceedings of the Society for Experimental Biology and Medicine* 70, 308-312.
- Waksman, S.A., Reilly, H.C., and Johnstone, D.B. (1946). Isolation of streptomycin-producing strains of Streptomyces griseus. *Journal of bacteriology* 52, 393.
- Waksman, S.A., and Woodruff, H.B. (1940). The soil as a source of microorganisms antagonistic to disease-producing bacteria. *Journal of bacteriology* 40, 581.
- Waksman, S.A., and Woodruff, H.B. (1941). Actinomyces antibioticus, a new soil organism antagonistic to pathogenic and non-pathogenic bacteria. *Journal of bacteriology* 42, 231.
- Wang, J.-P., Debbab, A., Hemphill, C.F.P., and Proksch, P. (2013). Optimization of enniatin production by solid-phase fermentation of Fusarium tricinctum. *Zeitschrift für Naturforschung C* 68, 223-230.
- Wang, M., Carver, J.J., Phelan, V.V., Sanchez, L.M., Garg, N., Peng, Y., Nguyen, D.D., Watrous, J., Kaponov, C.A., and Luzzatto-Knaan, T. (2016). Sharing and community curation of mass spectrometry data with Global Natural Products Social Molecular Networking. *Nature biotechnology* 34, 828-837.
- Wang, M., Jarmusch, A.K., Vargas, F., Aksenov, A.A., Gauglitz, J.M., Weldon, K., Petras, D., Da Silva, R., Quinn, R., and Melnik, A.V. (2020). Mass spectrometry searches using MASST. *Nature Biotechnology*, 1-4.
- Ward, A., and Campoli-Richards, D.M. (1986). Mupirocin. *Drugs* 32, 425-444.
- Weiss, L.E., Badalamenti, J.P., Weaver, L.J., Tascone, A.R., Weiss, P.S., Richard, T.L., and Cirino, P.C. (2008). Engineering motility as a phenotypic response to LuxI/Rf-dependent quorum sensing in Escherichia coli. *Biotechnology and bioengineering* 100, 1251-1255.
- Weisskopf, L., Heller, S., and Eberl, L. (2011). Burkholderia species are major inhabitants of white lupin cluster roots. *Applied and environmental microbiology* 77, 7715-7720.
- Werner, A., and Russell, A. (1999). Mupirocin, fusidic acid and bacitracin: activity, action and clinical uses of three topical antibiotics. *Veterinary Dermatology* 10, 225-240.
- Wessjohann, L. (1997). Epothilones: Promising Natural Products with Taxo-Like Activity. *Angewandte Chemie International Edition in English* 36, 715-718.
- Wheelhouse, N., and Longbottom, D. (2012). Endemic and emerging chlamydial infections of animals and their zoonotic implications. *Transboundary and emerging diseases* 59, 283-291.
- Yan, L., Boyd, K.G., and Burgess, J.G. (2002). Surface attachment induced production of antimicrobial compounds by marine epiphytic bacteria using modified roller bottle cultivation. *Marine Biotechnology* 4, 356-366.
- Yang, B., and Bogdanove, A. (2013). "Inoculation and virulence assay for bacterial blight and bacterial leaf streak of rice," in *Rice Protocols*. Springer), 249-255.



- Yang, L., Xiong, H., Lee, O.O., Qi, S., and Qian, P. (2007). Effect of agitation on violacein production in *Pseudoalteromonas luteoviolacea* isolated from a marine sponge. *Letters in Applied Microbiology* 44, 625-630.
- Young, G.P., Ward, P.B., Bayley, N., Gordon, D., Higgins, G., Trapani, J.A., McDonald, M.I., Labrooy, J., and Hecker, R. (1985). Antibiotic-associated colitis due to *Clostridium difficile*: double-blind comparison of vancomycin with bacitracin. *Gastroenterology* 89, 1038-1045.
- Zakataeva, N.P., Aleshin, V.V., Tokmakova, I.L., Troshin, P.V., and Livshits, V.A. (1999). The novel transmembrane *Escherichia coli* proteins involved in the amino acid efflux. *FEBS letters* 452, 228-232.
- Zakataeva, N.P., Kutukova, E.A., Gronskiy, S.V., Troshin, P.V., Livshits, V.A., and Aleshin, V.V. (2006). Export of metabolites by the proteins of the DMT and RhtB families and its possible role in intercellular communication. *Microbiology* 75, 438-448.
- Zhang, J., Zhang, A., Sun, Y., Cao, X., and Zhang, N. (2009). Treatment with immunosuppressants FTY720 and tacrolimus promotes functional recovery after spinal cord injury in rats. *The Tohoku journal of experimental medicine* 219, 295-302.
- Zhang, R., Yang, P., Huang, H., Yuan, T., Shi, P., Meng, K., and Yao, B. (2011). Molecular and biochemical characterization of a new alkaline beta-propeller phytase from the insect symbiotic bacterium *Janthinobacterium* sp. TN115. *Applied microbiology and biotechnology* 92, 317-325.
- Zhou, Z.-X., Jiang, H., Yang, C., Yang, M.-Z., and Zhang, H.-B. (2010). Microbial community on healthy and diseased leaves of an invasive plant *Eupatorium adenophorum* in Southwest China. *The Journal of Microbiology* 48, 139-145.
- Zhu, F., Chen, G., Chen, X., Huang, M., and Wan, X. (2011). Aspergicin, a new antibacterial alkaloid produced by mixed fermentation of two marine-derived mangrove epiphytic fungi. *Chemistry of Natural Compounds* 47, 767-769.
- Zhu, F., and Lin, Y. (2006). Marinamide, a novel alkaloid and its methyl ester produced by the application of mixed fermentation technique to two mangrove endophytic fungi from the South China Sea. *Chinese Science Bulletin* 51, 1426.

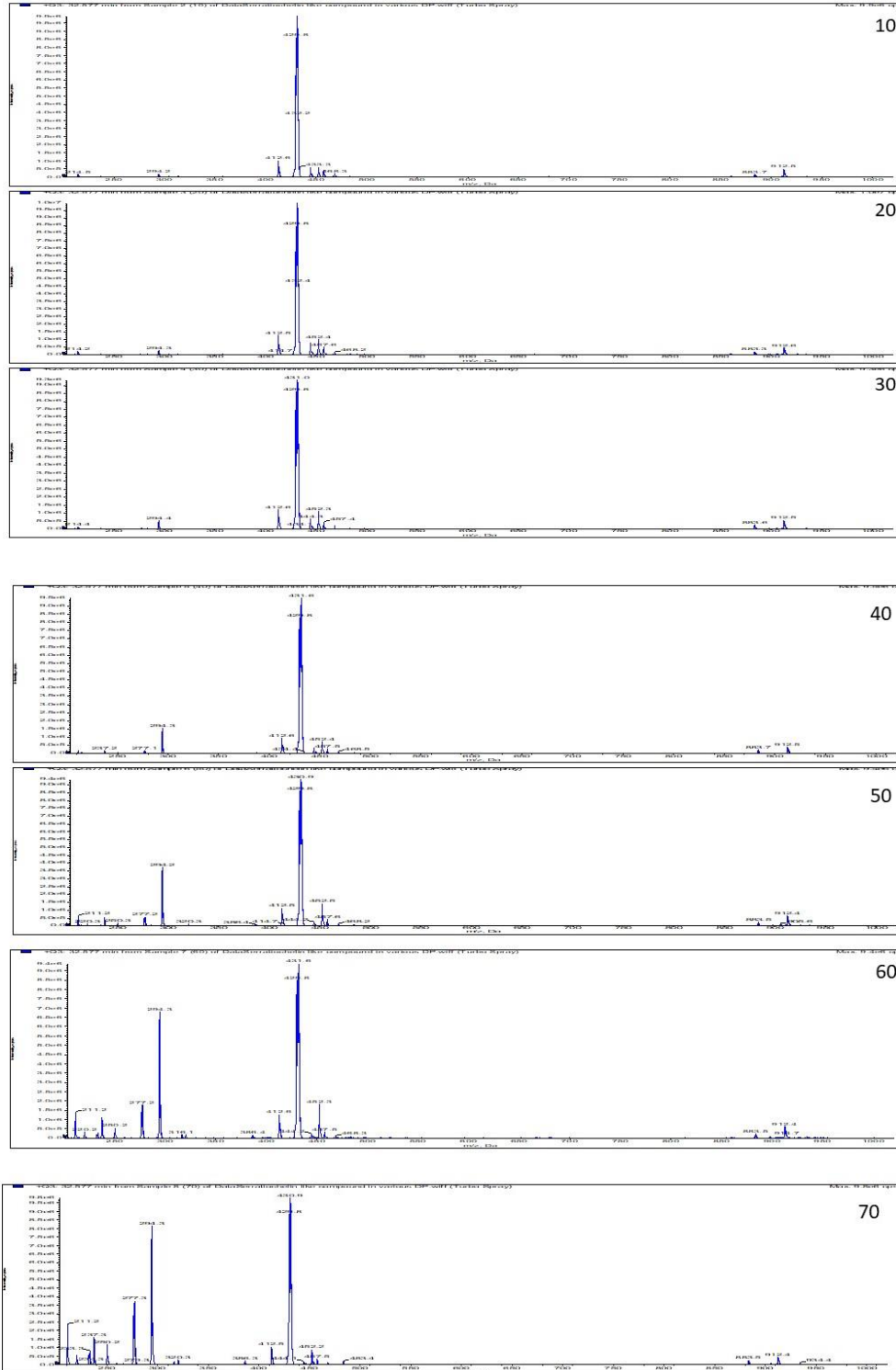
## Supplementary

Supplementary Figure 3-1 (FT-IR spectrum of tetrapeptide)

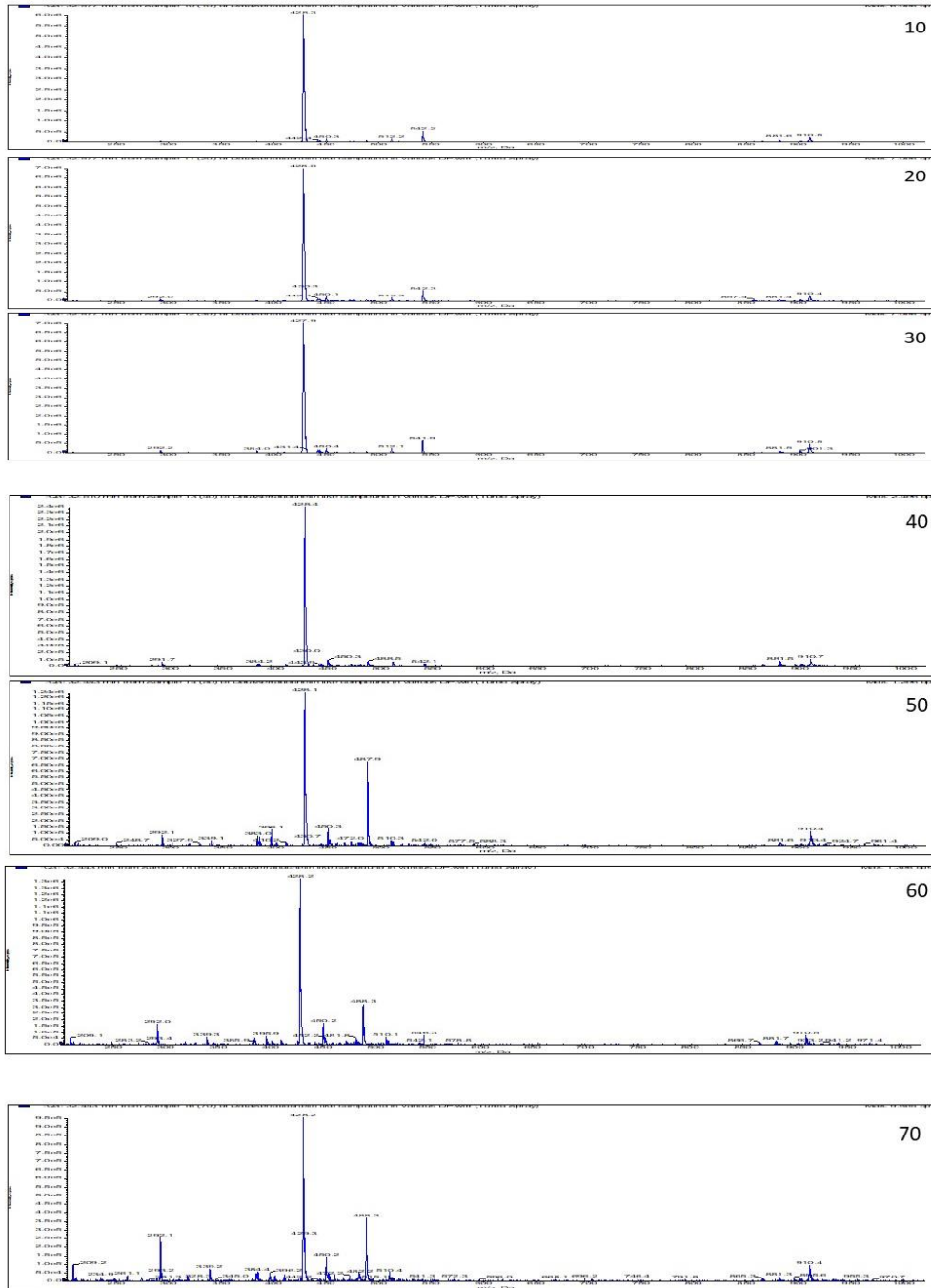


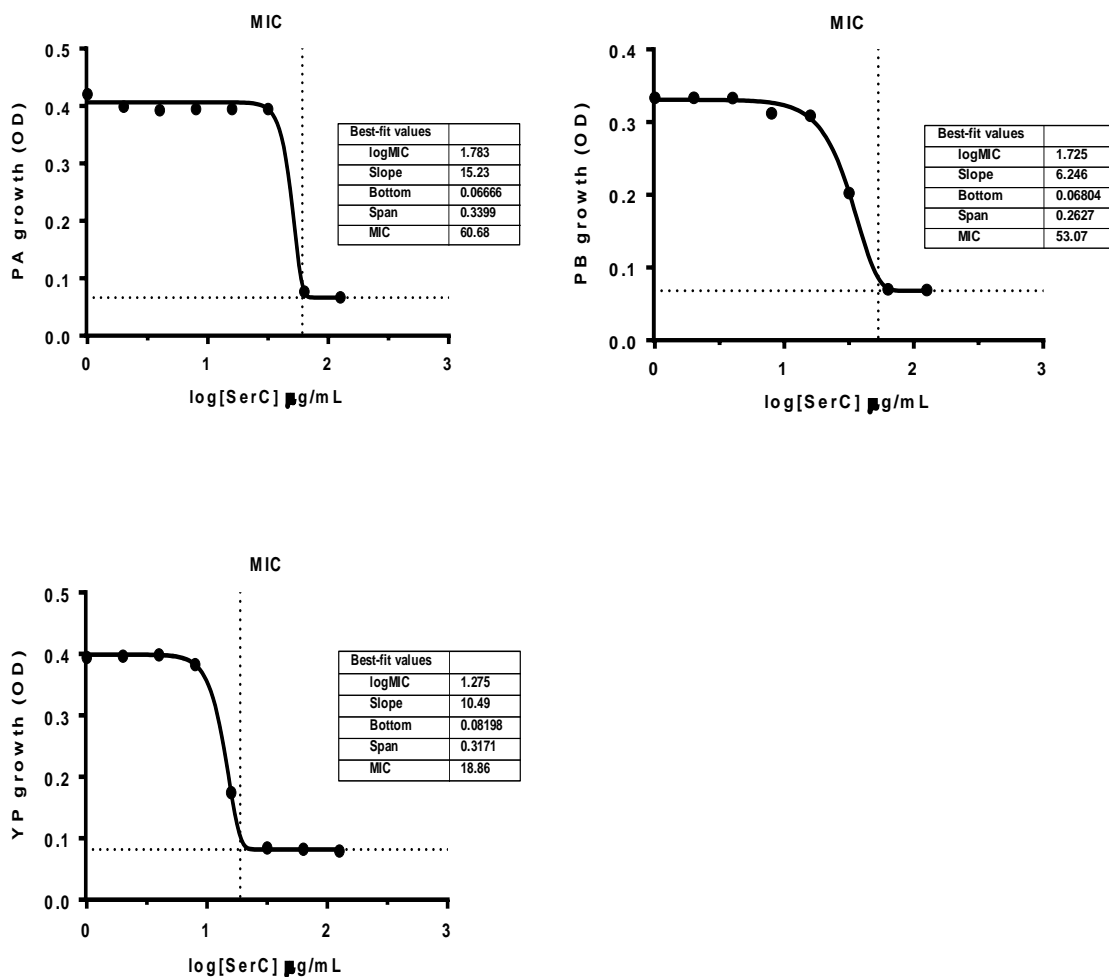
### Supplementary Figure 4-1 (MS serratiochelin C with different declustering potential)

#### Positive mode

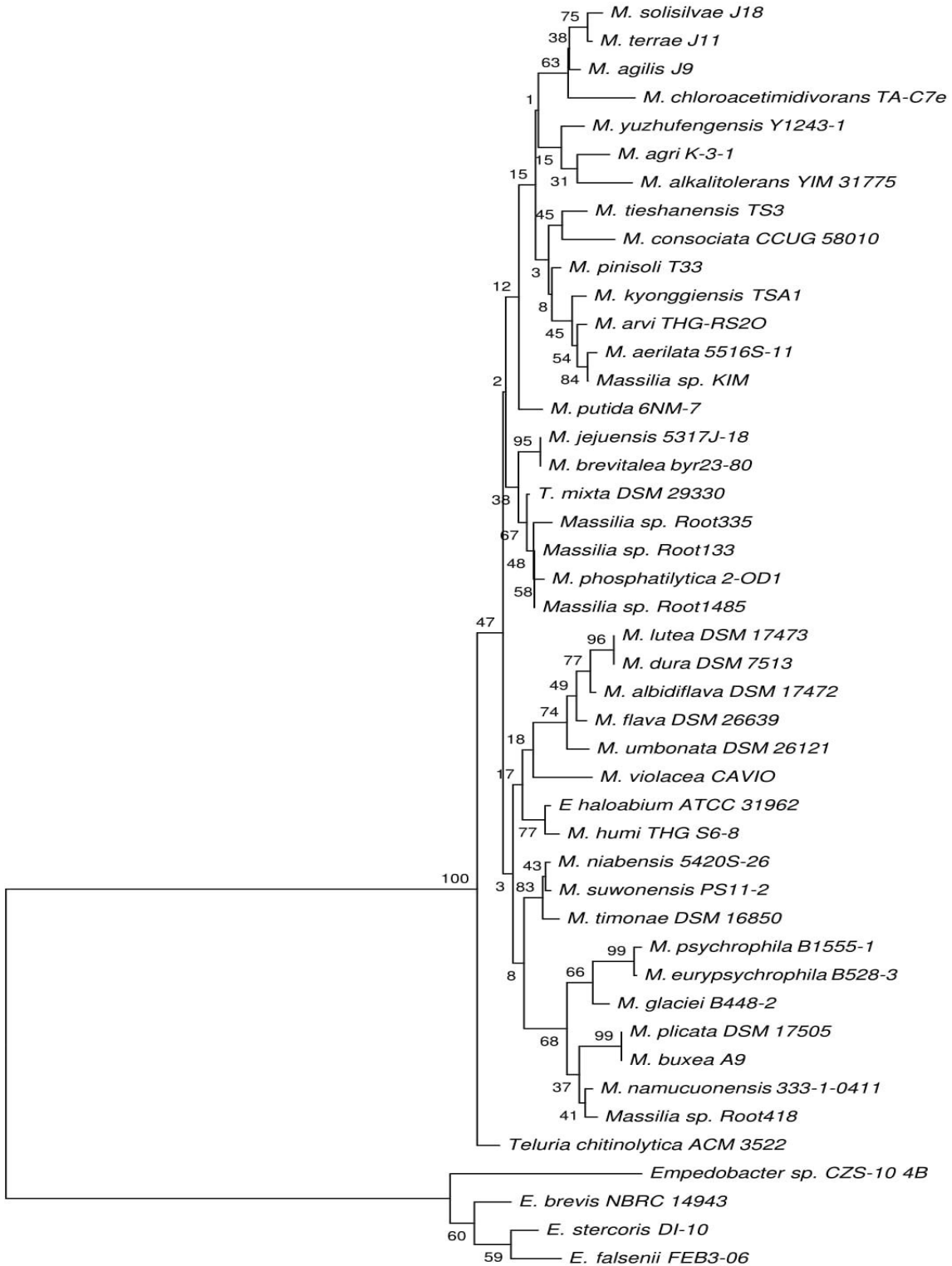


Negative mode

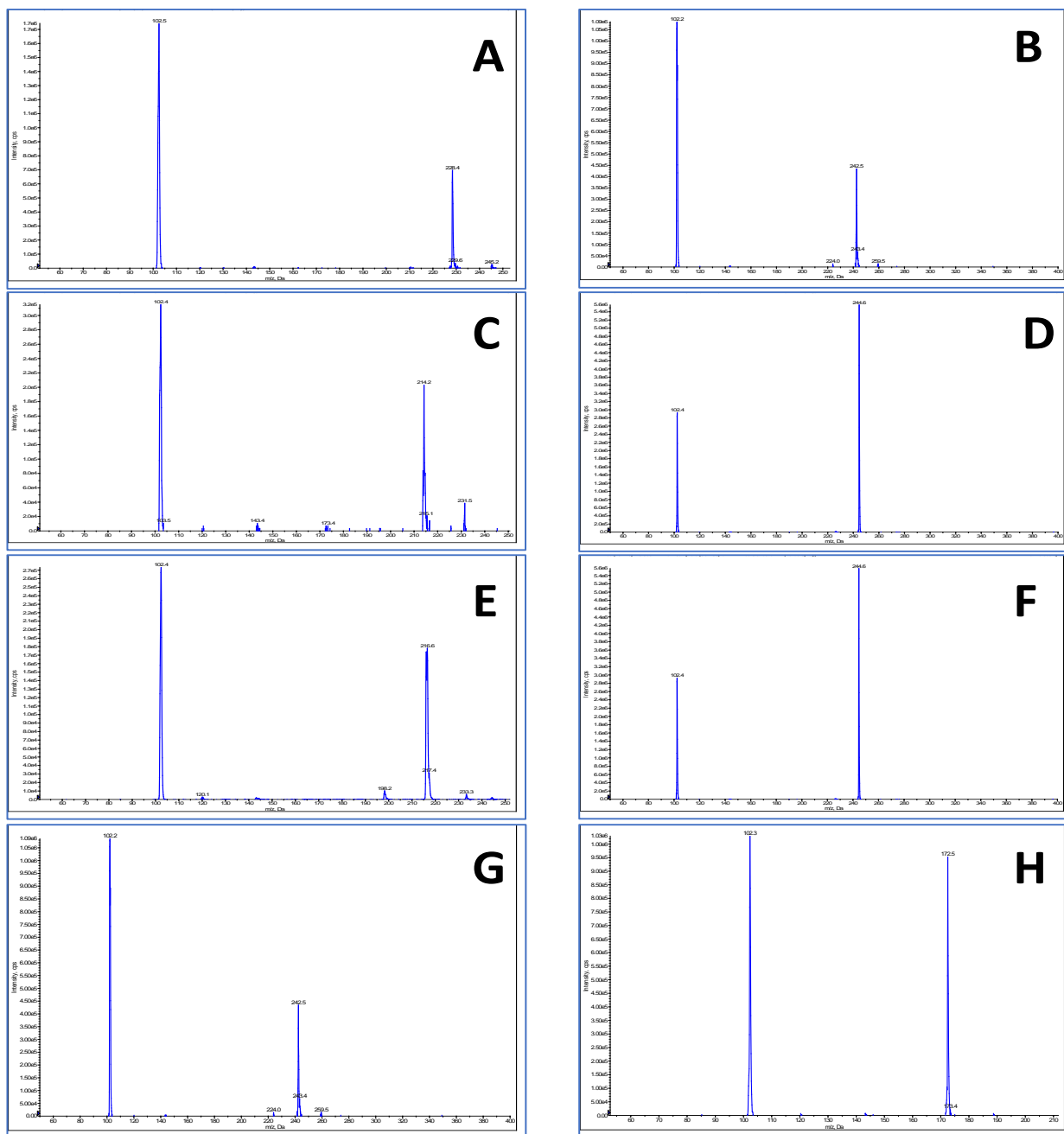


**Supplementary Figure 4-2** (Antibacterial activity of serratiochelin C)

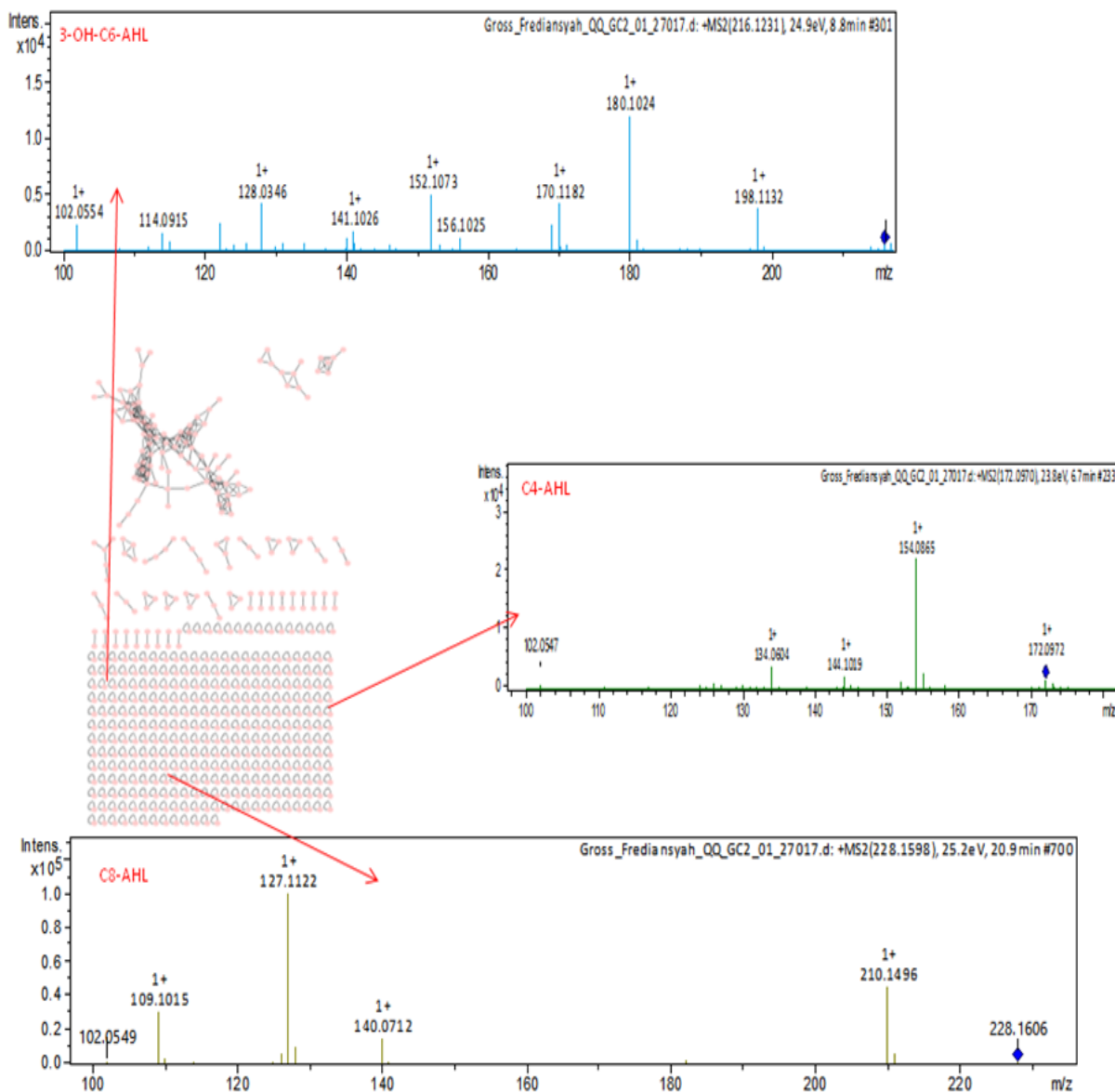
**Supplementary Figure 5-1** (Phylogenetic tree of *Massilia* and *Telluria*. A phylogenetic tree was constructed based on 16S rRNA. Neighbor-joining coupled with Tamura-Nei pairwise distance and 1000 bootstrap replicates were used in MEGA 7.0 for *T. chitinolytica*, *T. mixta*, *M. lutea*, *M. albidiflava*, *M. flava*, *M. umbonata*, *M. dura*, *M. plicata*, *M. lutea* and other *Massilia* that globally published. *Empedobacter* sp. CZS-10, *E. brevis* NRBC 1493, *E. stercoris* DI-10, and *E. falsenii* FEB3-06T was used as an out-group.)



**Supplementary Figure 5-2** (Parent mass (Q1) and a unique fragmentation (Q3) ion of  $102\pm 0.5$  represent as amino-butyrolactone in electrospray ionization with the positive mode from commercially AHL standard. (A) C8-AHL (B) C9-AHL (C) 3-oxo-C6-AHL (D) 3-oxo-C8-AHL (E) 3-OH-C6-AHL (F) 3-OH-C8-AHL (G) 3-OH-C10-AHL (H) C4-AHL.)

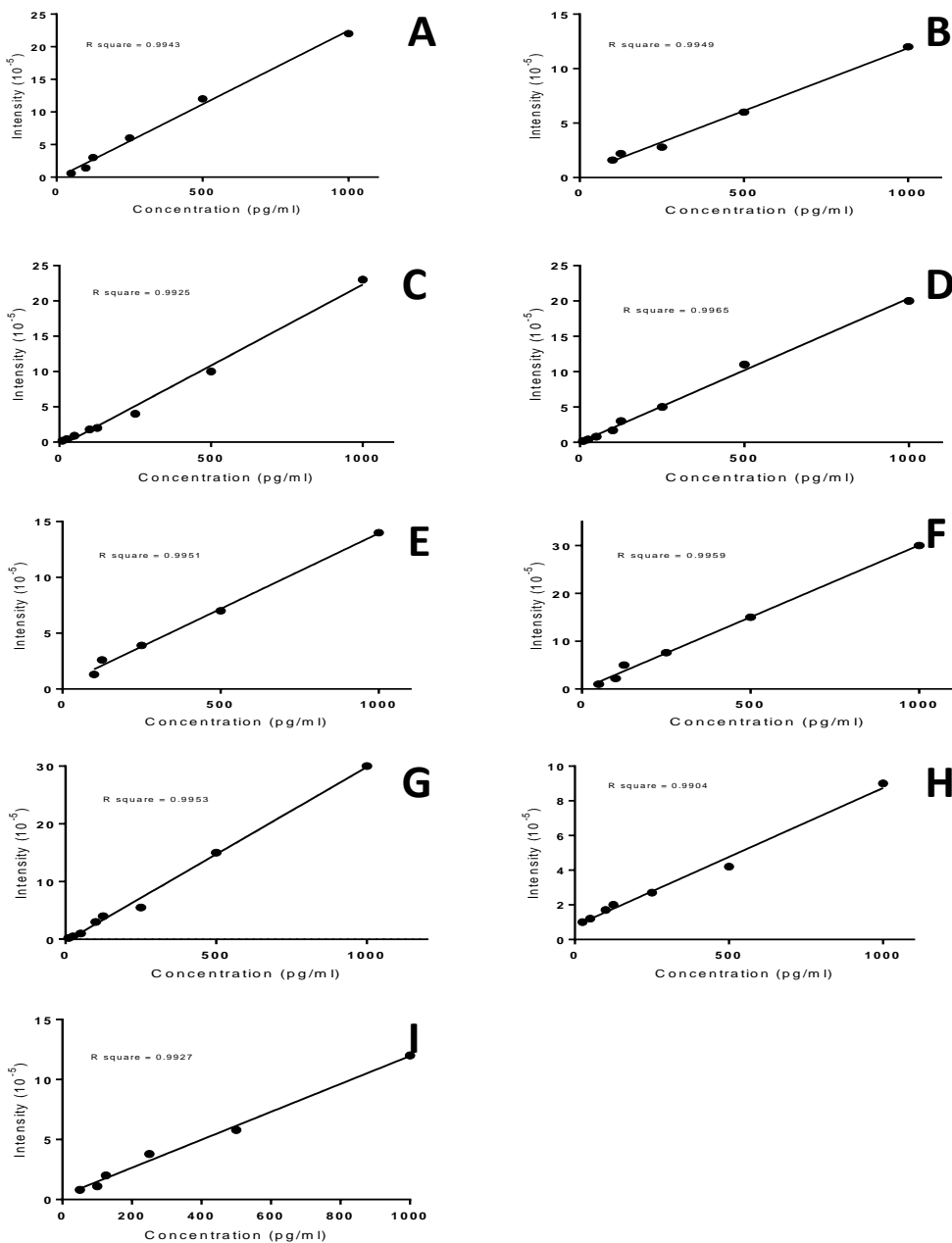


**Supplementary Figure 5-3** (Production of C8-AHL ([M+H]<sup>+</sup> m/z 228.1598, C4-AHL ([M+H]<sup>+</sup> m/z 172.), and 3-OH-C6-AHL ([M+H]<sup>+</sup> m/z 216.1231) in *T. chitinolytica* can be detected in HR-MS using +MS<sub>2</sub> with special fragmentation Q3 of 102.05±0.0054. The AHL's production by *T. chitinolytica* also could be analyzed using Global Natural Product Social Molecular Networking/GNPS (<https://gnps.ucsd.edu>) and visualized using Cytoscape software version 3.7.0 (<https://cytoscape.org/>))

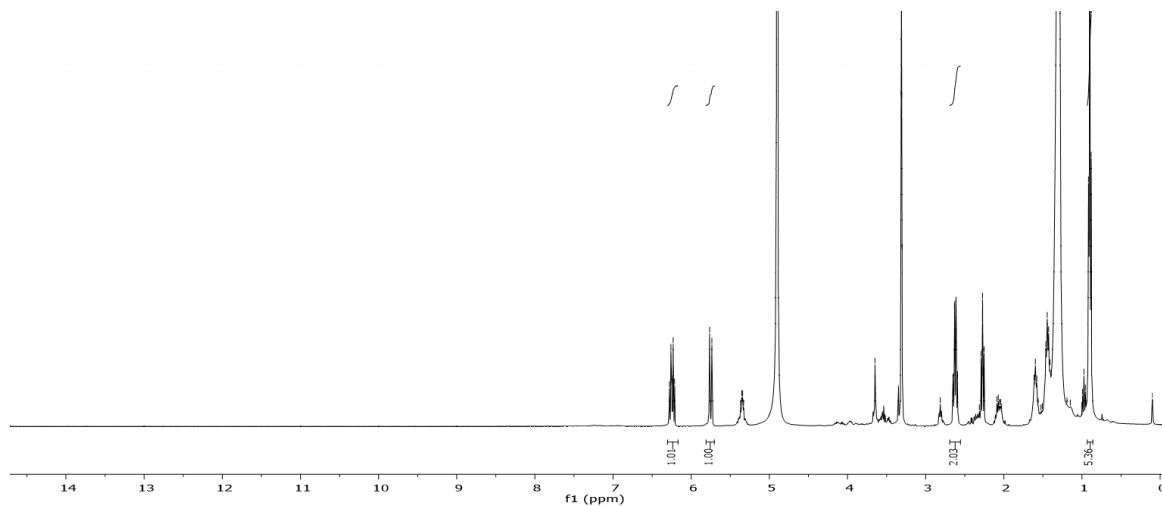




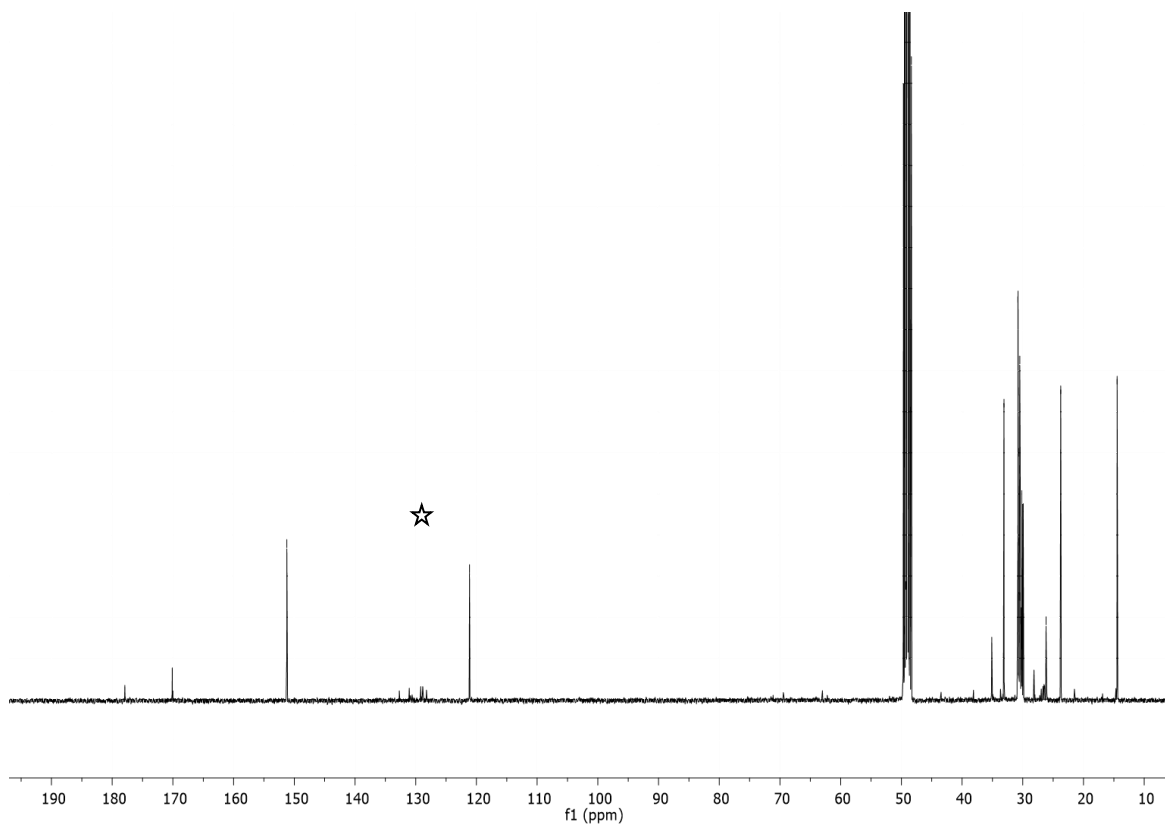
**Supplementary Figure 5-4.** (Calibration curves of AHL quantification. Data represent as Mean $\pm$ SEM from three independent replicates. Blackline visualized linear fit. (A) C8-AHL (B) C9-AHL (C) 3-oxo-C6-AHL (D) 3-oxo-C8-AHL (E) 3-OH-C6-AHL (F) 3-OH-C8-AHL (G) 3-OH-C10 AHL (H) C4-AHL (I) C6-AHL).



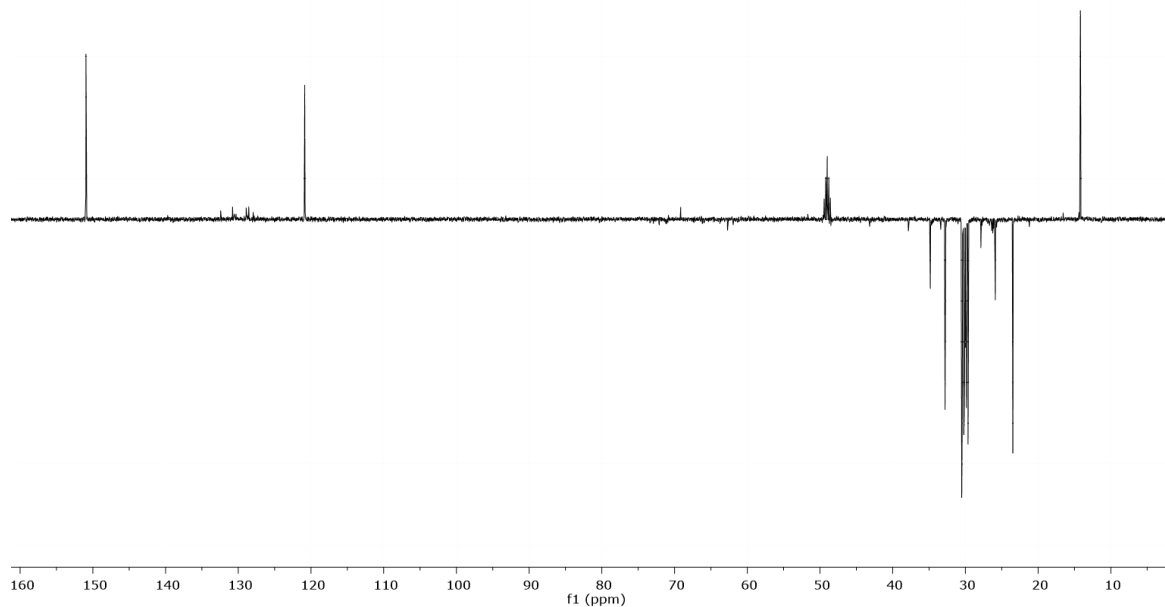
**Supplementary Figure 5-5** (Structure elucidation Fab from *Burkholderia glumae* ICMP 3729)



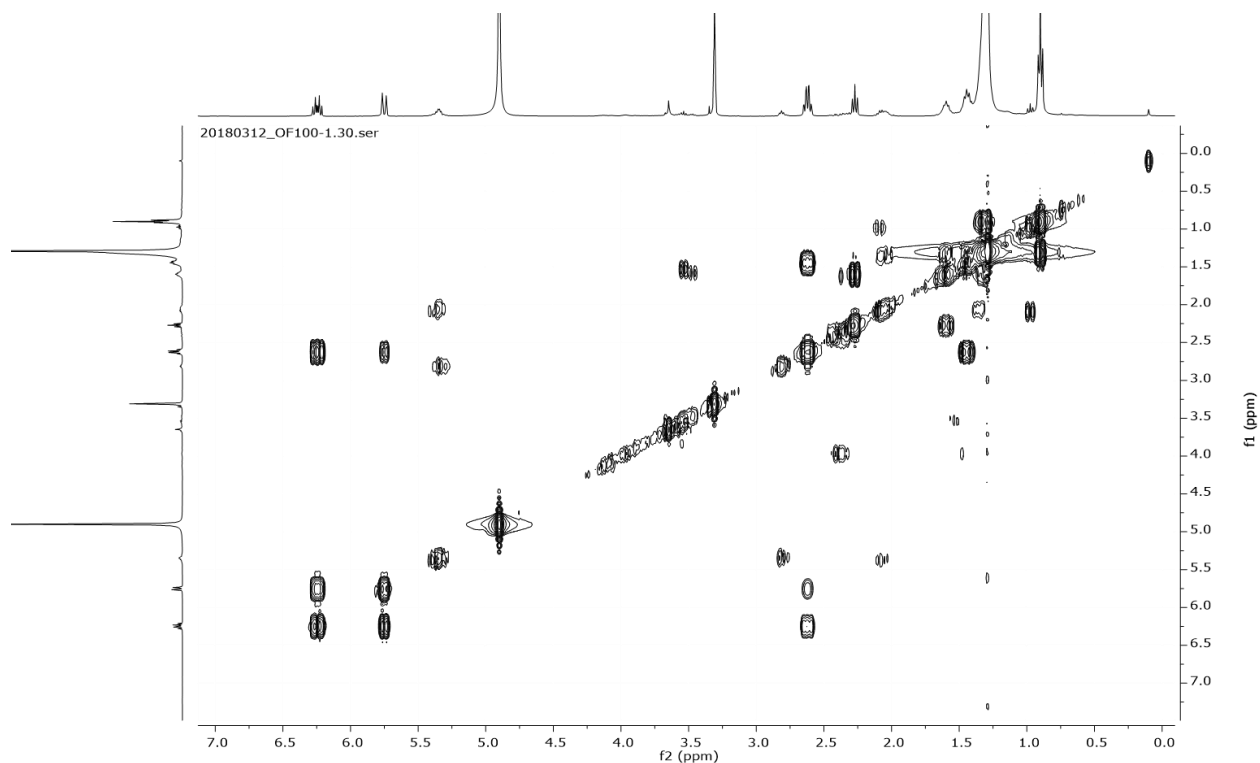
Proton NMR of fatty acid produced by *Burkholderia glumae* ICMP 3729



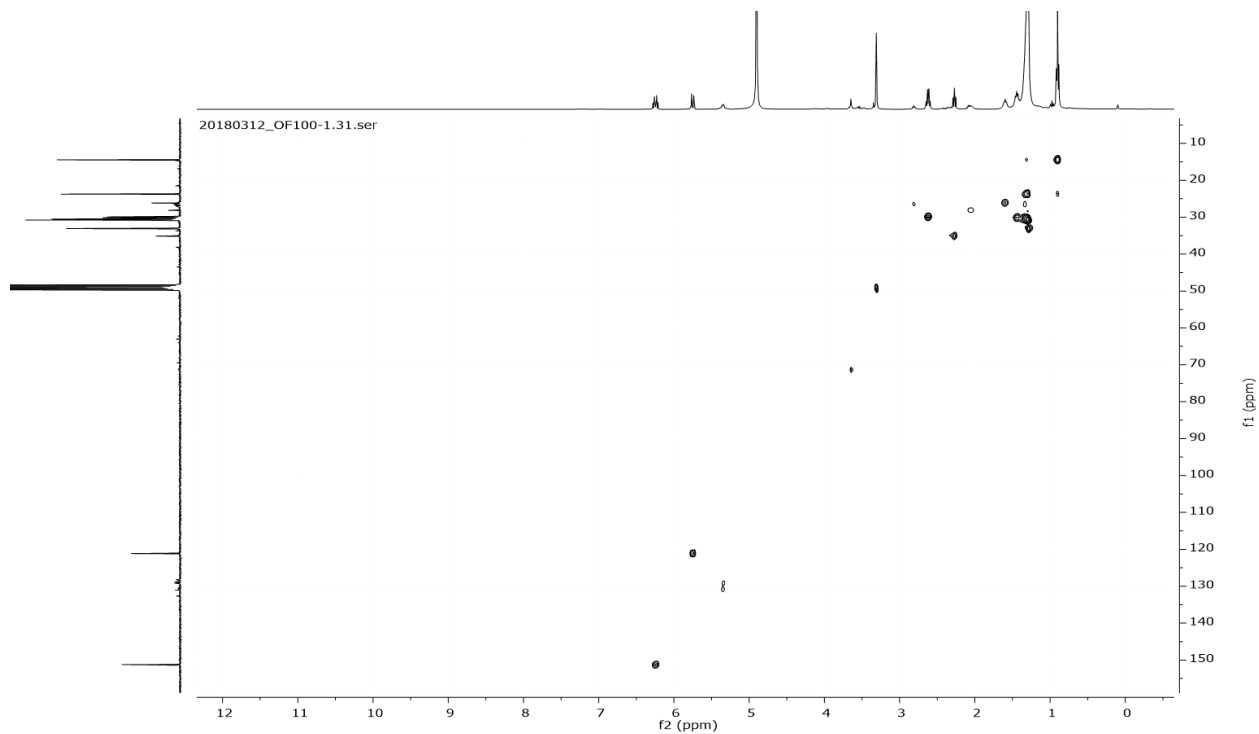
Carbon NMR of fatty acid produced by *Burkholderia glumae* ICMP 3729



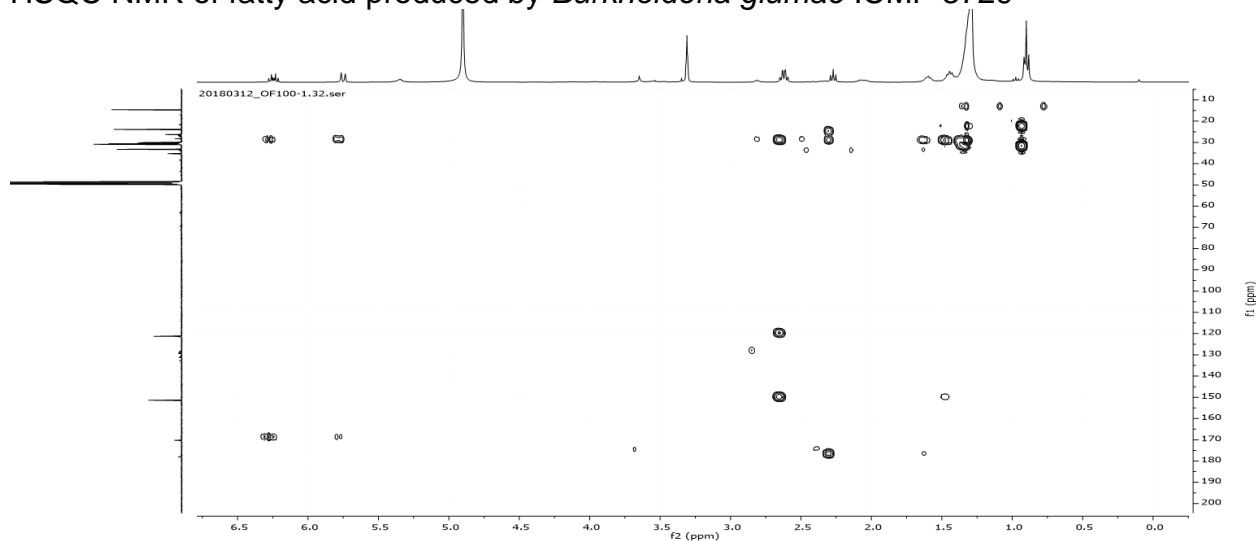
DEPT135 NMR of fatty acid produced by *Burkholderia glumae* ICMP 3729



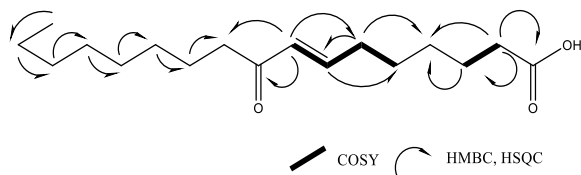
COSY NMR of fatty acid produced by *Burkholderia glumae* ICMP 3729



HSQC NMR of fatty acid produced by *Burkholderia glumae* ICMP 3729



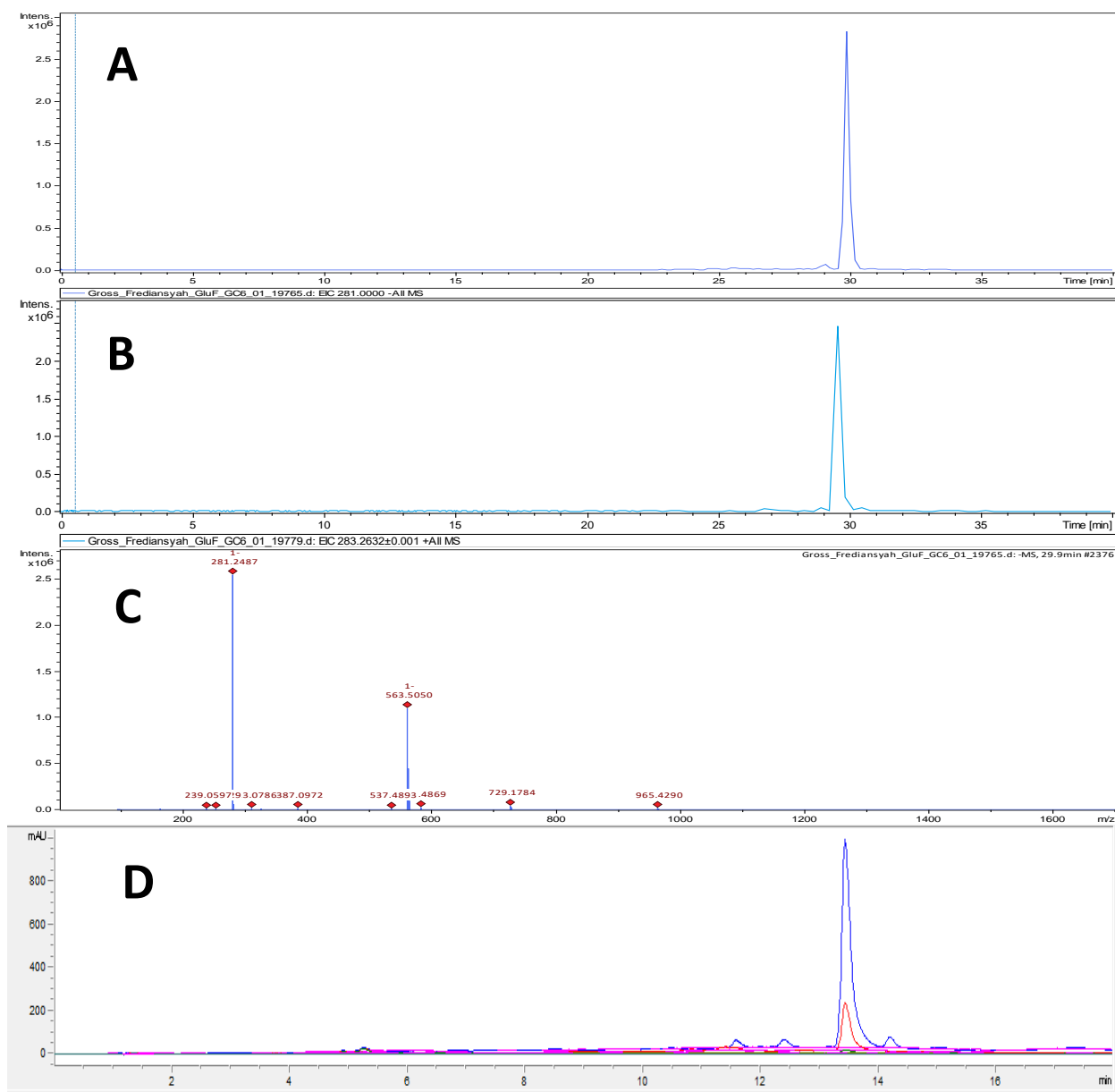
HMBC NMR of fatty acid produced by *Burkholderia glumae* ICMP 3729



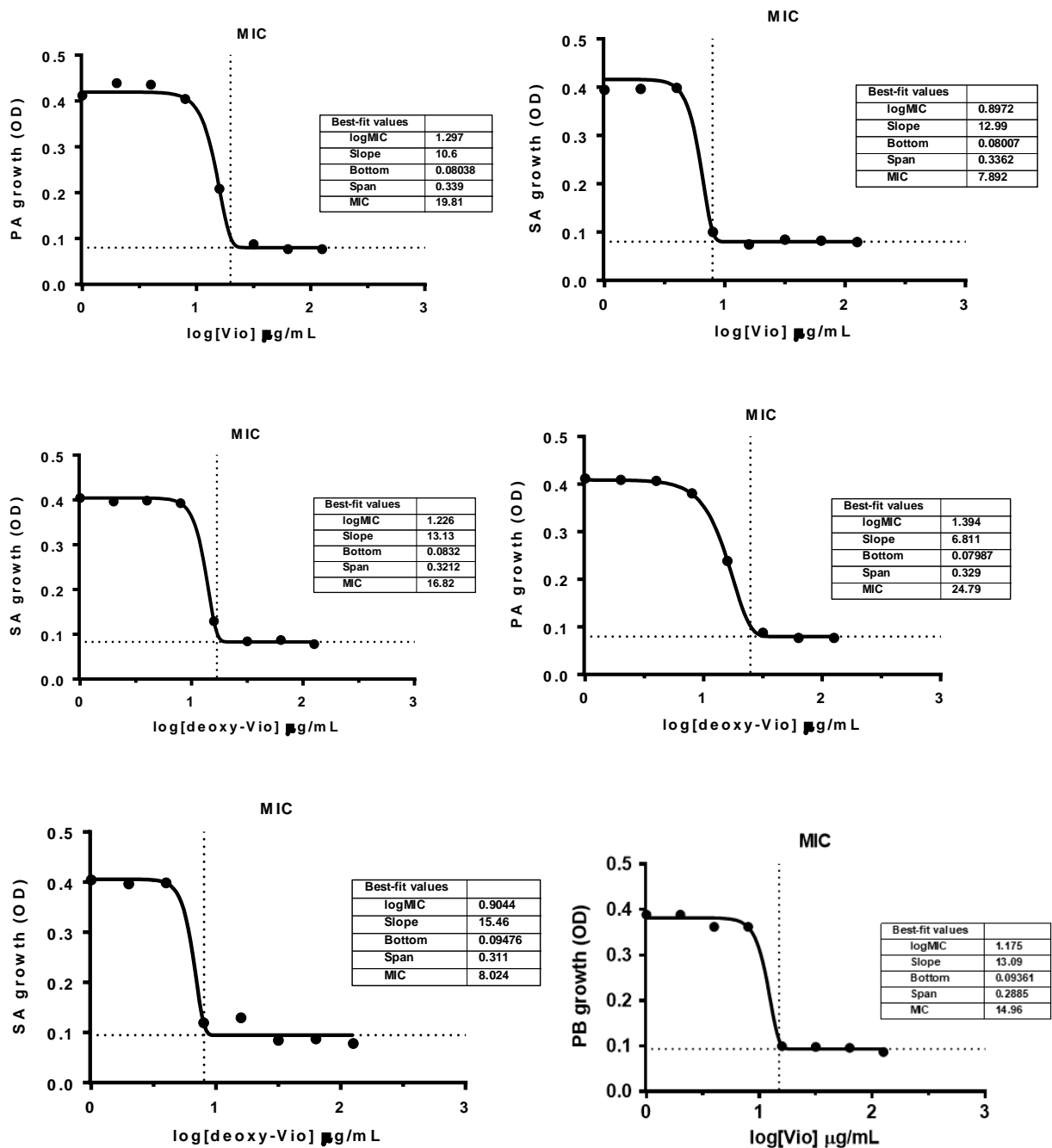
(*E*)-9-oxoheptadec-7-enoic acid  
 Chemical Formula: C<sub>17</sub>H<sub>30</sub>O<sub>3</sub>  
 Molecular Weight: 282.42

The generated final structure of fatty acid, FAb, produced by *Burkholderia glumae* ICMP 3729

**Supplementary Figure 5-6** (Mass of fatty acid produced by *Burkholderia glumae* ICMP 3729. (A) EIC [M+H]<sup>-</sup> 281, (B) EIC [M+H]<sup>+</sup> 283 and (C) [M+H]<sup>-</sup> 281.2487, [2M+H]<sup>-</sup> 563.5050, Chemical formula: C<sub>17</sub>H<sub>30</sub>O<sub>3</sub> (D) compound purification using *Aeris*<sup>TM</sup> 3.6 μm PEPTIDE XB-C18 100 Å, LC Column 100 x 2.1 mm)



**Supplementary Figure 6-1** (Antibacterial activity of dipeptides and violaceins)



-----end-----